

**Design, synthesis and optimization of
nucleotide-derived inhibitors and
probes for the ecto-nucleotidases
CD39 and CD73**

DISSERTATION

zur

Erlangung des Doktorgrades Dr. rer. nat.

der

Mathematisch-Naturwissenschaftlichen Fakultät

der

Rheinischen Friedrich-Wilhelms-Universität Bonn

vorgelegt von

Constanze Cerine Schmies

aus Wuppertal

Bonn 2019

Angefertigt mit Genehmigung der Mathematisch-Naturwissenschaftlichen Fakultät
der Rheinischen Friedrich-Wilhelms-Universität Bonn

Promotionskommission:

Erstgutachterin: Prof. Dr. Christa E. Müller

Zweitgutachter: Prof. Dr. Gerd Bendas

Fachnahes Mitglied: PD Dr. Ganna Staal

Fachfremdes Mitglied: Prof. Dr. Rainer Manthey

Tag der Promotion:

Erscheinungsjahr:

Diese Dissertation ist auf dem Hochschulserver der ULB Bonn elektronisch pub-
liziert: <http://nbn-resolving.de/urn:nbn:de:hbz:5n-56735>.

Die vorliegende Arbeit wurde in der Zeit von Oktober 2015 bis August 2019 am Pharmazeutischen Institut der Rheinischen Friedrich-Wilhelms-Universität Bonn unter der Leitung von Frau Prof. Dr. Christa E. Müller angefertigt.

Contents

1	Introduction	1
1.1	Purinergic signaling	1
1.1.1	Discovery of ATP	1
1.1.2	Purinergic receptors	2
1.1.3	ATP release and breakdown	4
1.2	Nucleoside triphosphate diphosphohydrolases	5
1.2.1	Crystal structure of CD39	6
1.2.2	Pathological role of CD39	9
1.2.3	Known inhibitors of CD39	11
1.2.3.1	Non-nucleotide-based CD39 inhibitors	11
1.2.3.2	Nucleotide-based CD39 inhibitors	13
1.3	<i>Ecto</i> -5'-nucleotidase	15
1.3.1	Pathological role of CD73	15
1.3.2	Crystal structure of CD73	16
1.3.3	Known inhibitors of CD73	19
1.4	Analytical assays	22
1.4.1	Malachite green assay	22
1.4.2	Capillary electrophoresis-UV assay	23
1.4.3	Fluorescence polarization immunoassay	24
1.4.4	Fast fluorescent CE assay	26
1.4.5	Radiometric assay	27
1.5	Synthesis of nucleotides	28
1.5.1	Monophosphorylation	28
1.5.2	Triphosphorylation	30
1.5.3	Diphosphorylation	30

2	Aims of the study	33
2.1	Development of novel inhibitors for CD39	33
2.2	Synthesis of inhibitors and tool compounds for CD73	33
2.2.1	Upscaling of the synthesis of AOPCP derivatives for <i>in vivo</i> testing of CD73 inhibitors	34
2.2.2	Development of a radioligand for CD73	34
2.2.3	Development of a fluorescent probe for CD73	34
2.2.4	Development of a PET-tracer for CD73	34
2.2.5	7-Deaza-AOPCP derivatives as novel CD73 inhibitors	35
3	Results and discussion - Part I: Development of novel inhibitors for CD39	37
3.1	Synthesis of adenosine derivatives	37
3.1.1	Modification of adenosine at the C2-position	38
3.1.2	Modification of adenosine at the C8-position	39
3.1.3	Modification of adenosine at the N ⁶ -position	43
3.1.4	Modification of adenosine at the C8- and N ⁶ -position	49
3.2	Triphosphorylation of adenosine derivatives	52
3.3	Monophosphorylation of adenosine derivatives	56
3.4	Pharmacological evaluation of ARL67156-derivatives	61
3.4.1	Structure-activity relationships of ARL67156-derivatives	61
3.4.2	Selectivity studies versus other <i>ecto</i> -nucleotidases	64
3.4.3	Metabolic stability of ARL67156-derivatives	66
3.5	Pharmacological evaluation of AMP-derivatives	67
3.5.1	Inhibitory potency of AMP-derivatives	67
3.5.1.1	SARs of C2-substituted AMP-derivatives	67
3.5.1.2	SARs of C8-substituted AMP-derivatives	68
3.5.1.3	SARs of N ⁶ -substituted AMP-derivatives	69
3.5.1.4	SARs of C8,N ⁶ -substituted AMP-derivatives	71
3.5.1.5	Most potent AMP derivatives	73
3.5.2	Selectivity studies versus other <i>ecto</i> -nucleotidases	73
3.5.3	Metabolic stability of AMP-derivatives	75

4 Results and discussion - Part II: Synthesis of inhibitors and tool compounds for CD73	79
4.1 Upscaling of the synthesis of AOPCP derivatives	79
4.1.1 Synthesis of PSB-12379 (123)	79
4.1.2 Synthesis of 2,6-dichloro-9- β -D-ribofuranosyl-purine	80
4.1.3 Synthesis of PSB-12489 (135)	82
4.2 Development of an AOPCP-derived radioligand for CD73	86
4.2.1 Synthesis of various cold ligands	86
4.2.2 Pharmacological evaluation of the cold ligands	87
4.2.3 Synthesis of the radioligand precursor	89
4.2.4 Generation of the tritium-labeled CD73 inhibitor	93
4.3 Development of an AOPCP-derived fluorescent probe	94
4.3.1 Design of an AOPCP-derived fluorescent probe for CD73	94
4.3.2 Synthesis route A	95
4.3.3 Synthesis route B	96
4.3.4 Synthesis route C	97
4.3.5 Synthesis route D	98
4.3.6 Pharmacological evaluation of the fluorescent probes	101
4.3.7 Fluorescence emission and absorption spectra	102
4.3.8 Evaluation of the binding of 158a and 158b to peripheral mononuclear blood cells by flow cytometry	103
4.4 Development of an AOPCP-derived PET-tracer	109
4.4.1 Synthesis of an AOPCP-derivative suitable for subsequent ^{18}F -labeling	111
4.4.2 Synthesis of the cold analog of the designed PET-tracer	112
4.4.3 Pharmacological evaluation of the PET-tracer	114
4.5 2-Chloro-7-deaza AOPCP-derived inhibitors of CD73	115
4.5.1 Synthesis of protected 2,6-dichloro-7-deazaadenosine	116
4.5.2 Synthesis of N^6 -substituted 2-chloro-7-deazaadenosine derivatives	118
4.5.3 Synthesis of N^6 -substituted 2-chloro-7-deaza-AOPCP derivatives	118
4.5.4 Pharmacological evaluation	122

5	Summary and outlook	125
5.1	Synthesis and evaluation of novel inhibitors for CD39	125
5.1.1	Structure–activity relationships of ARL67156 derivatives	125
5.1.2	Structure–activity relationships of AMP derivatives	126
5.2	Synthesis of inhibitors and tool compounds for CD73	128
5.2.1	Upscaling of the synthesis of AOPCP derivatives for <i>in vivo</i> testing of CD73 inhibitors	128
5.2.2	Development of a radioligand for CD73	129
5.2.3	Development of a fluorescent probe for CD73	130
5.2.4	Development of a PET-tracer for CD73	131
5.2.5	7-Deaza-AOPCP derivatives as CD73 inhibitors	131
6	Materials and methods	133
6.1	Chemicals	133
6.2	Instrumentation	133
6.3	Experimental procedures	135
6.4	Biological experiments	228
6.4.1	Pharmacological evaluation of 8-BuS-AMP and ARL67156 derivatives	228
6.4.2	Pharmacological evaluation of AOPCP derivatives at CD73	232
6.4.3	Flow cytometry analyses	236
7	List of abbreviations	239
8	List of Figures	243
9	List of Schemes	247
10	List of Tables	249
11	Literature	253

1 Introduction

1.1 Purinergic signaling

1.1.1 Discovery of ATP

90 years ago, in 1929, the molecule adenosine triphosphate (ATP) was first described by two distinct research groups in Heidelberg and Boston.^{1,2} A few years later, in 1941, it was discovered that muscle contraction and other energy-requiring processes were driven by the breakdown of ATP into adenosine diphosphate (ADP) and inorganic phosphate.³ For the first time, ATP was recognized as the main cellular energy source due to the energy-rich phosphate ester.³

The intracellular concentration of ATP is relatively high (1-10 mM) in contrast to its concentration in the extracellular space under physiological conditions (1-10 nM).⁴ Due to this concentration gradient and its small size, ATP can be released rapidly upon mechanical stress, cell damage, or as consequence of cell death.⁴ From an evolutionary point of view, ATP became probably the first extracellular signaling molecule, since cell damage would automatically lead to release of ATP into the extracellular space.⁵ Therefore, ATP is nowadays recognized as a universal danger signal and almost all cells or single-cell organisms possess a sensitivity towards ATP.⁵ Interestingly, already in 1929, Drury and Szent-Györgyi observed that ATP and adenosine had a potent effect on heart and blood vessels.⁶ However, it took another 40 years, until ATP was proposed to be a neurotransmitter.^{7,8} Initially, it was thought that ATP was released by non-adrenergic and non-cholinergic so called "*purinergic nerves*".^{7,8} Over the years it became, however, clear that ATP is more likely a co-transmitter in all peripheral and central nerves.^{9,10}

Since ATP is an ubiquitous molecule present in all types of cells, it seemed unlikely that ATP could act as a specific neurotransmitter. Therefore, the resistance against Burnstock's "*purinergic hypothesis*" of other biochemists was great and it took him more than 20 years until his model of purinergic signaling became accepted.¹¹

1.1.2 Purinergic receptors

The concept of receptors was first described in the beginning of the 20th century by John Newport Langley and Paul Ehrlich.^{12,13} Receptors are defined as cellular macromolecules or macromolecular complexes that transduce chemical signals.¹⁴ According to a simple model, receptors can be present in an active and an inactive conformation.^{14,15} Agonists, which are chemical compounds that can activate receptors, bind to the active conformation with high affinity, thereby stabilizing this conformation and activating the signal transduction cascade.¹⁴⁻¹⁶ In contrast, antagonists can bind to the active and inactive conformation of the receptor and lead to inactivation of the receptor or to the stabilization of the inactive state of the receptor, thereby inhibiting signal transduction.¹⁴

In order to induce signaling, extracellular nucleotides and nucleosides act on membrane-bound purinergic receptors. The first two families of purinergic receptors, P1 and P2, were identified based on the different activities of purine derivatives ATP, ADP, adenosine, and methylxanthines like caffeine on the respective receptor subtypes, and their effects on the second messenger system adenylate cyclase.¹⁷

P1 receptors are G protein-coupled receptors (GPCRs) and comprise four subtypes A_1 , A_{2A} , A_{2B} , and A_3 , all activated by adenosine (*Figure 1.1*).^{18,19} The A_1 receptor is highly expressed in brain, spinal cord, heart, stomach, eye, and adrenal gland.¹⁹ The A_{2A} receptor is expressed in brain, heart, spleen, lungs, immune cells, and blood vessels.¹⁹ The A_{2B} receptor is prominently expressed in cecum, colon and bladder whereas the A_3 receptor is highly expressed in lungs and liver.¹⁹ All adenosine receptors (ARs) couple to the second messenger system adenylate cyclase and either inhibit or stimulate this enzyme.^{18,19} ARs are a potential drug targets since stimulation of ARs can lead to various effects, including anti-inflammatory, anti-lipolytic, anti-convulsive, sedative, vasodilatory, immunosuppressive, anti-diuretic, and negative inotropic effects.¹⁸ Therefore, agonists as well as antagonists of ARs are investigated as potential drugs in many therapeutic areas like the respiratory and the cardiovascular systems, neuroprotection, pain processes, and inflammatory responses.¹⁸

The class of P2 receptors can be subdivided into nucleotide-activated ligand-gated ion channel (LGIC) P2X receptors, all activated by ATP, and G protein-coupled P2Y receptors, which are activated by ATP, ADP, uridine triphosphate (UTP), uridine

diphosphate (UDP), or UDP-glucose (Figure 1.1).^{20,21} P2X receptors are the only non-GPCR subclass in the purinergic receptor family and are expressed throughout the whole body, particularly in the central nervous system and in microglial cells, vas deferens, bladder, smooth muscle cells, and pain sensing neurons.^{22,23} P2Y receptors are distributed in brain, heart, kidney, liver, lung, pancreas, prostate and thymus, bone, and haematopoietic cells.²⁰ In general, short-term effects like for example neurotransmission, are mediated by P2X receptors and long-term effects like cell proliferation, differentiation, and migration are mediated by P2Y receptors.²⁰

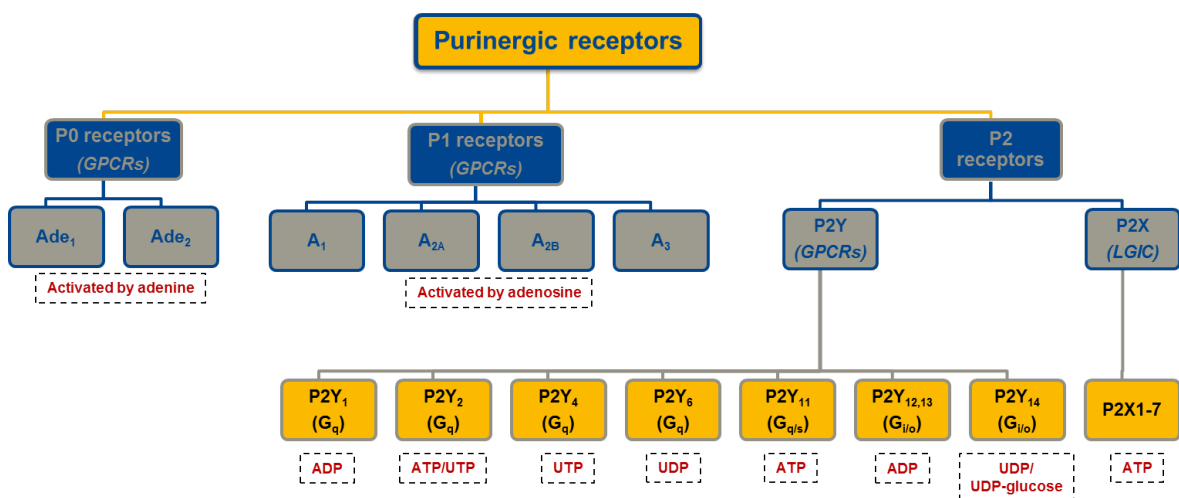


Figure 1.1: Overview of purinergic receptors and their endogenous ligands.

The youngest member of the purinergic receptor family is the P0 receptor also known as adenine receptor (AdeR).²⁴ P0 receptors belong to the family of GPCRs and are activated by the purine base adenine (Figure 1.1).^{25–27} Adenosine receptors (AdeR) have so far been found in rodents, including mouse, rat, and hamster. The rat AdeR was found to be expressed in small neurons of dorsal root ganglia, ovaries, kidney, and small intestine.^{25,26,28} The physiological role of adenine has not yet been identified, but a role in nociception was suggested.²⁵ Although the human AdeR has not been identified yet on a molecular level, increased concentrations of adenine were found in patients with chronic renal failure suggesting that adenine may play a role in human pathology as well.^{28,29}

1.1.3 ATP release and breakdown

Cell damage or cell lysis as consequence of organ injury, shock, or inflammatory conditions can lead to a massive leakage of endogenous nucleotides.³⁰ Next to these nonspecific mechanisms, endogenous nucleotides can also be released in a controlled manner. In excitatory or secretory tissues, like nerve terminals, pancreatic acinar cells, or circulating platelets, ATP and ADP are stored and released together with other neurotransmitters via calcium-mediated exocytosis.^{9,30,31}

In addition to that, endogenous nucleotides can be also be secreted by non-excitatory cells, including epithelial cells, smooth muscles and fibroblasts, astrocytes, circulating lymphocytes, monocytes, hepatocytes, and chondrocytes.³¹ Release has been reported to occur via three different processes, which include (1) diffusion through membrane ion channels, including connexin hemichannels, stretch- and voltage-activated channels; (2) active transport by nucleotide-specific ATP-binding cassette transporters such as the cystic fibrosis transmembrane conductance regulator, the multidrug resistance proteins, and the multiple organic anion transporters; and (3) cargo-vesicle trafficking and exocytotic granule secretion.^{20,30}

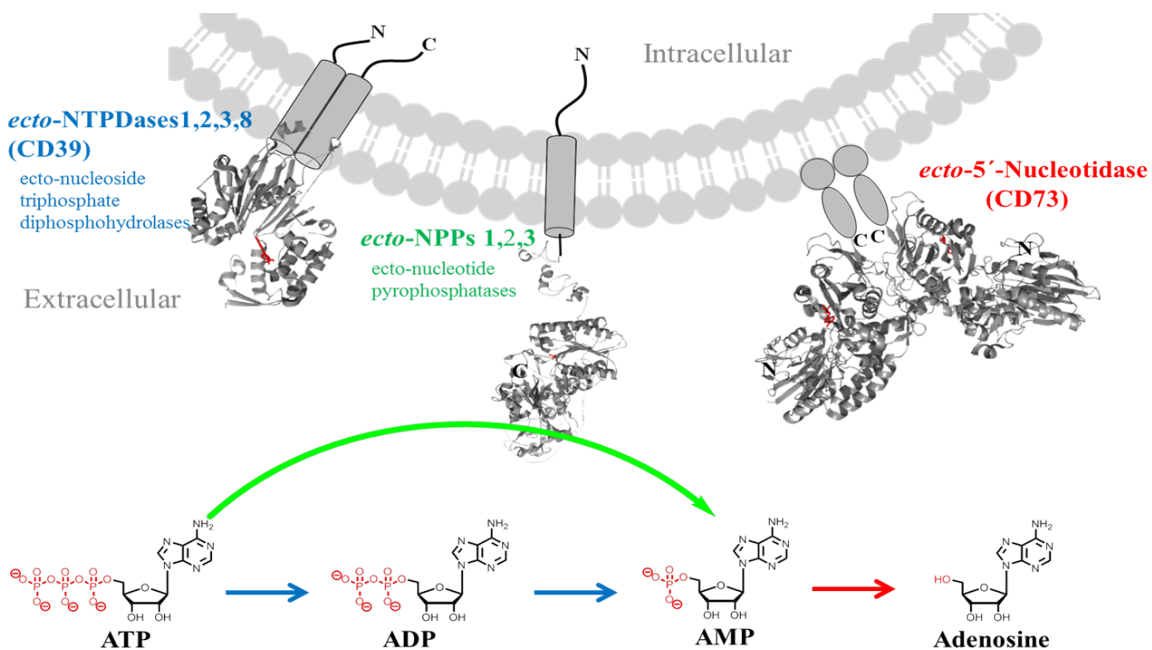


Figure 1.2: Pathways of extracellular nucleotide metabolism. NTPDases and NPPs are mainly responsible for the generation of adenosine monophosphate (AMP) from ATP and ADP, while *ecto-5'-nucleotidase (CD73)* hydrolyzes AMP to adenosine. This figure was taken from [32].

Upon release, various signaling pathways can be induced by ATP leading to dif-

ferent cellular effects. In order to terminate cell signaling, released nucleoside triphosphates (NTPs) need to be hydrolyzed in their respective nucleosides.²⁰ This is achieved by a cascade of enzymes called *ecto*-nucleotidases, which are located in the cell membrane with an extracellular catalytic site (*Figure 1.2*).^{4,20,21} This family of enzymes consists of four main classes: nucleoside triphosphate diphosphohydrolase (NTPDase), nucleotide pyrophosphatase/phosphodiesterase (NPP), *ecto*-5'-nucleotidase (CD73), and alkaline phosphatase (*Figure 1.2*).^{4,20,21} NTPDases and NPPs are mainly responsible for the generation of AMP from ATP and ADP, while CD73 hydrolyzes AMP to adenosine, which can be metabolized to inosine by adenosine deaminase.^{21,33} Adenosine can also be taken up by nucleoside transporters and be phosphorylated to AMP again by adenosine kinase.²¹

1.2 Nucleoside triphosphate diphosphohydrolases

NTPDases hydrolyze nucleoside tri- (NTP) and diphosphates (NDP) into the corresponding nucleoside monophosphates (NMP).²¹

An enzyme is a protein with catalytical properties and can therefore be considered a biocatalyst. The major role of enzymes is to lower the activation energy required for certain reactions within an organism and thereby to enhance the reaction rate.^{34,35} Often, co-factors, like cations or vitamins, are needed in order for the reaction to proceed, as well as specific reaction conditions, including pH and temperature.^{34,35} Enzymes possess specific binding sites, which enable the selective recognition and conversion of substrates.^{34,35} Iso-enzymes are enzymes that have a different amino acid sequence, but that metabolize the same substrate and therefore catalyze the same reaction.³⁵

Based on their cellular localization and substrate specificity, eight different NTPDase subtypes (NTPDase1-8) can be distinguished (*Figure 1.3*).²¹ NTPDases 4-7 are located on intracellular membranes, although soluble forms of NTPDase5 and 6 are also known.²¹ It is however, not expected that these soluble forms play a significant role in the hydrolysis of extracellular nucleotides. The extracellularly located isoenzymes NTPDase1, -2, -3, and -8 are closely related to each other and contain approximately 500 amino acids.²¹ A fully glycosylated monomer has a molecular mass of approximately 70-80 kDa.²¹

Although the extracellular NTPDases have a broad substrate specificity towards purine and pyrimidine nucleotides, NTPDase1 and -2 have a preference for adenine over uracil nucleotides.²¹ Extracellular NTPDases possess a dual specificity for nucleotide triphosphates and nucleotide diphosphates combined with a low base specificity.³⁷ In contrast to NTPDase1, NTPDase2, -3, and -8 release ADP after hydrolysis before it is further hydrolyzed to AMP, which can be explained by the fact, that NTPDase1 has equal preferences for ATP and ADP.^{21,36,38} However, when UTP is hydrolyzed by NTPDase1, accumulation of extracellular UDP is observed.³⁸

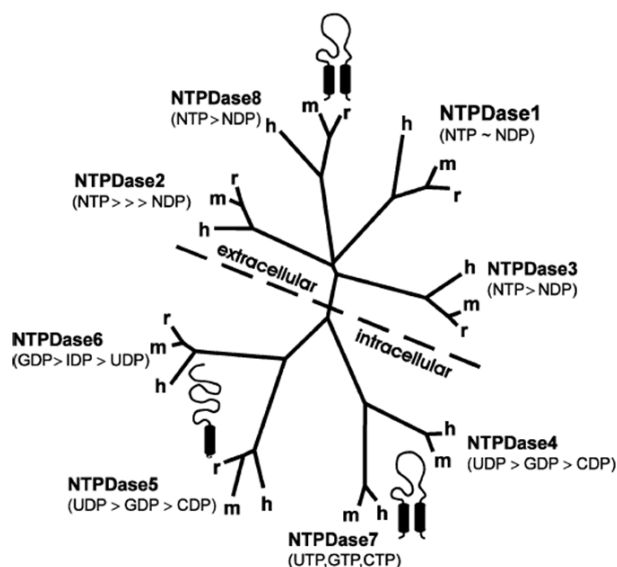


Figure 1.3: Phylogenetic tree of the NTPDase family based on amino acid sequence alignment. Members of the NTPDase family from rat (*r*), human (*h*), and mouse (*m*) are included. The length of the lines represents the differences between sequences. Substrate preferences are indicated in brackets. This figure was taken from [36].

1.2.1 Crystal structure of CD39

NTPDase1, -2, -3, and -8 are located at the cell surface and contain a large extracellular loop that harbors the active site and two transmembrane domains.²¹ The ligand binding pocket is formed by five highly conserved sequence motifs called the apyrase-conserved regions (ACRs), which are placed between two lobes that perform a butterfly-like domain closure after substrate binding.^{21,39} The ACRs are dependent on divalent metals (Ca^{2+} or Mg^{2+}) and are deactivated in their absence. Next to the ACRs, the four enzymes also share four additional conserved regions as well as ten conserved cysteine residues.⁴⁰

Structural X-ray analysis of a crystallized enzyme in complex with its substrate or inhibitor is useful for the characterization of the protein. Based on the structural information, new conclusions can be drawn concerning the catalytic mechanism, and computational models can be used for the rational design of new lead compounds. During the last couple of years, crystal structures of the *ecto*-domains of rat

NTPDase1 and -2, and of the homologous *L. pneumophila* NTPDase1 (LpNTPDase1) were published.^{37,39,41,42} These structures gave new insights into the molecular structure and functionality of NTPDase1 (Figure 1.4).

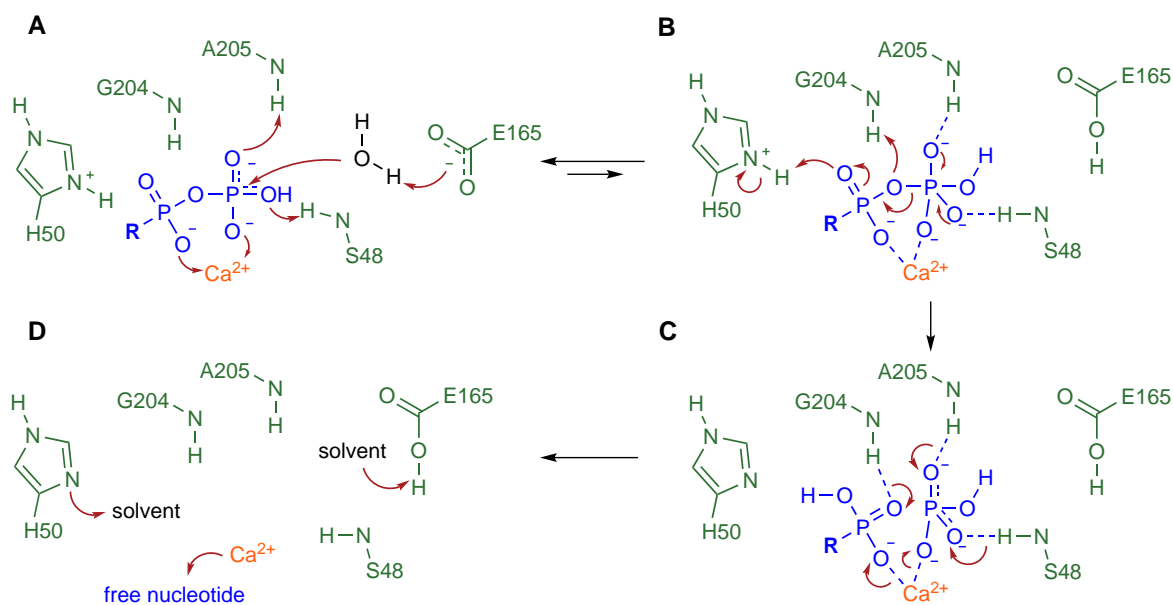


Figure 1.4: Schematic representation of the postulated reaction mechanism of NTPDase-mediated NTP (R = NMP) or NDP (R = nucleoside) hydrolysis. The catalytic mechanism was proposed after determination of the structure of the extracellular domain of rat NTPDase2 in complex with the nucleotide analog β,γ -imidoadenosine 5'-triphosphate (AMPPNP) and Ca^{2+} in a productive binding mode. A) Activation of the nucleophilic water by E165 and subsequent nucleophilic attack on the terminal phosphate. The negative charge of the phosphate groups is reduced by complex formation with a divalent metal cation. B) Collapse of the trigonal bipyramidal transition state. The negative charge of the transition state is stabilized by proton-donating hydrogen bonds from the phosphate-binding loops (e.g., S48, A205). Additional hydrogen bonds may exist. C) Product release. H50 may be responsible for protonation of the leaving group. D) Reconstitution of the active site. This figure was taken and modified from [21].

According to the proposed mechanism depicted in Figure 1.4, the nucleotide is in complex with a divalent cation, which is essential for proper functioning of the enzyme as already mentioned.²¹ The mechanism starts with activation of a water molecule by the carboxyl group of a highly conserved glutamate residue (E165) in the active site, which functions as a catalytical base. Subsequently, a nucleophilic attack of the activated water molecule on the terminal phosphate occurs. The negatively charged phosphate groups are reduced by the divalent cation. After collapse of the trigonal bipyramidal transition state, the product is released.^{21,37} It was also shown, that NTPDase can exist in an open inactive form and in a closed active conformation.^{37,42}

Crystal structures of NTPDase are currently available without any ligand or bound to non-competitive inhibitors, like the polyoxometalate decavanadate ($(V_{10}O_{28})^{6-}$).^{39,43} Non-competitive inhibitors are known to bind to a different site than the substrate binding site of the enzyme. Therefore, a crystal structure based upon co-crystallization with an non-competitive inhibitor might not represent the natural occurring conformation of the enzyme.

In contrast to human NTPDase1, rat NTPDase2 has been crystallized with natural substrate analogs.³⁷ Based on these data, a homology model of human NTPDase1 in its active conformation was generated, that allows investigation of ligand binding (*Figure 1.5*).

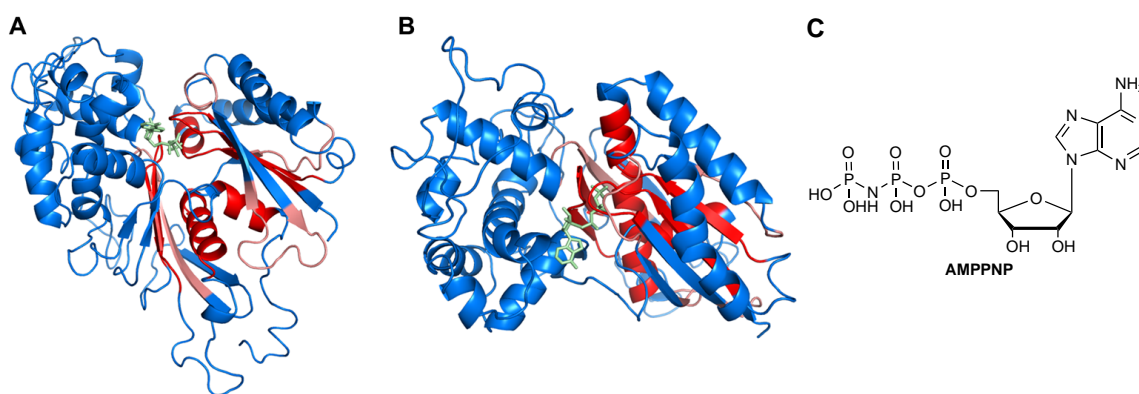


Figure 1.5: Homology model of human NTPDase1. The homology model of human NTPDase1 (blue) is shown from the front (A) and from the top (B). The truncated transmembrane domains would be located at the bottom. ACRs are colored in red and conserved regions (CRs) in extracellular domains of NTPDases are depicted in salmon. The ligand AMPPNP (pale green) is located in the binding pocket between two extracellular domains that close upon substrate binding. The structure of AMPPNP is depicted on the right site (C). The ligand has been taken from the rat NTPDase2 crystal structure (PDB identifier: 4BR5) to visualize the location of the binding pocket. This figure was taken and adapted from [44].

Homology modeling is the computational generation of a three-dimensional protein structure based on related structures.⁴⁴ For this purpose, already resolved crystal structures are considered as templates. The sequence identity of the chosen template should at least be 30%. Furthermore, it is essential that the important regions are conserved and that the chosen crystal structure is of high quality, especially in the important regions like for example the ligand binding site.

After the selection of one or more templates, a sequence alignment is made.⁴⁴ Based on this alignment the backbone and side-chain modeling is carried out, starting

with the backbone. In this process, a large number of models is produced which are scored. Based on the scores, the most appropriate model can be chosen which is not necessarily the one with the highest score. It might happen that gaps or some regions such as loops have to be remodeled because of the difference between template and target protein. This can be achieved by geometry if only up to three amino acids are involved, or by template-based or *de novo* methods. It can be searched for a similar loop in other structures that can function as template. Finally, the model is validated by the Ramachandran plot that can give an impression of the model's stability.⁴⁵

Pairwise sequence alignment of human, rat, and mouse NTPDase1 showed that rat and mouse share about 90% identity while the human form is about 75% identical with both rodent species.⁴⁴ The differences are mainly located in the extracellular loops, leading to the conclusion that the binding pockets are conserved. Therefore, the rat and mouse homologs can be used as templates for modeling of the human NTPDase1.

Based on the crystal structure of rNTPDase2, a homology model of hNTPDase1 in its substrate-bound conformation was generated in our group (*Figure 1.5*).⁴⁴

1.2.2 Pathological role of CD39

NTPDases have a broad tissue distribution and are expressed by various cell types like endothelial cells, vascular cells, and immune cells including natural killer cells, monocytes, dendritic cells, and activated T cells.²¹ Therefore, extracellular NTPDases play a role in various physiological processes including vascular haemostasis, immunoregulation, nociception, and development.⁴⁶⁻⁵³ Furthermore, they are important modulators of vascular inflammation and thrombosis, and play a role in cerebroprotection and cardioprotection.²¹ NTPDases are the major enzymes in the regulation of nucleotide metabolism at the surface of vascular smooth muscle cells and are involved in the regulation of the local vascular tone.²¹

Among the four extracellular isoenzymes, NTPDase1 is the most abundant and important isoenzyme, which was found to be expressed on various immune cells.²¹ It was first described in blood platelets in 1967 by Chambers *et al.* who studied the role of ATPases in ADP-induced platelet aggregation.⁵⁴ Being a lymphocyte activation marker, NTPDase1 is also termed CD39.²¹

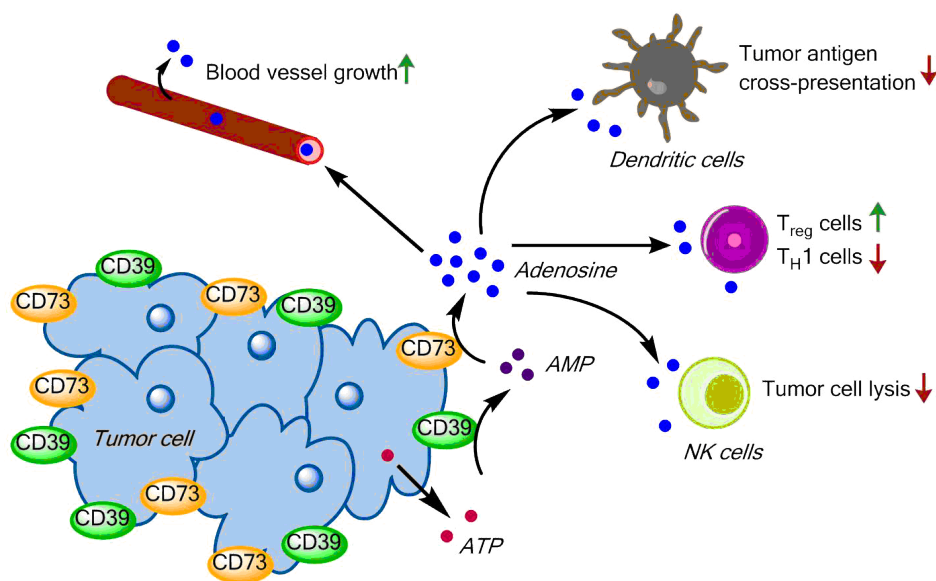


Figure 1.6: The role of CD39 overexpression in tumor progression. Increased expression of NTPDase1 (CD39) leads to an increased extracellular AMP concentration. Overexpression of CD73 results in the enhanced generation of adenosine, which promotes tumor growth, formation of new blood vessels and inhibits anti-cancer immune responses. T_{reg} cells = regulatory T cells; T_{H1} cells = T helper cells; NK cells = natural killer cells.

Extracellular ATP is a proinflammatory danger signal, while adenosine is anti-inflammatory and immunosuppressive. Therefore, CD39 is a major player in controlling immune responses.²¹ NTPDases are ubiquitously expressed, but many cancer cells show an overexpression of CD39 and CD73 leading to increased extracellular adenosine levels (Figure 1.6).⁵⁵ Increased CD39 expression has been reported to be involved in the progression of infectious diseases such as acquired immune deficiency syndrome (AIDS). Since adenosine promotes angiogenesis, tumor growth, and immunosuppression, inhibitors of CD39 may have potential for the treatment of various diseases, e.g. cancer, viral or bacterial infections, and immunodeficiency disorders.

In contrast to that, activation of CD39 can be of therapeutic relevance in inflammatory diseases like chronic obstructive pulmonary disease or graft-versus-host disease after transplantation.^{56,57} Furthermore, by hydrolysis of ADP, CD39 reduces platelet activation by P2Y₁ and P2Y₁₂ receptors and thereby the risk of thrombosis. Positive modulators of CD39 could therefore be used in the treatment of vascular diseases.⁵⁸

In summary it can be concluded that small molecules, inhibitors and activators of

CD39, are required for modulation of the enzyme to investigate its (patho)physiological roles, *e.g.*, in the context of the immune system, and its potential as a drug target.

1.2.3 Known inhibitors of CD39

An inhibitor is a compound that is able to slow down the rate of an enzymatic reaction. Reversible and an irreversible inhibitors exist.^{34,59} A reversible inhibitor can act via three different mechanisms, known as competitive, non-competitive, and mixed inhibition. In the case of competitive inhibition, the inhibitor binds to the free enzyme, thereby competing with the substrate for the same binding site. With increased substrate concentration, the inhibitor can be replaced again from the enzyme.^{34,60} In contrast, a non-competitive inhibitor binds to the enzyme-substrate complex at a different site of the enzyme than the substrate.^{34,60} During a mixed-type of inhibition, the inhibitor can bind to the free enzyme, as well as the enzyme-substrate complex at a different binding site. Therefore, by increasing the substrate concentration, the inhibition cannot be reversed.⁶⁰

For the determination of the potency of an inhibitor, two values are important, the half maximal inhibitory concentration (IC_{50}) and the inhibitory constant (K_i). While the K_i value is reflective of the binding affinity of the drug, the IC_{50} value is a measure of the effectiveness of a substance in inhibiting a specific biological or biochemical function.

Although crystal structures of multiple NTPDases have been resolved, the substrate specificity remains unknown. In the literature, few NTPDase1 inhibitors, that are weak and/or non-selective, have been described, including N^6 -diethyl-D- β,γ -dibromo-methylene-ATP (ARL67156), 8-butylthio-AMP (8-BuS-AMP), suramin and related compounds, polyoxometalates (PSB-POM-142), sulfonate dyes such as reactive blue 2 (RB2), pyridoxalphosphate-6-azophenyl-2',4'-disulfonic acids (PPADS), and anthraquinone derivatives.⁶¹⁻⁶⁸ These can be divided into two chemical classes: nucleotides (*Figure 1.7A*) and non-nucleotides (*Figure 1.7B*).

1.2.3.1 Non-nucleotide-based CD39 inhibitors

Suramin and RB2 are both commonly used non-selective inhibitors of P2Y receptors but they also have moderate, micromolar inhibitory activities against CD39 and

are therefore not selective.⁷³ Interestingly, both compounds contain an aromatic core substituted with sulfonate residues. Based on this observation Gendron *et al.* studied a series of naphtholsulfonate derivatives.⁷⁴ Out of this series, BGO136 was identified as an inhibitor of CD39 with a K_i value of $103 \mu\text{M}$ (Figure 1.7B).^{70,74} This compound also has an inhibitory activity against NTPDase2 (K_i of $150 \mu\text{M}$).^{70,74}

During structure-activity relationships (SARs) studies on RB2 to identify the pharmacophore, several 1-amino-2-sulfo-4-ar(alkyl)ylaminoanthraquinone derivatives were found to inhibit CD39.⁶⁹ The most potent compound out of this series contained a 2-naphthyl substitution and had a K_i value of $0.33 \mu\text{M}$.⁶⁹ However, this compound also exhibits low micromolar inhibitory potency against NTPDase3 (Figure 1.7B).⁶⁹

Another well-known P2 receptor inhibitor that also exhibits some inhibitory activity at CD39 is PPADS (Figure 1.7B).⁷¹

The pro-drugs clopidogrel and ticlopidine are known to irreversibly block P2Y₁₂ receptors after metabolic conversion into their active forms and thereby inhibit platelet aggregation.⁷² Additionally, Lecka *et al.* discovered that these drugs in their pro-drug forms are inhibitors for CD39 with K_i values in a moderate micromolar range (Figure 1.7B).⁷² Nevertheless, the K_i values are four fold lower than the expected concentrations of these drugs in patients' blood.⁷² This indicates, that the inhibition of CD39 by thienopyridines might be of clinical relevance.⁷² Ticlopidine was found to be a selective CD39 inhibitor with no effects on the activity of human NTPDase2, NTPDase3, NTPDase8, NPP1, and NPP3 (Figure 1.7B).⁷⁵

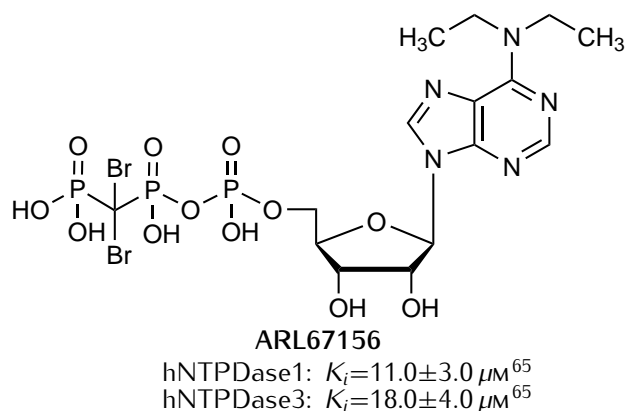
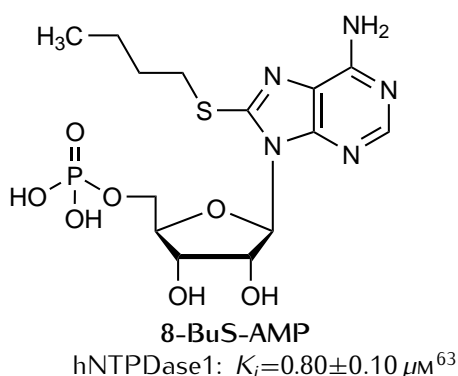
Polyoxometalates (POMs) like PSB-POM142 are anionic complexes that contain transition metal ions, such as tungsten, molbdenum, or vanadium, which are bridged by oxygen atoms.⁶⁸ These compounds are relatively stable and some of them are water-soluble at physiological pH.⁶⁸ Nevertheless, these compounds have a high molecular weight and they bear a lot of negative charges, which might restrict their pharmaceutical use because they could not be orally applied.⁶⁸ It was shown that polyoxometalates (POMs) exert different biological effects including anti-cancer, anti-bacterial, anti-protozoal, ant-viral, and anti-diabetic activities.⁶⁸ Although PSB-POM-142 exerts a low nanomolar K_i value against CD39, it is not very selective since it has also nanomolar potency against NTPDase2 and NTPDase3 (Figure 1.7B).⁶⁸

1.2.3.2 Nucleotide-based CD39 inhibitors

The weak competitive NTPDase1 and -3 inhibitor ARL67156 (K_i of $11 \pm 3 \mu\text{M}$ and $18 \pm 4 \mu\text{M}$ respectively), is relatively stable towards hydrolysis because the cleavage site is blocked by replacing the β,γ -oxygen atom of the triphosphate chain by a dibromo-methylene moiety yielding a phosphonate linkage.^{64,65} ARL67156 was shown to inhibit partially the mouse and human forms of NTPDase1 and NTPDase3 but had no effect on NTPDase2, NTPDase8, NPP3 and CD73 at concentrations of 50-100 μM (Figure 1.7A).⁶⁵ Furthermore, in contrast to other NTPDase inhibitors, ARL67156 had no effect on P2 receptors.³⁶ Although its K_i value is only modest, ARL67156 represents a good lead structure for the development of a potent, subtype-specific NTPDase1 inhibitor.

In 2000, 8-butylthio-ATP (8-BuS-ATP) was found to be the most potent competitive NTPDase1 inhibitor out of a series of C2- or C8-thioether-ATP derivatives.⁶⁶ In this series, the thioether side chain was varied in length, including ethyl to butyl and hexyl, and in bulkiness, from ethyl to cycloheptyl and *tert.*-butylmethylene.⁶⁶ From this series, 8-BuS-ATP was found to be almost completely resistant to NTPDase hydrolysis in contrast to ATP.⁶⁶ The authors concluded that analogs substituted with electron-donating groups at C8 were more resistant to hydrolysis than the corresponding C2-substituted analogs.⁶⁶ Furthermore, the resistance to the catalytic activity of the enzyme is depending on the nature of the substituent, since some C8-analogs displayed only weak resistance.⁶⁶ By nuclear magnetic resonance (NMR) analysis it was revealed that the C8-analogs prefer the *syn*-conformation, which is probably unfavorable for enzymatic hydrolysis, since the C2-analogs were found to be in the *anti*-conformation.⁶⁶ The authors hypothesized that in the *syn*-conformation the triphosphate chain might be shifted away from the catalytic amino acid residues.⁶⁶ Four C8-analogs were found to have K_i values in a range similar to those of ATP and ADP, but 8-BuS-ATP was the only analog identified as a competitive inhibitor, while the others were found to be non-competitive.⁶⁶ In a follow-up study, 8-BuS-AMP was found to be a subtype-specific NTPDase1 inhibitor that had only modest effects on NPPs and *ecto*-5'-nucleotidase (e5NT) in contrast to its corresponding ATP analog (Figure 1.7A).⁶³ Since the K_i value is already in the low micromolar range, this monophosphate derivative seems to be a promising lead structure for the development of potent, subtype-specific NTPDase1 inhibitors.

A Nucleotide-based inhibitors.



B Non-nucleotide-based inhibitors.

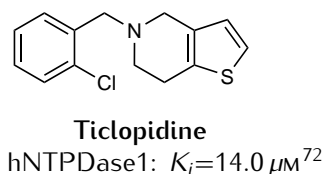
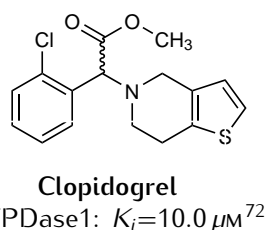
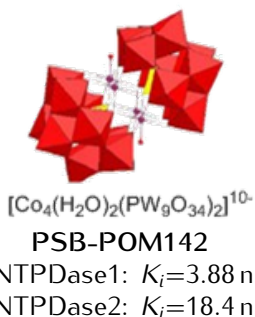
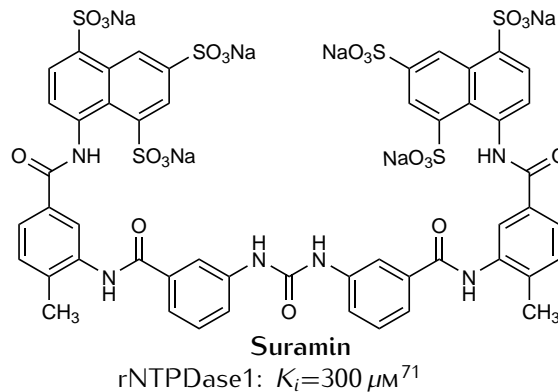
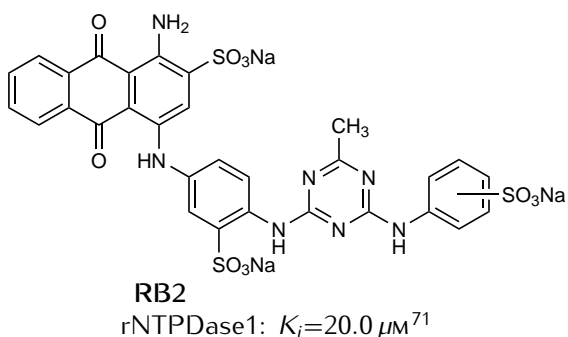
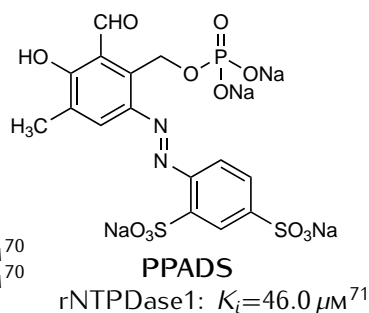
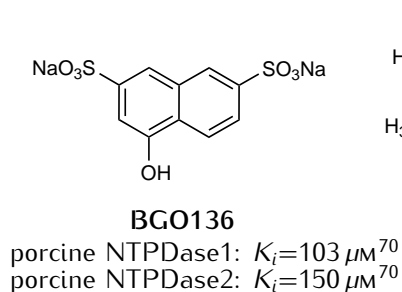
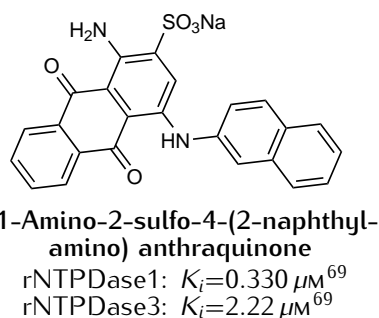


Figure 1.7: Known inhibitors of CD39. Various weak and/or non-selective inhibitors of NTPDases have been described. The corresponding K_i and/or IC_{50} values for CD39 are depicted. h = human. r = rat.

1.3 *Ecto*-5'-nucleotidase

The family of human *ecto*-5'-nucleotidases consists of seven isoenzymes, of which six have exclusively been found intracellularly.²¹ Sequence analysis showed that the membrane-bound *ecto*-5'-nucleotidase (e5NT), also referred to as CD73, can clearly be differentiated from the other six subtypes, which are phylogenetically unrelated and are either located in the cytosol or in the mitochondria. CD73 is a Zn²⁺-binding, glycosylphosphatidylinositol (GPI)-anchored homodimeric protein with a catalytic domain that is facing the extracellular medium.²¹

CD73 is part of the enzyme cascade that metabolizes ATP at physiological pH into adenosine.²¹ Although different ribo- and desoxyribonucleoside monophosphates can be hydrolyzed by CD73, the major substrate is AMP with K_M values in the range of 1-50 μM .²¹ ATP and ADP are competitive inhibitors of CD73 with K_i values in the low micromolar range ($K_i=8.90 \mu\text{M}$ and $K_i=3.38 \mu\text{M}$, respectively).²¹ They can bind to the catalytic site without being hydrolyzed which leads to a feed-forward inhibition. As long as the extracellular levels of tri- and diphosphates are high, the generation of extracellular adenosine will be delayed, until other *ecto*-nucleotidases such as CD39 have reduced the levels of tri- and diphosphates.

CD73 is a well studied *ecto*-nucleotidase which was first cloned from rat, human placenta, and the electric ray fish.²¹ Meanwhile, also the complementary DNA (cDNA) sequences of various other mammalian species have been identified.²¹ For example, the mouse CD73 cDNA is 86% and 92% identical to the human and rat cDNA, respectively. The apparent molecular mass of mammalian e5NT is 60-80 kDa for the monomer and 160 kDa for the dimer.

1.3.1 Pathological role of CD73

CD73 has a broad tissue distribution, and it is expressed by subpopulations of human T and B lymphocytes and also by a variety of tumor cells. The broad tissue distribution contributes to its involvement in various physiological and pathological functions, which are always related to the formation of adenosine by CD73. Adenosine plays a role in epithelial ion and fluid transport, epithelial and endothelial permeability, adaptation to hypoxia, ischemic preconditioning, inflammation, renal function, hypoxia, and platelet function.⁷⁶

Additionally, CD73 might have anti-nociceptive effects. Nociceptors or pain receptors can sense pain as a result of tissue damage. It was found that CD73 is expressed by peptidergic and non-peptidergic nociception (pain sensing) neurons and their axon terminals in spinal cord and spine. Therefore, CD73 can be used in the treatment of chronic pain involving A_1 adenosine receptors, which might have adenosine-dependent antinociceptive effects.⁷⁷

Furthermore, as already mentioned, various tumor cells overexpress CD39 and CD73 leading to increased extracellular anti-inflammatory adenosine levels (*Figure 1.6*).⁵⁵ The resulting activation of the A_{2B} adenosine receptors leads to cancer progression since this process is depending on vasodilatation, angiogenesis, and cytoprotective and immunosuppressive activities. Several studies have indicated that an increase in expression of CD73 is associated with tumor invasiveness and metastasis.⁷⁸ As an example, the expression level of CD73 seems to be associated with a poor prognosis in triple negative breast cancer and CD73 was proposed as a marker for breast cancer progression.^{79,80} "Triple negative" means, that the cancer cells are tested negative for estrogen receptors, progesterone receptors, and human epidermal growth factor receptor 2 (HER2), which means that the cancer will not respond to hormonal therapy or therapies that target the HER2 receptor. In mouse models of triple negative breast cancer, an overexpression of CD73 was correlated to chemoresistance to anthracycline treatment, like doxorubicin for example, due to suppression of an immune response via activation of A_{2A} receptors.⁸⁰ It was shown that targeted blockade of CD73 significantly prolonged the survival of mice with anthracycline-resistant metastatic breast cancer.⁸⁰

In summary it can be concluded that CD73 is an interesting drug target, and it is important to develop tool compounds to further investigate its (patho)physiological roles, e.g., in the context of the immune system *in vivo* and *in vitro*.

1.3.2 Crystal structure of CD73

CD73 functions as a noncovalent dimer and can exist in an open and in a closed conformation, and has been crystallized in both forms (*Figure 1.8*).

In total, five X-ray structures of the human CD73 have been resolved including two in complex with adenosine and two with inhibitors in an open conformation, as well as one in complex with α,β -methylene-ADP (AOPCP) in the closed conformation.⁸¹

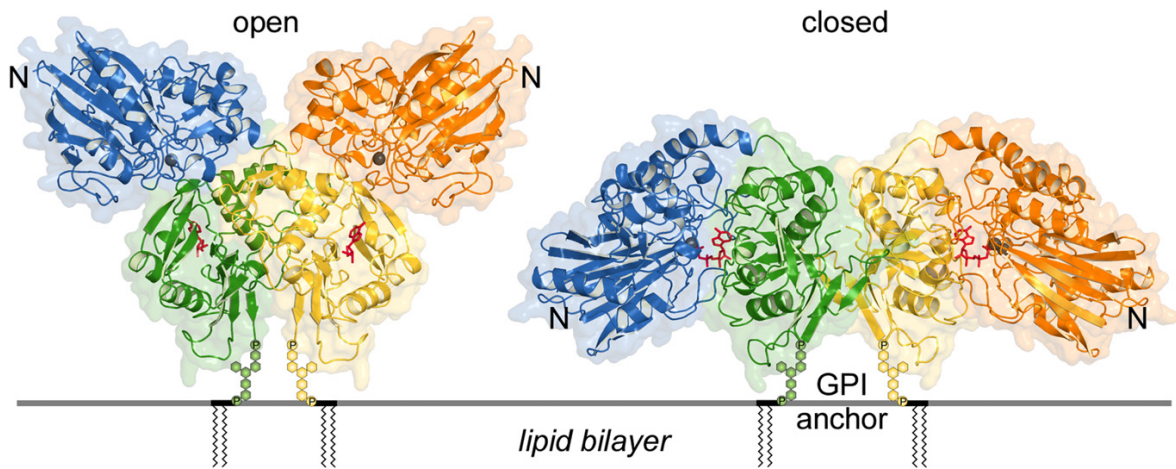


Figure 1.8: Crystal structure of human *ecto-5'-nucleotidase*. CD73 in an open conformation (left), and a closed conformation (right). The N- and C-terminal domains of one subunit of the dimer are shown in blue and green, respectively. The N- and C-terminal domains of the adjacent subunit are shown in orange and yellow, respectively. Ligands (adenosine and adenosine-5'-*O*-[(phosphonomethyl)phosphonic acid] (AOPCP) in the open and closed forms, respectively) are shown as red sticks while the metal ions are shown as gray spheres. Schematic representations of GPI anchors and the cell membrane are also shown. This figure was taken from [81].

CD73 is embedded in the membrane via a GPI anchor which is attached to serine-523 in the hydrophobic C-terminus, a residue that is conserved in all species.²¹ The C-terminal domain contains binding sites for the base and ribose moieties of the nucleotide substrates and is therefore responsible for substrate specificity.^{21,81} Furthermore, it contains the dimerization interface.⁸¹ Its structure is unique and has not been described in other proteins so far.²¹ In contrast to that, the N-terminal domain is related to the calcineurin superfamily of metallophosphatases, and it binds two metal ions (Zn^{2+}), which are important for the phosphohydrolase activity of the enzyme.^{21,81}

The N-terminal domain is attached to the C-terminus via an α -helix that contains a small hinge region, which enables the enzyme to undergo large domain movements and thereby switch between the open and closed conformations.⁸¹ Based on the crystal structures, it seems that the C-termini of the dimer both face the membrane and that the N-terminal domains extend into the extracellular space, where they can rotate freely to switch between the open and closed conformation. This implicates, that a large amount of water molecules needs to be displaced during domain movements.⁸¹ The active site is located in a space between the two domains and is therefore formed from residues of both domains.⁸¹ In the open form, the binding

pocket is accessible for the substrate to bind and the resulting cleavage product to leave.

It was found that adenosine is bound more than 17 Å away from the di-metal site.⁸¹ The nucleobase was found to be sandwiched between the side chains of two phenylalanine residues (F417 and F500) of the C-terminus forming a clamp for the adenosine base via strong hydrophobic π -stacking interactions (Figure 1.9).⁸¹ Adenosine is further positioned by hydrogen bonds between the ribose moiety and side chains of various arginine and aspartic acid residues (R354, R395, and D506).⁸¹

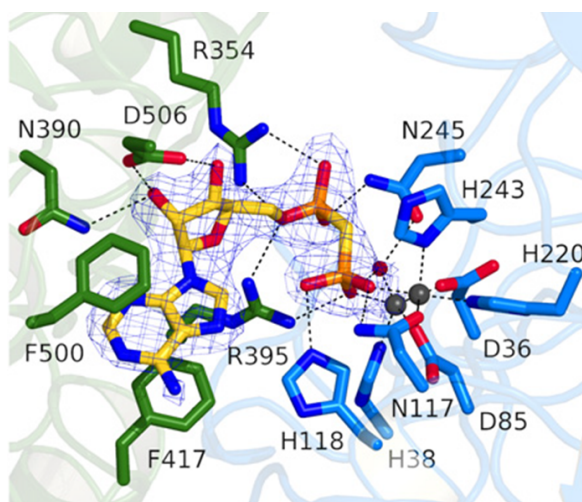


Figure 1.9: Binding mode of AOPCP to CD73. AOPCP bound at the CD73 active site of the closed conformation. The two zinc ions are shown as gray spheres. The protein residues of the C-terminal domain forming the substrate binding site are shown in green whereas the amino acids of the N-terminal domain are depicted in blue. Water molecules, unless coordinating metal ions, are omitted for clarity. The AOPCP omit-electron density map is shown in blue. This figure was taken from [81].

AOPCP is bound in a similar way with additional hydrogen bonds between the α - and the β -phosphonate group and the side chains of several asparagine, arginine, and histidine residues (N245, R354, R395 and N117, H118, R395 respectively).⁸¹ Additionally, the β -phosphonate group coordinates to both metal ions.⁸¹ In summary, this leads to polarization of the β -phosphonate group, which makes it more suitable for nucleophilic attack by water.⁸² A nucleophilic water is presumably coordinated to one of the metal ions, where it is in the perfect position for an in-line attack on the phosphorus atom.⁸³ However, water bridging the two metal ions might also be a possible candidate for the nucleophile.⁸² All in all, the transition state is stabilized by the two metal ions, the arginine and the catalytic histidine.⁸² Since no protein residue is positioned to protonate the leaving group, a water molecule might provide a proton.⁸² It is unclear if the domain rotation is also part of the catalytic cycle for the *ecto*-enzymes.⁸²

1.3.3 Known inhibitors of CD73

CD73 inhibitors have a great potential as novel drugs. Through their action, the extracellular level of adenosine can be reduced, *e.g.* in the tumor micro-environment, leading to the indirect blockage of adenosine P1 receptors. This would prevent the immunosuppressive effects of adenosine, and the tumor might get attacked by an immune response. In this section, the most important CD73 inhibitors described in the literature are presented.

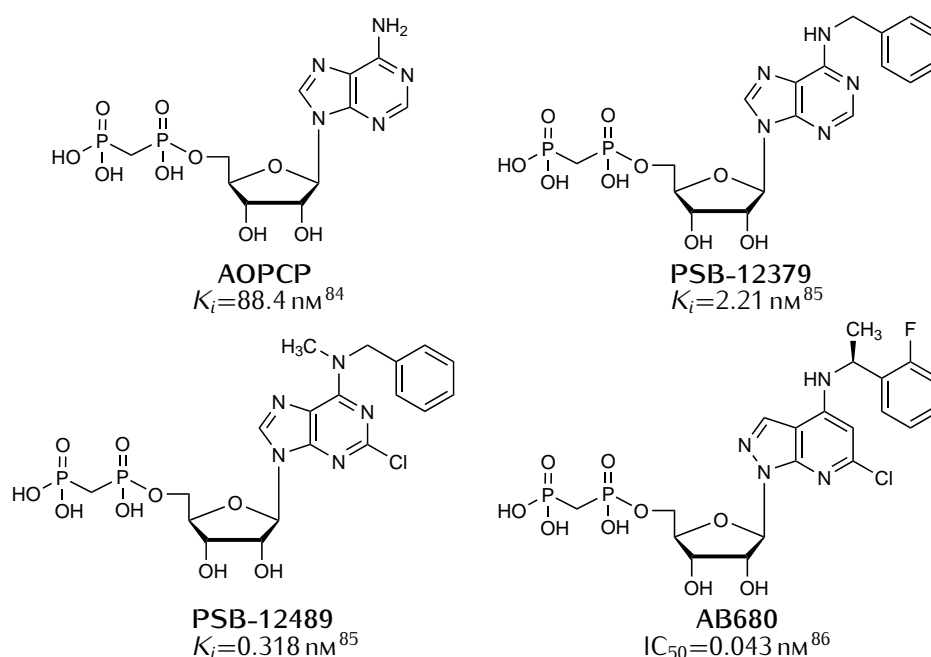


Figure 1.10: Known adenosine-based inhibitors of CD73. Various inhibitors of CD73 based on the structure of adenosine have been described. The corresponding K_i values for human CD73 are depicted.

ADP and ATP are competitive inhibitors of CD73 but are not suitable as drugs, since they are themselves substrates of the cascade of *ecto*-nucleotidases.²¹ In 1965, AOPCP was synthesized, a non-hydrolyzable analog of ADP in which the diphosphate group is exchanged by a diphosphonate group.⁸⁷ It was the first discovered adenine nucleotide-derived inhibitor of CD73 with a K_i value of 88.4 nM at soluble human CD73 (Figure 1.10).^{84,88,89} However, it has also been reported to inhibit NPP1 with a K_i value of 16.5 μM .⁹⁰

50 years after its discovery, a series of AOPCP derivatives was generated to identify potent and selective CD73 inhibitors.⁹¹ Substitution of the N^6 -position resulted in a number of potent CD73 inhibitors with K_i values in the low nanomolar range.

Substitution with benzyl yielded one of the most potent compounds out of this series (PSB-12379, *Figure 1.10*).⁹¹ PSB-12379 has a similar binding mode as AOPCP as revealed by co-crystallization with human CD73 (*Figure 1.11A*).⁹²

In the crystallography studies of PSB-12379 a sub-pocket was observed, which was targeted by chlorination of the C2-position.⁹² Additionally, those crystallography studies suggested a high flexibility of the *N*⁶-benzyl-group of PSB-12379, which was restricted by additional methylation. All together, 2-chlorination and *N*⁶-methylation resulted in the generation of a subnanomolar CD73 inhibitor (PSB-12489, *Figure 1.10*).⁹² Co-crystallization of PSB-12489 with human CD73 showed that chlorine forms a hydrogen bond with the N390 side chain and a water molecule coordinated to the carboxy-group of N499 (*Figure 1.11B*).⁹² Recently, a clinical trial phase I was started with the inhibitor AB680, which was developed based on previous findings by the company Arcus Biosciences *Inc.*^{92–95}

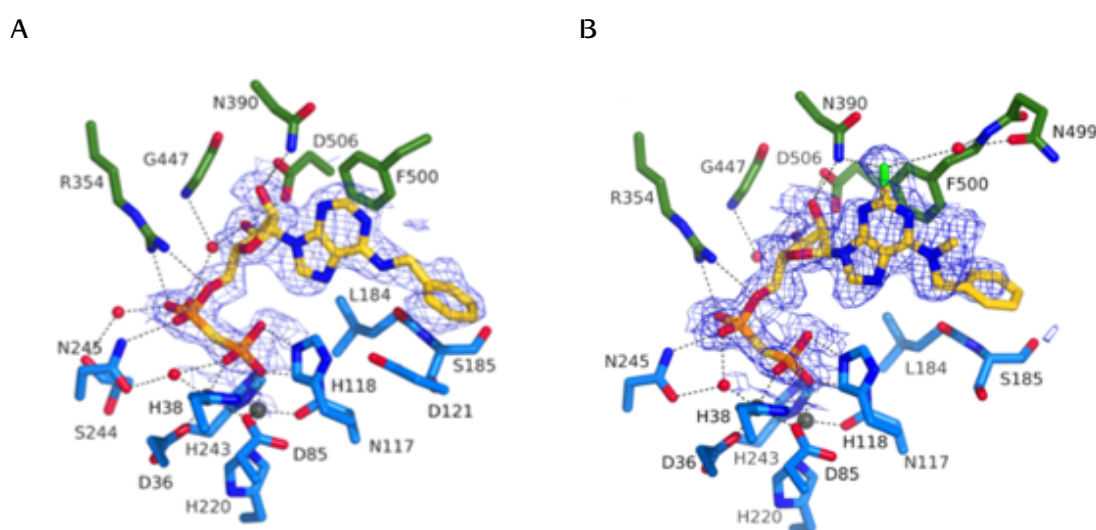


Figure 1.11: Binding modes of AOPCP analogs to human CD73. Co-crystal structures of human CD73 bound to PSB-12379 (A) or PSB-12489 (B) are depicted. The AOPCP derivatives are depicted in yellow. The substrate binding site is formed by the N-terminal (blue) and C-terminal (green) domain. This figure was taken from [92].

Besides Arcus Biosciences *Inc.*, two other companies filed patents with nucleotide mimetics as CD73 inhibitors. Vitae Pharmaceuticals *Inc.* focused on bioisosteric substitutions at the 5'-position as well as different modifications of the adenine base.⁹⁶ They described over 150 exemplary compounds from which 39 had a K_i value below 100 nM.⁹⁶ Calithera Biosciences *Inc.*, described more than 300 nucleotides and

nucleotide mimetic structures that were mainly derived from 2-chloro-2'-deoxy-2'-fluoroadenosine.⁹⁷ The 5'-position was substituted by dicarboxylic acids and different more bulky and lipophilic residues and the potencies were in the nanomolar range.⁹⁷

Next to adenine nucleotide-derived compounds also uracil nucleotide-derived compounds have been described as CD73 inhibitors, like for example the 5,6-dihydrouracil nucleotide mimetic PSB-11532 (Figure 1.12).⁹⁸ These molecules are uracil derivatives linked to a terminal dicarboxylate group via an alkyl linker and amide bonds at the 5'-position. Interestingly, PSB-11532 acts as non-competitive inhibitor at pH 5.6 and as an activator at pH 7.4. These kind of compounds might be used for the development of pH-dependent therapeutics as many tumor cells have lower pH values than normal cells.⁹⁸ However, the most potent antagonist from this class of compounds has only a micromolar potency.

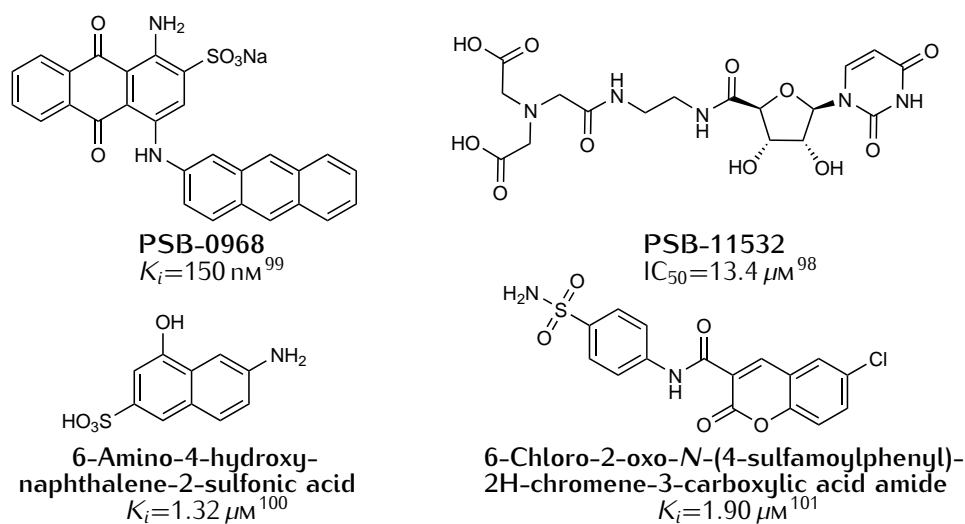


Figure 1.12: Other known inhibitors of CD73. Various inhibitors of CD73 and the corresponding K_i or IC_{50} values for rat CD73 are depicted.

In 2010, another class of CD73 inhibitors was identified by Baqi *et al.*⁹⁹ Anilinoanthraquinone derivatives related to the dye RB2 were found to inhibit CD73 competitively. The most potent compound from this series was PSB-0968 with a nanomolar potency (Figure 1.12). The sulfonate group at position 2 of the anthraquinone scaffold was found to be essential for CD73 inhibitory activity. Furthermore, among a series of different lipophilic substitutions, the anthracenyl substitution at position 4 was identified as an optimal residue, probably due to aromatic stacking interactions with the surrounding aromatic protein residues.⁹⁹

Later, in a structure-based virtual screening approach, new series of compounds were found to inhibit CD73.¹⁰¹ All of these hits contained two moieties. First, a nucleobase-mimicking heterocycle or a substituted benzene ring and second a sulfonamide group. The sulfonamide group probably interacts with a zinc ion present in the active site of the enzyme, and behaves therefore similar to a phosphate or phosphonate group. Out of these group of compounds, 6-chloro-2-oxo-*N*-(4-sulfamoylphenyl)-2H-chromene-3-carboxylic acid amide was identified as the most potent inhibitor of CD73, acting competitively (*Figure 1.12*).¹⁰¹

In 2013, sulfonic acid derivatives were studied as CD73 inhibitors.¹⁰⁰ These compounds showed only moderate potency with 9-amino-4-hydroxy-naphthalene-2-sulfonic acid as the most potent compound with a K_i value of $1.32 \mu\text{M}$. The structure-activity analysis suggests that amino, hydroxyl and sulfonic acid groups all are important for the activity.¹⁰⁰

1.4 Analytical assays

In order to study the potency of compounds at the different *ecto-nucleotidases*, assays are required to determine the enzymatic activity. There are several methods to measure the enzymatic activity of CD39 and CD73, involving luminescent, spectroscopic and chromatographic techniques. In the following sections, the common assay systems used in our group are described.

1.4.1 Malachite green assay

Inorganic phosphate released as a product of the enzymatic reaction can be detected with the malachite green assay, a colorimetric determination method.¹⁰² The assay is easy to handle and inexpensive, which is why it is often used as test system for *ecto-nucleotidases*. The assay is based upon the reaction of released phosphate with ammonium molybdate in the presence of sulfuric acid and malachite green.¹⁰³ Malachite green is a cationic triphenylmethane dye. At $\text{pH} > 2$, the majority of malachite green molecules will be deprotonated with an absorption maximum of $\sim 630 \text{ nm}$ (blue-green solution), whereas at $\text{pH} < 2$, the dye is protonated and the solution has a bright yellow colour.¹⁰⁴ Since the assay is carried out in the presence

of sulfuric acid, the dye will be protonated. However, only the deprotonated form is able to bind the resulting phosphomolybdate complex, which results in an increased blue-green coloring of the solution, depending on the amount of released phosphate (Figure 1.13).

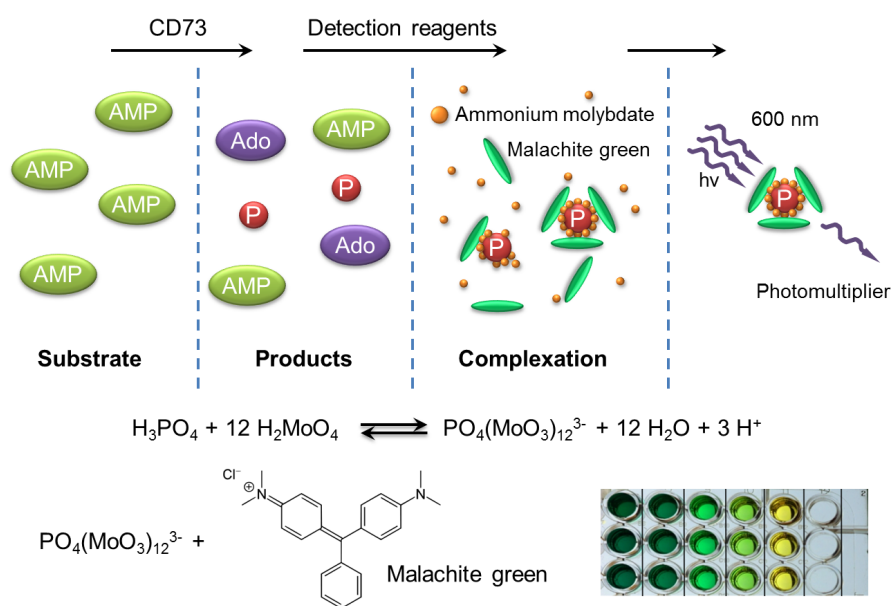


Figure 1.13: Principle of the malachite green assay. Inorganic phosphate is released as the enzymatic reaction proceeds and a phosphomolybdate complex is formed. A malachite green-phosphomolybdate complex is formed changing the color of the solution from bright yellow to blue-green depending on the amount of released phosphate. This figure was taken from [105].

The major drawback of this method is that only colorless compounds can be tested to avoid interference with the colorimetric detection. Furthermore, the assay is not very sensitive with a limit of detection of $1 \mu\text{M}$ phosphate, and is prone to mistakes due to the overall presence of phosphates. Nevertheless, this assay is used in our group for screening purposes since it is fast and high-throughput screening-compatible.

1.4.2 Capillary electrophoresis-UV assay

capillary electrophoresis (CE) is a technique in which charged analytes migrate through electrolyte solutions under the influence of an electric field.¹⁰⁶ Substrate and products can be separated from each other based on their electrophoretic mobility and are then detected by an ultra-violet (UV)-detector. The electrophoretic mobility of each molecule is the result of different mass-to-charge ratios.¹⁰⁷ The

greater the charge and the smaller the molecule, the faster the molecule migrates. By applying the CE assay coupled to a UV detector (CE-UV) assay, dephosphorylation reactions can be quantified by measuring the area under the curve of the substrate and its corresponding products. A schematic representation can be seen in *Figure 1.14*.

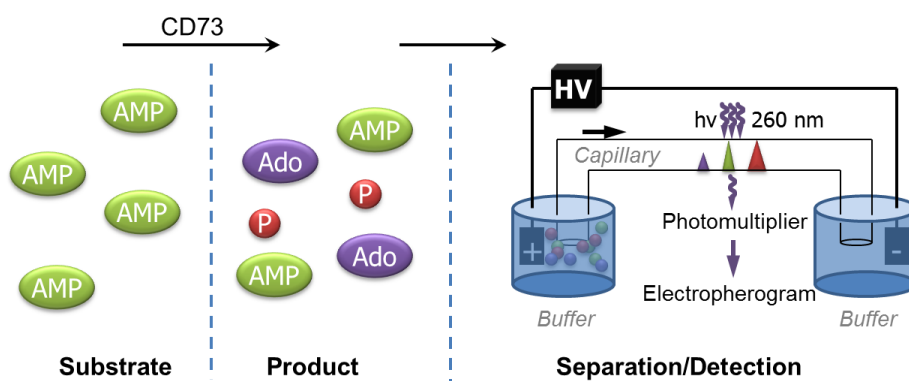


Figure 1.14: Principle of the capillary electrophoresis-UV assay. The CE-device consists of a capillary, two electrodes, a high voltage source (HV) and a detector. After injection of the sample, the inlet and outlet of the capillary are each put into buffered solution and an electric field is applied. Based on their charge, the analytes migrate through the capillary and can be detected and quantified. This figure was taken and modified from [105].

In a buffered solution, the different nucleotides ATP, ADP, and AMP, are present as charged species. Since ATP has the most negatively charged phosphate groups, it is the nucleotide with the fastest elution time and is detected first. Although a clear separation of all nucleotides can be achieved this method has also clear drawbacks. The limit of detection (LOD) is only 200 nM and the limit of quantification 600 nM. The assay is therefore not very sensitive. Furthermore it is a time-consuming method with each run taking around 20 min.

1.4.3 Fluorescence polarization immunoassay

Fluorescence polarization was first described by Perrin in 1923.¹⁰⁸ When a fluorophore is excited with polarized light, the light is emitted back at the same polarization plane, if the molecule does not rotate during excitation. However, if the molecule rotates, the light will be emitted at another polarization plane. The rotation-relaxation time is dependent on the viscosity of the solvent, the temperature, the molecular weight, and the gas constant. If the first two parameters are kept

constant, the fluorescence polarization is proportional to the molecular weight.¹⁰⁹

If vertically polarized light is used for excitation, the intensity of emitted light can be measured in the vertical and horizontal polarization plane, and a polarization value (P) can be calculated as in Eq. 1.4.1.¹¹⁰

$$P = \frac{I_{\text{vertikal}} - I_{\text{horizontal}}}{I_{\text{vertikal}} + I_{\text{horizontal}}} \quad (\text{Eq. 1.4.1})$$

Smaller molecules rotate faster which leads to a depolarization of emitted light in comparison with the excitement plane resulting in small P -values. Bigger molecules rotate slower and the emitted light stays polarized resulting in higher P -values.¹⁰⁹

The principle of fluorescence polarization immunoassay (FPIA) is based on the competition of a fluorescent-labeled molecule and a free non-labeled molecule for the binding to an antibody. The company BellBrook Labs has developed two FPIA assays for the detection of ADP and AMP.^{111,112} The detection reagent consists of a tracer, for example AMP labeled with the Alexa Fluor 688 dye, and an AMP-specific antibody. At first, the tracer is bound to the antibody. With the enzymatic reaction ongoing, non-labeled AMP is produced, which competes with the tracer for antibody binding. The free tracer is smaller than the antibody-bound tracer and therefore rotates faster. This leads to a decrease in fluorescence polarization and smaller P -value with higher AMP production (*Figure 1.15*).¹¹³

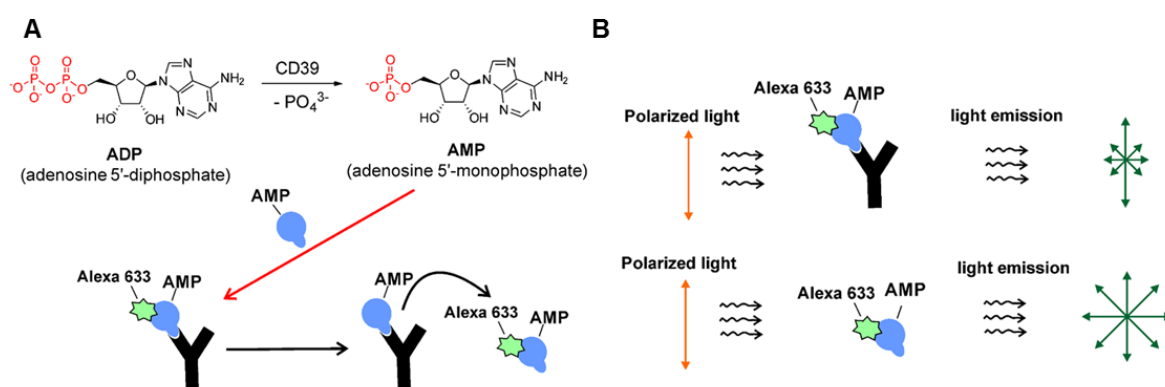


Figure 1.15: Principle of the fluorescence polarization immunoassay. A) Non-labeled AMP is generated by NTPDase1 and competes with labeled AMP. B) The free tracer rotates faster leading to smaller P values. The antibody-bound tracer is bigger and rotates therefore slower resulting in higher P values. This figure was taken and modified from [114].

FPIA is a fast and highly sensitive method ($\text{LOD} = 10 \text{ nM}$) for the detection of enzyme

activity. However, it is also an expensive and complex assay.

1.4.4 Fast fluorescent CE assay

The company Jena Bioscience GmbH (Jena, Germany) developed a fluorescent ATP derivative, N^6 -(6-fluoresceincarbamoyl)hexyl-ATP (FL-6-ATP), in which fluorescein is coupled to ATP via a hexyl linker at the N^6 -position. A new assay system was developed in our group based on the previously described CE-UV method.¹¹⁵ In contrast to the previous method, FL-6-ATP is used as substrate for CD39 and the conversion of FL-6-ATP into N^6 -(6-fluoresceincarbamoyl)hexyl-AMP (FL-6-AMP) is measured by capillary electrophoresis coupled to a laser-induced fluorescence (LIF) detector (*Figure 1.16*).¹¹⁵

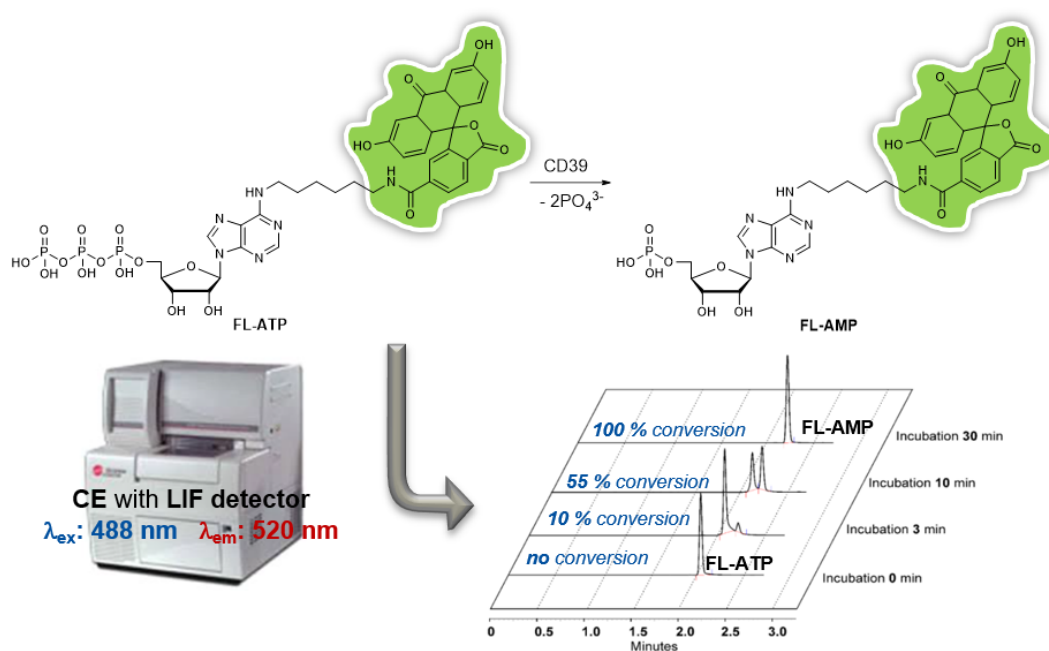


Figure 1.16: Principle of the fast fluorescent CE assay. FL-6-ATP is used as substrate for CD39. The enzymatic activity is related to the amount of FL-6-AMP generated. Substrate and product are separated by CE followed by detection with a LIF detector. This figure was taken and modified from [114].

It has been shown, that ATP and FL-6-ATP have similar K_M values with $11.4 \mu\text{M}$ and $19.6 \mu\text{M}$, respectively, making FL-6-ATP a suitable substrate. Furthermore, docking with the homology model of CD39 was performed, revealing that the enzyme contains a hydrophobic pocket near the natural ligand binding site in which the linker and the

fluorescein-tag fit perfectly (*Figure 1.17*).¹¹⁵ This might explain the similar enzyme kinetics for ATP and FL-6-ATP.

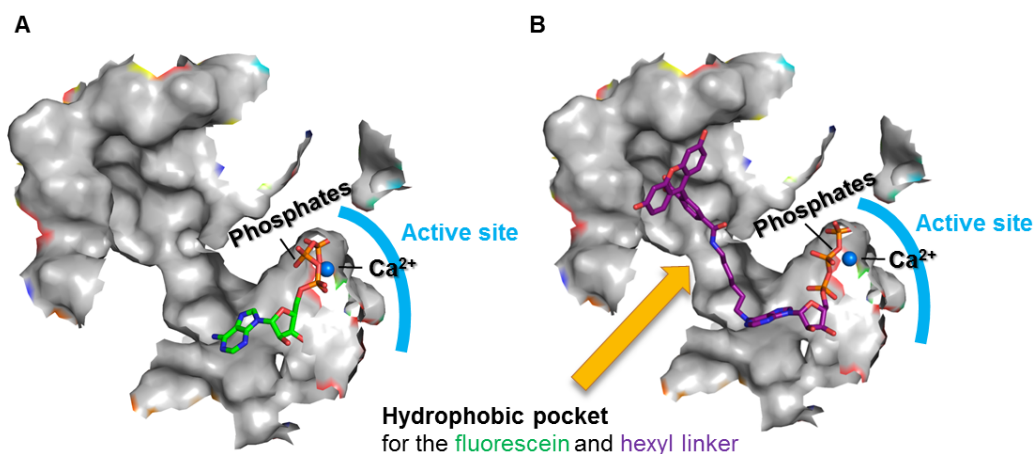


Figure 1.17: Molecular docking with ATP (A) and FL-ATP (B). This figure was taken and modified from [115].

The newly developed assay is highly sensitive with a limit of detection of 21.0 pM and a limit of quantification of around 65 pM.¹¹⁵ Although the assay is 8000-fold more sensitive than the CE-UV assay, it is still time-consuming. Furthermore, it is also expensive due to the costs of the required fluorescent substrate. Nevertheless, the assay is ideal for hit validation at CD39.

1.4.5 Radiometric assay

The radiometric assay is a highly sensitive CD73 assay method that was developed in our group a few years back.⁸⁴ In this assay, radio-labeled [2,8-³H]-adenosine-5'-monophosphate is used as a substrate. During the enzymatic reaction it is converted into [2,8-³H]adenosine. In order to quantify the amount of product formed, substrate and product need to be separated from each other. This can be achieved by precipitation of remaining substrate with lanthanum chloride. In the presence of sodium phosphate in an acidic milieu, this gives an insoluble salt whereas [2,8-³H]adenosine remains soluble in water. After filtration through glass fiber filters, filtrates are poured into scintillation vials containing the scintillation cocktail followed by quantification using scintillation counting (*Figure 1.18*).

Advantages of the assay include a very low limit of detection of 0.03 μM for adenosine,

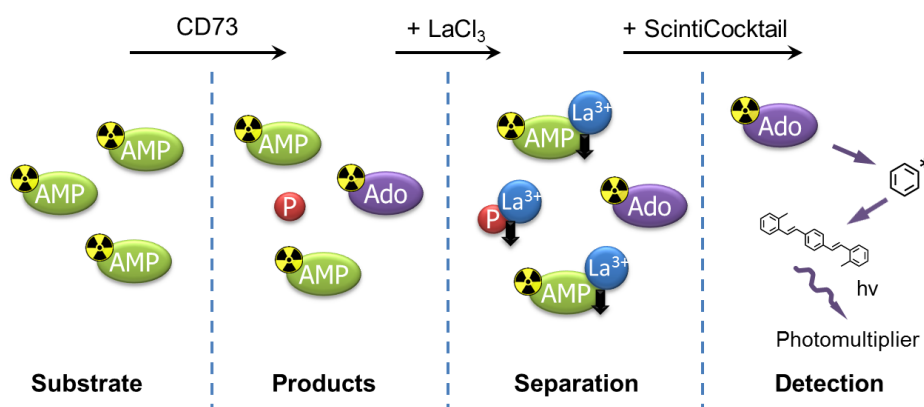


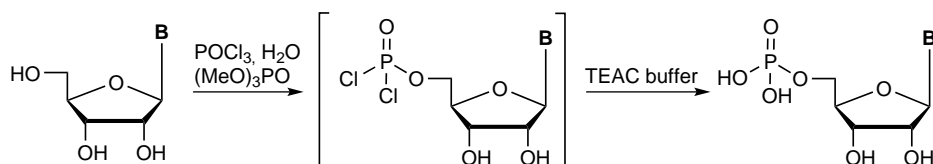
Figure 1.18: Principle of the radiometric assay. [2,8-³H]adenosine-5'-monophosphate CD73. The enzymatic activity is related to the amount of [2,8-³H]adenosine generated. Substrate and product are separated by precipitation and filtration followed by quantification of the product using scintillation counting. This figure was taken from [116].

suitability for high-throughput screening, and the absence of interference by colored compounds or inorganic phosphate. This assay was applied for the biological testing at CD73.

1.5 Synthesis of nucleotides

1.5.1 Monophosphorylation

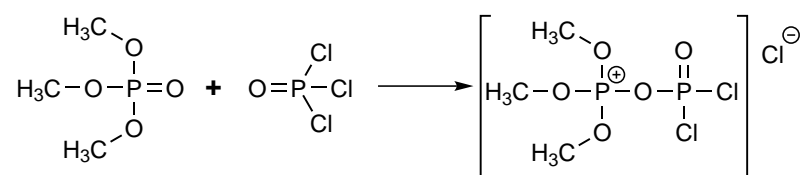
Nucleosides can be phosphorylated via different approaches. The most common method for selective monophosphorylation is the so called *Yoshikawa procedure*.¹¹⁷ In this one-pot-two-step procedure, the reaction of nucleoside with phosphoryl chloride (POCl_3) is facilitated by the use of trialkyl phosphate as a solvent, yielding a 5'-phosphorodichloridate intermediate (*Scheme 1.1*).



Scheme 1.1: The Yoshikawa procedure. Reaction of nucleoside with phosphoryl chloride will result in the formation of the reactive 5'-dichlorophosphate intermediate. The nucleoside monophosphate is generated by hydrolysis with triethylammonium hydrogencarbonate buffer (TEAC) buffer.

B = nucleobase.

The use of trialkyl phosphates as solvent has two advantages. First, nucleosides and phosphorylating agents are soluble in trialkyl phosphates leading to homogeneous solutions.¹¹⁸ Second, it is hypothesized that trialkyl phosphates and phosphoryl chloride are able to interact with each other thereby forming an active intermediate comparable to the complex formed between dimethylformamide (DMF) and phosphoryl chloride (*Scheme 1.2*).^{118,119}

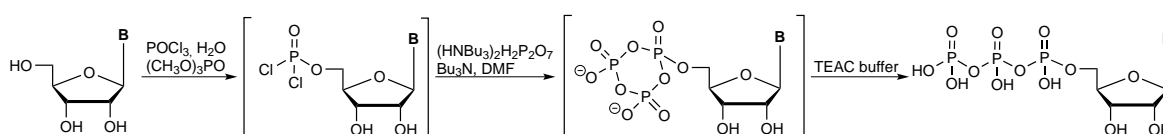


Scheme 1.2: Complex formation between trimethyl phosphate and phosphoryl chloride.

The 5'-nucleotide is obtained by rapid hydrolysis of the 5'-phosphorodichloridate intermediate. At first, Yoshikawa and colleagues used protected nucleosides for phosphorylation, but later on they discovered that selective monophosphorylation was possible when the phosphorylating agent was first treated with small amounts of water.^{117,120} It was reported that an acidic medium was required to prevent 2'- and 3'-*O*-phosphorylation, and addition of water led to the formation of hydrogen chloride.^{117,118,120} Kovács *et al.*, however, discovered that in the case of modified nucleobases containing unsaturated side chains, the presence of hydrogen chloride can lead to undesired side reactions.¹²¹ To prevent this, a base, 1,8-bis-(dimethylamino)naphthalene (proton sponge), was added to neutralize the generated hydrogen chloride, which had also the beneficial effect of accelerating the phosphorylation reaction.¹²¹ 1,8-Bis(dimethyl)naphthalene is a very strong base but at the same time a weak nucleophile, and is therefore called *proton sponge*.¹²² Due to the positive effect of the proton sponge on the reaction time, it is commonly used for monophosphorylation, also in the absence of unsaturated side chains.¹²³ Phosphorylation reactions according to the Yoshikawa procedure were also conducted in other solvents than trialkyl phosphates, *e.g.* 2-chlorophenol.^{118,124,125} Although some reactions showed high selectivity, these are not as widely used as reactions with trialkyl phosphates.

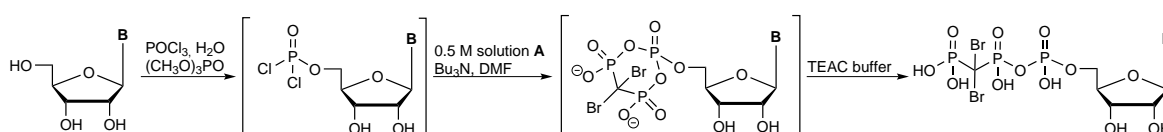
1.5.2 Triphosphorylation

The nucleophilic attack of phosphonato phosphate on an activated nucleoside is an efficient way to synthesize nucleoside triphosphates. One example of this approach is the extension of the Yoshikawa procedure, also called the *Ludwig procedure*, where the intermediate is not hydrolyzed but reacted with bis-tris-*N*-butylammonium phosphonato phosphate in anhydrous DMF (*Scheme 1.3*).¹²⁶



Scheme 1.3: Triphosphorylation via nucleophilic attack of phosphonato phosphate on an activated nucleoside. B = nucleobase.

Of course it is also possible to react the intermediate with a modified phosphonato phosphate solution, like for example tris-*N*-butylammonium-dibromomethylenebisphosphonate in anhydrous DMF, in order to synthesize compounds like ARL67156 that contain a β,γ -dibromomethylene bridge (*Scheme 1.4*).



Scheme 1.4: Synthesis of triphosphates containing a P_{β} - P_{γ} -dibromomethylene bridge. B = nucleobase. Solution A = tri-*N*-butylammonium dibromomethylenebisphosphonate solution in anhydrous DMF.

1.5.3 Diphosphorylation

Nucleosides can also be diphosphorylated. One way to achieve this is an intermediate method between the Yoshikawa procedure for monophosphorylation and the Ludwig procedure for triphosphorylation.^{117,121,126,127} The 5'-phosphorodichloridate intermediate is reacted with bis(tri-*N*-butylammonium) phosphate instead of the phosphonato phosphate followed by hydrolysis.

Another method to diphosphorylate a nucleoside is to use methylenebis(phosphonic dichloride), which is a similar reagent to phosphoryl chloride. Due to the central methylene group in methylenebis(phosphonic dichloride) the phosphorus centre is more electrophilic.¹²⁸ Therefore, methylenebis(phosphonic dichloride) is not only

more bulky but also more reactive than phosphoryl chloride. The phosphonylation reaction is carried in two steps (*Figure 1.19*). First, nucleosides or protected nucleosides are phosphonylated using methylenebis(phosphonic dichloride) leading to the formation of the 5'-[(phosphonomethyl)phosphonic dichloride] intermediate.¹²⁸ Second, rapid hydrolysis of the highly unstable intermediate with TEAC buffer will yield the desired α,β -methylene ADP (AOPCP) derivative.

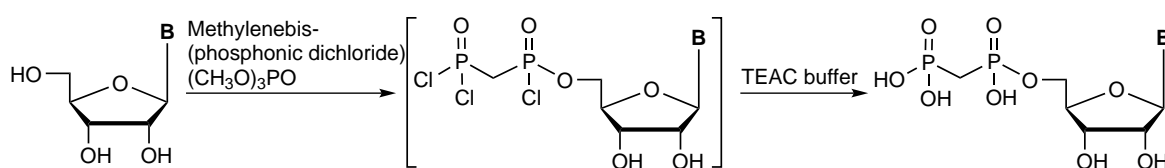


Figure 1.19: Diphosphonylation of nucleosides using methylenebis(phosphonic dichloride). Reaction of nucleoside with methylenebis(phosphonic dichloride) will result in the formation of the reactive 5'-[(phosphonomethyl)phosphonic dichloride] intermediate. Subsequent hydrolysis will give the nucleotide diphosphate. B = nucleobase.

During phosphonylation of nucleosides with methylenebis(phosphonic dichloride) there is a risk of 2'- and 3'-phosphorylation (II & III) in addition to the desired 5'-phosphorylation (I) (*Figure 1.20*). Apart from that, there is also a high risk of the formation of the nucleoside-3',5'-cyclomethylenebis(phosphonic acid) (IV) and the dinucleoside bisphosphonic acid (V). To avoid the formation of these side products, the reaction time needs to be carefully controlled.

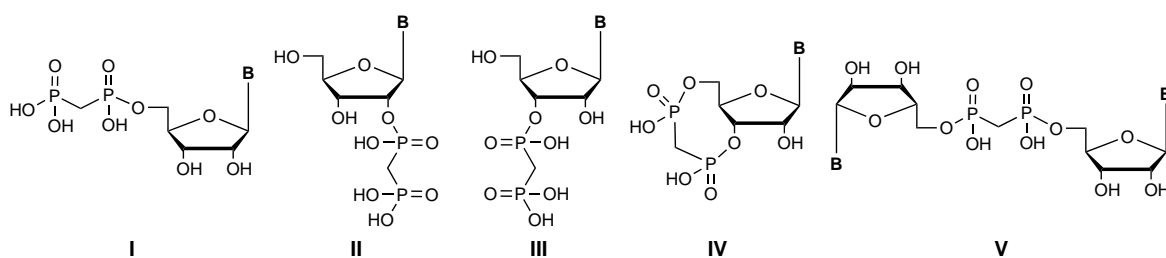


Figure 1.20: Possible phosphorylation products of nucleosides using methylenebis(phosphonic dichloride). I) 5'-phosphorylation, II) dinucleoside bisphosphonic acid, III) 2'-phosphorylation, IV) 3'-phosphorylation, and V) nucleoside-5',3'- cyclomethylenebis(phosphonic acid). B = nucleobase.

2 Aims of the study

2.1 Development of novel inhibitors for CD39

Although crystal structures of multiple NTPDases have been resolved and a catalytical mechanism has been proposed, no potent and selective inhibitors for CD39 are currently available. A wide range of non-selective CD39 inhibitors are known, which often show ancillary inhibition of other *ecto*-nucleotidases such as CD73. Due to its pathophysiological role, CD39 represents a potential drug target that requires further validation. For this purpose, potent, selective and metabolically stable inhibitors need to be identified, which represents the first objective of this thesis.

As already mentioned, 8-BuS-AMP was found to be an inhibitor of CD39 that had only modest effects on NPPs and CD73.⁶³ Since its K_i value at CD39 is in the low micromolar range, this nucleoside monophosphate may be a promising lead structure for the development of a potent, subtype-specific CD39 inhibitor. Therefore, a library of AMP derivatives was synthesized with modifications at the C2-, C8- and/or N^6 -position.

8-BuS-AMP and ARL67156 are promising lead structures whose structure-activity relationships as CD39 inhibitors are underexplored.

2.2 Synthesis of inhibitors and tool compounds for CD73

CD73 has become an important drug target for the immunotherapy of cancer. To fully explore its potential, also in the context of inflammatory diseases, we plan to design, develop, and synthesize various tool compounds.

2.2.1 Upscaling of the synthesis of AOPCP derivatives for *in vivo* testing of CD73 inhibitors

For a collaboration project, two AOPCP derivatives, PSB-12379 and PSB-12489, will be resynthesized on a larger scale to allow *in vivo* studies.

2.2.2 Development of a radioligand for CD73

In the past, very potent and selective inhibitors of CD73 have been developed based on the structure of AOPCP.^{91,92} Based on these results, a radioligand will be developed. First, different AOPCP-derived cold ligands will be synthesized and evaluated in biological assays. Then, a precursor for a hot ligand will be generated, which will be radioactively labeled by hydrogenation with radioactive tritium gas

2.2.3 Development of a fluorescent probe for CD73

Besides a radioligand, a fluorescent probe for CD73 is to be developed. For this purpose, 2-chloro-*N*⁶-benzyl-AOPCP (PSB-12651) will be used as a lead structure. In the *para*-position of the benzyl ring, a dye will be attached via a linker. Different types of dyes, fluorescein, cyanine, and boron-dipyrromethene (BODIPY), could be of interest. Since fluorescein is commercially available for a reasonable price, the proof-of-concept study will be done by introducing fluorescein. Flow cytometry will be used to compare the fluorescent small molecule probe with that of an established anti-CD73 antibody. Later on, when the synthetic route is established and the linker is optimized, probes containing various other dyes can be generated to provide a broad spectrum of fluorescent-labeled compounds with different properties.

2.2.4 Development of a PET-tracer for CD73

Positron electron tomography (PET) is an important method for the diagnosis of diseases *e.g.* in the field of oncology. CD73 is a biomarker for stem cells, undifferentiated cancer cells and inflamed tissues, and it would be highly desirable to have a radiotracer for CD73 to further investigate its biological role, and for use as a diagnostic tool. Therefore, 2-chloro-*N*⁶-benzyl AOPCP (PSB-12651) was chosen as

a starting point to develop and synthesize a ^{18}F -labeled AOPCP-derived inhibitor for CD73. At first, a cold tracer will be synthesized to evaluate its inhibitory potency followed by the synthesis of a precursor, which will be radioactively labeled with ^{18}F (*in collaboration*).

2.2.5 7-Deaza-AOPCP derivatives as novel CD73 inhibitors

AOPCP was the first discovered adenine nucleotide-derived inhibitor of CD73 with a K_i value of 197 nM.^{84,89} Recently, it was published that 7-deaza-AOPCP displays a two-fold higher inhibitory potency than AOPCP at the rat enzyme.¹²⁹ Therefore, the idea was born to elucidate the structure-activity relationships of this compound class further by generating a selection of 7-deaza-AOPCP derivatives.

3 Results and discussion - Part I:

Development of novel inhibitors for CD39

The first objective of this thesis is the evaluation of the SARs and the identification of potent, selective, and metabolically stable inhibitors for CD39. In this chapter, the synthesis of various ARL67156- and 8-BuS-AMP-derivatives will be described in addition to the pharmacological evaluation of those.

3.1 Synthesis of adenosine derivatives

8-BuS-AMP and ARL67156 are the only compounds in their class of compounds described so far. Except for some ATP derivatives, no other monophosphate or β,γ -dibromomethylene-triphosphate derivatives have been studied as CD39 inhibitors, yet.⁶⁶ Therefore, the structure-activity relationships of these classes of compounds have not been thoroughly evaluated. For this purpose, different modifications will be introduced at the adenine base (blue) and the phosphate chain (green) as indicated in *Figure 3.1*. In this chapter, the synthesis of the corresponding adenosine derivatives will be described.

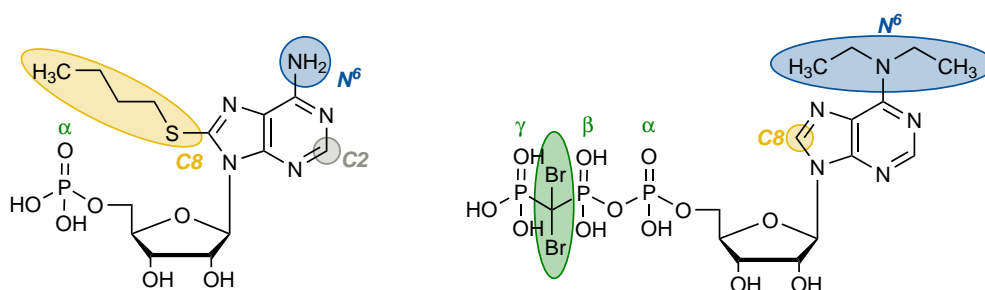
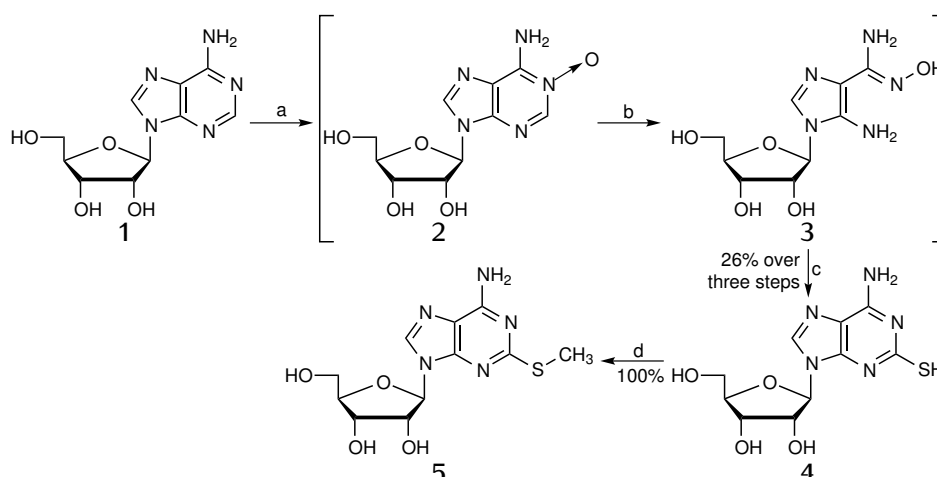


Figure 3.1: Modification places of the 8-BuS-AMP- and ARL67156-scaffolds.

3.1.1 Modification of adenosine at the C2-position

The first position that will be studied is the C2-position. Therefore, various C2-adenosine derivatives were synthesized.

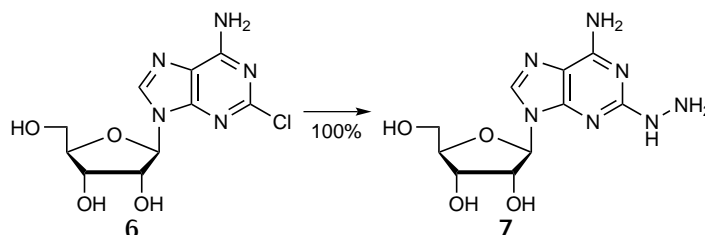
At first, 2-methylthioadenosine (**5**) was synthesized from the intermediate 2-thioadenosine (**4**), which was obtained via a three-step procedure. Adenosine (**1**) was oxidized by hydrogen peroxide in acetic acid (*Scheme 3.1*). Activated carbon was used to remove excess peroxide yielding the *N*¹-oxide (**2**).¹³⁰ Ring-opening (**3**) was achieved using sodium hydroxide followed by neutralization with HCl and removal of the formed sodium chloride yielding an amber-coloured gum-like material, which was used without further purification.¹³⁰ Treatment with a mixture of carbon disulfide, methanol, and water at 120°C in an autoclave gave compound **4**. Subsequent alkylation of **4** with iodomethane in the presence of sodium hydroxide in water, yielded 2-methylthio-adenosine (**5**).¹³¹



Scheme 3.1: Synthesis of C2-substituted adenosine derivatives. Reagents and conditions: a) H₂O₂, acetic acid, 50°C, overnight. b) 5 M NaOH (aq), reflux, 15 min. c) CS₂, methanol, H₂O, 120°C autoclave, 5 h. d) iodomethane, H₂O/EtOH 1:1, NaOH.

Next to 2-methylthioadenosine (**5**), also 2-hydrazinyladenosine was synthesized (*Scheme 3.2*). The reaction of commercially available 2-chloroadenosine (**6**) with hydrazine hydrate at room temperature followed by purification by silica gel column chromatography afforded compound **7** in quantitative yield (*Scheme 3.2*).¹³²

The structures of the synthesized nucleosides were confirmed by ¹H- and ¹³C-NMR spectroscopy (Table 3.1 and Table 3.2), in addition to HPLC analysis coupled to electrospray ionization mass spectrometry (LC/ESI-MS).



Scheme 3.2: Synthesis of 2-hydrazinyladenosine (7). Reagents and conditions: hydrazine hydrate, 10 h, room temperature.

Table 3.1: $^1\text{H-NMR}$ data of C2-substituted adenosine derivatives. Shifts (δ) in DMSO-d_6 [parts per million (ppm)]. Next to the signals of the substituents, a selection of characteristic ribose and purine protons is depicted.

Compound	Substituents	C'1-H	C'5-H ₂	C2-H	C8-H	C2-substituents
4	2-thio	5.75	3.64-3.52	-	8.21	11.90 (SH)
5	2-methylthio	6.09	3.63-3.51	-	8.21	2.46 (SCH ₃)
7	2-hydrazinyl	5.77	3.65-3.52	-	7.93	7.21 (NH) 6.82 (NH ₂)

Table 3.2: $^{13}\text{C-NMR}$ data of C2-substituted adenosine derivatives. Shifts (δ) in DMSO-d_6 [ppm]. Next to the signals of the substituents, a selection of characteristic ribose and purine carbons is depicted.

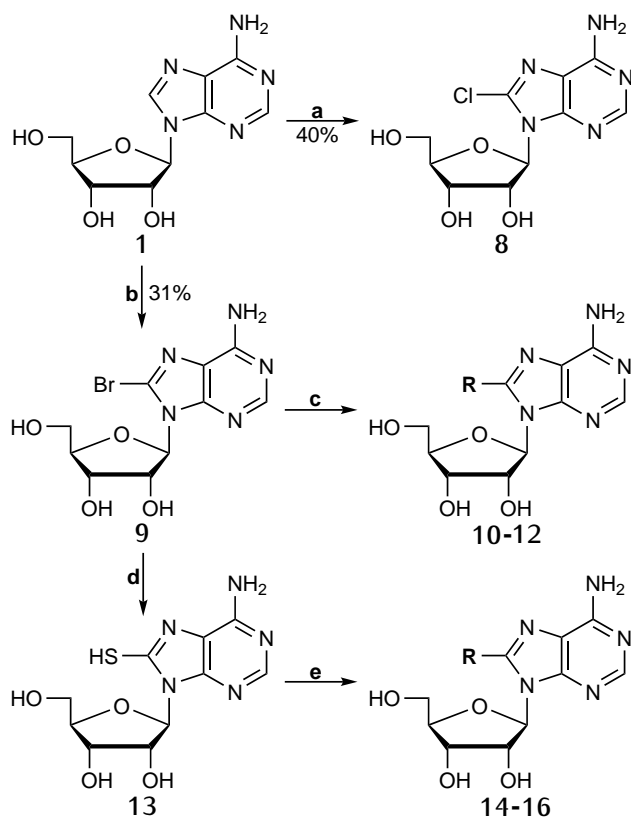
Compound	Substituents	C'1	C'5	C2	C8	C2-substituents
4	2-thio	87.20	61.58	161.60	139.82	-
5	2-methylthio	87.5	61.78	164.28	138.39	13.80
7	2-hydrazinyl	87.27	61.85	156.4	136.76	-

3.1.2 Modification of adenosine at the C8-position

8-BuS-AMP was identified as selective inhibitor of CD39 but with only moderate potency. In order to identify more potent inhibitors, analogs of 8-BuS-AMP were synthesized by changing the substitution at the C8-position.

In order to obtain C8-substituted adenosine derivatives, 8-bromoadenosine (**9**) was required as starting material. For this purpose, adenosine (**1**) was halogenated under acidic conditions using bromine (Scheme 3.3).^{91,133} The pH of the reaction was maintained by 0.1 M sodium acetate buffer pH 4.0. Excess bromine was removed by sodium bisulfite, and neutralization with NaOH followed by filtration afforded compound **9**.

The adenosine derivatives **10-12** were obtained by the reaction of **9** with the corresponding alkylamine in the presence of a base in ethanol (1:3) (Scheme 3.3).^{91,134,135} The addition of water was proven to be essential to obtain a homogeneous solution.



	-R	Yield
10	-NHCH ₃	89%
11		54%
12	-NH(CH ₂) ₃ CH ₃	100%
14	-SCH ₃	80%
15	-S(CH ₂) ₃ CH ₃	76%
16		30%

Scheme 3.3: Synthesis of C8-substituted adenosine derivatives. Reagents and conditions: a) benzoyl chloride, *meta*-chloroperoxybenzoic acid (mCPBA), DMF, 20 min, room temperature. b) bromine, sodium acetate buffer, pH 4.0, room temperature, overnight. c) alkylamine, Et₃N, H₂O/EtOH (1:3), reflux, 7-36 h. d) thiourea, EtOH, 1 h, reflux or NaSH, DMF, 100°C, 10 h. e) alkylhalide, H₂O/EtOH (1:1), NaOH.

If **9** was not dissolved completely, the reaction did not proceed.

The reaction of **9** with thiourea in ethanol gave the intermediate 8-thioadenosine (**13**), which was subsequently alkylated using the corresponding alkyl halide in a mixture of water and ethanol (1:1) and in the presence of sodium hydroxide yielding the compounds **14-16** (Scheme 3.3).^{91,123,131,136} Alternatively, **13** could also be obtained via the reaction of **9** with sodium hydrosulfide in DMF at 100°C.¹³⁷

Different approaches were tried to synthesize 8-chloroadenosine (**8**). Chlorination of **9** using *N*-chlorosuccinimide in DMF gave **8** in a mixture with **9**, and attempts to purify **8** by column chromatography or high performance liquid chromatography (HPLC) failed.⁹¹

Table 3.3: $^1\text{H-NMR}$ data of C8-substituted adenosine derivatives. Shifts (δ) in DMSO-d_6 [ppm]. Next to the signals of the substituents, a selection of characteristic ribose and purine protons is depicted.

Compound	Substituent	C'1-H	C'5-H ₂	C2-H	C8-substituents
8	8-chloro	5.85	3.67-3.52	8.20	-
9	8-bromo	5.83	3.67-3.51	8.11	-
10	8-methylamine	5.84	3.63	7.88	6.88 (NHCH ₃) 2.87 (NHCH ₃)
11	8-(4-phenyl)butylamine	5.88	3.61	7.87	7.25 (aryl) 7.19 (aryl) 7.15 (aryl) 6.89 (NHCH ₂) 2.60 (CH ₂ -aryl) 1.61 ((CH ₂) ₂)
12	8-butylamine	5.89	3.37-3.28	7.87	6.83 (NHCH ₂) 3.62 (NHCH ₂) 1.56 (CH ₂) 1.34 (CH ₂) 0.9 (CH ₃)
13	8-thio	6.33	3.65-3.49	8.11	12.52 (SH)
14	8-methylthio	5.72	3.52-3.66	8.04	2.71 (SCH ₃)
15	8-butylthio	5.77	3.68-3.50	8.04	3.32-3.27 (SCH ₂) 1.68 (CH ₂) 1.41 (CH ₂) 0.90 (CH ₃)
16	8-(5-methyl)hexylthio	5.77	3.66-3.51	8.04	3.28 (SCH ₂) 1.67 (CH ₂) 1.49 (CH(CH ₃) ₂) 1.39 (CH ₂) 1.16 (CH ₂) 0.84 (CHCH ₃) 0.83 (CHCH ₃)

Table 3.4: ^{13}C -NMR data of C8-substituted adenosine derivatives. Shifts (δ) in DMSO- d_6 [ppm]. Next to the signals of the substituents, a selection of characteristic ribose and purine carbons is depicted.

Compound	Substituent	C'1	C'5	C2	C8	C8-substituents
8	8-chloro	89.46	62.10	151.67	137.55	-
9	8-bromo	90.55	62.25	155.29	127.26	-
10	8-methylamine	86.65	61.79	152.68	148.48	29.24 (SCH ₃)
11	8-(4-phenyl)butylamine	86.55	61.87	152.46	148.60	142.39 (aryl), 128.48 (aryl), 128.42 (aryl), 125.82 (aryl), 56.22 (NHCH ₂), 42.27 (CH ₂ - aryl), 35.08 (CH ₂), 28.62 (CH ₂)
12	8-butylamine	86.50	61.80	152.43	148.56	42.19 (NHCH ₂), 31.03 (CH ₂), 19.83 (CH ₂), 13.95 (CH ₃)
13	8-thio	88.95	62.44	152.20	148.18	-
14	8-methylthio	88.89	62.34	154.58	149.84	14.77 (SCH ₃)
15	8-butylthio	89.01	62.36	154.67	184.05	32.22 (SCH ₂), 31.03 (CH ₂), 21.32 (CH ₂), 13.56 (CH ₃)
16	8-(5-methyl)hexylthio	89.03	62.37	150.56	154.69	37.95 (CH ₂ CH), 32.58 (SCH ₂), 29.25 (CH ₂), 27.47 (CH), 25.98 (CH ₂), 22.58 (CH(CH ₃) ₂)

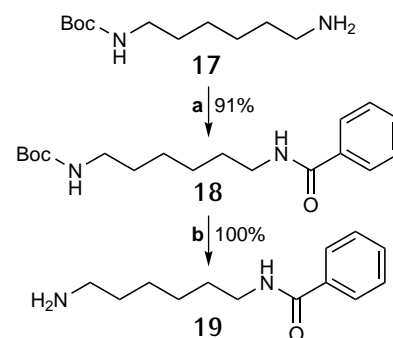
Chlorination of **13** using *N*-chlorosuccinimide in methanol did not lead to product formation at all.^{138,139} Therefore, a third approach was tried, starting from **1**. The reaction with benzoyl chloride and mCPBA in DMF and subsequent purification by column chromatography finally afforded compound **8** in high purity (*Scheme 3.3*).¹⁴⁰ The structures of the synthesized nucleosides were confirmed by ¹H- and ¹³C-NMR spectroscopy (Table 3.3 and Table 3.4), in addition to LC/ESI-MS analysis.

3.1.3 Modification of adenosine at the *N*⁶-position

ARL67156 is an inhibitor of CD39 but with only moderate potency. In order to identify more potent inhibitors, analogs of ARL67156 will be synthesized by changing the substitution at the *N*⁶-position.

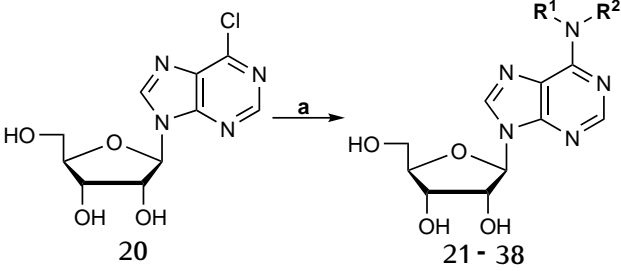
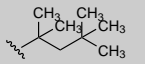
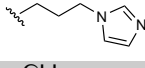
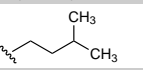
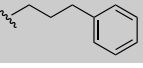
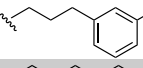
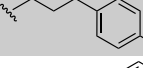
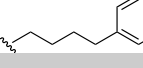
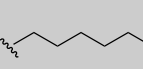
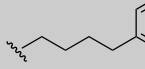
A small library of mono- or di-*N*⁶-alkylated adenosine derivatives was obtained by the reaction of commercially available 6-chloro-9-(β -D-ribofuranosyl)purine (**20**) with the appropriate alkylamine in the presence of triethylamine in absolute ethanol (*Table 3.5*). Purification by silica gel chromatography yielded the desired *N*⁶-substituted adenosine derivatives.⁹¹

Most of the required alkylamines were commercially available but some needed to be generated. For the synthesis of **29**, *N*-(6-aminohexyl)-benzamide (**19**) was obtained in a two-step procedure (*Scheme 3.4*). First, benzoic acid was pre-activated with 1-hydroxybenzotriazole (HOBt) and *N,N'*-dicyclohexylcarbodiimide (DCC) in tetrahydrofuran (THF), followed by the addition of *N*-*tert.*-butyloxycarbonyl (Boc)-protected 1,6-hexanediamine (**17**).¹⁴¹ After completion of the reaction, *N,N'*-dicyclohexylurea (DCU) was removed by filtration and the crude product was purified by silica gel chromatography. Deprotection of the Boc-group could be achieved by treatment with 6-8% trifluoroacetic acid (TFA) in dichloromethane (DCM) in the presence of a catalytical amount of water. Extraction with ethyl acetate yielded the desired primary amine **19** with moderate purity (90.4%).¹⁴¹



Scheme 3.4: Synthesis of *N*-(6-aminohexyl)-benzamide (**19**). Reagents and conditions: a) benzoic acid, HOBt, DCC, THF, room temperature, overnight. b) 6-8% TFA in DCM, room temperature, 6 h.

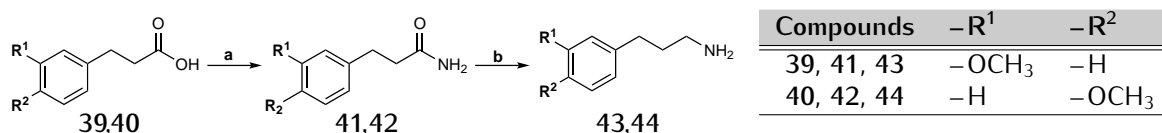
Table 3.5: Synthesis of N^6 -substituted adenosine derivatives. Reagents and conditions: a) mono- or dialkylamine, Et₃N, EtOH, reflux, 2-48 h.

							
-R ¹	-R ²	Yield	-R ¹	-R ²	Yield		
21	-H	-CH ₃	100%	30	-H	 34%	
22	-H	-CH ₂ CH ₃	100%	31	-H	 95%	
23	-H	-(CH ₂) ₅ CH ₃	99%	32	-CH ₃	-CH ₃	100%
24	-H	 95%	33	-CH ₃	-CH ₂ CH ₃	100%	
25	-H	 100%	34	-CH ₃	-(CH ₂) ₂ CH ₃	100%	
26	-H	 47%	35	-(CH ₂) ₂ CH ₃	-(CH ₂) ₂ CH ₃	100%	
27	-H	 43%	36	-CH ₂ CH ₃	-(CH ₂) ₂ CH ₃	65%	
28	-H	 88%	37	-CH ₂ CH ₃	-CH ₂ CH ₃	100%	
29	-H	 17%	38	-CH ₂ CH ₃	 58%		

For the synthesis of **26** and **27**, 3-methoxybenzenepropanamine (**43**) and 4-methoxybenzenepropanamine (**44**) were obtained by reduction of the corresponding carboxylic acids (*Scheme 3.5*).^{142,143} Firstly, the carboxylic acids **39** or **40** were converted to primary amides by reaction with 4-methylmorpholine and isobutylchloroformate. Quenching with ammonia in methanol led to the generation of the desired amides **41** or **42**, respectively, carbon dioxide and isobutanol. The amides **41** or **42** were then reduced using lithium aluminium hydride in THF yielding the desired amines **43** and **44**. These were then used for the synthesis of **26** and **27**, respectively.

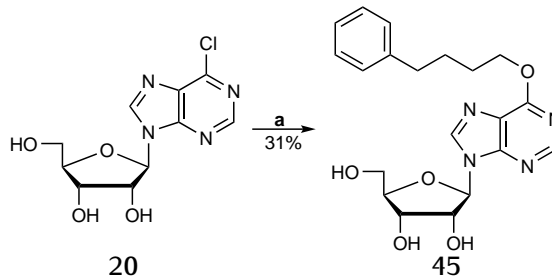
To investigate the importance of the nitrogen atom at the 6-position, an analog of N^6 -(4-phenyl)butyladenosine (**28**) was synthesized in which the nitrogen was replaced with an oxygen atom. For the synthesis of **45**, compound **20** was reacted

with sodium 4-phenylbutoxide in the appropriate alcohol (*Scheme 3.6*).¹⁴⁴ Sodium 4-phenylbutoxide was generated *in situ* by reaction of 4-phenylbutanol with elemental sodium.



Scheme 3.5: Synthesis of primary amines for the synthesis of 26 and 27. Reagents and conditions: a) three steps: I) 4-methylmorpholine, *iso*-butyl chloroformate, THF/toluene, 30 min, 0°C II) 7 M NH₃/methanol, 2 h, room temperature III) 10% K₂CO₃ (*aq*). b) two steps: I) LiAlH₄, dry THF, 0°C to reflux, 30 min II) H₂O, 15% NaOH (*aq*).

The reaction of 20 with sodium alkoxide is characterized as a salt metathesis reaction where there is an exchange of bonds between the two reacting chemical species. The reaction was performed by refluxing the reaction mixture at 100°C, and the progress of reaction was monitored by thin layer chromatography (TLC) in a DCM/methanol (9:1) mixture. After the reaction was completed the volatiles were removed *in vacuo* and the products were separated by silica gel column chromatography.



Scheme 3.6: Synthesis of 6-phenylbutoxyadenosine (45). Reagents and conditions: sodium 4-phenylbutoxide, 4-phenylbutanol, reflux, 100°C, 20 h.

The structures of the synthesized nucleosides were confirmed by ¹H- and ¹³C-NMR spectroscopy (Table 3.6 and Table 3.7), in addition to LC/ESI-MS analysis. In the ¹³C-NMR spectra of some *N*⁶-substituted adenosine derivatives, like for example 24, not all peaks from the *N*⁶-substituents are visible although the correct mass was found by LC/ESI-MS analysis. This is especially true for CH₂-groups that are adjacent to the *N*⁶-nitrogen atom, while the associated CH₃-groups can be detected. Furthermore, in the ¹H-NMR spectra, CH₂-groups adjacent to the *N*⁶-nitrogen atom of *N*⁶-disubstituted adenosine derivatives are displayed as very broad signals, that are often overlapping with signals from other sugar-derived protons.

Table 3.6: $^1\text{H-NMR}$ data of N^6 -substituted adenosine derivatives. Shifts (δ) in $\text{DMSO-d}_6^\#$ or CD_3OD^* [ppm]. Next to the signals of the substituents, a selection of characteristic ribose and purine protons is depicted.

Compound	N^6 -Substituents	C'1-H	C'5-H ₂	C2-H	C8-H	N^6 -substituents
21 [#]	N^6 -methyl	5.87	3.66–3.54	8.21	8.32	7.77 (NHCH ₃) 3.05 (NHCH ₃)
22 [#]	N^6 -ethyl	5.87	3.66–3.55	8.18	8.32	7.81 (NHCH ₂) 3.04 (CH ₂ CH ₃) 1.16 (CH ₂ CH ₃)
23 [#]	N^6 -hexyl	5.86	3.66–3.54	8.19	8.31	7.80 (NHCH ₂) 3.46 (NHCH ₂) 1.57 (CH ₂) 1.28 ((CH ₂) ₂) 1.18 (CH ₂) 0.85 (CH ₃)
24 [#]	N^6 - <i>iso</i> -pentyl	5.86	3.66–3.54	8.19	8.31	7.80 (NH) 3.49 (NHCH ₂) 1.62 (CH(CH ₃) ₂) 1.48 (CH ₂ CH ₂ CH) 0.89 (CH(CH ₃) ₂)
25 [#]	N^6 -(3-phenyl)propyl	5.87	3.66–3.55	8.19	8.33	7.89 (aryl) 7.28 (aryl) 3.50 (NHCH ₂) 2.63 (CH ₂ -aryl) 1.87 (CH ₂)
26 [#]	N^6 -(3-(3-methoxy)phenyl)-propyl	5.87	3.68–3.52	8.19	8.33	7.94 (NH) 7.17, 6.78–6.71 (aryl) 3.71 (OCH ₃) 3.16 (NHCH ₂) 2.61 (CH ₂ -aryl) 1.89 (CH ₂)
27 [#]	N^6 -(3-(4-methoxy)phenyl)-propyl	5.88	3.65–3.55	8.19	8.33	7.92 (NH) 7.12, 6.82 (aryl) 3.70 (OCH ₃) 3.16 (NHCH ₂) 2.57 (CH ₂ -aryl) 1.85 (CH ₂)
28 [#]	N^6 -(4-phenyl)butyl	5.87	3.68–3.52	8.18	8.31	7.86 (NH) 7.19 (aryl) 2.60 (CH ₂ CH ₂ -aryl) 1.61 ((CH ₂) ₂) 1.16 (NHCH ₂)
29 [#]	N^6 -(6-benzamide)hexyl	5.87	3.66–3.55	8.18	8.31	8.38 (NH) 7.81, 7.48, 7.43 (aryl) 3.46 (NHCH ₂) 3.23 (NHCH ₂) 1.59 (CH ₂) 1.51 (CH ₂) 1.34 ((CH ₂) ₂)
30 [#]	N^6 -(1,1,3,3-tetramethyl)-butyl	5.86	3.66–3.54	8.21	8.31	6.69 (NH) 2.00 (CH ₂) 1.54 ((CH ₃) ₂) 0.92 (C(CH ₃) ₃)
31 [#]	N^6 -(3-(imidazol-1-yl)propyl)	5.88	3.66–3.54	8.20	8.35	7.98 (NH) 7.71, 7.21, 6.91 (imidazole) 4.07 (NHCH ₂) 4.04 (NCH ₂) 2.69 (CH ₂)
32 [#]	N^6 -dimethyl	5.90	3.66–3.55	8.20	8.35	3.45 (N(CH ₃) ₂)
33 [#]	N^6 -ethyl- N^6 -methyl	5.90	3.66–3.54	8.20	8.35	4.04 (NCH ₂) 3.39 (NCH ₃) 1.17 (NCH ₂ CH ₃)

Continued on the next page

Table 3.6 – continued from previous page

Compound	N^6 -Substituents	C'1-H	C'5-H ₂	C2-H	C8-H	C8-substituents
34 [#]	N^6 -methyl- N^6 -propyl	5.89	3.66-3.54	8.19	8.35	3.16 (NCH ₂) [broad peak underneath previous peaks: NCH ₃] 1.64 (CH ₂) 0.87 (CH ₃)
35 [#]	N^6 -dipropyl	5.89	3.65-3.54	8.18	8.35	4.06 (N(CH ₂) ₂) 1.64 ((CH ₂) ₂) 0.89 ((CH ₃) ₂)
36*	N^6 -ethyl- N^6 -propyl	5.93	3.88-3.72	8.15	8.15	4.10-3.72 (2x NCH ₂) 1.73 (CH ₂) 1.25 (CH ₃) 0.95 (CH ₃)
37 [#]	N^6 -diethyl	5.89	3.66-3.54	8.19	8.34	4.03 (N(CH ₂ CH ₃) ₂) 1.19 (N(CH ₂ CH ₃) ₂)
38 [#]	N^6 -ethyl- N^6 -(4-phenyl)-butyl	5.89	3.66-3.55	8.18	8.35	7.24-7.15 (aryl) 4.06 (NCH ₂) 3.75 (NCH ₂) 2.62 (CH ₂ -aryl) 1.62 ((CH ₂) ₂) 1.16 (CH ₂ CH ₃)
45 [#]	O^6 -(4-phenyl)butyl	5.97	3.66-3.54	8.51	8.59	7.21 (aryl) 2.65 (OCH ₂ CH ₂) 1.81 (CH ₂ CH ₂ CH ₂) 1.72 (CH ₂ CH ₂ -aryl)

Table 3.7: ¹³C-NMR data of N^6 -substituted adenosine derivatives. Shifts (δ) in DMSO- $d_6^{\#}$ or CD₃OD* [ppm]. Next to the signals of the substituents, a selection of characteristic ribose and purine carbons is depicted.

Compound	N^6 -Substituents	C'1	C'5	C2	C8	N^6 -substituents
21 [#]	N^6 -methyl	88.05	61.7	152.46	139.74	24.44 (CH ₃)
22 [#]	N^6 -ethyl	88.07	61.80	152.47	139.72	34.24 (CH ₂), 12.63 (CH ₃)
23 [#]	N^6 -hexyl	88.10	61.83	152.50	139.69	48.73 (CH ₂) 45.77 (CH ₂) 31.18 (CH ₂) 26.20 (CH ₂) 22.21 (CH ₂) 14.04 (CH ₃)
24 [#]	N^6 - <i>iso</i> -pentyl	88.12	61.85	152.55	139.74	38.16 (CH ₂) 25.45 (CH) 22.66 (CH(CH ₃) ₂) [missing: NHCH ₂]
25 [#]	N^6 -(3-phenyl)propyl	88.08	61.82	152.50	139.78	140.97, 128.58, 128.44, 128.40, 126.19, 125.83 (aryl) 45.66 (CH ₂) 31.97 (CH ₂) 28.88 (CH ₂)
26 [#]	N^6 -(3-(3-methoxy)phenyl)-propyl	88.11	61.85	152.52	139.82	159.44, 143.60, 129.42, 120.73, 114.06, 111.39 (aryl) 55.04 (OCH ₃) 48.77 (CH ₂) 32.83 (CH ₂) 30.82 (CH ₂)

Continued on the next page

Table 3.7 – continued from previous page

Compound	N^6 -Substituents	C'1	C'5	C2	C8	C8-substituents
27 [#]	N^6 -(3-(4-methoxy)phenyl)-propyl	88.14	61.88	152.55	139.83	157.55, 133.84, 129.39, 113.08 (aryl) 55.14 (OCH ₃) 48.79 (CH ₂) 31.91 (CH ₂) 31.19 (CH ₂)
28 [#]	N^6 -(4-phenyl)butyl	88.06	61.79	152.44	139.68	142.31, 128.39, 128.29, 125.69 (aryl) 45.76 (CH ₂) 28.53 (CH ₂) 27.72 (CH ₂) 26.70 (CH ₂)
29 [#]	N^6 -(6-benzamide)-hexyl	88.10	61.83	152.49	139.71	166.21, 145.29, 134.90, 131.05, 128.31, 127.23 (aryl) 45.94 (CH ₂) 39.29 (CH ₂) 29.27 (CH ₂) 29.20 (CH ₂) 26.44 (CH ₂) 26.32 (CH ₂)
30 [#]	N^6 -(1,1,3,3-tetramethyl)-butyl	88.13	61.88	151.89	139.77	55.56 (<u>C</u> (CH ₂) ₂) 50.23 (CH ₂) 31.65(<u>C</u> (CH ₃) ₃) 31.40 ((CH ₃) ₂) 29.97 (C(<u>C</u> H ₃) ₃)
31 [#]	N^6 -(3-(imidazol-1-yl)propyl	88.09	61.83	152.50	139.93	137.43, 128.03, 119.70 (imidazol) 43.23 (CH ₂) 36.32 (CH ₂) 28.84 (CH ₂)
32 [#]	N^6 -dimethyl	87.94	61.68	151.82	138.69	11.57 (N(CH ₃) ₂)
33 [#]	N^6 -ethyl- N^6 -methyl	87.91	61.69	151.89	138.82	44.78 (NCH ₂) 35.47 (NCH ₃) 12.56 (CH ₃)
34 [#]	N^6 -methyl- N^6 -propyl	87.92	61.74	151.88	138.79	51.32 (NCH ₂) 48.75 (NCH ₃) 21.58 (CH ₂) 11.06 (CH ₃)
35 [#]	N^6 -dipropyl	87.92	61.92	151.88	138.89	56.17 ((CH ₂) ₂) 48.74 ((CH ₂) ₂) 18.70 (CH ₃) 11.18 (CH ₃)
36 [*]	N^6 -ethyl- N^6 -propyl	91.21	63.58	152.72	140.17	51.25 (NCH ₂) 44.72 (NCH ₂) 22.52 (CH ₂) 13.90 (CH ₃) 11.36 (CH ₃)
37 [#]	N^6 -diethyl	87.94	61.73	151.95	138.96	42.56 (N(<u>C</u> H ₂ CH ₃) ₂) 13.48 (N(CH ₂ <u>C</u> H ₃) ₂)
38 [#]	N^6 -ethyl- N^6 -(4-phenyl)-butyl	87.94	61.74	151.92	138.92	142.24, 128.41, 128.41, 125.77 (aryl) 48.74 (CH ₂ -aryl) 47.45 (NCH ₂) 35.07 (CH ₂) 28.37 ((CH ₂) ₂) 13.90 (CH ₃)
45 [#]	O^6 -(4-phenyl)butyl	87.92	61.57	151.95	142.43	142.03, 128.42, 128.37, 125.82 (aryl) 61.46 (OCH ₂) 34.85 (CH ₂ -aryl) 28.09 (CH ₂) 27.47 (CH ₂)

3.1.4 Modification of adenosine at the C8- and N⁶-position

Since the known inhibitors 8-BuS-AMP and ARL67156 have substitutions at C8 and N⁶, respectively, a combination of modifications at those position might be interesting to investigate. Therefore a small library of C8,N⁶-disubstituted adenosine derivatives was generated (Table 3.8). For this purpose, 6-chloro-9-(β-D-ribofuranosyl)purine (20) was substituted at the 6-position by the corresponding alkylamine in the presence of triethylamine in absolute ethanol as described before.⁹¹

Table 3.8: Synthesis of C8,N⁶-disubstituted adenosine derivatives. Reagents and conditions: a) mono- or dialkylamine, Et₃N, EtOH, reflux, 4-10 h. b) bromine, sodium-acetate buffer, pH 4.0, room temperature, overnight. c) For 50-56: alkylamine, Et₃N, EtOH, reflux, 18-48 h. For 57: two steps: I) thiourea, EtOH, 1 h, reflux or NaSH, DMF, 100°C, 10 h. II) 1-iodobutane, H₂O/EtOH (1:1), NaOH. For 58: 1-butanethiol, NaOH, EtOH, room temperature, 5 days.

21: R¹ = CH₃, R² = H
 22: R¹ = CH₂CH₃, R² = H
 32: R¹ = CH₃, R² = CH₃
 37: R¹ = CH₂CH₃, R² = CH₂CH₃

	-R ¹	-R ²	-R ³	Yield
46	-CH ₃	-H	-Br	25%
47	-CH ₂ CH ₃	-H	-Br	14%
48	-CH ₃	-CH ₃	-Br	21%
49	-CH ₂ CH ₃	-CH ₂ CH ₃	-Br	23%
50	-CH ₃	-H		37%
51	-CH ₃	-H	-NH(CH ₂) ₃ CH ₃	93%
52	-CH ₃	-CH ₃		33%
53	-CH ₃	-CH ₃	-NH(CH ₂) ₃ CH ₃	33%
54	-CH ₂ CH ₃	-CH ₂ CH ₃	-NHCH ₃	67%
55	-CH ₂ CH ₃	-CH ₂ CH ₃	-NH(CH ₂) ₃ CH ₃	100%
56	-CH ₂ CH ₃	-H	-NH(CH ₂) ₃ CH ₃	62%
57	-CH ₃	-H	-S(CH ₂) ₃ CH ₃	12%
58	-CH ₂ CH ₃	-CH ₂ CH ₃	-S(CH ₂) ₃ CH ₃	42%

Next, the 8-position was brominated under acidic conditions.^{91,133} The pH of the reaction was maintained by 0.1 M sodium acetate buffer pH 4.0. Excess bromine was removed by sodium bisulfite and neutralization with NaOH followed by filtration

Table 3.9: $^1\text{H-NMR}$ data of C8, N^6 -disubstituted adenosine derivatives. Shifts (δ) in $\text{DMSO-d}_6^\#$ or CD_3OD^* [ppm].
Next to the signals of the substituents, a selection of characteristic ribose and purine protons is depicted.

Compound	Substituents	C'1-H	C'5-H ₂	C2-H	C8-substituents	N^6 -substituents
50 [#]	8-cyclopropylamino- N^6 -methyl	5.87	3.61	7.98	6.86 (NHCH) 5.82 (NHCH) 0.66 (CH ₂) 0.45 (CH ₂)	7.05 (NHCH ₃) 2.93 (NHCH ₃)
51 [#]	8-butylamino- N^6 -methyl	5.89	3.62	7.95	6.83 (NHCH ₂) 3.36 (NHCH ₂) 1.56 (H ₂) 1.33 (CH ₂) 0.89 (CH ₂ CH ₃)	6.77 (NHCH ₃) 2.92 (NHCH ₃)
52 [#]	8-(4-phenyl)butylamino- N^6 -dimethyl	5.91	3.62	7.95	7.24–7.16 (aryl) 6.88 (NHCH ₂) 4.10 (NCH ₂) 2.60 (CH ₂ –aryl) 1.62 ((CH ₂) ₂)	3.34 (N(CH ₃) ₂)
53 [*]	8-butylamino- N^6 -dimethyl	6.04	3.88–3.81	8.00	2.97 (NHCH ₂) 1.71 (CH ₂) 1.46 (CH ₂) 1.02 (CH ₃)	3.47 (N(CH ₃) ₂)
54 [#]	N^6 -diethyl-8-methylamino	5.87	3.62	7.94	6.81 (NHCH ₃) 3.08 (NCH ₃)	3.87 (N(CH ₂) ₂) 1.16 (N(CH ₂ CH ₃) ₂)
55 [#]	8-butylamino- N^6 -diethyl	5.90	3.61	7.93	6.83 (NHCH ₂) 3.16 (NHCH ₂) 1.57 (CH ₂) 1.33 (CH ₂) 0.88 (CH ₃)	3.85 (N(CH ₂) ₂) 1.15 ((CH ₃) ₂)
56 [#]	8-butylamino- N^6 -ethyl	5.88	3.61	7.93	6.82 (NHCH ₂) 3.48 (NHCH ₂) 1.32 ((CH ₂) ₂) 0.87 (CH ₃)	6.78 (NHCH ₂) 2.76 (NHCH ₂) 1.13 (CH ₃)
57 [#]	8-butylthio- N^6 -methyl	5.77	3.68–3.49	8.13	3.26 (SCH ₂ CH ₂) 1.67 (CH ₂) 1.40 (CH ₂) 0.89 (CH ₃)	7.63 (NHCH ₃) 2.96 (NHCH ₃)
58 [#]	8-butylthio- N^6 -diethyl	5.72	3.65–3.51	8.10	3.25 (SCH ₂) 1.72 (CH ₂) 1.40 (CH ₂) 0.89 (CH ₃)	4.15–3.65 (N(CH ₂) ₂) 1.19 ((CH ₃) ₂)

Table 3.10: ^{13}C -NMR data of C8, N^6 -disubstituted adenosine derivatives. Shifts (δ) in DMSO- $d_6^{\#}$ or CD_3OD^* [ppm].
Next to the signals of the substituents, a selection of characteristic ribose and purine carbons is depicted.

Compound	Substituents	C'1	C'5	C2	C8-substituents	N^6 -substituents
50 [#]	8-cyclopropylamino- N^6 -methyl	86.49	61.75	151.58	25.01 (CH) 6.83 (CH ₂) 6.19 (CH ₂)	18.67 (CH ₃)
51 [#]	8-butylamino- N^6 -methyl	86.45	61.79	151.35	42.17 (NHCH ₂) 31.00 (CH ₂) 19.78 (CH ₂) 13.91 (CH ₃)	27.44 (CH ₃)
52 [#]	8-(4-phenyl)butylamino- N^6 -dimethyl	86.48	61.78	150.63	142.34, 128.41, 128.36, 125.76 (aryl) 42.09 (CH ₂) 40.24 (CH ₂) 37.91(CH ₂) 34.97 (CH ₂)	28.53 (CH ₃) 28.45 (CH ₃)
53 [*]	8-butylamino- N^6 -dimethyl	87.05	61.69	150.65	37.40 (NHCH ₂) 31.16 (CH ₂) 19.78 (CH ₂) 12.79 (CH ₃)	42.00 ((CH ₃) ₂)
54 [#]	N^6 -diethyl-8-methylamino	86.55	61.78	150.62	28.98 (NHCH ₃)	45.90 (CH ₂) 42.07 (CH ₂) 14.04 (CH ₃) 8.74 (CH ₃)
55 [#]	8-butylamino- N^6 -diethyl	86.44	61.82	150.43	56.20 (CH ₂) 30.95 (CH ₂) 19.74 (CH ₂) 18.72 (CH ₃)	42.19 (CH ₂) 41.95 (CH ₂) 14.08 (CH ₃) 13.87 (CH ₃)
56 [#]	8-butylamino- N^6 -ethyl	86.48	61.82	151.37	42.19 (NHCH ₂) 31.03 (CH ₂) 19.82 (CH ₂) 13.64 (CH ₃)	56.20 (NHCH ₂) 15.51 (CH ₃)
57 [#]	8-butylthio- N^6 -methyl	89.04	62.41	151.47	32.27 (SCH ₂) 31.11 (CH ₂) 21.37 (CH ₂) 13.59 (CH ₃)	27.17 (NHCH ₃)
58 [#]	8-butylthio- N^6 -diethyl	88.99	62.44	151.54	42.61 (SCH ₂) 31.39 (CH ₂) 21.56 (CH ₂) 13.60 (CH ₃)	31.88 (N(CH ₂) ₂) [missing: (CH ₃) ₂]

afforded the desired compounds **46–49**. Last but not least, the bromo-group was substituted with an alkylamine in the presence of triethylamine in absolute ethanol to obtain compounds **50–56**.⁹¹

In order to obtain compounds **57** and **58**, the corresponding 8-bromo derivatives **46** and **49**, respectively, were reacted with thiourea in ethanol to give the intermediate 8-thio derivatives, which were subsequently alkylated using the corresponding alkyl halide in a mixture of water and ethanol (1:1) and in the presence of sodium hydroxide yielding compounds **57** and **58**.^{91,123,131,136}

The structures of the synthesized nucleosides were confirmed by ¹H- and ¹³C-NMR spectroscopy (Table 3.9 and Table 3.10), in addition to LC/ESI-MS analysis.

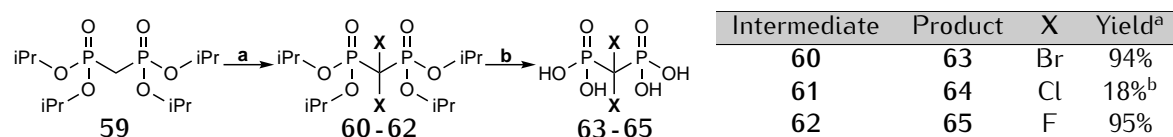
3.2 Triphosphorylation of adenosine derivatives

To explore the structure-activity relationships of ARL67156, a library of ARL67156 derivatives was created by triphosphorylation of several adenosine derivatives described in *Chapter 3.1*.

The adenosine derivatives were submitted to phosphorylation according to the Ludwig procedure as described in *Chapter 1.5.2* with small adjustments. Shortly, lyophilized nucleosides were dissolved in trimethylphosphate and reacted with phosphoryl chloride (POCl₃) in the presence of proton sponge to yield the reactive 5'-dichlorophosphate intermediates.^{117,123} The intermediate was reacted with tris-*N*-butylammonium-dibromomethylene-bisphosphonate (**63**) in anhydrous DMF followed by hydrolysis with TEAC buffer (*Table 3.11*).^{123,145}

Dibromomethylenebisphosphonate (**63**) was synthesized from tetraisopropyl methylenebisphosphonate (**59**) (*Scheme 3.7*).^{145–147} Bromination using sodium hypobromite, that was generated *in situ* at 0°C from bromine and sodium hydroxide, was carried out at low temperature in order to slow down the conversion of hypobromite to bromide and bromate. The brominated intermediate **60** was deprotected by refluxing with hydrochloric acid for 24 hours.^{145,146} Finally, the bisphosphonic acid **63** was simply converted to the corresponding tri-*N*-butylammonium salt by dissolution of the acid in 50% aqueous ethanol and subsequent drop-wise addition of tri-*N*-butylamine until the pH reached 7.8–8.0 followed by evaporation and lyophilization.^{145,146}

After completion of the phosphorylation reaction, trimethylphosphate was removed



Scheme 3.7: Synthesis of dihalogenmethylenebisphosphonate. Reagents and conditions: a) for **60**: NaOH, bromine, 0°C, 30 min; for **61**: NaOCl, 0°C, 30 min; for **62**: *N*-fluorobenzenesulfonimide (NFSi), sodium bis(trimethylsilyl)amide (NaHMDS), anhydrous THF, room temperature, 10h. b) 6 M *aq* HCl, reflux, 24 h. ^aYield over both steps. ^bYield underestimated because of product loss due to technical problems.

from the crude reaction mixture by extraction with *tert*-butylmethylether followed by lyophilization of the water layer. The nucleotides were first purified by anion exchange chromatography on a sepharose column using a fast protein liquid chromatography (FPLC) apparatus by applying a linear gradient (5→80%, 0.5 M *aqueous* ammonium bicarbonate buffer in water).¹⁴⁸ The neutral impurities (*e.g.* nucleosides) should elute first, followed by charged species (mono-, di, and finally triphosphates). Additionally to the desired triphosphates, monophosphates were also collected and isolated. The products were further purified by HPLC on reverse-phase C18 material in order to remove inorganic phosphates and buffer components and to yield the desired triphosphates and the corresponding monophosphates (*Table 3.11*).^{91,123}

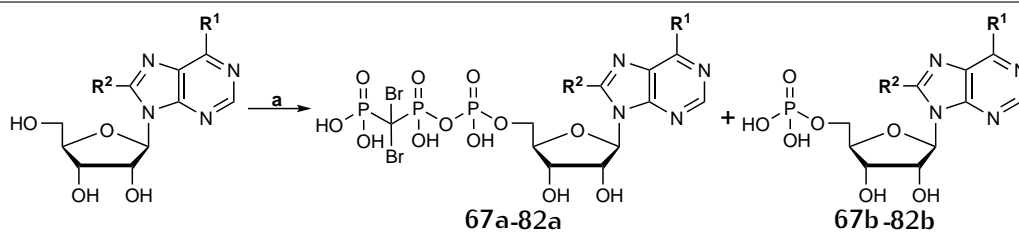
Unfortunately, it was not possible to isolate **67a**, **74a**, and **82a** due to different reasons. The bulky lipophilic substituent of **67a** caused the desired triphosphate to elute at the FPLC later than the other triphosphates, which led to loss of the product. For **74a** and **82a** degradation of the triphosphate into the diphosphate was observed in the ³¹P-NMR spectrum after purification by HPLC, indicating that the compounds are chemically unstable. Furthermore, **76b** and **78b** could also not be isolated due to the low conversion of the adenosine derivatives to the monophosphates.

To investigate the structure-activity relationships of the triphosphate moiety, variants of the β,γ -dibromomethylene group are of interest. The naked β,γ -methylene-ATP (**66**), without any substituents attached to the methylene group, is commercially available and does not need to be synthesized. β,γ -Dibromomethylene-ATP (**83**) was synthesized according to the procedure described above (*Scheme 3.8*).^{117,123,145}

Additionally, β,γ -dichloro- (**61**) and β,γ -difluorobisphosphonic acid (**62**) were synthesized (*Scheme 3.7*) to generate β,γ -dichloro- and β,γ -difluoromethylene-ATP.

For the synthesis of β,γ -dichlorobisphosphonic acid (**61**), tetraisopropyl methylene-

Table 3.11: Synthesis of ARL67156-derivatives. Reagents and conditions: a) three steps: I) trimethylphosphate, POCl₃, proton sponge, 0–4°C, 4–5 h. II) 0.5 M Bu₃N · CBr₂(PO₃H)₂ solution in anhydrous DMF, Bu₃N, 0–4°C, 5 min. III) 0.5 M TEAC buffer pH 7.4–7.6, room temperature, 1 h.



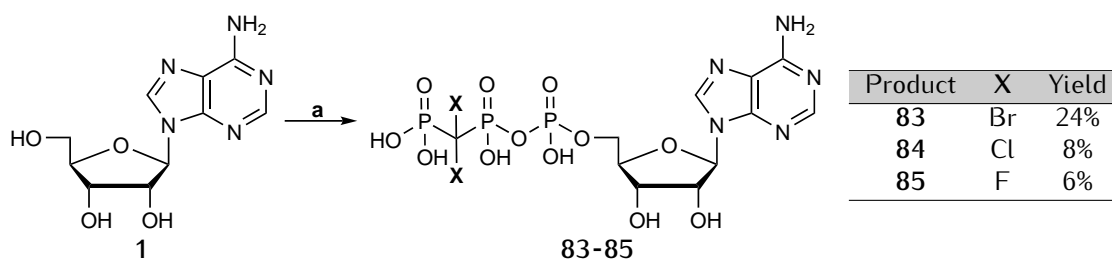
	–R ¹	–R ²	Yield		–R ¹	–R ²	Yield
67a	–NH ₂		–*	75a	–N(CH ₂ CH ₃) ₂	–H	4%
67b			3%	75b			36%
68a	–NH ₂		2.5%	76a	–NHCH ₃		2%
68b			10%	76b			–*
69a	–N(CH ₃) ₂	–H	1%	77a	–NHCH ₃		2.3%
69b			3%	77b			22%
70a		–H	12%	78a	–N(CH ₃) ₂		1.8%
70b			14%	78b			–*
71a		–H	9%	79a	–N(CH ₂ CH ₃) ₂	–NHCH ₃	4%
71b			17%	79b			5%
72a	–N((CH ₂) ₂ CH ₃) ₂	–H	8%	80a	–NHCH ₃		3%
72b			43%	80b			51%
73a		–H	6%	81a	–N(CH ₂ CH ₃) ₂		4%
73b			14%	81b			41%
74a	–N(CH ₂ CH ₃) ₂		–*	82a	–NH ₂		–*
74b			25%	82b			4%

*Purification not successful.

bisphosphonate (**59**) was reacted with sodium hypochlorite at 0°C.¹⁴⁶ Unfortunately, the reaction did not proceed completely and therefore, the intermediate needed to be purified by silica gel column chromatography, and most of the product was lost due to technical problems with the fraction collector. However, the yield was still sufficient to proceed further with the synthesis of β,γ -dichloromethylene-ATP (**84**).

For the synthesis of β,γ -difluorobisphosphonic acid (**62**), tetraisopropyl methylenebisphosphonate (**59**) was reacted with NaHMDS and NFSi in THF at room temperature.¹⁴⁹ One likely formed side product of the reaction is β,γ -monofluorobisphosphonic acid, which has a similar retention factor (R_f) as the desired product, making the purification process very difficult. In order to achieve completion of the reaction, NaHMDS and NFSi were not added at once. Instead, 1 M solutions in anhydrous THF were generated and 0.3 equivalents of each chemical were added approximately every 2 minutes until the exothermic reaction was over.¹⁴⁹ With continuous reaction,

a white suspension was generated. The resulting suspension was filtered and the filter cake was washed with hexane yielding the pure product.¹⁴⁹



Scheme 3.8: Synthesis of β,γ -dibromomethylene-ATP analogs. a) three steps: I) trimethylphosphate, POCl_3 , proton sponge, $0-4^\circ\text{C}$, 4-5 h. II) $0.5\text{ M Bu}_3\text{N} \cdot \text{CX}_2(\text{PO}_3\text{H})_2$ solution in anhydrous DMF, Bu_3N , $0-4^\circ\text{C}$, 5 min. III) 0.5 M TEAC buffer pH 7.4-7.6, room temperature, 1 h.

The halogenated intermediates **61** and **62** were deprotected by refluxing with hydrochloric acid for 24 hours as described before.^{145,146} In the next step, the bisphosphonic acids (**64** and **65**) were converted to the corresponding tri-*N*-butylammonium salts by dissolution of the acid in 50% aqueous ethanol and subsequent drop-wise addition of tri-*N*-butylamine until the pH reached 7.8-8.0 followed by evaporation and lyophilization.^{145,146} Triphosphorylation of adenosine (**1**) and subsequent purification was carried out as described before (Scheme 3.8).^{117,123,145}

The structures of the synthesized nucleotides were confirmed by ^1H -, ^{13}C , and ^{31}P -NMR spectroscopy (Table 3.12), in addition to LC/ESI-MS analysis performed in both positive and negative mode.

Table 3.12: ^{31}P -NMR data of ARL67156 derivatives. Shifts (δ) in D_2O [ppm].

Triphosphate	Substituents	P_α	P_β	P_γ	Monophosphate	P_α
67a	8-(4-phenyl)-butylamine	-	-	-	67b	0.36
68a	8-butylthio	-10.62	-0.69	7.46	68b	0.88
69a	N^6, N^6 -dimethyl	-10.65	-0.73	7.48	69b	0.59
70a	N^6 -ethyl- N^6 -methyl	-10.62	0.22	7.58	70b	2.06
71a	N^6 -methyl- N^6 -propyl	-10.62	-0.23	7.56	71b	2.66
72a	N^6, N^6 -dipropyl	-10.59	0.78	7.64	72b	1.91
73a	N^6 -ethyl- N^6 -propyl	-10.59	1.10	7.68	73b	2.58
74a	8-butylamino- N^6, N^6 -diethyl	-	-	-	74b	0.72
75a	N^6, N^6 -diethyl	-10.61	0.40	7.61	75b	4.03

Continued on the next page

Table 3.12 – continued from previous page

Triphosphate	Substituents	P _α	P _β	P _γ	Monophosphate	P _α
76a	8-cyclopropylamine- <i>N</i> ⁶ -methyl	-11.16	-0.84	7.51	76b	-
77a	8-butylamine- <i>N</i> ⁶ -methyl	-11.26	-0.87	7.48	77b	0.38
78a	8-butylamine- <i>N</i> ⁶ , <i>N</i> ⁶ -dimethyl	-12.61	-2.22	6.15	78b	-
79a	<i>N</i> ⁶ , <i>N</i> ⁶ -diethyl-8-methylamine	-10.77	0.27	7.14	79b	0.65
80a	8-butylthio- <i>N</i> ⁶ -methyl	-10.64	0.70	7.49	80b	1.33
81a	8-butylthio- <i>N</i> ⁶ , <i>N</i> ⁶ -diethyl	-10.64	-0.74	7.48	81b	1.00
82a	8-butylamino	-	-	-	82b	1.14
83	-	-10.58	-0.50	7.56	-	-
84	-	-10.55	0.16	7.83	-	-
85	-	-10.68	-4.56	3.40	-	-

3.3 Monophosphorylation of adenosine derivatives

To explore the structure-activity relationships on 8-BuS-AMP, a library of AMP-derivatives was created by monophosphorylation of several adenosine derivatives described in *Chapter 3.1*.

The adenosine derivatives were submitted to phosphorylation according to the Yoshikawa procedure with small adjustments as described in *Chapter 1.5.1 (Table 3.13)*.^{117,123} Shortly, lyophilized nucleosides were dissolved in trimethylphosphate and reacted with POCl₃ to yield the reactive 5'-dichlorophosphate intermediates. Hydrolysis with TEAC buffer yielded the desired nucleoside monophosphates. To remove the trimethylphosphate, the crude reaction mixture was extracted with *tert.*-butylmethylether. The nucleosides were purified by HPLC on reverse-phase C18 material in order to remove inorganic phosphates and buffer components yielding the desired monophosphates.

Next to the described C2-substituted adenosine derivative **7**, also commercially available 2-chloroadenosine (**6**) and 2-aminoadenosine (**86**) were submitted to monophosphorylation to yield **87** and **103**, respectively.

Table 3.13: Monophosphorylation of adenosine derivatives. Reagents and conditions: a) two steps: I) trimethylphosphate, POCl₃, proton sponge, 0-4°C, 4-5 h. II) 0.5 M TEAC buffer pH 7.4-7.6, room temperature, 1 h.

87-103

Nucleoside	Monophosphate	-R ¹	-R ²	-R ³	Yield
6	87	-Cl	-NH ₂	-H	84%
7	88	-NHNH ₂	-NH ₂	-H	58%
8	89	-H	-NH ₂	-Cl	69%
10	90	-H	-NH ₂	-NHCH ₃	23%
14	91	-H	-NH ₂	-SCH ₃	81%
16	92	-H	-NH ₂		24%
21	93	-H	-NHCH ₃	-H	74%
22	94	-H	-NHCH ₂ CH ₃	-H	65%
23	95	-H	-NH(CH ₂) ₅ CH ₃	-H	22%
24	96	-H		-H	18%
30	97	-H		-H	13%
31	98	-H		-H	17%
38	99	-H		-H	28%
45	100	-H		-H	7%
52	101	-H	-N(CH ₃) ₂		22%
56	102	-H	-NHCH ₂ CH ₃	-NH(CH ₂) ₃ CH ₃	56%
86	103	-NH ₂	-NH ₂	-H	45%

In addition to the nucleosides shown in Table 3.13, some other adenosine derivatives containing larger *N*⁶-substituents like for example, 3-propylphenyl (25) or 4-phenylbutyl (28), were submitted to phosphorylation according to the above de-

scribed procedure. However, instead of the desired 5'-*O*-monophosphates, mixtures of multiple monophosphates were obtained (*Figure 3.2A*). Interestingly, in the LC/ESI-MS analysis, only one peak with the desired mass was detected, but ^{31}P -NMR clearly showed the presence of multiple phosphorus atoms (*Figure 3.2A*).

This phenomenon was also observed for 2-methylthioadenosine (**5**) but not when smaller N^6 -substituents like ethyl or methyl were introduced, indicating that longer, and more bulky N^6 -substituents facilitate phosphorylation at the 2'- or 3'- position. Unfortunately, the different monophosphates elute at the same time from the HPLC and are therefore not separable. Next to the formation of undesired side products, a second complication occurred. During the purification by HPLC it was observed that unreacted proton-sponge is eluted around the same time from the column as the unprotected AMP-derivatives with long N^6 -substituents, which led to significant loss of product.

In order to solely obtain the desired 5'-monophosphates, the hydroxy groups at the 2'- and 3'-position of the adenosine derivatives **25-29** were protected using 2,2-dimethoxypropane and acetone in the presence of sulfuric acid (*Table 3.14*).^{91,150}

The 2',3'-*O*-isopropylidene-protected adenosine derivatives **104-109** were submitted to phosphorylation according to the Yoshikawa procedure as described before but without the use of the proton sponge (*Table 3.14*).^{117,123} As already mentioned, separation of the unreacted proton sponge and the desired AMP-derivatives is difficult. Usually, proton sponge is used to achieve selective phosphorylation at the 5'-position. However, by using 2',3'-protecting groups no proton sponge needs to be used for the phosphorylation of the protected intermediates since phosphorylation can only occur at the desired 5'-position. Therefore, purification of the desired AMP-derivatives is much easier.

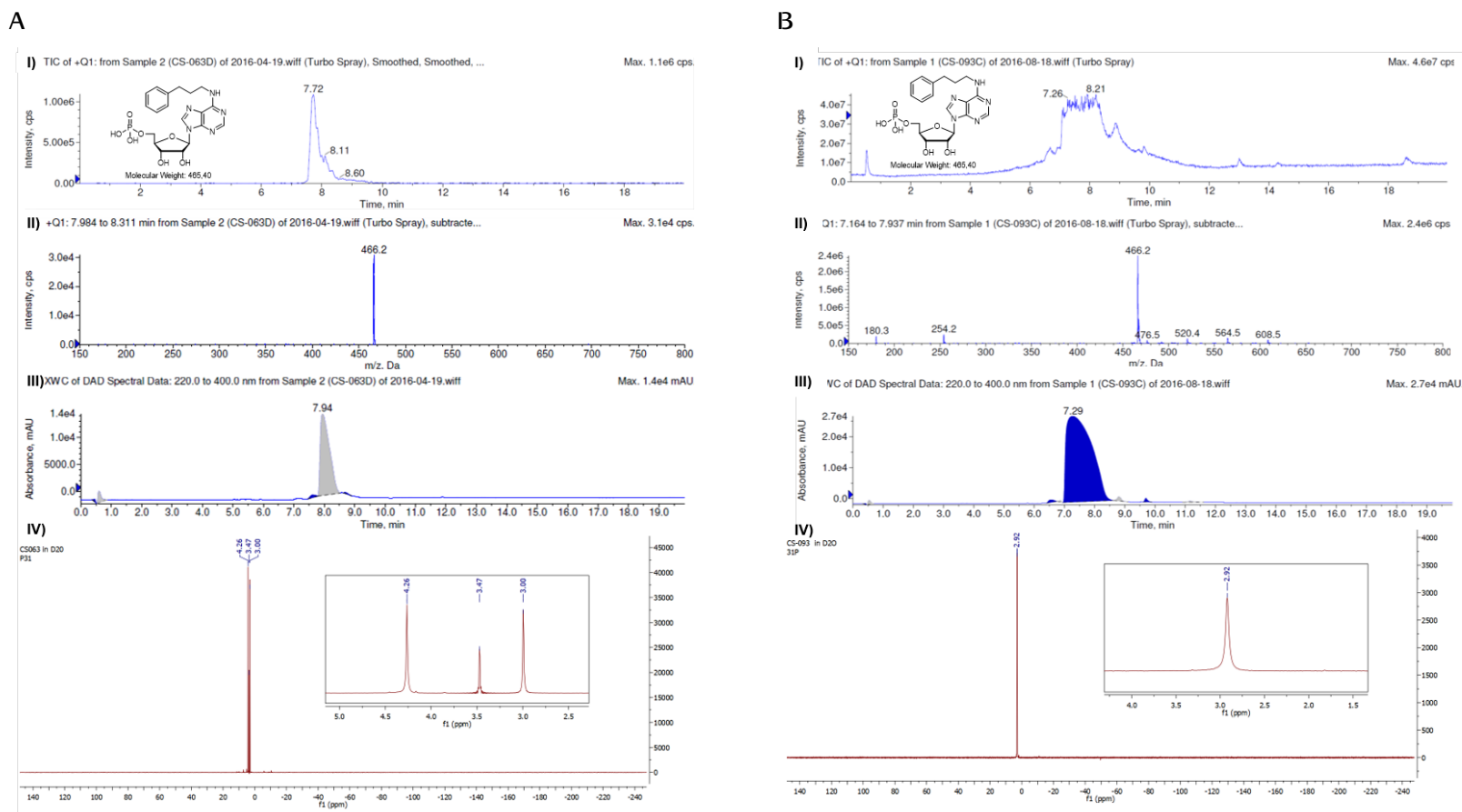
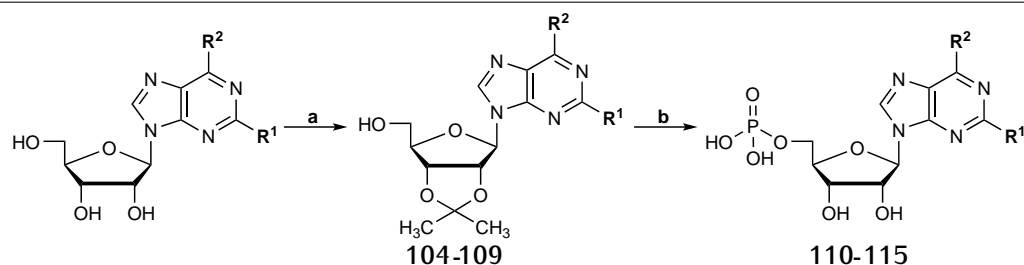


Figure 3.2: Analytical spectra of 111. A) LC/ESI-MS and ^{31}P -NMR spectra recorded after direct phosphorylation of 25. B) LC/ESI-MS and ^{31}P -NMR spectra recorded after phosphorylation of 105 and subsequent deprotection. I) Total ion count (TIC) chromatogram. II) Mass spectrum of the main peak. III) UV chromatogram measured with a diode array detector (DAD) from 200.0 - 400.0 nm. IV) ^{31}P -NMR spectrum recorded in D_2O and measured at 243 MHz.

Table 3.14: Protection and subsequent phosphorylation of adenosine derivatives. Reagents and conditions: a) acetone, 2,2-dimethoxypropane, sulfuric acid, room temperature, 20 min. b) two steps: I) trimethylphosphate, POCl₃, 0–4°C, 6–7 h II) 0.5 M TEAC buffer pH 7.4–7.6, room temperature, 15 min. b) H₂O, 7–8% TFA, DCM, room temperature, 2 h.



Nucleoside	Intermediate	Monophosphate	–R ¹	–R ²	Yield
5	104	110	–SCH ₃	–NH ₂	8%
25	105	111	–H		18%
26	106	112	–H		34%
27	107	113	–H		10%
28	108	114	–H		14%
29	109	115	–H		15%

By cutting out the proton sponge, some other aspects have to be taken into account. As already mentioned in *Chapter 1.5*, the proton sponge usually accelerates the phosphorylation reaction. Therefore, the reaction time of the phosphorylation of protected nucleosides needed to be prolonged by 2–3 hours. Another function of the proton sponge is to neutralize hydrogen chloride that is formed during phosphorylation. Because of the absence of proton sponge, the phosphorylation took place in an acidic medium. This led to the partial deprotection of 2',3'-isopropylidene groups, as observed by LC/ESI-MS analysis.

After purification by HPLC the protected AMP derivatives were treated with 7–8% TFA in water and DCM to achieve complete deprotection. Nucleotides were precipitated using cold diethyl ether followed by a second purification by HPLC yielding the desired monophosphates 110–115.⁹¹ As can be seen in *Figure 3.2B* using 111 as

an example, solely the 5'-monophosphate was obtained as confirmed by LC/ESI-MS and ^{31}P -NMR analyses.

The structures of the synthesized nucleotides were confirmed by ^1H -, ^{13}C -, and ^{31}P -NMR spectroscopy (Table 3.15), in addition to LC/ESI-MS analysis performed in both positive and negative mode.

Table 3.15: ^{31}P -NMR data of 8-BuS-AMP derivatives. Shifts (δ) in D_2O [ppm].

Compound	Substituents	P_α	Compound	Substituents	P_α
87	2-chloro	3.99	99	N^6 -ethyl- N^6 -(4-phenyl)butyl	1.34
88	2-hydrazinyl	4.09	100	6-(4-phenyl)butoxide	2.56
89	8-chloro	1.76	101	8-(4-phenyl)-butylamino- N^6, N^6 -dimethyl	1.31
90	8-methylamino	3.35	102	8-butylamino- N^6 -ethyl	0.29
91	8-methylthio	2.78	103	2-amino	2.62
92	8-(5-methyl)hexyl	1.43	110	2-methylthio	4.09
93	N^6 -methyl	4.22	111	N^6 -(3-phenyl)propyl	2.95
94	N^6 -ethyl	2.80	112	N^6 -(3-(3-methoxy)-phenyl)propyl	0.41
95	N^6 -hexyl	0.92	113	N^6 -(3-(4-methoxy)-phenyl)propyl	1.21
96	N^6 -iso-pentyl	1.64	114	N^6 -(4-phenyl)butyl	1.57
97	N^6 -(1,1,3,3-tetramethyl)butyl	1.93	115	N^6 -(<i>N</i> -benzamide)hexyl	0.86
98	N^6 -(3-(imidazol-1-yl)propyl)	2.27			

3.4 Pharmacological evaluation of ARL67156-derivatives

3.4.1 Structure-activity relationships of ARL67156-derivatives

The synthesized ARL67156-derivatives (Chapter 3.2) were tested for their inhibitory potency at human CD39 by applying the fast fluorescent CE assay (FFCE) method, which was described in Chapter 1.4.4.¹¹⁵ The biological testing was performed by

Laura Schäkel, Sangyong Lee and Xihuan Luo. The test results are summarized in *Table 3.16*. The determined K_i values were $0.973 \mu\text{M}$ and $1.19 \mu\text{M}$ for commercial and synthesized ARL67156 (**75a**) at human CD39, respectively. These values were approximately tenfold lower than the literature value ($11.0 \mu\text{M}$) which had been determined in a malchite green assay at human CD39.⁶⁵

Table 3.16: Potency of ARL67156 analogs and derivatives as CD39 inhibitors. The test was performed by using $0.5 \mu\text{M}$ FL-ATP as a substrate and human umbilical cord membrane preparations natively expressing CD39.

Compound	R ¹	R ²	-X	$K_i \pm \text{SEM} (\mu\text{M})^a$ (or % inhibition at $10 \mu\text{M}$)
ARL67156 75a		-H	-Br	0.973 ± 0.239^b , 1.19 ± 0.12^c <i>lit. value: 11.0 ± 3.0^{65}</i>
68a	-NH ₂		-Br	1.13 ± 0.23
69a		-H	-Br	33.1 ± 19.3
70a		-H	-Br	6.48 ± 2.60
71a		-H	-Br	4.04 ± 2.12
72a		-H	-Br	2.68 ± 1.11

Continued on the next page

Table 3.16 – continued from previous page

Compound	R ¹	R ²	-X	$K_i \pm \text{SEM} (\mu\text{M})^a$ (or % inhibition at 10 μM)
73a		-H	-Br	2.22 ± 0.02
76a			-Br	5.72 ± 0.86
77a			-Br	1.51 ± 0.40
78a			-Br	≈ 10 (54 ± 5 %)
79a			-Br	12.0 ± 0.7
80a			-Br	> 10 (39 ± 2 %)
81a			-Br	7.48 ± 1.29
116 ^d		-H	-Br	> 10 (4 ± 11 %)
117 ^d		-H	-Br	4.82 ± 0.21
β,γ -methylene-ATP ^e (118)	-NH ₂	-H	-H	> 10 (23 ± 6 %)
83	-NH ₂	-H	-Br	5.26 ± 0.22
84	-NH ₂	-H	-Cl	9.53 ± 1.46
85	-NH ₂	-H	-F	10.6 ± 0.4

^a SEM = standard error of the mean.

^b The K_i value was obtained with ARL67156 synthesized in our laboratory.

^c The K_i value was obtained with commercial ARL67156 from *Sigma* (Steinheim, Germany).

^d The compound was synthesized by Dr. The Hung Vu.

^e The compound was obtained from *Sigma* (Steinheim, Germany).

The results show that further derivatization of the diethyl-group at the N⁶-position, for example by shortening or prolongation of the alkyl substituents, did not improve inhibitory potency (69a-73a). In this series, substitution with dipropyl (72a) or ethylpropyl (73a) resulted in the two most potent compounds, but they were still weaker than the original diethyl substitution (75a).

The hybrid of ARL67156 and 8-BuS-AMP, 81a, had a seven-fold lower potency

then ARL67156. A combination of the β,γ -dibromomethylene-triphosphate group of ARL67156 with the 8-butylthio-group of 8-BuS-AMP (**68a**) showed a K_i value similar to that of ARL67156. Additional methylation at the N^6 -amino group (**80a**) led to a significant loss in inhibitory potency. However, replacement of the sulfur atom with a nitrogen atom (**77a**) increased the inhibitory potency and resulted in a K_i value similar to that of ARL67156. Interestingly, as soon as the N^6 -position was disubstituted as in **78a**, the inhibitory potency decreased.

Replacement of the butylamino group by a cyclopropylamino group (**76a**) at the 8-position led to a fourfold decrease in the inhibitory potency. Further studies of an aromatic substitution at the N^6 -position of ARL67156 showed that substitution of a benzyl group (**116**) abolished the inhibitory potency while substitution of a phenylethyl group resulted in a low micromolar inhibitory potency (**117**).

Additionally, structure-activity relationships of the triphosphonate-moiety were investigated. The unsubstituted β,γ -methylene group resulted in only 23% inhibition at 10 μM (**118**). Furthermore, the dealkylation of the N^6 -group of ARL67156 led to a fivefold decrease in the inhibitory potency compared with ARL67156 (**83**). The replacement of the dibromo substitution in the β,γ -position by dichloro (**84**) or difluoro groups (**85**) led to a two-fold reduction in inhibitory potency (compared with **83**).

Unfortunately, it has so far not been possible to identify a more potent inhibitor than ARL67156. Compounds **68a** and **77a** were the two most promising candidates with K_i values similar to that of ARL67156 (**75a**). Their concentration-inhibition curves are depicted in *Figure 3.3*.

3.4.2 Selectivity studies versus other *ecto*-nucleotidases

Compounds **68a**, **75a**, and **77a** were further investigated at other extracellular *ecto*-nucleotidases including NTPDase2, -3, and -8, NPP1, -3, -4, and -5, as well as CD73 (*Table 3.17*). In addition, compounds **68a**, **75a**, and **77a** were also evaluated on cyclic ADP ribose hydrolase (CD38), which is an extracellular *ecto*-nucleotidase expressed on various immune cells including CD4⁺, CD8⁺, B lymphocytes and natural killer cells.¹⁵¹ CD38 catalyzes the synthesis and hydrolysis of cyclic ADP-ribose (cADPR) from nicotinamide adenine dinucleotide⁺ (NAD⁺) to ADP-ribose (ADPR) as well as the synthesis of nicotinic acid adenine dinucleotide phosphate (NAADP) from

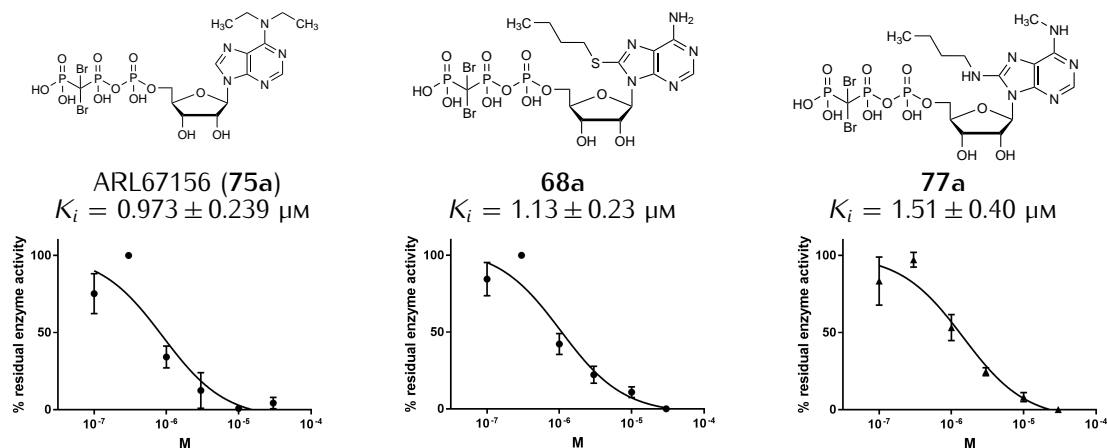


Figure 3.3: Concentration-inhibition curves of the most potent ARL67156 derivatives. The compounds were tested for inhibition of CD39 by using $0.5 \mu\text{M}$ FL-6-AMP as a substrate and human umbilical cord membrane preparations natively expressing CD39. Error bars represent the standard error of the mean (SEM) of three independent experiments performed by Dr. S. Lee.

nicotinamide adenine dinucleotide phosphate⁺ (NADP⁺).¹⁵¹ These selectivity studies were performed by Laura Schäkel, Vittoria Lopez, Salahuddin Mirza, and Riham Idris.

Table 3.17: Potency of ARL67156 derivatives at human NTPDase2, 3, and 8, NPP1-4, CD73, and CD38. IC₅₀ curves were approximated from the screening data and K_i values were calculated using the Cheng-Prusoff equation (Eq. 6.4.2). This analysis was performed by Laura Schäkel.

Enzyme	estimated $K_i \pm \text{SEM}^a (\mu\text{M})$ (or % inhibition)		
	75a	68a	77a
NTPDase1	0.973 ± 0.239	1.13 ± 0.23	1.51 ± 0.40
NTPDase2 ^b	90.5 ± 15.1	19.6 ± 1.1	48.3 ± 2.4
NTPDase3 ^b	26.3 ± 5.8	11.7 ± 5.0	12.3 ± 16.9
NTPDase8 ^b	1010 ± 981	225 ± 69	1232 ± 3275
NPP1 ^c	13.0 ± 0.7	12.4 ± 0.9	22.5 ± 3.2
NPP3 ^d	169 ± 29	138 ± 37	94.9 ± 22.6
NPP4 ^e	67.4 ± 9.0	116 ± 8	116 ± 8
NPP5 ^d	108 ± 23	134 ± 28	80.6 ± 10.1
CD73 ^f	6.83 ± 0.30	1.90 ± 0.00	3.97 ± 2.43
CD38 ^d	109 ± 14	137 ± 15	75.3 ± 16.4

^a SEM = standard error of the mean.

^b Three independent experiments at $50 \mu\text{M}$ and $100 \mu\text{M}$ test concentration.

^c Two independent experiments each in duplicate at $20 \mu\text{M}$ test concentration.

^d Two independent experiments each in duplicate at $10 \mu\text{M}$ and $100 \mu\text{M}$ test concentration.

^e Two independent experiments each in duplicate at $20 \mu\text{M}$ test concentration.

^f Three independent experiments each in duplicate at $50 \mu\text{M}$ test concentration.

For better comparability IC_{50} curves were approximated from the screening data and K_i values were estimated using the Cheng-Prusoff equation (Table 3.17 and Figure 3.4). ARL67156 is known to be an inhibitor of all NTPDases.⁶⁵ Therefore it is no surprise, that this test series confirmed ARL67156 (**75a**) and its derivatives **68a** and **77a** to be unselective towards NTPDase3. Surprisingly, ARL67156 was selective towards NTPDases2 and -8. Compound **68a** is approximately 17-fold less potent at NTPDase2 than at NTPDase1 while **77a** exhibits an approximately 30-fold lower K_i value at NTPDase2 than at NTPDase1. The activity of NTPDase8 was not inhibited by any of the compounds. Similar to this, NPP3-5, and CD38 were not significantly inhibited. NPP1 was moderately inhibited by each of the compounds with K_i values approximately 10- to 15-fold lower compared to NTPDase1. All three compounds were unselective towards CD73.

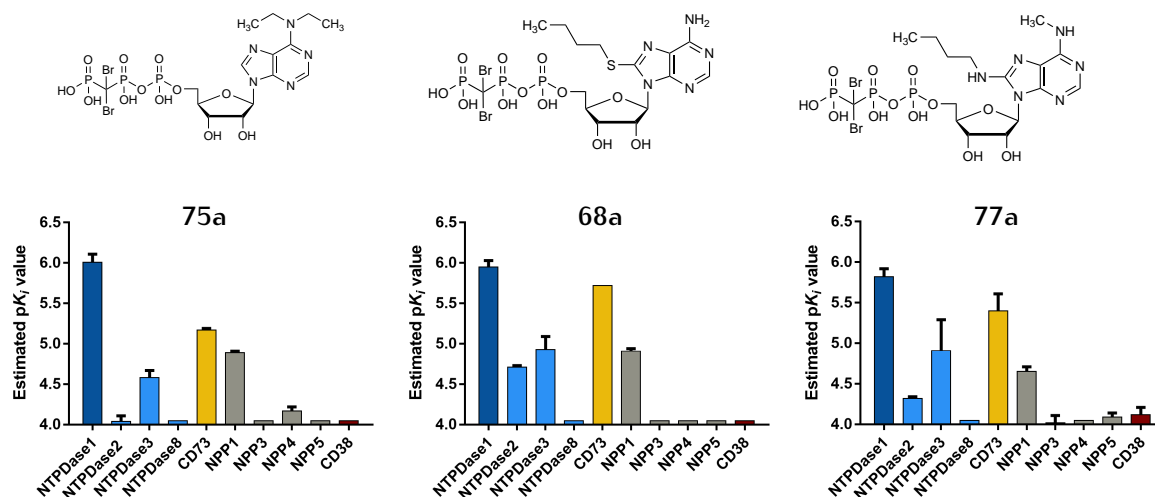


Figure 3.4: Selectivity of ARL67156-derived CD39 inhibitors. Inhibitory potency of ARL67156 (**75a**) and its derivatives **68a** and **77a** at human *ecto*-nucleotidases.

3.4.3 Metabolic stability of ARL67156-derivatives

In addition to K_i -determination and selectivity studies, the inhibitors **68a**, **75a**, and **77a** were studied for metabolic stability by *Pharmacelsus* (Saarbrücken, Germany), a preclinical contract research organization that develops and conducts pharmacological, biological and bioanalytical *in vitro* and *in vivo* testing.

All three compounds appeared to be metabolically unstable in the presence of mouse and human liver microsomes since the analytes could not be detected by LC/ESI-MS

analysis. To ensure that degradation was caused by microsomal enzymes and not due to chemical instability, the stock solutions were also analyzed by LC/ESI-MS analysis, and in all cases the desired mass was found. Since ARL67156 (**75a**) is commonly used as a CD39 inhibitor, these results are quite surprising, especially, because it has always been assumed in biological studies that ARL67156 is metabolically stable because of its β,γ -dibromomethylene-group.^{64,65}

3.5 Pharmacological evaluation of AMP-derivatives

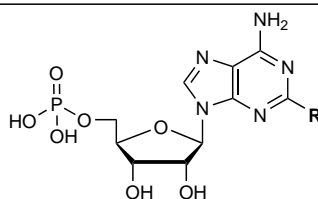
3.5.1 Inhibitory potency of AMP-derivatives

The synthesized AMP-derivatives (*Chapter 3.2 and 3.3*) were tested for their inhibitory potency at CD39 by applying the FFCE method, which was described in *Chapter 1.4.4*.¹¹⁵ The biological testing was done by Laura Schäkel, Sangyong Lee and Xihuan Luo.

3.5.1.1 Structure-activity relationships of C2-substituted AMP-derivatives

The obtained C2-substituted AMP derivatives were investigated for their inhibitory potency at human CD39 (*Table 3.18*).

Table 3.18: Potency of C2-substituted AMP derivatives as CD39 inhibitors. The test was performed by using 0.5 μM FL-ATP as a substrate and human umbilical cord membrane preparations natively expressing CD39.



Compound	R	$K_i \pm \text{SEM}$ (μM) ^a (or % inhibition at 10 μM)
AMP ^b	-H	> 10 (10 \pm 6 %)
87	-Cl	> 10
88	-NHNH ₂	> 10 (25 \pm 4 %)
103	-NH ₂	> 10 (6 \pm 3 %)

Continued on the next page

Table 3.18 – continued from previous page

Compound	R	$K_i \pm \text{SEM} (\mu\text{M})^a$ (or % inhibition at $10 \mu\text{M}$)
110	-SCH ₃	> 10

^a SEM = standard error of the mean.

^b The compound was obtained from *Sigma* (Steinheim, Germany).

Substitution with chloro (**87**), amino (**103**), and methylthio (**110**) at position 2 resulted in no inhibition of enzymatic activity at a high concentration of $10 \mu\text{M}$. In contrast, substitution with a hydrazine group (**88**) at that position led to weak inhibition of human CD39.

3.5.1.2 Structure-activity relationships of C8-substituted AMP-derivatives

The synthesized C8-substituted AMP derivatives were investigated for their inhibitory potency at human CD39 (Table 3.19). The 8-BuS-AMP (**68b**) synthesized in our laboratory showed a similar K_i value as reported in literature (Table 3.19).

Replacement of the sulfur atom at the 8-position of 8-BuS-AMP with nitrogen (**82b**) led to loss of the inhibitory potency (Table 3.19). Shortening of butylthio in **68b** to methylthio (**91**) resulted in a five-fold decrease in inhibitory potency. However, replacement of the sulfur atom of **91** with a nitrogen atom (**90**) increased inhibitory activity to a similar K_i value as that of 8-BuS-AMP.

Changing butylthio into a more bulky residue like (1-methyl)hexylthio (**92**) led to a more than tenfold decrease in potency. Substitution with a bulky amino substituent resulted in a compound with even less activity (**67b**). Replacement of the 8-butylthio group with a chlorine (**89**), bromine (**119**) or azido (**120**) group led to significantly reduced inhibitory potency. Surprisingly, substitution with *p*-chlorophenylthio (**121**) at position 8 gave a compound with similar inhibitory potency as observed for **91**.

Table 3.19: Potency of C8-substituted AMP derivatives as CD39 inhibitors. The test was performed by using 0.5 μM FL-ATP as a substrate and human umbilical cord membrane preparations natively expressing CD39.

Compound	R	$K_i \pm \text{SEM}$ (μM) ^a (or % inhibition at 10 μM)
8-BuS-AMP 68b		0.457 \pm 0.036 <i>lit. value:</i> 0.8 \pm 0.1 ⁶³
67b		> 10 (25 \pm 13%)
82b		> 10 (36 \pm 14%)
89	-Cl	7.30 \pm 0.81
90		0.660 \pm 0.072
91		2.22 \pm 0.31
92		5.91 \pm 1.32
119 ^b	-Br	\geq 10 (43 \pm 6%)
120 ^b	-N ₃	\approx 10 (49 \pm 10%)
121 ^b		2.67 \pm 0.81

^a SEM = standard error of the mean. ^b Purchased from *Biolog* (Bremen, Germany).

3.5.1.3 Structure-activity relationships of N^6 -substituted AMP-derivatives

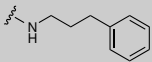
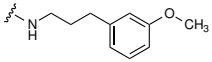
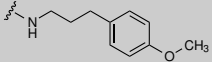
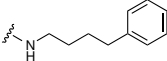
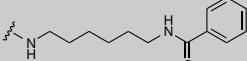
Next, a number of AMP derivatives with N^6 -modifications were investigated (*Table 3.20*). In general, (di)-alkylation of the N^6 -position (**69b-97**) resulted in no or only slight inhibition of human CD39. An exception was observed with the di-propyl derivative (**72**) which displayed 57% inhibition of the enzyme at 10 μM .

Table 3.20: Potency of N^6 -substituted AMP derivatives as CD39 inhibitors. The test was performed by using $0.5 \mu\text{M}$ FL-ATP as a substrate and human umbilical cord membrane preparations natively expressing CD39.

Compound	R	$K_i \pm \text{SEM} (\mu\text{M})^a$ (or % inhibition at $10 \mu\text{M}$)
69b		> 10
70b		> 10
71b		> 10
72b		15.5 ± 4.1
73b		> 10 ($13 \pm 8\%$)
75b		> 10 ($9 \pm 1\%$)
93		> 10
94		> 10 ($2 \pm 2\%$)
95		≥ 10 ($43 \pm 4\%$)
96		≥ 10 ($40 \pm 5\%$)
97		> 10 ($6 \pm 2\%$)
98		> 10 ($11 \pm 2\%$)
99		7.25 ± 1.52
100		≥ 10 ($47 \pm 5\%$)

Continued on the next page

Table 3.20 – continued from previous page

Compound	R	$K_i \pm \text{SEM} (\mu\text{M})^a$ (or % inhibition at $10 \mu\text{M}$)
111		> 10 ($14 \pm 6\%$)
112		> 10
113		> 10 ($13 \pm 1\%$)
114		1.40 ± 0.12
115		> 10 ($15 \pm 7\%$)

^a SEM = standard error of the mean.

An imidazolpropyl (**98**), or a phenylpropyl substitution with and without a methoxy group in the *meta*- or *para*-position of the ring (**111–113**) resulted in no significant inhibition of human CD39. Interestingly, a phenylbutyl-group instead of a phenylpropyl-group led to increased inhibitory activity with a K_i value of $1.40 \mu\text{M}$ (**114**). However, ethyl-substitution of the nitrogen atom of **114** (**99**) or its replacement by an oxygen atom (**100**) led to reduced inhibitory potency. The prolongation of the phenylbutyl-group and insertion of an amide group as in **115** also led to a loss of the inhibitory potency.

3.5.1.4 Structure-activity relationships of C8, N^6 -disubstituted AMP-derivatives

In addition to the C8- and the N^6 -monosubstituted AMP-derivatives, also a number of AMP derivatives with a combination of those modifications was investigated to study whether they are additive (Table 3.21). Most of the compounds described in this section were isolated as side products of the triphosphorylation reaction described in Chapter 3.2, and not based on the design of CD39 inhibitors.

Table 3.21: Potency of N^6 -C8-disubstituted AMP derivatives as CD39 inhibitors. The test was performed by using $0.5 \mu\text{M}$ FL-ATP as a substrate and human umbilical cord membrane preparations natively expressing CD39.

Compound	R ¹	R ²	$K_i \pm \text{SEM} (\mu\text{M})^a$ (or % inhibition at $10 \mu\text{M}$)
74b			> 10 ($17 \pm 4\%$)
77b			2.51 ± 0.40
79b			≥ 10 ($45 \pm 3\%$)
80b			1.83 ± 0.33
81b			4.56 ± 0.30
101			≥ 10 ($45 \pm 4\%$)
102			> 10 ($36 \pm 14\%$)

^a SEM = standard error of the mean.

Di-ethylation of 8-BuS-AMP at the N^6 -position like in ARL67156 (**81b**) resulted in a tenfold decrease of the inhibitory potency. Replacement of the sulfur atom with a nitrogen atom (**74b**) further decreased the inhibitory potency to 17% at the investigated concentration of $10 \mu\text{M}$. Interestingly, by losing one ethyl group at the N^6 -position (**102**), the inhibitory potency was increased to 36% at the investigated concentration. Those results are not surprising since the corresponding mono-substitutions of AMP (N^6 -diethyl, N^6 -ethyl, and 8-aminomethyl) also did not result in inhibitory potency. In case of **81b**, it seems as if the 8-substituent is rescuing the inhibitory potency. Combination of the mono-substitutions N^6 -methyl and 8-butylamino resulted in a compound which is only five-fold less potent than 8-BuS-AMP (**77b**), similar to the corresponding N^6 -methyl derivative (**80b**). A com-

ination of the diethyl group as in ARL67156 at the N^6 -position with a methyl-amino group at position 8 (**79b**) also did not result in the generation of a potent compound. A combination of di-methylation at the N^6 -position and introduction of a phenyl-butylamino group at the 8-position led to a decrease of potency (**101**).

3.5.1.5 Most potent AMP derivatives

Unfortunately, it was not possible to identify a more potent inhibitor than 8-BuS-AMP. The compounds **90** and **114** were the two most promising candidates with K_i values similar to that of 8-BuS-AMP (**68b**). The concentration-inhibition curves are depicted in *Figure 3.5*. At present, it is unclear whether a combination of the best C8- and N^6 -substitutions could be beneficial.

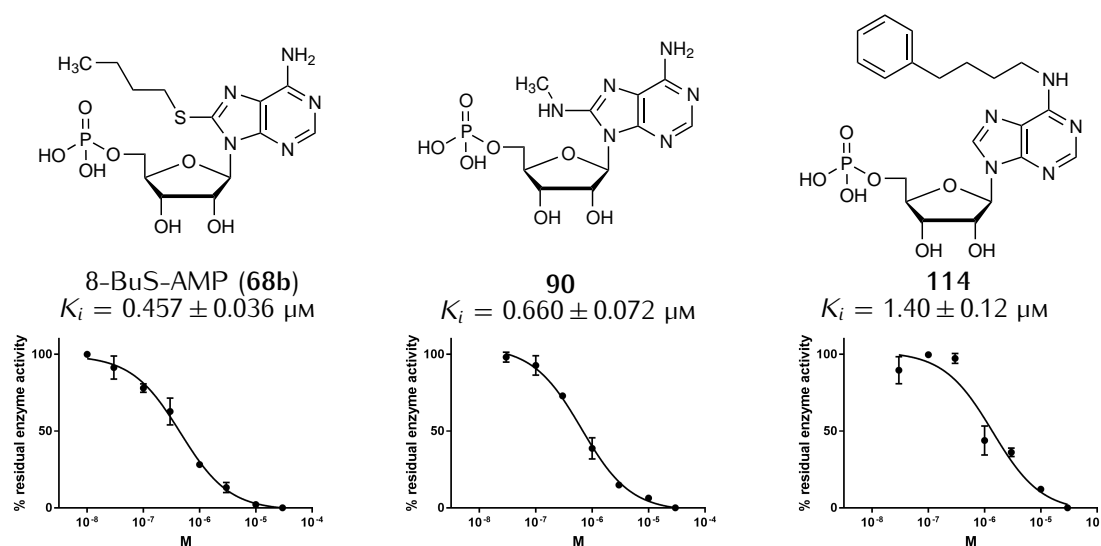


Figure 3.5: Concentration-inhibition curves of the most potent 8-BuS-AMP derivatives. The compounds were tested for inhibition of CD39 by using $0.5 \mu\text{M}$ FL-6-AMP as a substrate and human umbilical cord membrane preparation of CD39. Error bars represent the standard error of the mean (SEM) of three independent experiments performed by Dr. S. Lee.

3.5.2 Selectivity studies versus other *ecto*-nucleotidases

Compounds **68b**, **90**, and **114** were further investigated at other extracellular *ecto*-nucleotidases like NTPDase2, -3, and -8, NPP1, -3, -4, and -5, CD38, as well as CD73 (*Table 3.22*). The selectivity studies were performed by Laura Schäkel, Vittoria Lopez, Salahuddin Mirza, and Riham Idris.

Table 3.22: Potency of 8-BuS-AMP derivatives at human NTPDase2, 3, and 8, NPP1-4, CD73, and CD38. IC₅₀ curves were approximated from the screening data and K_i values were calculated with the Cheng-Prusoff equation (Eq. 6.4.2). This analysis was performed by Laura Schäkel.

Enzyme	estimated $K_i \pm \text{SEM}^a (\mu\text{M})$ (or % inhibition)		
	68b	90	114
NTPDase1	1.10 ± 0.67	0.660 ± 0.072	1.40 ± 0.12
NTPDase2 ^b	84.6 ± 42.2	529.1 ± 364.9	1.26 ± 0.65
NTPDase3 ^b	99.5 ± 45.0	65.5 ± 11.0	60.6 ± 3.5
NTPDase8 ^b	> 1000 (-18 %)	> 1000 (-15 %)	> 1000 (0 %)
NPP1 ^c	51.4 ± 2.1	29.5 ± 0.0	23.7 ± 7.6
NPP3 ^d	95.5 ± 34.3	171.9 ± 36.7	111.7 ± 34.2
NPP4 ^e	33.6 ± 10.8	35.6 ± 4.0	24.6 ± 1.1
NPP5 ^d	187.0 ± 42.0	206.6 ± 33.5	99.8 ± 14.6
CD73 ^f	6.2 ± 0.6	131.9 ± 3.3	0.46 ± 0.00
CD38 ^d	173.5 ± 29.9	227.6 ± 46.2	99.7 ± 13.4.

^a SEM = standard error of the mean.

^b Three independent experiments at 50 μM and 100 μM test concentration.

^c Two independent experiments each in duplicate at 20 μM test concentration.

^d Two independent experiments each in duplicate at 10 μM and 100 μM test concentration.

^e Two independent experiments each in duplicate at 20 μM test concentration.

^f Three independent experiments each in duplicate at 50 μM test concentration.

For better comparability, IC₅₀ curves were approximated from the screening data and K_i values were calculated using the Cheng-Prusoff equation and plotted (Figure 3.6).

8-BuS-AMP (**68b**) was selective towards NTPDase2, -3, and -8 but displayed a moderate effect on the activity of NPP1 and -4, while NPP3 and -5, and CD38 remained virtually unaffected. CD73, however, was strongly inhibited by **68b**. This is in contrast to what is described in literature since 8-BuS-AMP was reported to be inactive at NTPDase2, -3, and -8, and CD73, while NPP1 and -3 were found to be slightly inhibited.⁶³ Nevertheless, 8-BuS-AMP is still most potent at NTPDase1.

Compound **114** also shows a high inhibition of CD73 (99% at 50 μM), while compound **90** only causes moderate inhibition of CD73. Compound **114** strongly inhibits NTPDase2 and CD73, and moderately inhibits NTPDase3, and NPP1 and -4, while NTPDase8, NPP3 and -5, and CD38 remain unaffected. Compound **90** moderately inhibits NTPDase3, NPP1 and -4, and CD73 but is selective towards NTPDase2 and -8, NPP3 and -5, and CD38 and therefore appears to have the best selectivity

profile.

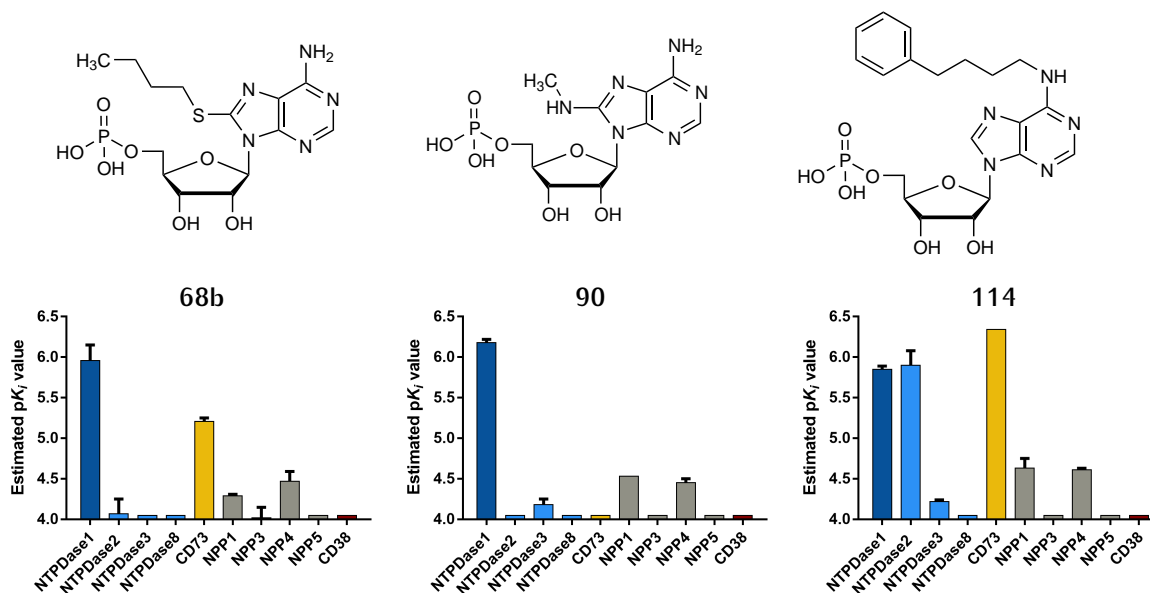
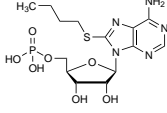
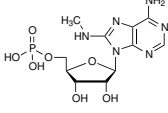
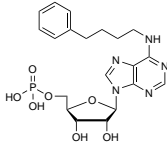


Figure 3.6: Selectivity of 8-BuS-AMP-derived CD39 inhibitors. Inhibitory potency of 8-BuS-AMP (**68b**) and its derivatives **90** and **114** at human *ecto*-nucleotidases.

3.5.3 Metabolic stability of AMP-derivatives

In addition to the K_i -determination and selectivity studies, compounds **68b**, **90**, and **114** were studied by *Pharmacelsus* (Saarbrücken, Germany) for metabolic stability in mouse and human liver microsomes. As can be seen in *Table 3.23*, 8-BuS-AMP (**68b**) is highly stable. In contrast, **90** is not stable at all, while **114** possesses some stability with a half-life of 15 and 6 min in the presence of mouse or human liver microsomes, respectively.

Table 3.23: Biological evaluation of 8-BuS-AMP-derived inhibitors for metabolic stability. 10 mM stock solutions were made in water. Microsomal stability was tested at a final concentration of 1 μ M (n = 2). $t_{1/2}$ = half-time. CL_{int} = internal clearance.

Compound	Reference	68b	90	114
Structures	Verapamil			
Metabolic Stability (mouse liver microsomes)				
$t_{1/2}$ (min)	5	> 60	n.a. ^a	15
CL_{int} (μ l/min/mg protein)	257.2	7.6	n.a. ^a	92.2
Metabolic Stability (human liver microsomes)				
$t_{1/2}$ (min)	10	> 60	n.a. ^a	6
CL_{int} (μ l/min/mg protein)	143.8	3.0	n.a. ^a	248.0

^an.a. = no analyte detected

4 Results and discussion – Part II: Synthesis of inhibitors and tool compounds for CD73

The second objective of this thesis is to develop various tool compounds for CD73 and to investigate a new class of compounds to develop novel CD73 inhibitors.

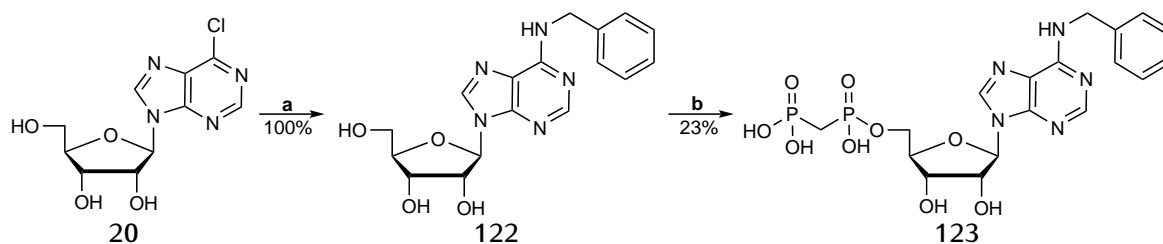
4.1 Upscaling of the synthesis of AOPCP derivatives

In the past, very potent and selective inhibitors of CD73 have been developed in our group.^{85,91} For a collaboration, two specific CD73 inhibitors needed be resynthesized, PSB-12379 and PSB-12489. Since they would like to conduct *in vivo* studies, they requested about 100 mg of each compound. Therefore, an upscaling and therefore modification of the existing synthesis route is needed. Parts of this chapter have been published in *Bhattarai et al. 2019*.⁹²

4.1.1 Synthesis of PSB-12379 (123)

The first compound that was resynthesized, is *N*⁶-benzyladenosine-5'-*O*-[(phosphonomethyl)phosphonic acid] (123, PSB-12379). The corresponding adenosine derivative 122 was synthesized starting from commercially available 20, which was reacted with *N*-benzylamine in the presence of triethylamine in absolute ethanol followed by purification by silica gel column chromatography (*Scheme 4.1*).⁹¹ Phosphonylation of 122 using methylenebis(phosphonic dichloride) followed by hydrolysis with aqueous TEAC buffer gave the desired AOPCP derivative 123.¹²⁸

To remove the trimethylphosphate, the crude reaction mixture was extracted with *tert.*-butylmethylether. The nucleoside was purified by HPLC on reverse-phase C18 material in order to remove inorganic phosphates and buffer components, which afforded the desired compound 123 with high purity.



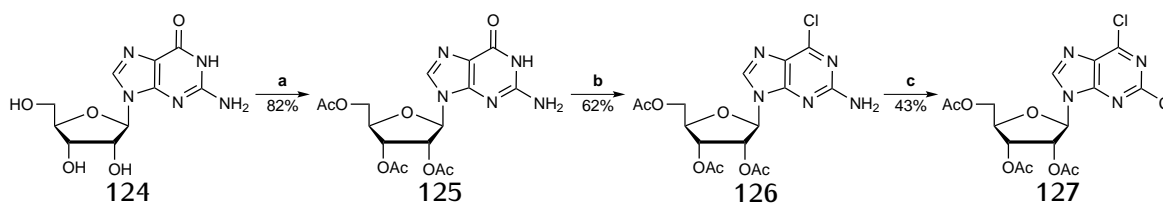
Scheme 4.1: Synthesis of PSB-12379 (123). Reagents and conditions: a) benzylamine, Et₃N, absolute EtOH, reflux, 4 h. b) two steps: I) methylenebis(phosphonic dichloride), PO(OCH₃)₃, argon, 0°C, 30 min; II) 0.5 M TEAC buffer pH 7.4-7.6, room temperature, 1 h.

The structures of the synthesized nucleoside and nucleotide were confirmed by ¹H- and ¹³C-NMR spectroscopy (Table 4.1 and Table 4.2), in addition to LC/ESI-MS performed in both positive and negative mode. The nucleotide was additionally investigated by ³¹P-NMR spectroscopy (Table 4.3).

4.1.2 Synthesis of 2,6-dichloro-9-(2',3',5'-tri-*O*-acetyl-β-D-ribofuranosyl)-purine

For the synthesis of the second compound, *N*⁶-benzyl-2-chloro-*N*⁶-methyladenosine-5'-*O*-[(phosphonomethyl)-phosphonic acid] (135, PSB-12489), the starting material, 2,6-dichloropurine-ribofuranoside, is not commercially available but has to be synthesized.

The common method for the synthesis of 2,6-dichloropurine-nucleosides used in our laboratory involves four steps: (1) protection of guanosine, (2) chlorination at C6-position, (3) chlorination at C2-position, and (4) deprotection (Scheme 4.2).^{85,152-154}



Scheme 4.2: Synthesis of 2,6-dichloropurine-ribofuranoside. Reagents and conditions: a) 4-dimethylaminopyridine (DMAP), acetonitrile, *N,N*-dimethylethylamine, room temperature, 15 min. b) two steps: I) *N,N*-dimethylaniline, tetraethylammonium chloride, phosphoryl chloride, room temperature, 7 min, argon II) 90°C, 13 min. c) acetyl chloride, anhydrous DCM, benzyltriethylammonium nitrite (BETA-NO₂), 0-4°C, argon, 5 h.

The chlorination of the keto-functional group at the 6-position of guanosine requires

protection at the 2'-, 3'-, and 5'-hydroxyl groups as they are all susceptible to chlorination. As protecting group, acetyl was chosen, because it can be removed under mild alkaline conditions since nucleosides are unstable in highly acidic medium. Protection of the 2'-, 3'-, and 5'-hydroxyl groups of guanosine was carried out using acetic anhydride, DMAP and *N*-ethyl dimethylamine at 40°C for one hour to achieve **125** (*Scheme 4.2*).¹⁵² Acetic anhydride is a versatile reagent for acylation. Bases such as DMAP and pyridine function as catalysts in the acylation reaction. The excess of acetic anhydride was quenched after the completion of the reaction by adding ice and stirring for additional 30 minutes. The resulting product was obtained by extraction with dichloromethane in high yield and purity.

Compound **125** was then chlorinated at the 6-position to give 2-amino-6-chloro-2',3',5'-*O*-acetyl-purine riboside (**126**) using phosphorus oxychloride, *N,N*-dimethylaniline and tetraethylammonium chloride followed by purification by silica gel column chromatography (*Scheme 4.2*).¹⁵³

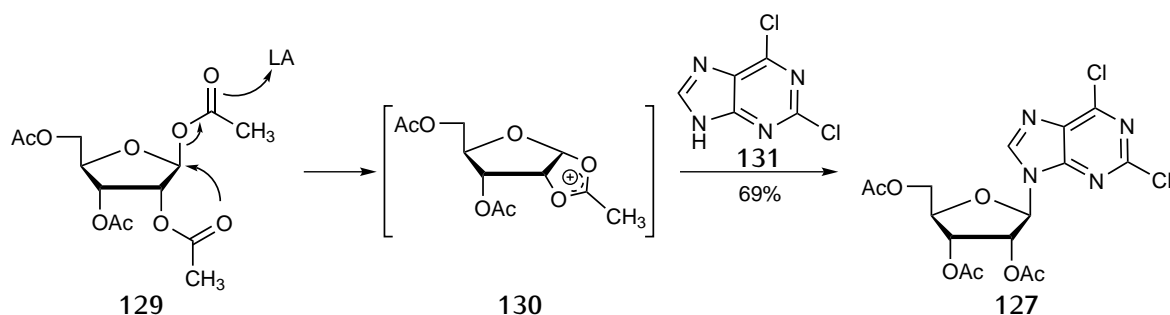
Compound **126** was converted into 2,6-dichloro-2',3',5'-tri-*O*-acetyl purine riboside (**127**) via a Sandmeyer reaction, which utilizes diazonium salts to convert anilines to aryl chlorides.¹⁵⁵ The aromatic amino group is converted to a diazonium salt by BETA-NO₂ (**128**) followed by its displacement with a nucleophile, in this case acetyl chloride, resulting in the formation of a halide (*Scheme 4.2*).¹⁵⁴ BETA-NO₂ is not commercially available so it is prepared from the benzyltriethylammonium chloride by replacing chloride with nitrate using ion exchanger. Compound **127** was purified by silica gel column chromatography and obtained in moderate yield.

The above described method for the synthesis of **127** is labor-intensive, and dangerous to apply due to the huge amount of phosphorus oxychloride used in the second step. Phosphorus oxychloride is on the list of extremely hazardous substances¹ because it is corrosive and reactive. It reacts violently with water and moisture and is not compatible with a list of chemicals including alcohols. After applying the previous method a couple of times with only moderate yield over three steps, another way to synthesize **127** was tested, the fusion method. In this method, a melt of C'-1 acetoxysugar is reacted with the purine base in presence of a Lewis acid as catalyst under reduced pressure to give the desired acylated nucleoside via

¹As defined in Section 302 of the U.S. Emergency Planning and Community Right-to-Know Act (42 U.S.C. 11002). The list can be found as an appendix to 40 C.F.R. 355. Updates as of 2006 can be seen on the Federal Register, 71 FR 47121 (August 16, 2006)

an *in situ* made C'-1 halosugar (Scheme 4.3).¹⁵⁶ As Lewis acid trifluoromethanesulfonic acid (CF₃SO₃H) was used. This method works best for purines that contain electron-withdrawing groups and have low melting points.

For the stereochemical control, neighbouring group participation plays an important role. Ionization of the leaving group at C'-1 of the sugar leads to the formation of a carbocation that is then captured by the carbonyl group of the adjacent acyl group to form an acyloxonium ion (**130**) on the lower face of the sugar.¹⁵⁶ Next, nucleophilic displacement of the base (**131**) occurs from the opposite site, which gives the natural β -anomer.¹⁵⁶ Since the formation of the acyloxonium ion is independent of the initial configuration of the sugar, this allows good stereocontrol.¹⁵⁶ This phenomenon is known as *Baker's 1,2-trans rule*.



Scheme 4.3: Nucleoside condensation reaction. LA = Lewis acid. Reagents and conditions: CF₃SO₃H, 0.9 bar, 1 h, 85°C → room temperature.

By applying the fusion method, acetylated 2,6-dichloropurine-ribofuranoside (**127**) was obtained with good yield and high purity after recrystallization from absolute ethanol. No further purification was needed, which makes this an excellent procedure for the synthesis on a higher scale. The β -conformation of the nucleoside was further confirmed by rotating frame Overhauser effect spectroscopy (ROESY)-NMR analysis (Figure 4.1).

4.1.3 Synthesis of PSB-12489 (**135**)

Going back to the synthesis of PSB-12489 (**135**), the next step is the deprotection of **127** with sodium methoxide in methanol. This, however, did not result in the formation of 2,6-dichloropurine-ribose (**132**). Instead, the chloro groups were replaced by methoxy groups giving 2,6-dimethoxy-9- β -D-ribofuranosylpurine (**133**) with high yield (Scheme 4.4). The chloro-group at the C6-position is less stable

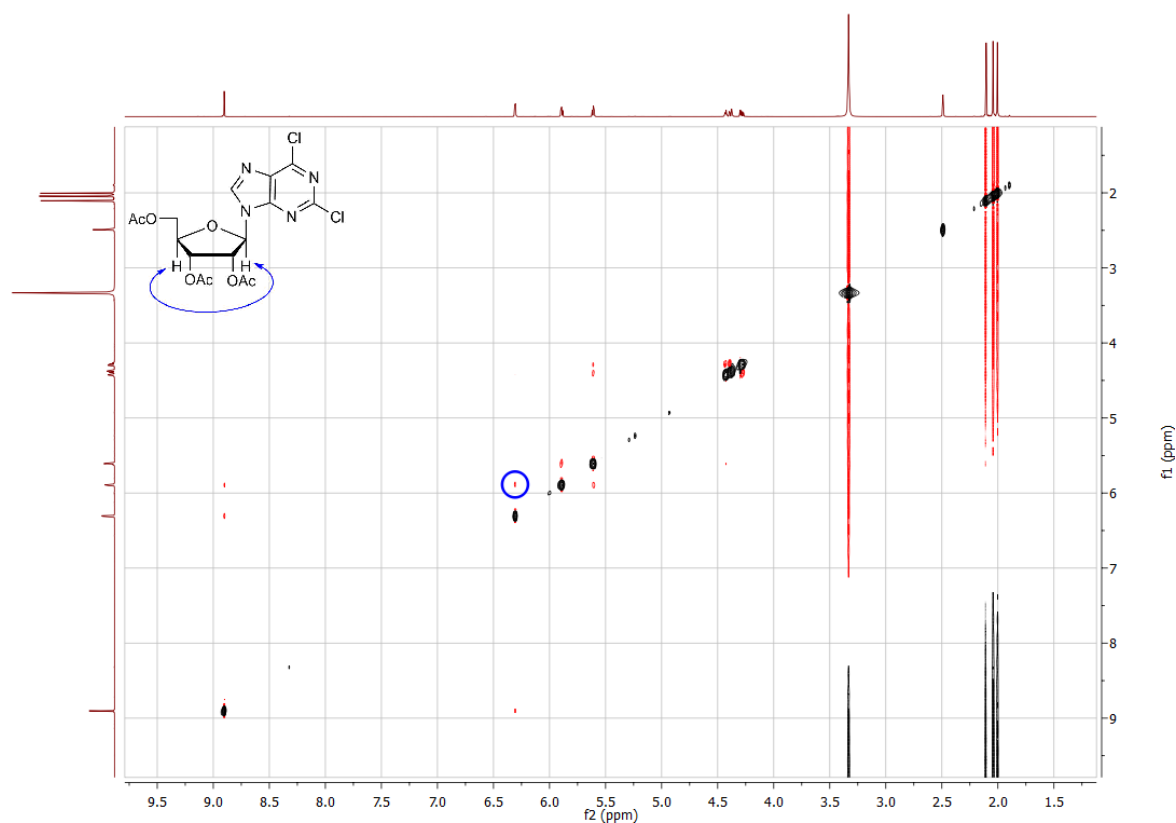
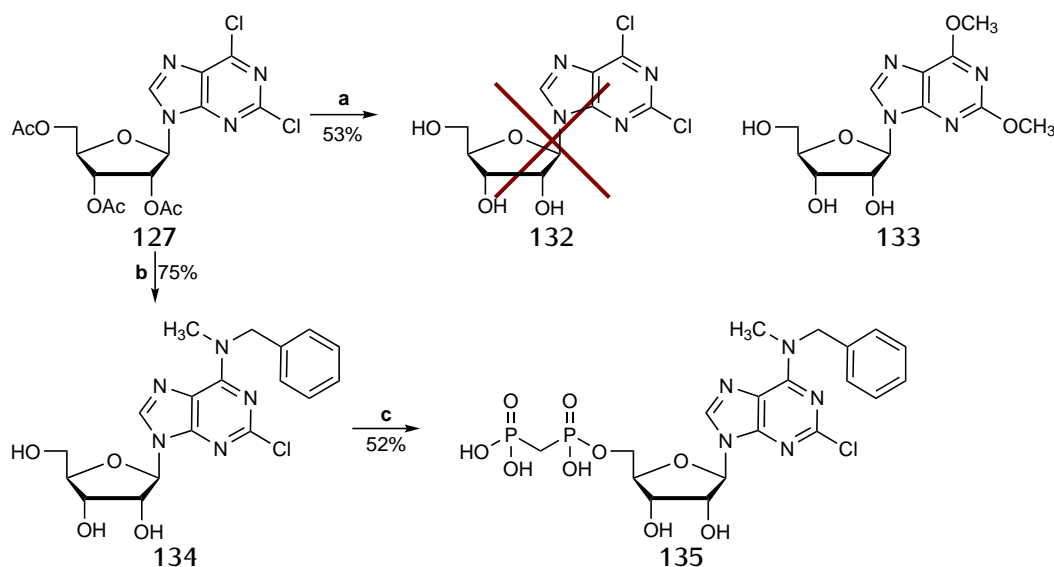


Figure 4.1: ROESY-NMR spectrum of **127**. The coupling of the C'1-H and the C'4-H is circled in blue.

than at the C2-position. Therefore, the 6-chloro group is often replaced during deprotection reaction, like for example by an amino group upon deprotection with ammonia in ethanol.¹⁵⁷ To prevent this, **127** was substituted first at the C6-position with *N*-benzylmethylamine in the presence of triethylamine in absolute ethanol. LC/ESI-MS-analysis revealed, that during the coupling reaction, partial deprotection of the acetyl groups took place. This is in agreement with the findings of Meier *et al.* who described a fast deprotection method for nucleosides based on a triethylamine-catalyzed methanolysis of acetate in aqueous medium.¹⁵⁸ Therefore, prior to purification by silica gel column chromatography, the crude mixture was first reacted with sodium methoxide in methanol to achieve full deprotection.

Interestingly, next to the desired product **134**, also the 2,6-disubstituted compound was obtained. These two compounds appear as one spot on thin layer chromatography and therefore, separation by column chromatography was, unfortunately, not successful after several attempts. Because of this, reverse phase HPLC was used



Scheme 4.4: Synthesis of PSB-12489 (135). Reagents and conditions: a) 2% NaOMe, methanol, room temperature, 10 min. b) two steps: I) *N*-benzylmethylamine, Et₃N, absolute EtOH, reflux, 5h. II) 0.5% NaOCH₃, methanol, room temperature, 10 min. b) two steps: I) methylenebis(phosphonic dichloride), PO(OCH₃)₃, 0°C, 30 min II) 0.5 M TEAC buffer pH 7.4-7.6, room temperature, 1 h.

for purification. Establishment of a proper method was somehow difficult, since the two products elute around 90% of methanol in water. Finally, it was found that only when starting the gradient at a low concentration of methanol (20% in water) followed by an isocratic phase at 90% methanol in water, separation was achieved yielding the desired compound **134** in pure form.

As a final step, phosphorylation of **134** was achieved using methylenebis(phosphonic dichloride) in trimethylphosphate followed by hydrolysis with aqueous TEAC buffer. To remove the trimethylphosphate, the crude reaction mixture was extracted with *tert.*-butylmethylether. Purification by HPLC on reverse-phase C18 material in order to remove inorganic phosphates gave the desired AOPCP derivative **135**.¹²⁸

The structure of the synthesized nucleosides and nucleotide was confirmed by ¹H- and ¹³C-NMR spectroscopy (Table 4.1 and Table 4.2), in addition to LC/ESI-MS performed in both positive and negative mode. The nucleotide was additionally investigated by ³¹P-NMR spectroscopy (Table 4.3). In the ¹³C-NMR spectra of **134** and **135** not all peaks from the purine base and the *N*⁶-substituents are visible although all protons are visible in the ¹H-NMR spectra and the correct mass was found by LC/ESI-MS analysis. This phenomenon was often observed when disubstituted adenosine derivatives were analyzed, as mentioned in Chapter 3.1.3.

Table 4.1: $^1\text{H-NMR}$ data of PSB-12379 and PSB 12489 and the corresponding adenosine derivatives. Shifts (δ) in $\text{DMSO-d}_6^\#$ or D_2O^* [ppm]. Next to the signals of the substituents, a selection of characteristic ribose and purine protons is depicted.

Compound	Substituents	C'1-H	C'5-H ₂	C2-H	C8-H	N ⁶ -substituents	$\alpha,\beta\text{-CH}_2$
122 [#]	N ⁶ -benzyl	5.89	3.68-3.53	8.19	8.36	7.45-7.18 (aryl), 3.95 (NHCH ₂)	-
123 [*]	N ⁶ -benzyl	6.11	4.17	8.20	8.50	7.40-7.29 (aryl), 4.77 (NHCH ₂)	2.21
134 [#]	2-chloro-N ⁶ ,N ⁶ -benzylmethyl	5.85	3.67-3.52	-	8.42	7.34-7.26 (aryl), 3.16 (NCH ₂), 3.10 (NCH ₃)	-
135 [*]	2-chloro-N ⁶ ,N ⁶ -benzylmethyl	6.05	4.17	-	8.40	7.32 (aryl), 5.31 (NCH ₂), (NCH ₃)	2.20

Table 4.2: $^{13}\text{C-NMR}$ data of PSB-12379 and PSB 12489 and the corresponding adenosine derivatives. Shifts (δ) in $\text{DMSO-d}_6^\#$ or D_2O^* [ppm]. Next to the signals of the substituents, a selection of characteristic ribose and purine carbons is depicted.

Compound	Substituents	C'1	C'5	C2	C8	N ⁶ -substituents	$\alpha,\beta\text{-CH}_2$
122 [#]	N ⁶ -benzyl	88.07	61.78	152.42	140.00	135.97, 128.67, 128.61, 128.31, 128.15, 127.24 (aryl), 42.90 (NHCH ₂)	-
123 [*]	N ⁶ -benzyl	89.74	66.26	155.70	142.27	141.22, 135.50, 131.88, 131.57, 130.18, 129.77 (aryl), 45.86 (NHCH ₂)	30.69
134 [#]	2-chloro-N ⁶ ,N ⁶ -benzylmethyl	87.46	61.42	152.76	139.18	128.75, 127.44, 118.60 (aryl), 56.16 (NCH ₂), 18.67 (NCH ₃)	-
135 [*]	2-chloro-N ⁶ ,N ⁶ -benzylmethyl	89.74	66.41	153.86	141.12	139.58, 131.67, 130.48, 130.11 (aryl), 49.49 (NCH ₂), 11.06 (NCH ₃)	30.18

Table 4.3: ^{31}P -NMR data of PSB-12379 and PSB 12489. Shifts (δ) in D_2O [ppm].

Compound	Substituents	P_α	P_β
123	N^6 -benzyl	14.53	19.12
135	2-chloro- N^6, N^6 -benzylmethyl	15.47	18.46

4.2 Development of an AOPCP-derived radioligand for CD73

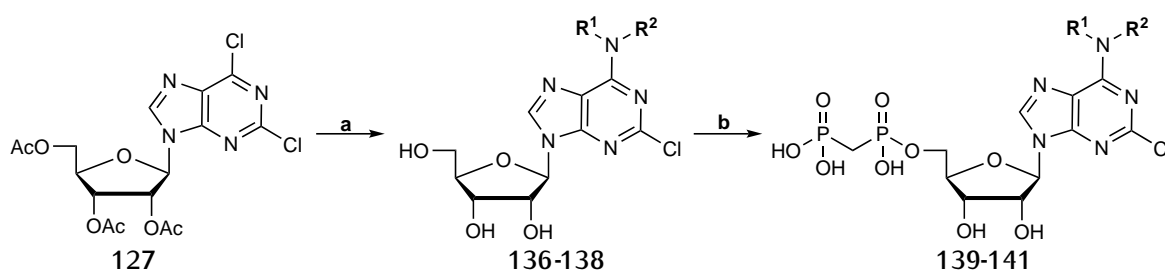
During the past years, potent and selective inhibitors of CD73 have been developed in our group. Based on these results, a radioligand will be developed. As radioactive label, tritium was chosen, which is the naturally occurring isotope of hydrogen, and is commonly used as radioactive label. The process of developing a radioligand involves several steps. First, "cold ligands" will be synthesized, which are not radioactively labeled. These cold ligands should ideally contain a functional group that can be easily labeled with tritium, like for example a propyl group. After biological evaluation, a suitable compound will be chosen and a precursor will be synthesized. In the case of a propyl group, this means that the same compound containing a propargyl-group will be synthesized. This precursor can then be submitted to catalytic hydrogenation with tritium gas to get the final so called "hot ligand".¹⁵⁹

4.2.1 Synthesis of various cold ligands

Based on previous results, different AOPCP-derived cold ligands (139–141) were designed. For the synthesis of these, acetyl-protected 2,6-dichloropurine-ribofuranoside (127) was used as starting material for the synthesis of the cold ligands. Compound 127 is not commercially available but has to be synthesized as described in Section 4.1.2. The C6-position was substituted with an N,N -dialkyl-amine in the presence of triethylamine in absolute ethanol followed by purification by silica gel column chromatography. After deprotection using sodium methoxide, the 2-chloro- N^6 -disubstituted nucleosides were phosphonylated using methylenebis(phosphonic dichloride) in trimethylphosphate followed by hydrolysis with aqueous TEAC buffer. To remove the trimethylphosphate, the crude reaction mixture was extracted with

tert.-butylmethylether. Purification by HPLC on reverse-phase C18 material in order to remove inorganic phosphates gave the desired AOPCP derivatives **139-141** (Scheme 4.5).¹²⁸

The structure of the synthesized nucleosides and nucleotide were confirmed by ¹H- and ¹³C-NMR spectroscopy (Table 4.7 and Table 4.8), in addition to LC/ESI-MS performed in both positive and negative mode. The nucleotide was additionally investigated by ³¹P-NMR spectroscopy (Table 4.6).



Product	-R ¹	-R ²	Yield
136			66%
139	-(CH ₂) ₂ CH ₃	-benzyl	91%
137	-CH ₃	-benzyl-(α -methyl)	58%
140		-benzyl-(α -methyl)	51%
138	-(CH ₂) ₂ CH ₃	-benzyl-(α -methyl)	13%
141		-benzyl-(α -methyl)	20%

Scheme 4.5: Synthesis of α,β -methylene-*N*⁶-disubstituted-2-chloro-ADP derivatives. Reagents and conditions: a) two steps: I) di-alkylamine, Et₃N, absolute EtOH, reflux, 5 h. II) 0.5% NaOCH₃, methanol, room temperature, 10 min. b) two steps: I) methylenebis(phosphonic dichloride), PO(OCH₃)₃, 0°C, 30 min II) 0.5 M TEAC buffer pH 7.4-7.6, room temperature, 1 h.

4.2.2 Pharmacological evaluation of the cold ligands

The previously described cold ligands were tested in a radiometric assay (Section 1.4.5) to determine the *K_i*-values for CD73 (Figure 4.2).¹²⁹ The biological testing was done by Christian Renn.

Compounds **140** and **141** both contain a chiral center in the *N*⁶-substituent and both compounds are probably obtained as racemic mixtures. The stereochemistry of the corresponding amines was, however, not defined by the supplier. Nevertheless, the stereochemistry does most likely not play an important role since Dr. Bhattarai, a previous member of our group, already investigated this matter. He synthesized *N*⁶-((*S*)-1-phenylethyl)-2-chloro AOPCP and *N*⁶-((*R*)-1-phenylethyl)-2-chloro AOPCP, and both compounds had similar *K_i* values with 0.92 nM and 1.12 nM, respectively.⁸⁵

Furthermore, **139** and **141** have similar K_i values although they only differ at the position of the chiral center in **141**. This also indicates that the stereochemistry does not play a role in this case.

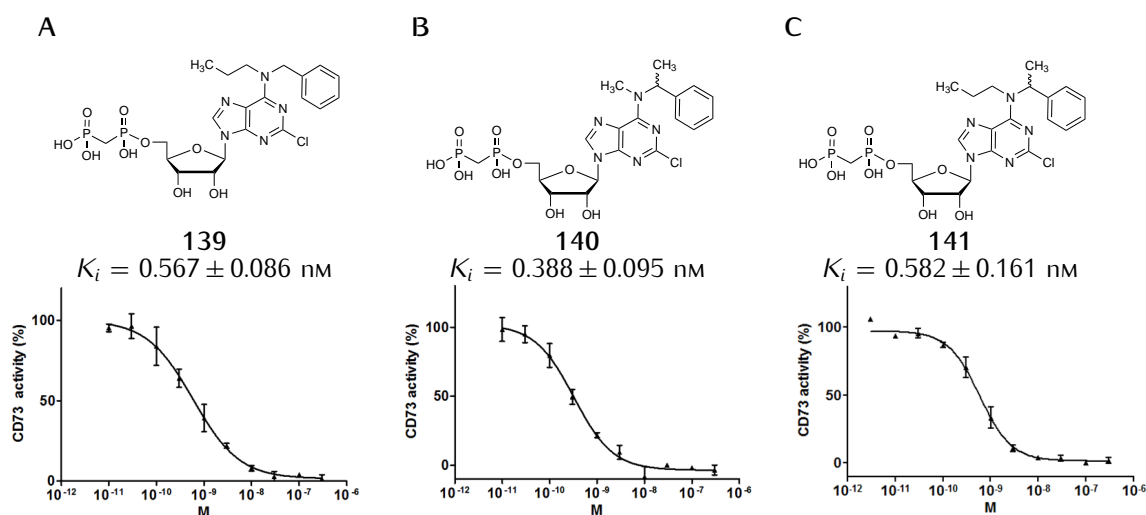


Figure 4.2: Potencies at rat CD73 of cold ligands. The compounds were tested for inhibition of CD73 by using $5 \mu\text{M}$ $[2,8\text{-}^3\text{H}]\text{AMP}$ as a substrate and soluble rat CD73. Depicted are the structures, the calculated K_i value, and the mean value concentration inhibition curves ($n = 3$) of each compound. Error bars represent the standard error of the mean (SEM).

In addition to the K_i -determinations, the compounds were sent to *Pharmacelsus* (Saarbrücken, Germany), a preclinical contract research organization that develops and conducts pharmacological, biological and bioanalytical *in vivo* and *in vitro* testing. All three cold ligands were tested for their metabolic stability in mouse and human liver microsomes. Furthermore, the plasma protein binding in human plasma was tested. As can be seen in *Table 4.4*, compounds **139**–**141** are metabolically highly stable but, unfortunately, also display a high plasma protein binding capacity.

The synthesized cold ligands all have a submicromolar potency against CD73 and are metabolically stable, and are therefore all suitable to develop a radioligand. Comparing the three compounds, it can be said, that the presence of a propyl-group is advantageous since a propargyl-group can be easily hydrogenated. Compounds **139** and **141** have very similar K_i values, but finally, **139** was chosen as suitable candidate because of the absence of a stereochemical center. Therefore, the potency of **139** was further evaluated at other preparations of CD73, including soluble human

Table 4.4: Biological evaluation of CD73 inhibitors (139-141) for their pharmacological properties. 10 mM stock solutions in water were made. Microsomal stability was tested with a final concentration of 1 μ M (n = 2). plasma protein binding (PPB) was tested with a final concentration of 10 μ M substrate (n = 2). $t_{1/2}$ = half-time. CL_{int} = internal clearance. SD = standard deviation

Compound	Reference	139	140	141
Metabolic Stability (Mouse)				
$t_{1/2}$ (min)	5 [‡]	7702	330	630
CL_{int} (μ l/min/mg protein)	263.1 [‡]	0.2	4.2	2.2
Metabolic Stability (Human)				
$t_{1/2}$ (min)	6 [‡]	> 60	> 60	> 60
CL_{int} (μ l/min/mg protein)	217.3 [‡]	-0.02	-2.8	-0.2
Plasma protein binding crossfiltration				
PPB (% \pm SD)*	97.3 \pm 0,01*	99.6 \pm 0.02	99.6 \pm 0.01	99.9 \pm 0.02

[‡]Reference item: Verapamil. *Mean value calculated from filtrate and retentate. *Reference item: Warfarin.

CD73 and CD73 obtained from membrane preparation of triple-negative breast cancer cells (MDA-MB-231), which natively express CD73. It was found that compound 139 is even more potent at human variants of CD73 as can be seen in Table 4.5.

Table 4.5: Inhibitory potency of 139 at different preparations of CD73.

Enzyme preparation	$K_i \pm$ SEM (nM) of 139
rat soluble CD73	0.567 \pm 0.086
human soluble CD73	0.073 \pm 0.001
human CD73 in MDA-MB-231 cell membranes	0.089 \pm 0.010

The compound was tested using 5 μ M [2,8-³H]AMP as a substrate.

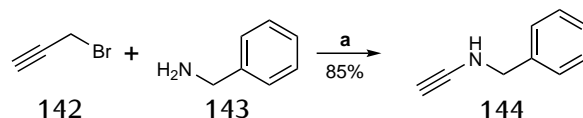
4.2.3 Synthesis of the radioligand precursor

Compound 139 was chosen as a template for the synthesis of the radioligand precursor. For the synthesis of the precursor, the corresponding propargylamine was first synthesized by stirring propargyl bromide (142) with benzylamine (143) overnight at room temperature (Scheme 4.6a).¹⁶⁰

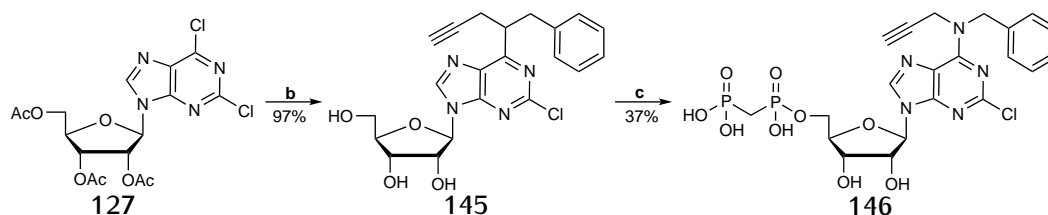
Next, the acetyl-protected 2,6-dichloropurine-ribofuranoside (127) was reacted with *N,N*-benzylpropargylamine 144 in the presence of triethylamine in absolute ethanol followed by purification by silica gel column chromatography as described before.⁹¹ After deprotection using sodium methoxide, 145 was phosphorylated using methylenebis(phosphonic dichloride) in trimethylphosphate followed by hydrolysis with aqueous TEAC buffer.⁹¹ To remove the trimethylphosphate, the crude reac-

tion mixture was extracted with *tert.*-butylmethylether. Purification by HPLC on reverse-phase C18 material in order to remove inorganic phosphates gave the desired AOPCP derivative **146** (Scheme 4.6b).

a Synthesis of propargylamine.



b Synthesis of radioligand precursor.



Scheme 4.6: Synthesis of 2-chloro- N^6,N^6 -benzylpropargyl AOPCP. Reagents and conditions: a) room temperature, overnight. b) two steps: I) **144**, Et_3N , absolute EtOH, reflux, 18 h. II) 0.5% NaOCH_3 , methanol, room temperature, overnight. c) two steps: I) methylenebis(phosphonic dichloride), $\text{PO}(\text{OCH}_3)_3$, 0°C , 30 min II) 0.5 M TEAC buffer pH 7.4–7.6, room temperature, 1 h.

The structures of the synthesized compounds were confirmed by ^1H - and ^{13}C -NMR spectroscopy (Table 4.7 and Table 4.8), in addition to LC/ESI-MS performed in both positive and negative mode. The nucleotide was additionally investigated by ^{31}P -NMR spectroscopy (Table 4.6).

Table 4.6: ^{31}P -NMR data of the cold ligands and the precursor. Shifts (δ) in D_2O [ppm].

Compound	N^6 -Substituents	P_α	P_β
139	N^6,N^6 -benzylpropyl	14.63	19.15
140	N^6,N^6 -(α -methyl)benzylmethyl	14.07	17.14
141	N^6,N^6 -(α -methyl)benzylpropyl	16.84	17.92
146	N^6,N^6 -benzylpropargyl	15.02	18.7

Table 4.7: $^1\text{H-NMR}$ data of the cold ligands, the precursor, and the corresponding adenosine derivatives. Shifts (δ) in $\text{DMSO-d}_6^\#$ or D_2O^* [ppm]. Next to the signals of the substituents, a selection of characteristic ribose and purine protons is depicted.

Compound	N^6 -Substituents	C'1-H	C'5-H ₂	C8-H	N^6 -substituents	α,β -CH ₂
136 [#]	N^6, N^6 -benzylpropyl	5.96	3.93-3.79	8.21	7.37-7.27 (aryl) 5.61 (1x NCH ₂) 5.04 (1x NCH ₂) 4.13 (1x NCH ₂) 3.64 (1x NCH ₂) 1.72 (CH ₂ CH ₂ CH ₃) 0.95 (CH ₂ CH ₃)	-
139*	N^6, N^6 -benzylpropyl	6.01	4.16	8.37	7.30-7.23 (aryl) 5.27 (NCH ₂) 3.93 (NCH ₂) 1.61 (CH ₂ CH ₂ CH ₃) 0.84 (CH ₂ CH ₃)	2.16
137 [#]	N^6, N^6 -(α -methyl)benzylmethyl	5.87	3.68-3.53	8.44	7.36-7.27 (aryl) 3.37 (NCH) 2.84 (NCH ₃) 1.62 (CHCH ₃) 1.08 (NCH ₃)	-
140*	N^6, N^6 -(α -methyl)benzylmethyl	6.06	4.18	8.43	7.39-7.31 (aryl) 3.19 (NCH) 3.02 (NCH ₃) 1.67 (CHCH ₃)	2.21
138 [#]	N^6, N^6 -(α -methyl)benzylpropyl	5.87	3.66-3.53	8.43	7.38-7.26 (aryl) 3.13 (NCH), 1.64 (CHCH ₃), 1.39 (CH ₂ CH ₃) 0.74 (CH ₂ CH ₃)	-
141*	N^6, N^6 -(α -methyl)benzylpropyl	6.01	4.15	8.36	7.21 (aryl) 3.35 (N(CH)CH ₂) 1.57 (CHCH ₃) 1.28 (CH ₂ CH ₂ CH ₃) 0.63 (CH ₂ CH ₃)	2.26
145 [#]	N^6, N^6 -benzylpropagyl	5.88	3.67-3.52	8.50	7.3 (aryl) 5.6 + 4.39 (N(CH ₂) ₂), 3.72 (C \equiv CH) 3.26 + 3.22 (N(CH ₂) ₂)	-
146 [#]	N^6, N^6 -benzylpropagyl	6.08	4.17	8.46	7.36 (aryl) 5.30 (NCH ₂) 4.65 (NCH ₂) 2.64 (C \equiv CH)	2.19

Table 4.8: ^{13}C -NMR data of the cold ligands, the precursor, and the corresponding adenosine derivatives. Shifts (δ) in $\text{DMSO-d}_6^\#$ or D_2O^* [ppm]. Next to the signals of the substituents, a selection of characteristic ribose and purine carbons is depicted.

Compound	N^6 -Substituents	C'1	C'5	C8	N^6 -substituents	α,β -CH ₂
136 [#]	N^6,N^6 -benzylpropyl	88.12	63.67	139.38	129.90, 129.17, 128.74, 120.79 (aryl), 22.83 (NCH ₂ -aryl), 21.58 (CH ₂), 15.73 (CH ₂), 11.48 (CH ₃)	-
139 [*]	N^6,N^6 -benzylpropyl	89.71	66.36	140.02	131.50, 130.26, 130.12, 120.78 (aryl), 55.64 (NCH ₂), 55.60 (NCH ₂), 27.95 (CH ₂), 13.10 (CH ₃)	30.37
137 [#]	N^6,N^6 -(α -methyl)benzylmethyl	87.47	65.04	139.00	128.70, 127.49, 127.02, 118.65 (aryl), 54.33 (NCH), 29.60 (CH ₃) 16.50 (CH ₃)	-
140 [*]	N^6,N^6 -(α -methyl)benzylmethyl	89.67	66.39	140.87	131.48, 130.44, 129.91, 121.08 (aryl), 57.83 (NCH), 18.70 (CH ₃), 11.06 (CH ₃)	30.19
138 [#]	N^6,N^6 -(α -methyl)benzylpropyl	87.42	61.46	139.39	128.60, 127.55, 127.32, 118.61 (aryl), 54.87 (NCH), 23.27 (CH ₂), 21.12 (CH ₂), 17.06 (CH ₃), 11.22 (CH ₃)	-
141 [*]	N^6,N^6 -(α -methyl)benzylpropyl	89.77	66.57	140.75	131.25, 130.35, 130.18, 120.95 (aryl), 49.10 (CH ₂), 22.16 (CH ₂), 19.13 (CH-aryl), 13.34 (CH ₃), 11.04 (CH ₃)	29.85
145 [#]	N^6,N^6 -benzylpropagyl	87.53	61.36	139.88	128.72, 128.25, 128.16, 127.60, 126.77, 118.65 (aryl) 73.89 (NCH ₂), 73.85 (C), 51.41 (CH) 36.77 (CH ₂)	-
146 [#]	N^6,N^6 -benzylpropagyl	89.81	66.41	139.25	131.66, 130.68, 130.57, 121.88 (aryl), 76.18 (NCH ₂), 73.09 (C), 54.39 (CH) 40.79 (CH ₂)	30.32

4.2.4 Generation of the tritium-labeled CD73 inhibitor

The precursor together with the cold ligand as a reference compound were sent to *RC TRITEC* (Teufen, Switzerland) for tritium labeling. The labeling was successful providing a new radioligand for ligand binding studies ($[^3\text{H}]\text{PSB-17230}$). According to the company, the radiochemical purity is $>99\%$, which means that more than 99% of the total radioactivity in the sample is present as the desired radiolabeled species (see *Figure 4.3*). The specific activity was determined to be 108 Ci/mmol (29.6 TBq/mmol) indicating the incorporation of almost four ^3H atoms per molecule.

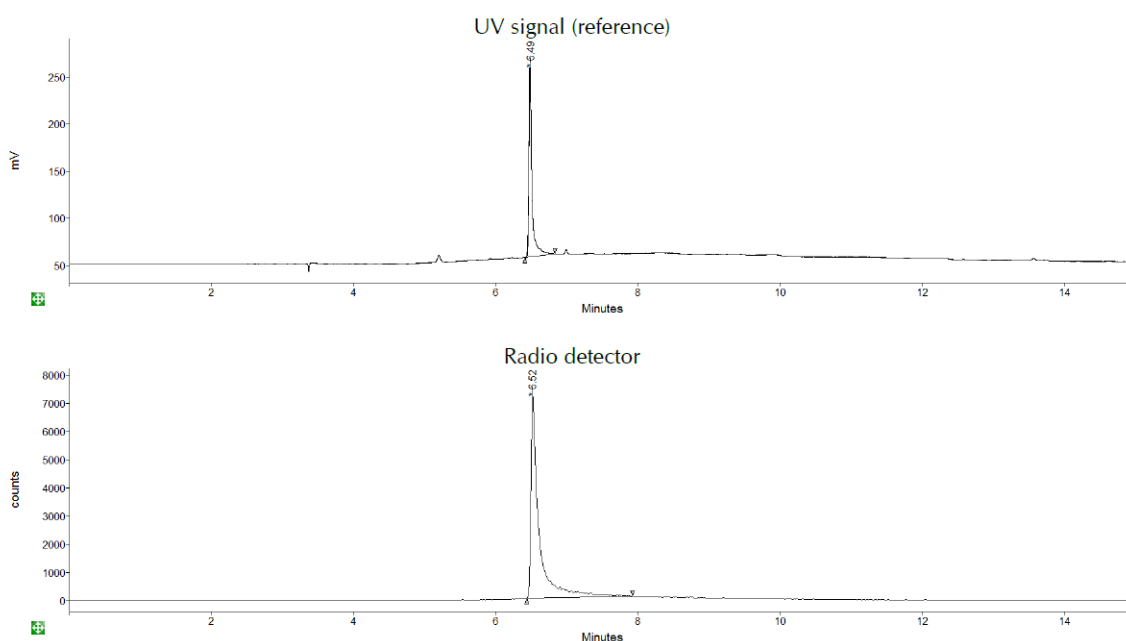


Figure 4.3: HPLC chromatogram after tritium labeling. Up: HPLC chromatogram of the cold ligand. Down: HPLC chromatogram of the hot ligand. HPLC program: 5-95% MeCN/10 mM NH_4OAc buffer pH 10 in 14.5 min, 1 ml/min.

4.3 Development of an AOPCP-derived fluorescent probe for CD73

4.3.1 Design of an AOPCP-derived fluorescent probe for CD73

To monitor the expression levels of CD73, a fluorescent probe molecule with a high binding affinity that can be used instead of an antibody, is highly desirable. The ADP analog α,β -methylene-ADP (AOPCP, $K_i = 88.4$ nM, human CD73) was the first described potent competitive inhibitor of CD73.^{84,91} Since its discovery, significantly more potent AOPCP-based inhibitors have been developed by our group that display high selectivity and metabolic stability.⁸⁵ One of these compounds, PSB-12651, was selected as a lead structure to develop potent fluorescent CD73 inhibitors with high binding affinity. The idea was to attach a fluorescent dye to the benzyl ring in the N^6 -position of the adenine core structure via a linker moiety (Figure 4.4). To optimize the binding properties of the target compounds, multiple factors have to be taken into account, including the linker length, the lipophilicity of the linker, the connection between the linker and the CD73 inhibitor, and the fluorophore. The obtained fluorescent CD73 inhibitors will be useful tools for research and diagnostic applications.

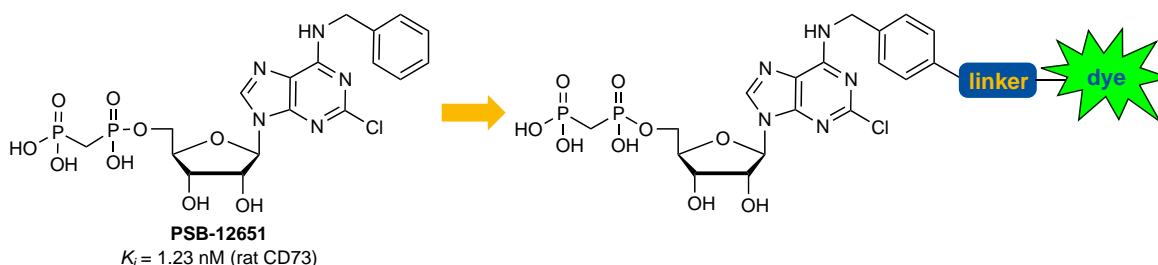


Figure 4.4: Design of an AOPCP-derived fluorescent probe for CD73. PSB-12651 will serve as lead structure for the development of a fluorescent probe.

As initial fluorophore fluorescein (**150**) was chosen. It was first described in 1871 by *von Bayer*.¹⁶¹ Fluorescein is a strongly fluorescent molecule with an absorption maximum at 492 nm and an emission maximum at 517 nm.¹⁶² Furthermore, fluorescein derivatives have a high quantum efficiency ($\varphi = 0.92$ at pH > 8.55).¹⁶² A major drawback of fluorescein is that in an aqueous environment, it can be present as cation, neutral, anion, or dianion depending on the pH.¹⁶³ The differently charged species possess different spectroscopic properties. The pK_a value of fluorescein is

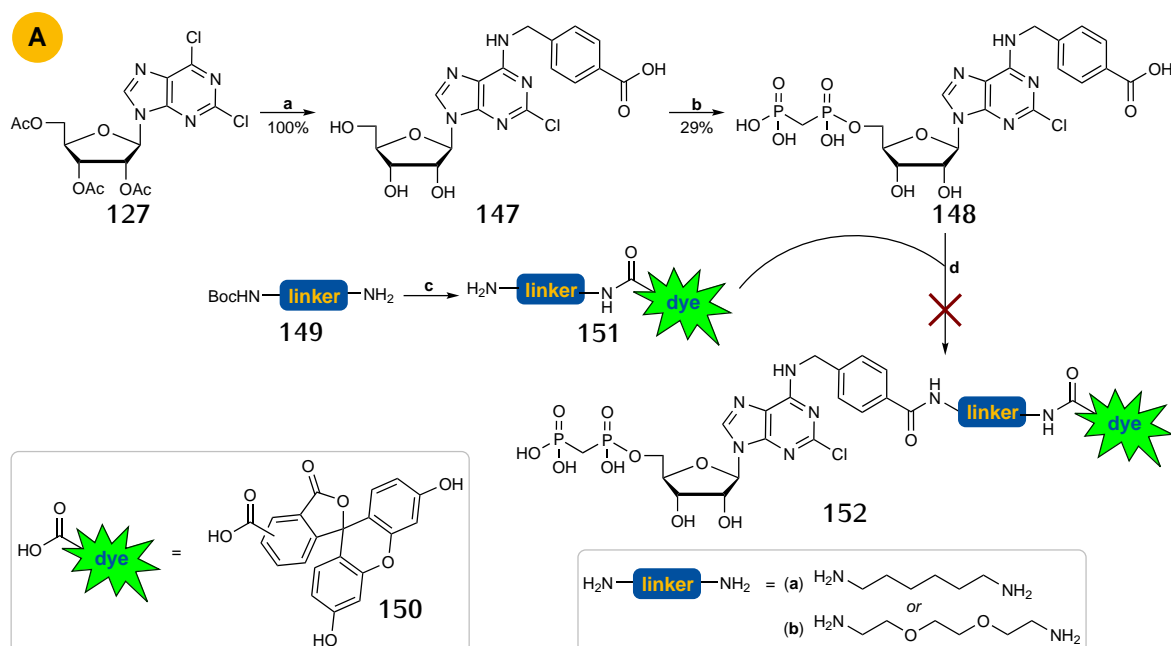
6.4 which is why at physiological pH, the majority of fluorescein is present in its instable yellow spirolacton form ($\varphi = 0.37$ at pH > 5.4).¹⁶³ Furthermore, fluorescein derivatives or conjugates possess a low photostability which leads to restrictions regarding the limit of detection.¹⁶⁴ Additionally, fluorescein conjugates have a broad emission spectrum which makes it difficult to study multiple targets at the same time with different dyes.¹⁶⁴ Nevertheless, fluorescein derivatives are suitable for biological experiments in which fluorescein is covalently attached to biomolecules such as nucleotides. However, it is not an ideal candidate due to its described properties. In the beginning, fluorescein was chosen as dye because it is commercially available and non-toxic, and therefore a good candidate for a first proof-of-principle study.

4.3.2 Synthesis route A

To synthesize **152**, acetyl-protected 2,6-dichloropurine-ribofuranoside (**127**) was used as starting material. For the first approach, **127** was first substituted at the C6-position with 4-(aminobenzyl)benzoic acid in the presence of triethylamine in absolute ethanol followed by purification by silica gel column chromatography (*Scheme 4.7*).⁹¹ After deprotection using sodium methoxide, the 2-chloro-*N*⁶-substituted nucleoside **147** was phosphorylated using methylenebis(phosphonic dichloride) in trimethylphosphate followed by hydrolysis with aqueous TEAC buffer.¹²⁸ To remove the trimethylphosphate, the crude reaction mixture was extracted with *tert.*-butylmethylether. Purification by HPLC on reverse-phase C18 material in order to remove inorganic phosphates gave the desired AOPCP derivative **148**.

Next, a Boc-protected linker molecule (**149**) was coupled to pre-activated 5(6)-carboxyfluorescein (**150**) with standard amide coupling reagents, including HOBt and DCC in anhydrous THF.¹⁴¹ Two different linker molecules were chosen, *N,N*-Boc-hexanediamine (**149a**) and *N*-Boc-2,2'-(ethylenedioxy)diethylamine (**149b**). These linker molecules differ in length and lipophilicity and will therefore allow structure-activity relationship studies on the final fluorescent probe molecules. Deprotection of the Boc-group could be achieved by treatment with 6-8% TFA in DCM in the presence of a catalytical amount of water yielding the labeled linker molecules **151a** and **151b**.¹⁴¹

Finally, the AOPCP-derivative **148** was tried to be coupled to the labeled linker molecules **151a** and **151b** after activation with HOBt and DCC.¹⁴¹ Unfortunately,



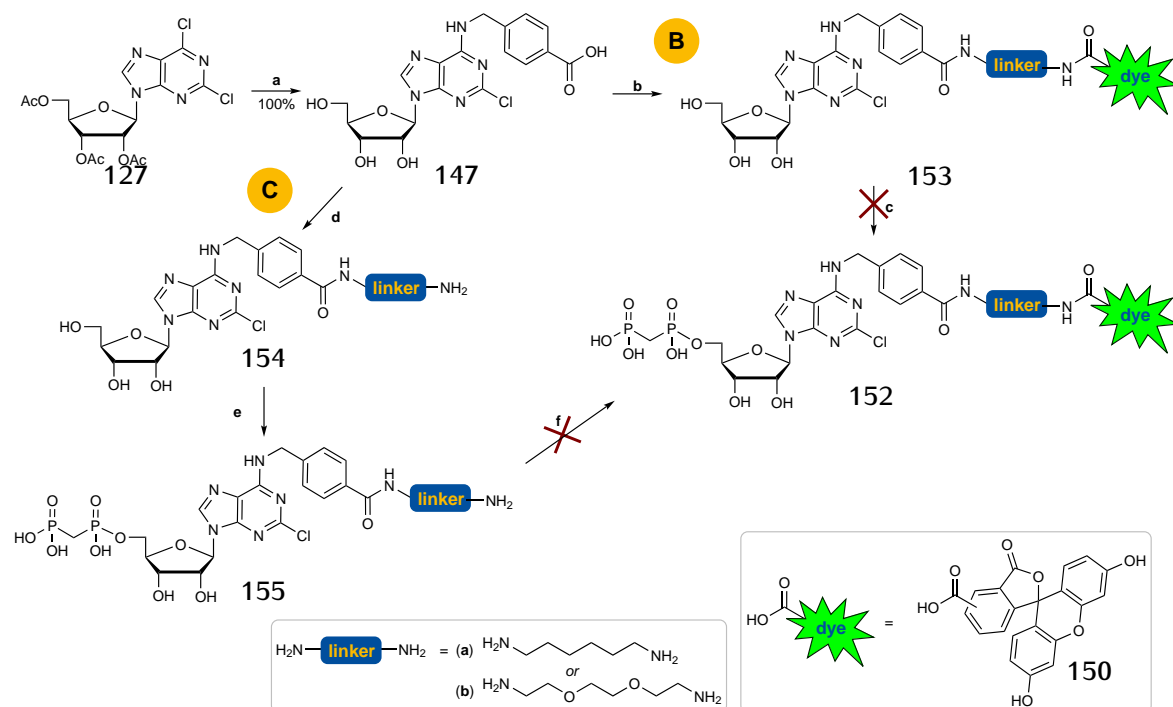
Scheme 4.7: Attempted synthesis route A to obtain 152. Reagents and conditions: a) 4-(aminomethyl)benzoic acid, Et_3N , absolute EtOH, reflux, 5 h. b) two steps: I) methylenebis(phosphonic dichloride), $\text{PO}(\text{OCH}_3)_3$, argon, 0°C , 30 min; II) 0.5 M TEAC buffer pH 7.4–7.6, room temperature, 1 h. c) two steps: I) 150, HOBt, DCC, THF, room temperature, overnight. II) 6–8% TFA in DCM, room temperature, 6 h. d) 151, HOBt, DCC, THF, room temperature, overnight.

the reaction did not take place according to LC/ESI-MS analysis. Only the starting materials of the reaction could be detected. The reactions were repeated in DMF instead of THF to improve the solubility of the phosphonate. Still, the reactions did not take place. Next to the solubility problems, the phosphonate group might also interfere with pre-activation of the carboxy-group. Therefore another approach was tested to synthesize 152.

4.3.3 Synthesis route B

For the second approach, 147 was coupled to the labeled-linker molecules 151a and 151b before the phosphonylation step (route B in Scheme 4.8). The amide coupling was performed as described before with HOBt and DCC in anhydrous THF.¹⁴¹ The desired products 153a and 153b were successfully obtained after purification by reverse phase HPLC (RP-HPLC).

Next, both compounds were submitted to phosphonylation using methylenebis(phos-



Scheme 4.8: Attempted synthesis routes B & C to obtain 152. Reagents and conditions: a) 4-(aminomethyl)benzoic acid, Et_3N , absolute EtOH, reflux, 5 h. b) **151**, HOBT, DCC, THF, room temperature, overnight. c) two steps: I) methylenebis(phosphonic dichloride), $\text{PO}(\text{OCH}_3)_3$, argon, 0°C , 30 min; II) 0.5 M TEAC buffer pH 7.4–7.6, room temperature, 1 h. d) two steps: I) **149**, HOBT, DCC, THF, room temperature, overnight. II) 6–8% TFA in DCM, room temperature, 6 h. e) two steps: I) methylenebis(phosphonic dichloride), $\text{PO}(\text{OCH}_3)_3$, argon, 0°C , 30 min; II) 0.5 M TEAC buffer pH 7.4–7.6, room temperature, 1 h. f) **150**, HOBT, DCC, THF, room temperature, overnight.

phonic dichloride) in trimethylphosphate followed by hydrolysis with aqueous TEAC buffer.¹²⁸ To remove the trimethylphosphate, the crude reaction mixture was extracted with *tert.*-butylmethylether. Purification by RP-HPLC gave, however, solely the starting compounds **153a** and **153b**.¹²⁸ The reason why the reaction did not take place, might be the insufficient solubility of the labeled nucleosides in trimethylphosphate.

4.3.4 Synthesis route C

Since it seems to be unbeneficial to have the carboxylic acid and the phosphonate present when performing an amide coupling, and because the labeled nucleoside is not soluble in trimethylphosphate which prevents phosphonylation, a third approach to obtain **152** was pursued (*route C in Scheme 4.8*). Again, **147** was used as starting

material. In the first step, it was coupled to only the Boc-protected linker molecules without the dye using the same coupling reagents as described before.¹⁴¹ After purification by silica gel chromatography, removal of the Boc-group was achieved by treatment with 6-8% TFA in DCM in the presence of a catalytical amount of water. Purification by RP-HPLC yielded the desired nucleosides **154a** and **154b**. Next, the nucleosides were phosphonylated using methylenebis(phosphonic dichloride) in trimethylphosphate followed by hydrolysis with aqueous TEAC buffer.¹²⁸ To remove the trimethylphosphate, the crude reaction mixture was extracted with *tert*-butylmethylether. Purification by RP-HPLC gave the desired nucleotides **155a** and **155b**.

In the final step, 5(6)-carboxyfluorescein (**150**) was pre-activated with HOBt and DCC in anhydrous THF, followed by the addition of **155** to get the desired compound **152**. LC/ESI-MS analysis, however, revealed, that again the reaction did not take place. Instead, a new isomer can be seen in the LC/ESI-MS, indicating that the fluorescein did react to form a side product with a mass of 391.1 in the positive mode. The difference in mass between 5(6)-carboxyfluorescein and the formed side product is 15, indicating that maybe a methyl group has attached to the dye. This phenomenon has already been observed before, when *N,N*-Boc-hexanediamine-HCl instead of *N,N*-Boc-hexanediamine was used for the coupling to 5(6)-carboxyfluorescein. This indicates that the presence of counter ions might interfere with the reaction process. Unfortunately, phosphates are usually present in complex with a counter ion.

4.3.5 Synthesis route D

The synthesis of an AOPCP-based fluorescent probe might be easier if not an amide coupling is used to attach the linker-dye construct but instead a nucleophilic substitution reaction using Et₃N and ethanol as described before. This, however, requires the phosphonylation of a 6-chloroadenosine derivative prior to the coupling of an amine to the C6-position, since phosphonylation of a labeled nucleoside was already shown to be unsuc-

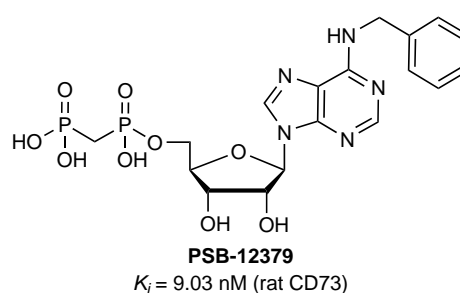
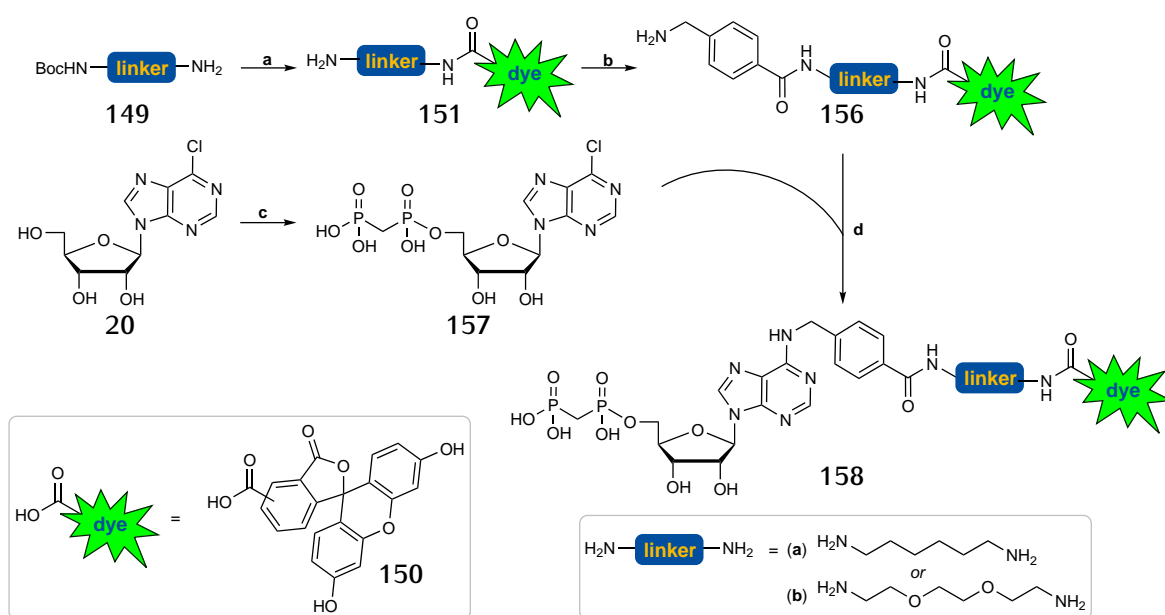


Figure 4.5: Structure of PSB-12379.

cessful (*route B in Scheme 4.8*). Phosphonylation also requires a free hydroxy-group at the 5'-position. As shown before, deprotection of 2',3',5'-tri-O-acetyl-2,6-dichloropurine-ribofuranoside (**127**) led to the generation of 2,6-dimethoxy-9- β -D-ribofuranosylpurine (**133**). PSB-12651, the lead structure for developing the fluorescent probe, is a derivative of PSB-12379. PSB-12379 has the same substitution at the N^6 -position but lacks the 2-chloro group (*Figure 4.5*). Its K_i value is still in the low nanomolar range with 9.03 nM at rat CD73. Therefore, it was chosen to synthesize a fluorescent probe without the 2-chloro group, making the nucleophilic substitution at the N^6 -position possible after phosphonylation.

For this purpose, the linker-dye constructs (**151a** and **151b**) were coupled to pre-activated 4-(Boc-aminobenzyl)benzoic acid using with HOBt and DCC in anhydrous THF followed by deprotection with 6-8% TFA in DCM in the presence of a catalytical amount of water (*Scheme 4.9*).¹⁴¹ Purification by RP-HPLC yielded the desired compounds **156a** and **156b**.



Scheme 4.9: Synthesis route to obtain **158**. Reagents and conditions: a) two steps: I) **150**, HOBt, DCC, THF, room temperature, overnight. II) 6-8% TFA in DCM, room temperature, 6 h. b) two steps: I) 4-(aminomethyl)benzoic acid, HOBt, DCC, THF, room temperature, overnight. II) 6-8% TFA in DCM, room temperature, 6 h. c) two steps: I) methylenebis(phosphonic dichloride), $\text{PO}(\text{OCH}_3)_3$, argon, 0°C, 30 min; II) 0.5M TEAC buffer pH 7.4-7.6, room temperature, 1 h. d) Et_3N , EtOH, reflux, overnight.

Table 4.9: $^1\text{H-NMR}$ data of fluorescent CD73 probe. Shifts (δ) in MeOD* or D₂O* [ppm]. Next to the signals of the substituents, a selection of characteristic ribose and purine protons is depicted.

	158a*	158b [‡]
C'1-H	6.13	6.09
C'5-H ₂	4.21	4.18
C8-H	8.61	8.30
N ⁶ -benzyl	7.75 (aryl) 7.50 (aryl) 3.45 (NHCH ₂ -aryl)	6.62 (aryl) 6.57 (aryl) 4.50 (NHCH ₂)
linker	3.05 (NHCH ₂) 2.87 (NHCH ₂) 1.50 (CH ₂) 1.44 (CH ₂) 1.36 (CH ₂) 0.97 (CH ₂)	3.73 (CH ₂) 3.63 (CH ₂) 3.60 (CH ₂) 3.51 (CH ₂) 3.45 (CH ₂) 3.25 (CH ₂)
fluorescein	8.33 + 7.64 (CH=CCO or CH=CH) 8.26 + 8.22 (C=CH) 7.98 + 7.35 (CH=CCO) 7.09 (2x C=CH) 6.60 (4x CHCOH)	7.88 (CH=CH) 7.52 (C=CH) 7.48 (C=CH) 7.27 (CH=CO) 7.20 (CH=CO) 7.06 (CH=COH) 7.03 (2x CH=COH)
α,β -CH ₂	2.51	2.17

Table 4.10: $^{13}\text{C-NMR}$ data of fluorescent CD73 probe. Shifts (δ) in MeOD* or D₂O* [ppm]. Next to the signals of the substituents, a selection of characteristic ribose and purine carbons is depicted.

	158a*	158b [‡]
C'1	88.76	90.06
C'5	64.73	66.39
C8	141.08	139.05
N ⁶ -benzyl	169.78, 141.96, 134.10, 129.03, 128.80, 54.11	161.19, 145.48, 134.11, 130.32, 129.98, 45.31
linker	49.15, 47.65, 30.16, 27.61, 27.40, 21.21	71.85, 71.67, 71.56, 71.47, 42.61, 42.17
fluorescein	182.43, 174.23, 174.04, 170.89, 170.24, 160.17, 159.73, 159.49, 137.17, 136.48, 135.98, 134.36, 132.44, 131.56, 130.59, 129.71, 129.20, 128.58, 124.44, 113.24, 104.81	176.62, 172.57, 171.74, 160.95, 160.77, 160.23, 160.11, 155.34, 137.31, 136.89, 136.17, 134.95, 134.30, 131.64, 131.19, 130.47, 116.04, 115.55, 106.47, 106.25
α,β -CH ₂	41.18	30.37

In parallel, 6-chloro- β -D-ribofuranosyl-purine (**20**) was phosphonylated using methylenebis(phosphonic dichloride) in trimethylphosphate followed by hydrolysis with aqueous TEAC buffer.¹²⁸ To remove the trimethylphosphate, the crude reaction mixture was extracted with *tert.*-butylmethylether. Purification by HPLC on reverse-phase C18 material in order to remove inorganic phosphates gave the desired AOPCP derivative **157**.

In the next step, **156a** or **156b** were coupled to **157** by reflux in absolute ethanol in the presence of a base.⁹¹ Finally, purification by RP-HPLC gave the desired products **158a** and **158b**.

The structures of the synthesized nucleotides were confirmed by ^1H -, ^{13}C -, and ^{31}P -NMR spectroscopy (*Table 4.9-Table 4.11*), in addition to LC/ESI-MS analysis performed in both positive and negative mode.

Table 4.11: ^{31}P -NMR data of fluorescent CD73 probe. Shifts (δ) in D_2O [ppm].

	158a	158b
P_α	11.35	14.96
P_β	20.51	18.88

4.3.6 Pharmacological evaluation of the fluorescent probes

Both fluorescent probes were tested in a radiometric assay (*Section 1.4.5*) to determine their K_i -values of CD73. The biological testing was done by Christian Renn and Riham Idris according to published procedure.¹²⁹ The inhibitory potencies of **158a** and **158b** were evaluated at soluble human CD73. Compound **158a** was additionally evaluated at a soluble rat CD73 and membrane preparations of triple-negative breast cancer cells (MDA-MB-231) which natively express CD73. The concentration-inhibition curves were plotted and the mean IC_{50} values from three independent experiments were used to calculate the K_i values (*Table 4.12*).

The inhibitory potency of the second fluorescent probe **158b** is fourfold lower than the potency of the first probe **158a** at human soluble CD73. This is probably due to the nature of the linker, which is more hydrophilic in **158b** than in **158a**. This leads to the conclusion that more lipophilic linker structures are better tolerated by CD73.

Table 4.12: Inhibitory potency of 158a and 158b at different enzyme preparations.

Enzyme preparation	$K_i \pm \text{SEM}$ [nM]	
	158a	158b
rat soluble CD73	26.0 ± 1.9	<i>n.d.</i>
human soluble CD73	2.98 ± 0.77	12.6 ± 0.7
human CD73 in MDA-MB-231 cell membranes	4.59 ± 1.18	<i>n.d.</i>

The compounds were tested using $5 \mu\text{M}$ [2,8- ^3H]AMP as a substrate. *n.d.* = *not determined*

Compound **158a** has a similar K_i -value at soluble human CD73 and membrane preparation of MDA-MB-231 cells. At rat CD73, the K_i -value is, however, eightfold lower.

4.3.7 Fluorescence emission and absorption spectra

As already mentioned, the spectroscopic properties of fluorescein rely heavily on the pH value of the reaction medium. Therefore, fluorescence absorption and emission spectra of both probes were recorded in the range from 300 to 800 nm in different media including water, phosphate-buffered saline (PBS) pH 7.4, which resembles a physiological pH, and sodium acetate buffer pH 4. The excitation wavelength was set corresponding to the absorbance maxima of the corresponding compound. It can be seen that the fluorescence intensity is low in water and almost abolished at pH 4 (*Figure 4.6A-4.6B*). The absolute data were subsequently normalized in order to determine the *Stokes shift* (*Figure 4.6C-4.6D*).

Table 4.13: Measured absorption and emission maxima and calculated *Stokes shift* of **158a** and **158b**. The excitation wavelength was set corresponding to the absorbance maxima of the corresponding compound.

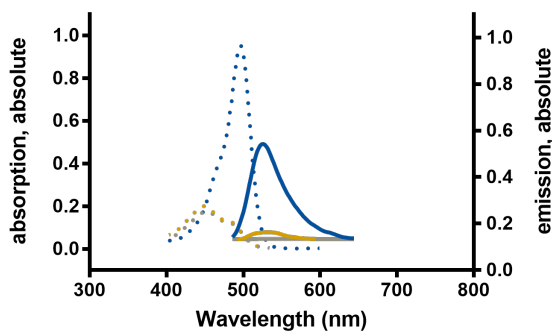
Medium	158a			158b		
	λ_{ex} (nm)	λ_{em} (nm)	λ_{S} (nm)	λ_{ex} (nm)	λ_{em} (nm)	λ_{S} (nm)
H ₂ O	449.0	530.0	81.0	451.0	524.0	73.0
NaOAc buffer pH 4	452.0	552.0	100.0	453.0	540.0	87.0
PBS	496.0	526.0	30.0	498.0	524.0	26.0

λ_{ex} = absorption maximum; λ_{em} = emission maximum; λ_{S} = Stokes shift.

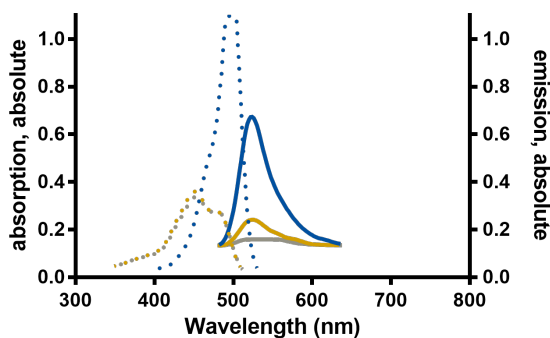
The *Stokes shift* is the difference between the absorption maximum and the emission maximum and is named after the Irish physicist George Gabriel Stokes.¹⁶⁵ The measured absorption and emission maxima and the calculated *Stokes shifts* are depicted in *Table 4.13*. As can be seen, the *Stokes shift* in water and buffer is much better than the one in PBS. While looking at the absolute spectra, however, it be-

comes clear that the fluorescence intensity is much higher in PBS than in water or buffer.

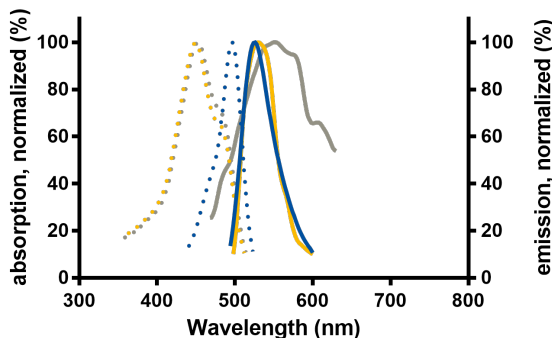
A Absolute data of 158a.



B Absolute data of 158b.



C Normalized data of 158a.



D Normalized data of 158b.

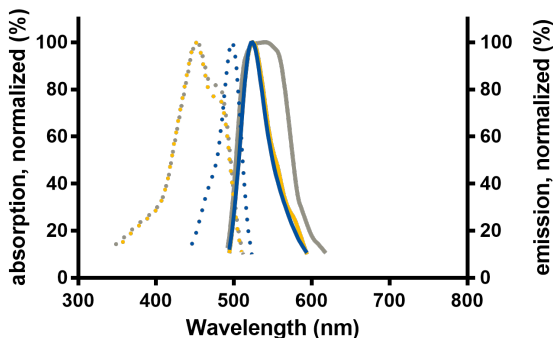


Figure 4.6: Absorption and emission spectra of 158a and 158b. Depicted are the absorption (dotted lines ···) and emission (solid lines —) curves measured in different media: water (yellow), PBS (blue), and sodium acetate buffer pH 4 (grey). Fluorescence spectra were recorded from 300–800 nm.

4.3.8 Evaluation of the binding of 158a and 158b to peripheral mononuclear blood cells by flow cytometry

To analyze molecules expressed by a cell, typically on the cell surface, flow cytometry can be applied.¹⁶⁶ In comparison with other methods, *e.g.* microscopy, flow cytometry allows the measurement of a large amount of cells in a short time, and provides information on a single cell basis.¹⁶⁶ Briefly, a sample containing cells is suspended in liquid and the suspension is subsequently broken down into tiny

droplets.¹⁶⁶ Next, the cells pass a laser beam one at a time and based on the characteristics of the cell and its components, the light is scattered.¹⁶⁶ The scattering of the light is analyzed by two detectors: the forward scatter (FSC) gives information about the size of the cell while the side scatter (SSC) gives information about the granularity.¹⁶⁶ Additionally, any fluorescent molecule present will fluoresce. To capture multichannel images of cells, the scattered and fluorescent light is collected by appropriately positioned lenses, and a combination of beam splitters and filters steers the scattered and fluorescent light to the appropriate detectors.¹⁶⁶ This technique can also be used to sort cells based on characteristic probes and separating them in an electric field (fluorescence-activated cell sorting (FACS)).

Flow cytometry was used for the proof-of-principle study of the fluorescent CD73 inhibitors, **158a** (PSB-18332) and **158b** (PSB-19416). The experiments were performed in the group of Prof. Dr. Eva Tolosa (Institute of Immunology, University Medical Center Hamburg-Eppendorf, Germany).

To investigate the binding of **158b** to CD73 on cells, a titration of **158b** was performed on peripheral blood mononuclear cells (PBMCs) freshly isolated from blood of a healthy donor. PBMCs consist of lymphocytes and monocytes. Lymphocyte subsets, as B cells and CD8 T cells are known to express CD73 and are therefore suitable to analyze the binding of the compounds.⁷⁶ The cells were incubated with different concentrations of **158b** (*Figure 4.7*). To evaluate the efficiency of **158b** as a dye for labeling CD73, PBMCs were first stained with a commercial phycoerythrin (PE)-labeled anti-human CD73 antibody as a control.

As can be seen in *Figure 4.7*, staining with the anti-human CD73 resulted two populations, with 14.5% of the cells being CD73-positive (*Figure 4.7*). When **158b** was used, only one population was observed with a concentration-dependent shift of the peak towards a more positive signal (*Figure 4.7*). In addition to the data shown in *Figure 4.7*, PBMCs were also incubated with 1 nM, and 10 nM, and 100 μ M of **158b**. The results were, however, similar to the experiments with 100 nM or 10 μ M of **158b**, respectively.

The concentration-dependent high background signal might be due to non-specific lipophilic interactions. To reduce those, different conditions were tested, including fixation of the membrane (*Figure 4.8A*), co-incubation with protein (*Figure 4.8B*) or detergent (*data not shown*), and extra washing with detergent (*Figure 4.8C*).

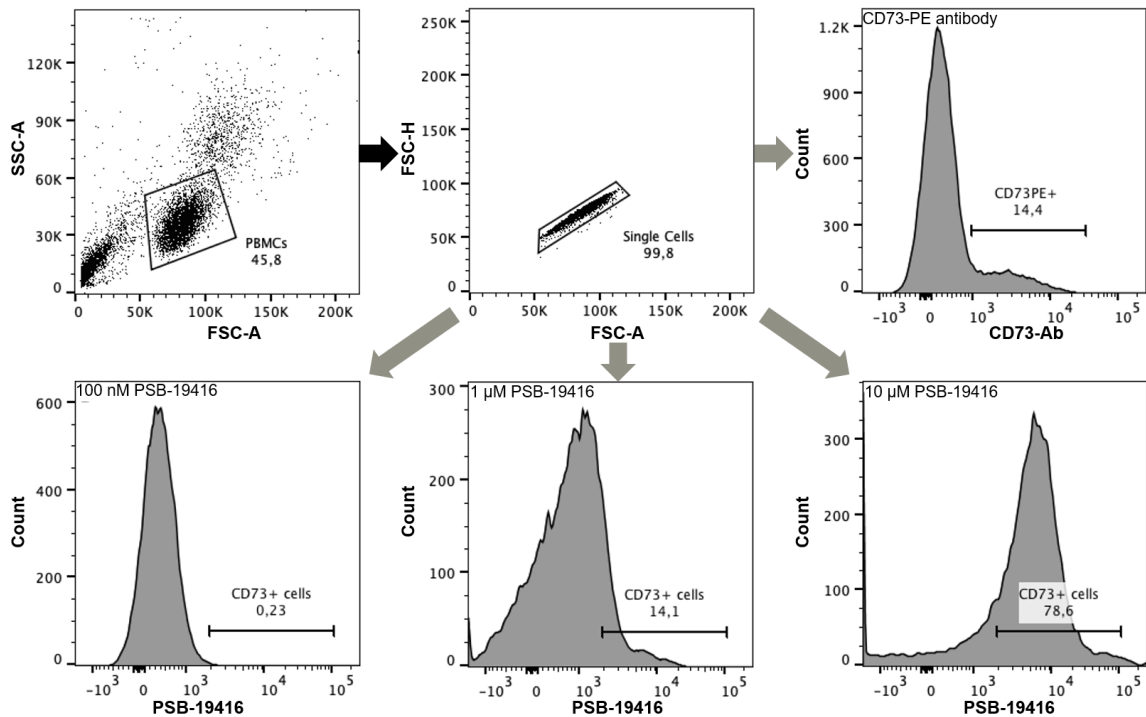


Figure 4.7: Titration of **158b** on PBMCs. A) PBMCs, analyzed by flow cytometry, were stepwise gated on lymphocytes and single cells regarding their size and granularity. The expression of CD73 was analyzed either by using a commercially available anti-CD73 antibody ($0.8 \mu\text{g}/\text{ml}$) or different concentrations of **158b**.

After fixation of the cell membrane with fixation buffer, two populations could be observed after incubation with **158b** (Figure 4.8A). The percentage of CD73-positive cells was, however, higher than after staining with the anti-CD73 antibody (45.9% CD73-positive cells with **158b** compared to 14.4% with CD73 antibody, see Figure 4.8). Furthermore, both populations were clearly shifted to the right, which indicates non-specific interactions.

Co-incubation with bovine serum albumin (BSA) did not have any effect on the signal compared to the incubation performed in Figure 4.7 (Figure 4.8B). Co-incubation with permeabilization buffer, which contains detergents, gave a similar result (*data not shown*).

In another setup, cells were fixed and permeabilization buffer was used to wash the cells after incubation (Figure 4.8C). In comparison with merely incubation with $10 \mu\text{M}$ **158b** (Figure 4.8A), this resulted in a significant shift to the left of both populations, indicating that background signals were reduced. The percentage of CD73 positive

cells was, however, still twice as high as in the control with the CD73 antibody (*Figure 4.7*).

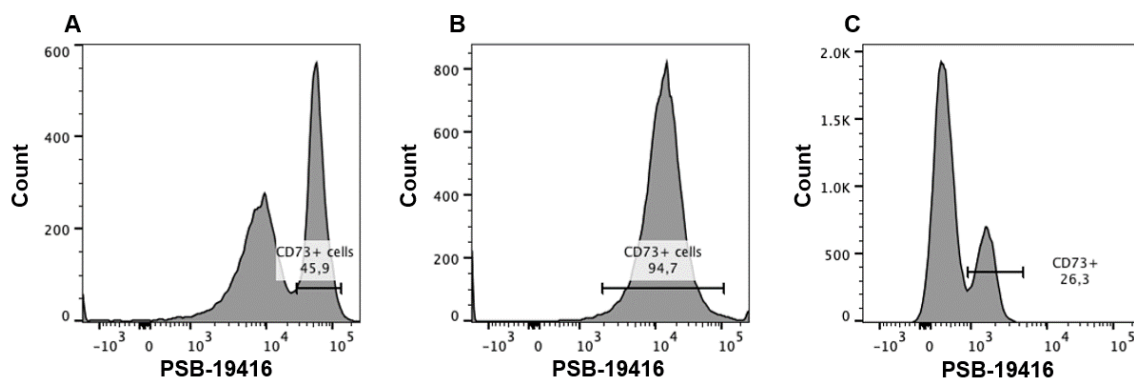


Figure 4.8: Testing of different conditions to reduce the concentration-dependent shift of the **158b** peak. PBMCs were incubated with $10\ \mu\text{M}$ **158b** under different conditions. A) Fixation of cells prior to the incubation with **158b**. B) Fixation of cells prior to the incubation with **158b** and subsequent co-incubation with permeabilization buffer. C) Fixation of cells prior to the incubation with **158b** and washing with permeabilization buffer after the incubation. Cells in shown histograms were previously gated on single cells.

To compare the two different fluorescent CD73 inhibitors, the incubation of the cells was repeated with both compounds (*Figure 4.9*). Here, the cells were fixed before the incubation with the inhibitor and were washed with permeabilization buffer after the incubation (*Figure 4.9*).

As can be seen in *Figure 4.9E*, the histogram after staining with **158b** looks different than that in *Figure 4.8A*, although the conditions were almost identical. The only difference is that in case of *Figure 4.9E*, also a co-staining with anti-CD8a and anti-CD19 antibodies took place prior to membrane fixation (*data for those antibodies not shown*). The shift to the right was decreased and the population of CD73-positive cells was increased. When the experiment was repeated, the same result was obtained as in *Figure 4.9E*, indicating that this effect indeed might be caused by pre-staining with other antibodies.

In comparison with **158a**, the two populations can much clearer be distinguished when the cells were incubated with **158b** (*Figure 4.9C+E*). After washing with detergent, this observation is even more prominent (*Figure 4.9D+F*). Furthermore, the background signal seems to be less with **158b** than with **158a**, which could be due to the more lipophilic character of **158a**.

Interestingly, after fixation of the cell membrane, staining with anti-CD73 antibody

led to a drastic reduced signal for CD73 compared to staining with the antibody before fixation (*Figure 4.9A+B*). This makes experiments challenging in which you want to test the competition of the binding of the anti-CD73 antibody and the fluorescent inhibitor.

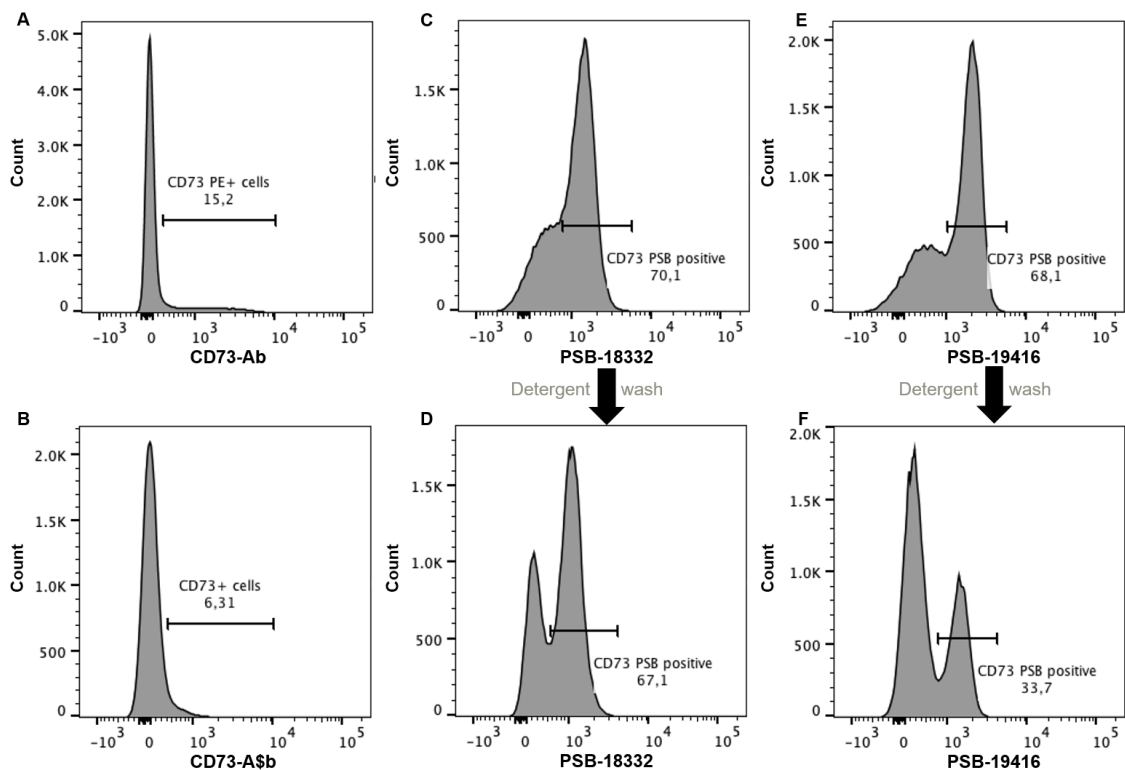


Figure 4.9: Comparison of anti-CD73-PE antibody, 158a, and 158b. A) Staining with PE anti-human CD73 (0.8 $\mu\text{g/ml}$) prior to fixation. B) Staining with PE anti-human CD73 (0.8 $\mu\text{g/ml}$) after fixation. C) Staining with 158a after fixation. D) Staining with 158a after fixation, and with detergent wash. E) Staining with 158b after fixation. F) Staining with 158b after fixation, and with detergent wash.

Anyway, co-staining of the anti-CD73 antibody and both fluorescent inhibitors was performed (*Figure 4.10*). For this, PBMCs were first stained with the CD73 antibody, followed by fixation of the cell membrane and subsequent incubation with 158a (*Figure 4.10A*) or 158b (*Figure 4.10B*).

In *Figure 4.10* on the left side, the CD73-antibody staining can be seen in a histogram, being similar for both sub-experiments. Single cells were further analyzed regarding their co-expression of the anti-CD73 antibody and the fluorescent inhibitors (*Figure 4.10 dot plots on the right*). CD73-positive and CD73-negative cells both have two sub-populations one being 158 positive (*upper right corner of the*

dot plot) and the other being negative (*lower right corner of the dot plot*). There are cells which are double positive for the antibody and the inhibitors, however, the inhibitors do not mark all cells indicated as CD73-positive by the antibody. Furthermore, some cells are positive for the compounds but not for the antibody (*upper left corner of the dot plot*), indicating non-specific binding. The difference between **158a** and **158b** is that the separation between the two populations is more distinct for **158b**.

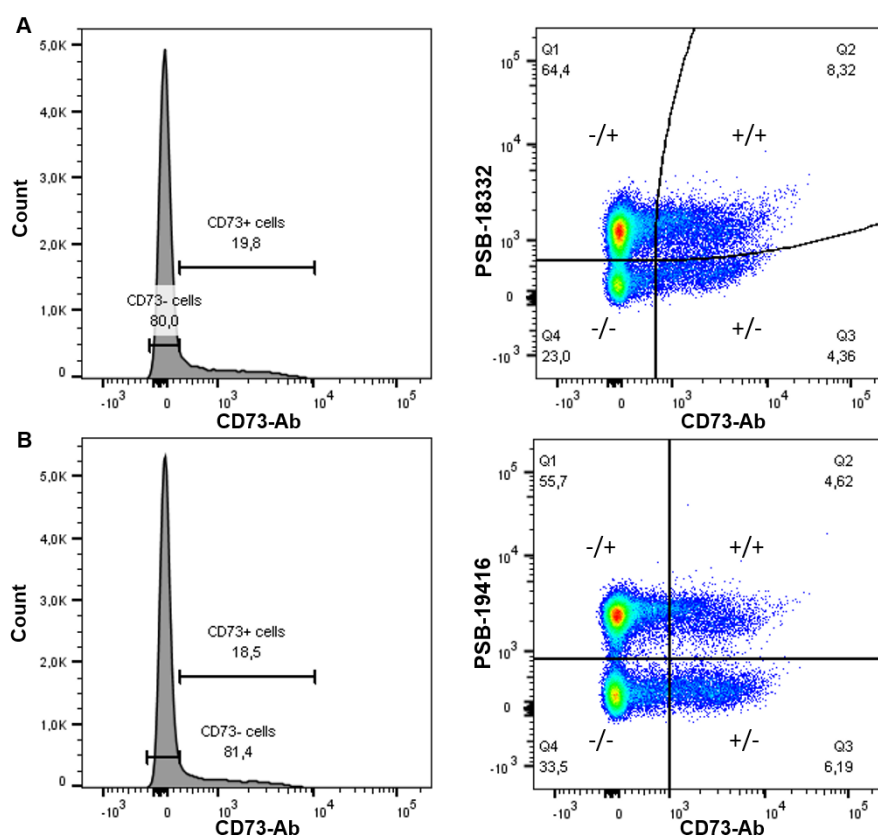


Figure 4.10: Co-staining of PBMCs with an anti-CD73 antibody and **158a** or **158b**. Cells were incubated with anti-CD73 antibody (0.8 $\mu\text{g/ml}$) followed by fixation, incubation with 10 μM **158a** (A) or **158b** (B), and washing with permeabilization buffer. Cells were gated on single cells. Left: Histogram of the anti-CD73 antibody signal. Right: Dot plot of co-staining by anti-CD73 antibody and inhibitors. ++ = double positive for antibody and inhibitor. +/- = positive for antibody but negative for inhibitor. -/+ = negative for antibody and positive for inhibitor. -/- = double negative for antibody and inhibitor.

These experiments show that the fluorescent CD73 inhibitors **158a** and **158b** bind to the surface of PBMCs. However, they possess a high capacity of nonspecific binding, for which reason the marked cells cannot be compared to cells which are

defined as CD73-positive by a commercially available antibody. The improvement of the specificity needs to be addressed in the future.

4.4 Development of an AOPCP-derived PET-tracer for CD73

An often used technique in diagnostics is positron emission tomography (PET). It is a nuclear imaging technique that provides images of the biodistribution of a radiotracer *in vivo*.¹⁶⁷ The speed of acquisition allows the determination of the pharmacokinetics of the uptake of a radiotracer.¹⁶⁷ PET can give novel insights for drug discovery and development, and for the identification of off-targets of a potential drug candidate, and, importantly, on target engagement.¹⁶⁷ Therefore PET is utilized more and more for clinically relevant targets, *e.g.* as diagnostics or for clinical development of drugs.¹⁶⁷ CD73 is a potential biomarker for cancer cells and it would be highly desirable to have a radiotracer for CD73 as a diagnostic tool, and to further study its biological role.

Table 4.14: Half-lives of the different positron-emitting radionuclides. Data taken from [167].

Nuclide	Half-life (min)
¹⁵ O	2
¹³ N	10
¹¹ C	20
¹⁸ F	110

The principle behind PET is that radiolabeled molecules with positron-emitting nuclides are administered and that the emission signal is measured.¹⁶⁷ These nuclides ideally have short half-lives.¹⁶⁷ Therefore, ¹⁵O, ¹³N, ¹¹C, and ¹⁸F are often used.¹⁶⁷ ¹⁸F has the most ideal half-life in comparison with the other radionuclides (*Table 4.14*), and is therefore often used for the labeling of radiopharmaceuticals.¹⁶⁷ Fluorine is frequently used in the field of medicinal chemistry due to its favorable physical properties.¹⁶⁷ Fluorine has a small *van der Waals* radius (1.47 Å) and a high electronegativity.¹⁶⁷ Furthermore, it can form stronger bonds with carbon (C-F energy bond of 112 kcal/mol) than for example hydrogen (C-H energy bond of 98 kcal/mol) which leads to a higher thermostability and oxidation resistance.¹⁶⁷ In addition, it is also resistant to metabolism. Because of its size and valence electrons, fluorine is a bioisoster of hydrogen, and because of its size and electronegativity it is also a bioisoster of oxygen.¹⁶⁷ Next to the short half-life, ¹⁸F also has a high positron decay ratio (97%) and a low positron energy (maximum

0.635 MeV), which results in a short diffusion range (<2.4 mm) thereby increasing the resolution of PET images.¹⁶⁷ Because of its advantages, several selective fluorination reagents for electrophilic and nucleophilic incorporation have been developed that allow synthesis of ¹⁸F-containing molecules in large quantities.¹⁶⁷ Since ¹⁸F has such a short half-life, the incorporation of ¹⁸F preferably is done in the late stage of the synthetic route.¹⁶⁷

An imaging agent has to possess a high target specificity, and biomolecules like oligonucleotides, peptides, or proteins are often used. Radioactive labeling with ¹⁸F can be done via direct or indirect methods.¹⁶⁷ Using a direct method, ¹⁸F is directly reacted with a molecule and subsequent purification will give the desired imaging agent.¹⁶⁷ This procedure is similar to the method applied for the synthesis of the previously described tritiated radioligand, in which an alkyne group was directly reacted with tritium gas. The indirect method consist of the synthesis of a radiolabeled prosthetic group which is subsequently conjugated to the biomolecule that has been modified for site-specific reaction.¹⁶⁷ For selecting a labeling method, the reaction conditions and the stability of the biomolecule have to be taken into account since for direct substitutions nonphysiological conditions of pH and temperature are often used.¹⁶⁷

Our aim was to develop an imaging probe for CD73. The structure of the radioligand (139) that has been described before in *Chapter 4.2* was chosen to be used as a template for the tracer (*Figure 4.11*).

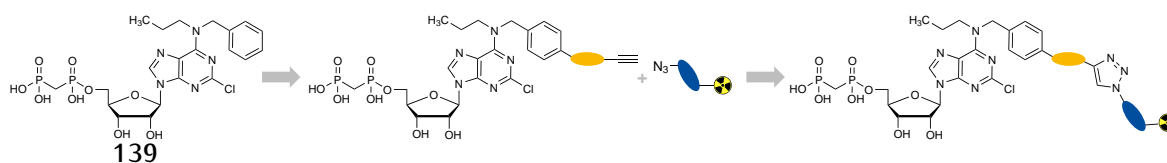


Figure 4.11: AOPCP-derived PET tracer for CD73. Compound 139 will serve as a lead structure for the development of a PET tracer.

The development of the fluorescent probe in *Chapter 4.3* showed, that addition of a moiety to the *para*-position of the *N*⁶-benzyl-ring is well tolerated by CD73. Therefore, we chose to add a moiety for site-specific fluorine labeling at that position (*Figure 4.11*). As a labeling strategy we decided to use the indirect method, since the nucleotide might not be stable enough to use a direct method. Furthermore, site-specific introduction of fluorine might be difficult on the nucleotide scaffold itself.

Biomolecules can be conjugated to a prosthetic group through amine- or thiol-reactive groups via different reaction types including acylation, alkylation, amidation, or by using the so called *click chemistry*.¹⁶⁷ Click chemistry belongs to the class of bioorthogonal reactions.¹⁶⁷ These reactions can take place in living tissue without interacting with the biological system.¹⁶⁷ Next to the high selectivity of bioorthogonal reactions, these reactions are also rapid and can take place in biological media, which is why this chemistry is often used to conjugate ¹⁸F-containing prosthetic groups to biomolecules.¹⁶⁷

For the development of the CD73-targeted radiotracer, the copper(I)-catalyzed azide-alkyne cycloaddition (CuAAC) was chosen as a conjugation method. The *Huisgen* cycloaddition is a 1,3-dipolar cycloaddition of an azide and an acyclic alkyne to yield a 1,2,3-triazole which is highly stable to oxygen, light, and also in an aqueous environment.^{168,169} The presence of copper lowers the required reaction temperature and shortens the reaction time to overcome the activation barrier of triazole formation.¹⁶⁷ Alkynes and azides are both biologically inert which is why the reaction can be classified as bioorthogonal.¹⁶⁷ This also has the benefit that no other protecting groups are necessary and that the reaction can be carried out in the presence of water and oxygen.¹⁶⁷

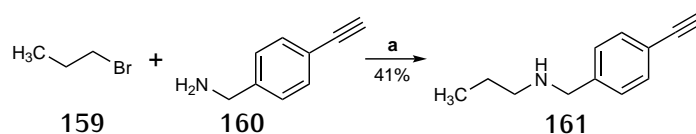
Typically, CuSO₄ is used as a source for copper, which is reduced to Cu(I) *in situ* in the presence of a reducing agent like sodium ascorbate.¹⁶⁷ It is proposed that Cu(I) coordinates to the terminal alkyne to form a copper(I) acetylide.^{167,170} It was reported that the reaction is most efficient in water and in the presence of polytriazole ligands such as tris(benzyltriazolylmethyl)amine (TBTA).^{167,170}

4.4.1 Synthesis of an AOPCP-derivative suitable for subsequent ¹⁸F-labeling

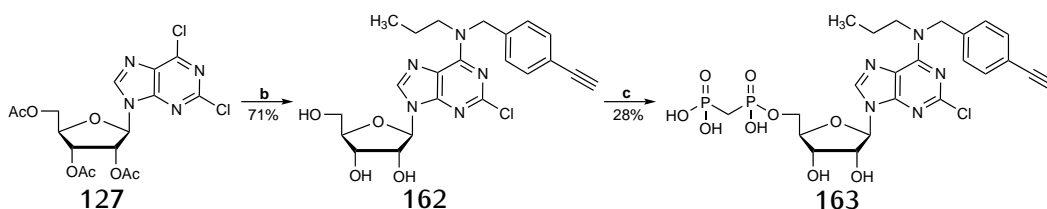
Compound **139** (*Figure 4.11*) was chosen as a template for the synthesis of the PET tracer precursor. For the synthesis of the precursor, the corresponding alkyne-containing amine was first synthesized by stirring 1-bromopropane (**159**) with (4-ethynylphenyl)methanamine (**160**) overnight at room temperature (*Scheme 4.10a*).¹⁶⁰

Next, the acetyl-protected 2,6-dichloropurine-ribofuranoside (**127**) was reacted with *N,N*-(4-ethynyl)-benzylproylamine (**161**) in the presence of triethylamine in abso-

a Synthesis of an alkyne-containing amine.



b Synthesis of the PET precursor.



Scheme 4.10: Synthesis of *N*⁶-(4-ethynyl)benzyl-2-chloro-*N*⁶-propyl AOPCP. Reagents and conditions: a) CH₃OH, rt, overnight. b) two steps: I) **161**, Et₃N, absolute EtOH, reflux, 18 h. II) 0.5% NaOCH₃, methanol, room temperature, overnight. c) two steps: I) methylenebis(phosphonic dichloride), PO(OCH₃)₃, 0°C, 30 min II) 0.5 M TEAC buffer pH 7.4–7.6, room temperature, 1 h.

lute ethanol followed by purification by silica gel column chromatography as described before.⁹¹ After deprotection using sodium methoxide, **162** was phosphorylated using methylenebis-(phosphonic dichloride) in trimethylphosphate followed by hydrolysis with aqueous TEAC buffer.⁹¹ To remove the trimethylphosphate, the crude reaction mixture was extracted with *tert.*-butylmethylether. Purification by HPLC on reverse-phase C18 material in order to remove inorganic phosphates gave the desired AOPCP derivative **163** (Scheme 4.10b).

4.4.2 Synthesis of the cold analog of the designed PET-tracer

In order to test the pharmacological potency of the designed PET tracer structure, the precursor needs to be clicked to the cold fluorine-containing ligand (**165**). 2-Fluoroethylazide was obtained by the reaction of 2-fluoroethyl-4-methylbenzenesulfonate (**164**) with sodium azide in DMF (Scheme 4.11a).¹⁷¹ Since attempts to isolate neat 2-fluoroethylazide can result in an explosion, the reaction mixture was filtered and crude **165** was used for the click reaction.¹⁷¹

The click reaction between **165** and **166** was performed in the presence of sodium ascorbate and premixed CuSO₄ and TBTA in a mixture of water, THF and *tert.*-butanol.¹⁷² The crude product was filtered and subsequently purified by HPLC on reverse-phase C18 material yielding the desired AOPCP derivative **166** (Scheme 4.11).

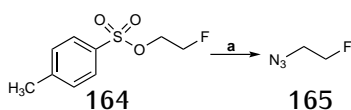
Table 4.15: $^1\text{H-NMR}$ data of the PET-tracer and its precursor. Shifts (δ) in D_2O [ppm]. Next to the signals of the substituents, a selection of characteristic ribose and purine protons is depicted.

	163	166
C'1-H	6.01	6.02
C'5-H ₂	4.17	4.18
C8-H	8.37	8.27
N^6 -substituent	7.30 (aryl) 7.18 (aryl) 5.29 (NCH ₂) 3.90 (NCH ₂) 1.62 (CH ₂ CH ₃) 1.25 (C≡CH) 0.84 (CH ₃)	8.40 (triazolyl)) 7.67 (aryl) 7.36 (aryl) 4.93- 4.85 (NCH ₂) 4.77 (NCH ₂) 3.15 (NCH ₂) 1.67 (CH ₂ F) 1.34 (CH ₂ CH ₃) 0.91 (CH ₃)
α,β -CH ₂	2.17	2.18

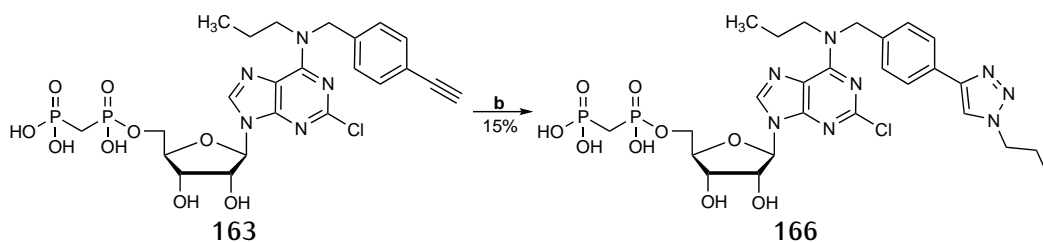
Table 4.16: $^{13}\text{C-NMR}$ data of of the PET-tracer and its precursor. Shifts (δ) in D_2O [ppm]. Next to the signals of the substituents, a selection of characteristic ribose and purine carbons is depicted.

	163	166
C'1	89.78	89.68
C'5	66.41	66.51
C8	141.06	141.04
N^6 -substituent	134.97, 130.31, 123.07, 120.82, 85.92, 81.00, 57,61, 53,51, 23,79, 13.11	143.88, 131.31, 130.98, 128.64, 125.38, 120.81, 85.48, 55.52, 53.76, 53.63, 22.14, 15.63
α,β -CH ₂	30.37	28.06

a Synthesis of 2-fluoroethylazide.



b Synthesis of the cold PET tracer.



Scheme 4.11: Synthesis of 2-chloro-*N*⁶-(4-(1-(2-fluoroethyl)-1,2,3-triazol-4-yl)-benzyl)-*N*⁶-propyl AOPCP. Reagents and conditions: a) sodium azide, anhydrous DMF, rt, 24 h. b) 165, 1 M sodium ascorbate in H₂O, CuSO₄, TBTA, THF/H₂O/*t*-BuOH (3:1:1), room temperature, 18 h.

The structures of the synthesized nucleotides were confirmed by ¹H-, ¹³C-, and ³¹P-NMR spectroscopy (Table 4.15-Table 4.17), in addition to LC/ESI-MS performed in both positive and negative mode. The ¹⁹F-substituted, nonradioactive inhibitor was additionally investigated by ¹⁹F-NMR spectroscopy (Table 4.17).

Table 4.17: ³¹P- and ¹⁹F-NMR data of the PET-tracer and its precursor (shifts (δ) in D₂O given in ppm).

	163	166
P _α	14.89	0.39
P _β	18.94	16.44
F	-	-75.62

4.4.3 Pharmacological evaluation of the PET-tracer

The precursor and the "cold" version of the PET-tracer were both evaluated in a radiometric CD73 assay (Section 1.4.5) to determine their *K_i*-values for CD73 (Figure 4.2).¹²⁹ The biological testing was done by Riham Idris. The inhibitory potency of 166 was evaluated at three different preparations of CD73, including membrane preparations containing rat CD73, soluble human CD73, and membrane preparations of triple-negative breast cancer cells (MDA-MB-231), which natively express CD73. In addition to that, the inhibitory potency of 163 at human soluble CD73

was investigated. The concentration-inhibition curves were plotted, and the mean IC_{50} -value from three independent experiments was used to calculate the K_i -values (Table 4.18).

At human soluble CD73, the inhibitory potency of the precursor (**163**) was in the subnanomolar concentration range. After click reaction with the fluoroethyl-group, the inhibitory potency was three-fold lower, which is still very potent, indicating that the modifications in *para*-position of the benzyl ring are well tolerated. This is in agreement with the previous results. The K_i value for **166** determined with membrane preparations of triple-negative breast cancer cells (MDA-MB-231) which natively express CD73 is similar to the K_i value determined at soluble CD73. As observed in previous experiments, the inhibitory potency of **166** was decreased slightly at rat CD73.

Table 4.18: Inhibitory potency of **163** and **166** at different enzyme preparations.

Enzyme preparation	$K_i \pm SEM$ [nM]	
	163	166
rat soluble CD73	<i>n.d.</i>	6.09 ± 0.74
human soluble CD73	0.372 ± 0.030	1.02 ± 0.11
human CD73 in MDA-MB-231 cell membranes	<i>n.d.</i>	2.78 ± 0.47

The compounds were tested using $5 \mu\text{M}$ $[2,8\text{-}^3\text{H}]\text{AMP}$ as a substrate. *n.d.* = not determined.

4.5 2-Chloro-7-deaza AOPCP-derivatives as novel inhibitors for CD73

Recently, it was published that 7-deaza-AOPCP displays a two-fold higher inhibitory potency than AOPCP on soluble rat CD73.¹²⁹ Therefore, the idea was born to elucidate the structure-activity relationships of this compound class further by generating a selection of 7-deaza-AOPCP derivatives. The first targets were 7-deaza derivatives of the most potent AOPCP derivatives described so far to study the effect of the presence or absence of the nitrogen atom at the 7-position.

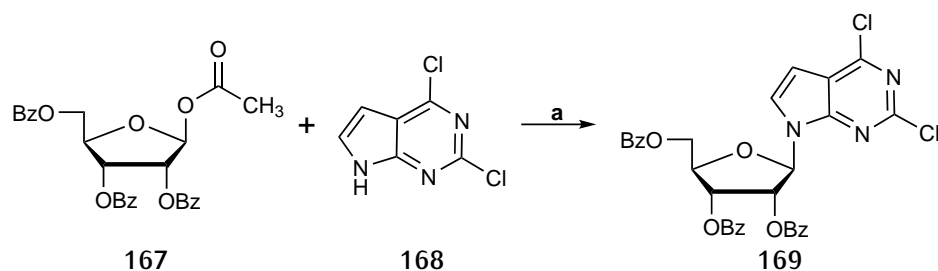
4.5.1 Synthesis of protected 2,6-dichloro-7-deazaadenosine

For the synthesis of 7-deaza AOPCP derivatives, 7-deaza-2,6-dichloropurine-ribofuranoside was chosen as starting material. For its synthesis, the condensation method described in *Chapter 4.1.2* was applied. The coupling was not successful since the melting point of 2,6-dichloropurine is above 300°C, and therefore no homogenous reaction mixture could be formed and therefore no reaction occurred.

Next, the Vorbrüggen glycosylation procedure was tested. It is a one-pot reaction in which first silylation of the purine base takes place followed by reaction with the protected sugar in the presence of a Lewis acid.¹⁷³ During the Vorbrüggen reaction, an intermediate is formed as described for the condensation method (*Chapter 4.1.2*). Upon addition of a Lewis acid like trimethylsilyl trifluoromethanesulfonate (TMSOTf), an oxonium ion is formed from the sugar.¹⁵⁶ Next, a nucleophilic attack of the nucleobase takes place from the opposite side, which will give the natural β -anomer according to *Baker's 1,2-trans rule*.¹⁵⁶ In addition to the neighboring group participation, also the coordination of the Lewis acid to the nucleophile plays an important role.¹⁷⁴ Due to the basic character of silylated nucleobases, σ -complexes are formed with the Lewis acid.¹⁷⁵ Those σ -complexes react much slower in further reactions.¹⁷⁵ It was shown that the stronger the Lewis acid is, the more tightly it is bound to the *N1* of the nucleobase.¹⁷⁵ Since TMSOTf is a much weaker Lewis acid than SnCl₄, it is a superior catalyst for nucleoside synthesis.¹⁷⁵

For the synthesis of **169**, 7-deaza-2,6-dichloropurine (**168**) was first suspended in anhydrous acetonitrile. Upon addition of the silylating agent bis(trimethylsilyl)acetamide (BTSA), the solution became clear indicating that silylation was completed since the unsilylated purine base is not soluble in acetonitrile.¹⁷⁶ Next, 1'-*O*-acetyl-2',3',5'-tri-*O*-benzoyl- β -D-ribofuranose and the Lewis acid TMSOTf were added.¹⁷⁶ The reaction was stirred at 50°C for 16 hours followed by evaporation (*Scheme 4.12*).¹⁷⁶

LC/ESI-MS analysis revealed that the desired product was formed but also large amounts of starting material were still present. The applied reaction conditions were adapted from a paper that describes an optimized synthesis route to obtain tubercidin (7-deazaadenosine), which possesses antibiotic activity.¹⁷⁶ The authors investigated the effect of different parameters, including the reaction temperature, the sugar : nucleobase ratio, and the reaction time. Unfortunately, this optimization



Scheme 4.12: Synthesis of protected 7-deaza-2,6-dichloropurine riboside (**169**). Reagents and conditions: BTSA, TMSOTf, acetonitrile, 50°C, 16 h.

process was not described in detail. Since the conversion of the reaction was low, the reaction was tried to be optimized by varying the amount and kind of Lewis acid used, the time and temperature of the pre-activation, and the reaction time and temperature (*Table 4.19*). After evaporation, LC/ESI-MS analysis of the crude residue was performed in order to determine the conversion. Unfortunately, it was not possible to improve the reaction conditions. An explanation for the low conversion might be the low reactivity of the pyrrole nitrogen towards glycosylation due to the absence of the nitrogen in the 7 position.¹⁷⁶

Table 4.19: Optimization of the synthesis of 169. Different reaction parameters were varied in order to improve the conversion of the Vorbrüggen glycosylation.

Conditions	I	II	III	IV	V	VI	VII	VIII	IX	X
Lewis acid	TMSOTf	TMSOTf	TMSOTf	TMSOTf	TMSOTf	TMSOTf	SnCl ₄	SnCl ₄	SnCl ₄	TMSOTf
eq	1.4	1.4	1.4	1.4	1.4	1.4	1	2	2	2
Activation	rt	60°C	rt	rt	rt	rt	rt	rt	rt	rt
	15 min	30 min	15 min	15 min	15 min	15 min	15 min	15 min	15 min	15 min ^a
Temperature	50°C	50°C	rt	40°C	50°C	50°C	50°C	50°C	50°C	50°C
Time	16 h	16 h	16 h	16 h	24 h	48 h	16 h	16 h	48 h	16 h
Conversion	38%	25%	5%	18%	15%	17%	30%	32%	33.5%	40%

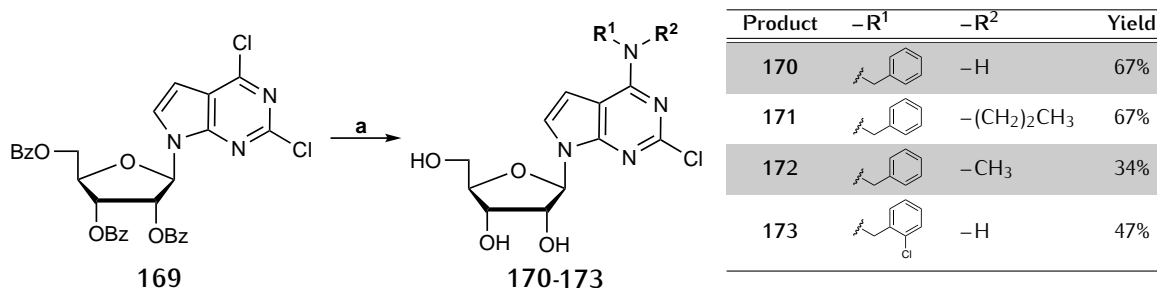
^aAdditionally, also pre-activation of the sugar with TMSOTf was carried out at room temperature for 15 min.

According to Ingale *et al.*, side products and remaining starting material can be removed easily by chromatographic work-up since they possess completely different R_f -values.¹⁷⁶ This, however, was not true for the purification of crude **169** by silica gel chromatography since already by using 0.5% methanol in DCM, both starting materials and the desired product eluted together. Therefore, it was decided to continue with the substitution at the 6-position without any purification except for filtration over silica gel to remove polar or charged impurities.

4.5.2 Synthesis of N^6 -substituted 2-chloro-7-deazaadenosine derivatives

Substitution at the 6-position was done as described before by refluxing crude **169** with the corresponding alkylamine in absolute ethanol in the presence of a base (*Scheme 4.13*).⁹¹

Since deprotection of the benzoyl groups occurred already during the substitution reaction due to the presence of triethylamine, deprotection was directly carried out using sodium methoxide in methanol without an extra purification step in between. After completion of the reaction the solvent was evaporated, and the crude mixture was purified by silica gel chromatography (CH₃OH/DCM 1:9) yielding the desired nucleosides **170-173**.



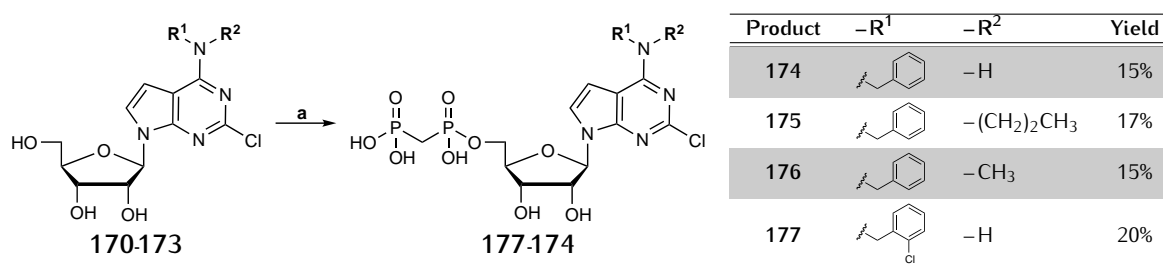
Scheme 4.13: Synthesis of N^6 -substituted 2-chloro-7-deazaadenosine derivatives. Reagents and conditions: a) two steps: I) alkylamine, Et₃N, absolute EtOH, reflux, 18h. II) 1 M NaOMe, methanol, room temperature, overnight.

LC/ESI-MS analysis, however, showed that an isomeric mixture of the α and β anomers was obtained although based on the mechanism of the reaction and the use of the weak Lewis acid TMSOTf solely the β -anomer was expected. Unfortunately, the retention times of both isomers are too similar to achieve separation by RP-HPLC. Therefore, the isomeric mixtures of the four nucleosides were used for the phosphorylation.

4.5.3 Synthesis of N^6 -substituted 2-chloro-7-deaza-AOPCP derivatives

Phosphorylation of **170-173** was carried out using methylenebis(phosphonic dichloride) in trimethylphosphate followed by hydrolysis with aqueous TEAC buffer as de-

scribed before.⁹¹ To remove the trimethylphosphate, the crude reaction mixture was extracted with *tert.*-butylmethylether. Purification by HPLC on reverse-phase C18 material gave the desired AOPCP derivatives **174-177** (Scheme 4.14). Phosphonylation apparently increased the difference in retention times of the two anomers since it was now possible to separate the α and β anomers. α -Anomers were not isolated since the quantity was not sufficient.



Scheme 4.14: Phosphonylation of N^6 -substituted 2-chloro-7-deazaadenosine derivatives.

Reagents and conditions: a) two steps: I) methylenebis(phosphonic dichloride), PO(OCH₃)₃, 0°C, 30 min II) 0.5 M TEAC buffer pH 7.4-7.6, room temperature, 1 h.

The structures of the synthesized nucleotides were confirmed by ¹H-, ¹³C-, and ³¹P-NMR spectroscopy (Table 4.20-Table 4.22), in addition to LC/ESI-MS performed in both positive and negative mode. Additionally, ROESY-NMR analysis confirmed the formation of the desired β -anomers (*data not shown*). For the 7-deaza-AOPCP derivatives with a monosubstitution at the N^6 -position (**174** and **177**), ³¹P-NMR analysis revealed the formation of a mixture of different monophosphates with the desired 5'-diphosphonate as main synthesis product (approximately 70% in both cases). This was not observed for the other two 7-deaza-AOPCP derivatives (**175** and **176**), indicating that the substitution at the N^6 -position has an effect on the selectivity of the phosphonylation.

Table 4.20: ³¹P-NMR data of the 7-deaza-AOPCP derivatives. Shifts (δ) in D₂O [ppm].

Compound	Substituents	P _{α}	P _{β}
174	2-chloro- N^6 -benzyl	15.14	18.55
175	2-chloro- N^6, N^6 -benzylpropyl	15.02	18.92
176	2-chloro- N^6, N^6 -benzylmethyl	15.08	18.84
177	2-chloro- N^6 -(2-chloro)benzyl	15.29	18.45

Table 4.21: ¹H-NMR data of the 7-deazaadenosine and 7-deaza-AOPCP-derivatives. Shifts (δ) in DMSO-d₆[#] or D₂O* [ppm]. Next to the signals of the substituents, a selection of characteristic ribose and purine protons is depicted.

Compound	Substituents	C'1-H	C'5-H ₂	C7-H	C8-H	Substituents	α,β-CH ₂
170 [#]	2-chloro-N ⁶ -benzyl	5.26	3.62	7.10	8.03	7.33 (aryl) 7.28 (aryl) 7.20 (aryl) 4.60 (NHCH ₂)	-
171 [#]	2-chloro-N ⁶ ,N ⁶ -benzylpropyl	5.04	3.73-3.67	7.27	7.41	7.33 (aryl) 4.97 (NCH ₂) 3.63-3.55 (NCH ₂) 1.71 (CH ₂ CH ₃) 0.89 (CH ₃)	-
172 [#]	2-chloro-N ⁶ ,N ⁶ -benzylmethyl	4.92	3.49-3.43	7.30	7.36	7.32 (aryl) 7.29 (aryl) 7.28 (aryl) 3.63 (NCH ₂) 2.25 (NCH ₃)	-
173 [#]	2-chloro-N ⁶ -(2-chloro)benzyl	5.08	3.56	7.09	8.01	7.43 (aryl) 7.25 (aryl) 7.14 (aryl) 4.69 (NHCH ₂)	-
174 [*]	2-chloro-N ⁶ -benzyl	4.91	3.89	7.22	7.43	7.42 (aryl) 3.70 (NHCH ₂)	2.06
175 [*]	2-chloro-N ⁶ ,N ⁶ -benzylpropyl	5.12	3.56-3.40	7.33	7.57	7.33 (aryl overlapping with CH=C) 4.35 (NCH ₂) 4.02 (NCH ₂) 1.65 (CH ₂) 0.78 (CH ₂ CH ₃)	2.16
176 [*]	2-chloro-N ⁶ ,N ⁶ -benzylmethyl	5.00	3.99	7.32	7.52	7.42 (aryl) 4.87 (NCH ₂) 3.08 (NCH ₃)	2.14
177 [*]	2-chloro-N ⁶ -(2-chloro)benzyl	4.90	3.86	7.22	7.45	7.33 (aryl) 3.55 (NHCH ₂)	2.02

Table 4.22: ^{13}C -NMR data of the 7-deazaadenosine and 7-deaza-AOPCP derivatives. Shifts (δ) in DMSO- d_6 [#] or D₂O* [ppm]. Next to the signals of the substituents, a selection of characteristic ribose and purine carbons is depicted.

Compound	Substituents	C'1	C'5	C7	C8	N ⁶ -substituents	α,β -CH ₂
170[#]	2-chloro-N ⁶ -benzyl	86.49	60.68	99.53	120.88	128.50, 128.33, 128.27, 127.45, 127.34 (aryl) 126.73 (aryl) 43.17 (NHCH ₂)	-
171[#]	2-chloro-N ⁶ ,N ⁶ -benzylpropyl	86.31	63.66	104.62	132.53	129.99, 129.81, 129.31, 129.15, 128.52 (aryl) 54.61 (NCH ₂) 52.68 (NCH ₂) 21.90 (CH ₂) 11.96 (CH ₃)	-
172[#]	2-chloro-N ⁶ ,N ⁶ -benzylmethyl	84.56	61.84	101.69	122.02	128.57, 128.22, 128.13, 127.82, 127.19, 126.72 (aryl) 54.58 (NCH ₂) 35.55 (NCH ₃)	-
173[#]	2-chloro-N ⁶ -(2-chloro)benzyl	86.46	60.63	99.67	121.12	132.00, 129.22, 128.38, 128.00, 127.20 (aryl) 41.81 (NHCH ₂)	-
174*	2-chloro-N ⁶ -benzyl	87.20	66.48	102.79	123.35	131.78, 131.66, 131.52, 130.44, 130.22, 129.88 (aryl) 47.19 (NHCH ₂)	30.30
175*	2-chloro-N ⁶ ,N ⁶ -benzylpropyl	85.82	66.64	106.47	126.28	131.60, 131.52, 130.81, 130.34 (aryl) 55.55 (NCH ₂) 54.57 (NCH ₂) 22.96 (CH ₂) 13.36 (CH ₃)	30.40
176*	2-chloro-N ⁶ ,N ⁶ -benzylmethyl	85.80	66.60	105.19	125.82	133.46, 132.51, 132.43, 132.03, 131.64, 130.47 (aryl) 58.85 (NCH ₂) 34.80 (NCH ₃)	30.38
177*	2-chloro-N ⁶ -(2-chloro)benzyl	87.17	66.49	102.88	123.26	135.94, 132.51, 131.86, 130.20 (aryl) 45.63(NCH ₂)	30.28

4.5.4 Pharmacological evaluation

The four 7-deaza AOPCP-derivatives were submitted to pharmacological evaluation applying the radiometric CD73 assay that was described in *Section 1.4.5*.¹²⁹ The biological testing was done by Riham Idris. Since the main synthesis product was the 5'-monophosphate for all four derivatives, it was decided to evaluate the inhibitory potency of all compounds, although the results should be treated carefully for **174** and **177**.

The mean IC₅₀ from three independent experiments was used to calculate the K_i value (*Table 4.23*). For comparison, the K_i values of the corresponding AOPCP-derivatives are also depicted in *Table 4.23*. In general, it can be said that, surprisingly, the inhibitory potency decreases significantly upon replacing the nitrogen at the 7-position with a carbon.

Table 4.23: Inhibitory potencies of the 7-deaza AOPCP derivatives 174-177. For comparison, the K_i values of the corresponding AOPCP derivatives are depicted.

7-deaza-AOPCP analogs	$K_i \pm \text{SEM}$ (nM) at soluble human CD73	$K_i \pm \text{SEM}$ (nM) of the corresponding AOPCP-derivatives at soluble	
		human CD73	rat CD73
7-deaza-AOPCP	88.6 ± 4.0 (rat CD73) ¹²⁹	88.4 ± 4.0 ⁹¹	197 ± 53 ⁸⁴
174	305 ± 59	<i>n.d.</i>	1.23 ± 0.04 ⁸⁵
175	5990 ± 0.62	0.073 ± 0.001 (139)	0.567 ± 0.086 (139)
176	413 ± 29	0.318 ± 0.020 ⁹²	0.746 ± 0.246 ⁹²
177	55.4 ± 7.1	0.387 ± 0.034 ¹⁷⁷	0.341 ± 0.060 ⁸⁵

The compounds were tested at human soluble CD73 using 5 μM [2,8-³H]AMP as a substrate. *n.d.* = not determined.

In case of **175**, there is a 80 000- fold decrease of the inhibitory potency at soluble human CD73 compared to the AOPCP-derivative **139**. **175** was also evaluated at rat CD73 resulting in an even lower K_i value with 7.64 ± 0.36 μM. This is in agreement with previous experiments, in which it was observed that usually the AOPCP-derivatives are equipotent or more potent at human CD73 than at rat CD73, suggesting that also the other 7-deaza AOPCP-derivatives would be even less active at rat CD73.

5 Summary and outlook

CD39 and CD73 belong to the family of membrane-bound *ecto*-nucleotidases that are involved in the hydrolysis of extracellular, pro-inflammatory ATP into anti-inflammatory, immunosuppressive, tumor growth-stimulating, and angiogenic adenosine. Therefore, CD39 and CD73 possess great potential as novel drug targets for the (immuno)therapy of cancer and infections.

5.1 Synthesis and evaluation of novel inhibitors for CD39

The first objective of this thesis was to identify potent, selective, and metabolically stable inhibitors for CD39 based on the lead structures of 8-BuS-AMP and the ATP-analog ARL67156. For this purpose, adenosine derivatives bearing modifications at the C2-, C8-, and N⁶-position were generated and submitted to phosphorylation according to the Ludwig procedure or Yoshikawa procedure, yielding a library of ARL67156 or AMP derivatives, respectively. In case of the ARL67156 derivatives, also modifications of the phosphate chain were introduced by replacing the dibromo-substitution of the β,γ -methylene bridge in ARL67156 with hydrogen, dichloro or difluoro substitution. In total, 16 ARL67156 derivatives and 37 AMP derivatives were obtained and evaluated.

5.1.1 Structure-activity relationships of ARL67156 derivatives

The SARs of the synthesized ARL67156 derivatives at human CD39 are summarized in *Figure 5.1* and *Figure 5.2*.

It has not been possible so far to identify a more potent inhibitor than ARL67156. Compounds **68a** and **77a** were the two most promising candidates with K_i values similar to that of ARL67156 (**75a**). Co-incubation with human and mouse liver microsomes showed that all ARL67156 derivatives are metabolically unstable.

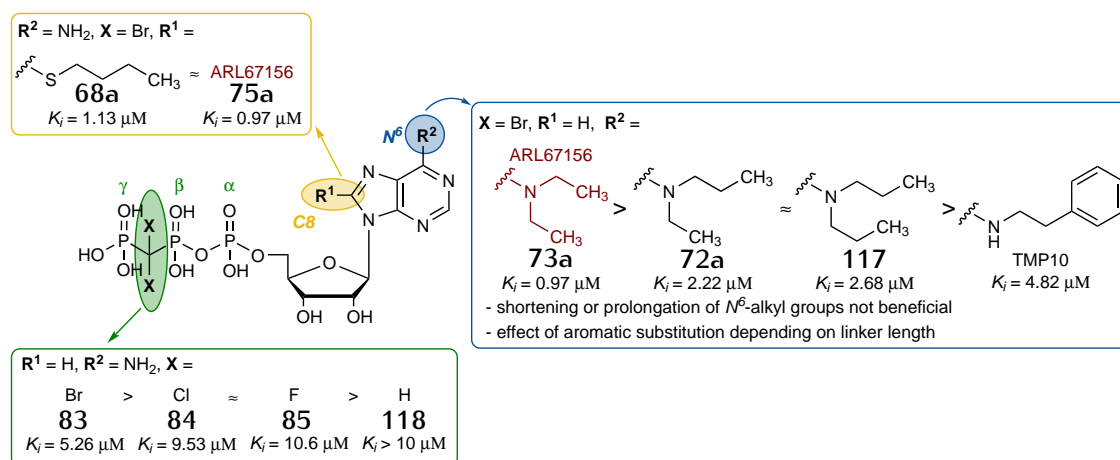


Figure 5.1: Structure-activity relationships of single modifications of the ARL67156-scaffold at human CD39.

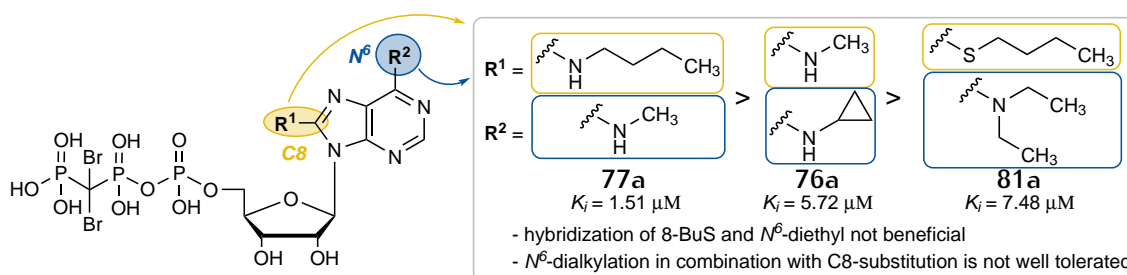


Figure 5.2: Structure-activity relationships of combined modifications of the ARL67156-scaffold at human CD39.

Compounds **68a**, **75a**, and **77a** were further investigated at other extracellular human *ecto*-nucleotidases for their selectivity. None of the compounds was selective for NTPDase1, instead also NTPDase3, NPP1, and CD73 were significantly inhibited.

In the future, it has to be investigated whether other modifications like substitution at the C2-position or replacement of the nitrogen at the 7-position with a carbon would be tolerated. Furthermore, stability issues could be addressed by introducing an additional α,β -methylene group in the phosphate chain.

5.1.2 Structure-activity relationships of AMP derivatives

The synthesized AMP-derivatives were tested for their inhibitory potency at human CD39. The results of the SARs are summarized in *Figure 5.3* and *Figure 5.4*. It

has not been possible so far to identify a more potent inhibitor than 8-BuS-AMP. The compounds **90** and **114** were the two most promising candidates with K_i values similar to that of 8-BuS-AMP (**68b**). All three compounds were tested for their metabolic stability in mouse and human liver microsomes. 8-BuS-AMP (**68b**) was found to be quite stable, while **90** was unstable. Compound **114** possessed some stability with a half-life of 15 or 6 minutes in the presence of mouse or human liver microsomes, respectively.

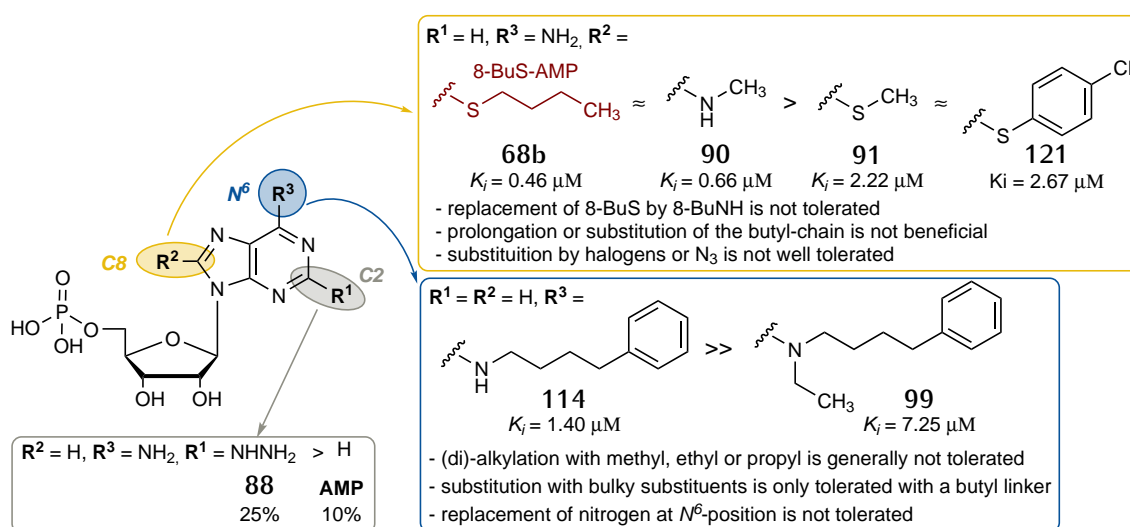


Figure 5.3: Structure-activity relationships of single modifications of the 8-BuS-AMP-scaffold at human CD39.

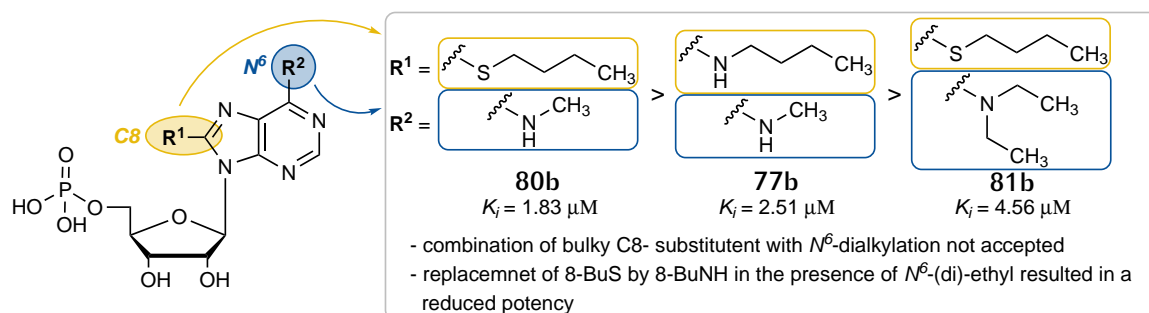


Figure 5.4: Structure-activity relationships of combined modifications of the 8-BuS-AMP-scaffold at human CD39.

Compounds **68b**, **90**, and **114** were further investigated at other extracellular human *ecto*-nucleotidases. Compound **90** had the best selectivity profile in this screening since only NTPDase3 was significantly inhibited in addition to CD39 and the effect on the activity of the other *ecto*-nucleotidases was low or absent. Thus, **90** would be

a preferable CD39 inhibitor for *in vitro* studies, while 8-BuS-AMP (**68b**) is superior for *in vivo* experiments. Compound **114** could serve as multitarget ligand that inhibits multiple enzymes of the same enzyme cascade at the same time.

In the future, it has to be further investigated whether a combination of certain C8- and N^6 -substitutions could be beneficial. Furthermore, C2-substitutions should be combined with C8- and N^6 -modifications to evaluate whether dual modifications would be additive.

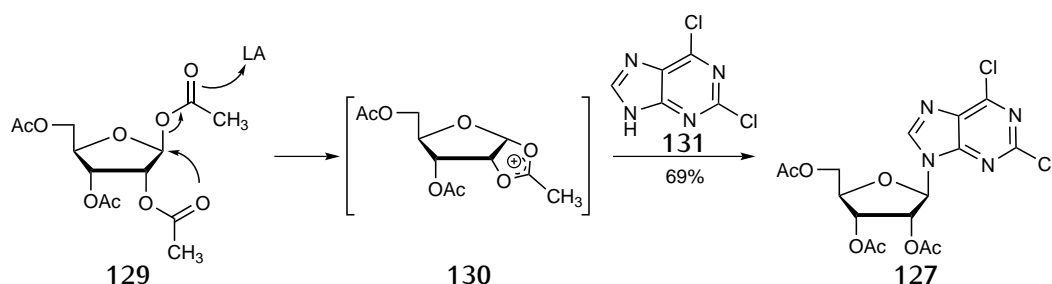
5.2 Synthesis of inhibitors and tool compounds for CD73

The second objective of this thesis was to synthesize and develop a variety of tool compounds for CD73 and to investigate a new class of CD73 inhibitors.

5.2.1 Upscaling of the synthesis of AOPCP derivatives for *in vivo* testing of CD73 inhibitors

In the past, potent, selective and metabolically stable AOPCP-based inhibitors for CD73 had been developed. To provide those compounds to collaborators for further studies, large amounts have to be obtained. The common method for the synthesis of the starting material 2,6-dichloropurine-ribofuranoside used in our laboratory was labor-intensive, and dangerous to apply due to the huge amount of phosphorus oxychloride required in the second step. Therefore, optimization of the synthesis route was required. An alternative strategy to synthesize **127** was tested, in which the C'1-acetoxysugar is melted and reacted with the purine base in the presence of a Lewis acid (*Scheme 5.1*).¹⁵⁶

- By applying this *fusion method*, acetylated 2,6-dichloropurine-ribofuranoside (**127**) was obtained in good yield (69%) and high purity after recrystallization from absolute ethanol
 - No further purification was needed, which makes this an excellent procedure for synthesis on a larger scale



Scheme 5.1: Optimized procedure for the synthesis of 127. LA = Lewis acid. Reagents and conditions: $\text{CF}_3\text{SO}_3\text{H}$, 0.9 bar, 1 h, 85°C \rightarrow room temperature.

- Two AOPCP derivatives, PSB-12379 (123) and PSB-12489 (135), were synthesized on a large scale (> 100 mg)

5.2.2 Development of a radioligand for CD73

A radioligand binding assay is a useful method to study the interaction of compounds with a receptor as well as the affinity of that compound. Such an assay could, for example, be applied to investigate ligand binding kinetics, or for *ex vivo* diagnostic purposes. To establish such an assay in our laboratory, a radioligand for CD73 was developed based on the structure of PSB-12489 (135).

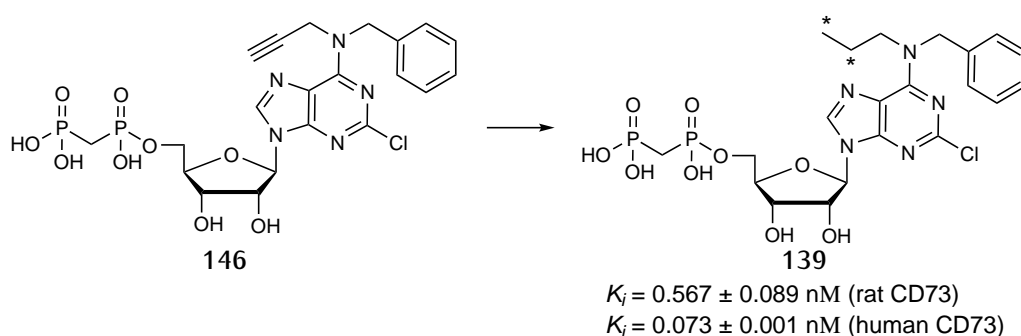


Figure 5.5: Structures of a novel radioligand (139) for CD73 and its precursor (146).

- Three different AOPCP-derived cold ligands (139–141) with high inhibitory potencies and high metabolic stability were obtained
- Compound 139 was chosen as a suitable candidate
- A precursor containing a propargyl-group instead of a propyl-group at the N^6 -position was generated (146)

- Tritium labeling was achieved providing a new radioligand with a high specific activity of 108 Ci/mmol (29.6 TBq/mmol) and high purity of >99% (Figure 5.5)
- The new radioligand binding assay is currently under development; preliminary results are promising (PhD thesis of Riham Idris)¹⁷⁸

5.2.3 Development of a fluorescent probe for CD73

To monitor the expression levels of CD73, a fluorescent probe with a high binding affinity that can be used instead of an antibody, is highly desirable. PSB-12379 was selected as a lead structure to develop potent fluorescent CD73 inhibitors with high binding affinity. The idea was to attach a fluorescent dye to the benzyl ring in the *N*⁶-position of the adenine core structure via a linker moiety.

- As initial fluorophore, fluorescein (**150**) was chosen because it is commercially available containing a carboxylate function and non-toxic
- Two fluorescent probes containing different linker molecules were successfully synthesized (**158a** and **158b**, Figure 5.6)
- Both compounds displayed K_i values in the low nanomolar range
- The inhibitory potency of **158b** was four-fold lower than the potency of **158a** at human soluble CD73 possibly indicating that more lipophilic linker structures are better tolerated by CD73

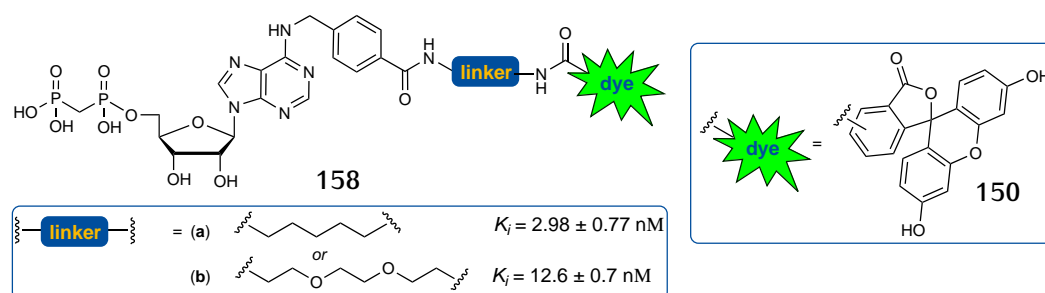


Figure 5.6: Novel fluorescent markers for CD73.

For proof-of-principle studies, both fluorescent inhibitors, **158a** and **158b**, were evaluated by flow cytometry and their performance as CD73 probes was compared to that of an established anti-CD73 antibody. These experiments showed, that the fluorescent CD73 inhibitors possessed high nonspecific binding, which needs to be addressed in the future.

5.2.4 Development of a PET-tracer for CD73

Positron emission tomography (PET) is an important method in the diagnosis of diseases *e.g.* in the field of oncology. A fluorine-containing AOPCP-derived inhibitor for CD73 was developed based on the structure of 2-chloro-*N*⁶-benzyl-AOPCP (Figure 5.7).

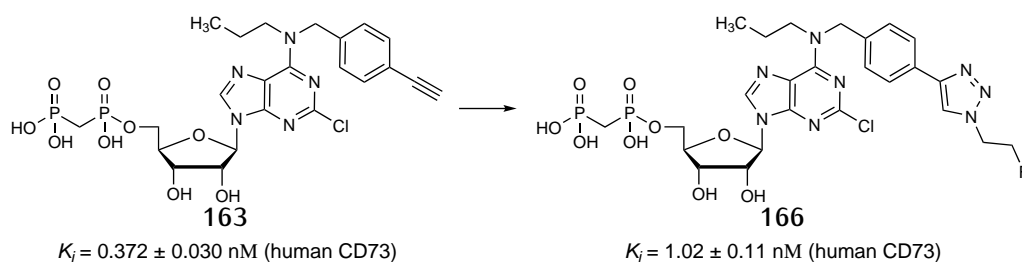


Figure 5.7: Cold version of novel PET-tracer (163) and its precursor (166).

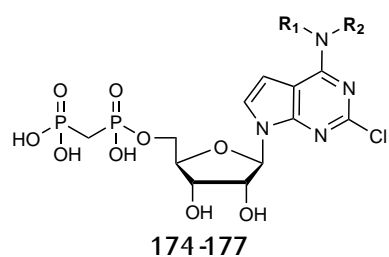
- A cold version of the potential tracer (166) with a K_i -value of 1.02 nM was successfully obtained
- The precursor 163 was successfully generated on a large scale and ^{18}F -labeling will be performed in collaboration

In the near future, *in vivo* studies will be conducted.

5.2.5 7-Deaza-AOPCP derivatives as CD73 inhibitors

Recently, 7-deaza-AOPCP was observed to display a two-fold higher inhibitory potency than AOPCP at rat CD73.¹²⁹ Therefore, a series of 7-deaza-AOPCP derivatives was synthesized and studied based on some of the most potent AOPCP derivatives known so far (Figure 5.8).

The inhibitory potency was significantly decreased at human CD73 upon replacing the nitrogen at the 7-position by a carbon (Figure 5.8). In the future, the potency of 7-deaza-AOPCP at the different enzyme preparations should be reevaluated. Additionally, it should be elucidated whether the 2-chloro substitution is still beneficial in 7-deaza-AOPCP derivatives.



Product	-R ₁	-R ₂	K _i ± SEM (nM)
174		-H	305 ± 59
175		-(CH ₂) ₂ CH ₃	5990 ± 0.62
176		-CH ₃	413 ± 29
177		-H	55.4 ± 7.1

Figure 5.8: Inhibitory potency of N⁶-substituted 2-chloro-7-deaza-AOPCP derivatives at human CD73.

6 Materials and methods

6.1 Chemicals

Unless stated otherwise, all reagents were commercially obtained from various producers (Acros, Fluorochem, Merck, Carbosynth, Santa Cruz, Sigma Aldrich, and TCI) and used without further purification. Commercial solvents of specific reagent grades were used, without additional purification or drying.

If no further details are given the reaction was conducted under ambient atmosphere and temperature. The reactions were monitored by TLC using *Merck silica gel 60 F254* aluminum sheets and using DCM/methanol (9:1 or 3:1) as the mobile phase. The TLC plates were analyzed by staining with potassium permanganate or by ultra-violet (UV) light irradiation at wavelength (λ): 254 nm. Column chromatography was carried out with silica gel 0.040–0.060 mm, pore diameter ca. 6 nm.

6.2 Instrumentation

Semi-preparative HPLC was performed on a *Knauer Smartline 1050 HPLC system* equipped with a *Eurospher-100 C18* column, 250 mm x 20 mm, particle size 10 μ m. The UV absorption was detected at 254 nm. Fractions were collected, and appropriate fractions were pooled, diluted with water, and lyophilized several times, using a *CHRIST ALPHA 1-4 LSC* freeze dryer, to remove the NH_4HCO_3 buffer, yielding the nucleotides as white powders.

Anion exchange chromatography was performed on a FPLC instrument (*ÄKTA FPLC*, from *Amersham Biosciences*) with an *HiPrep Q Fast Flow (FF)* sepharose column, 16 x 100 mm (*GE Healthcare Life Sciences*). Elution of the nucleoside triphosphates was achieved with a linear gradient (5–100%, 0.5 M aqueous ammonium bicarbonate buffer in water, 8 column volumes, flow 1 ml/min). The neutral impurities (e.g. nucleosides) eluted first, followed by charged species (mono-, and finally triphosphates).

Mass spectra were recorded on an *API 2000* mass spectrometer (Applied Biosystems, Darmstadt, Germany) with a turbo ion spray ion source coupled with an *Agilent 1100*

HPLC system (Agilant, Böblingen, Germany) using a *EC50/2 Nucleodur C18 Gravity 3 μ m* (Macherey-Nagel, Düren, Germany), or on a *micrOTOF-Q* mass spectrometer (Bruker, Köln, Germany) with ESI-source coupled with a HPLC *Dionex Ultimate 3000* (Thermo Scientific, Braunschweig, Germany) using an *EC50/2 Nucleodur C18 Gravity 3 μ m* column (Macherey-Nagel, Düren, Germany). The LC-MS samples were prepared by dissolving 1 mg/ml of compound in H₂O/CH₃OH (1:1) containing 2 mM ammonium acetate. A sample of 10 μ L, or 1 μ L respectively, was injected into an HPLC instrument, and elution was performed with a gradient of water/methanol (containing 2 mM ammonium acetate) from 90:10 to 0:100 for 20 min at a flow rate of 250 μ L/min, or with a gradient of water/acetonitrile (containing 2 mM ammonium acetate) from 90:10 to 0:100 for 9 min at a flow rate of 0.3 ml/min. UV absorption was detected from 220 to 400 nm using a DAD.

NMR spectra were recorded on a *Bruker Avance 500* and 600 MHz spectrometers. DMSO-*d*₆, CD₃OD, or D₂O were used as solvent. ³¹P-NMR spectra were recorded at 25°C; phosphoric acid was used as an external standard. For spectra recorded in D₂O, 3-(Trimethylsilyl)propionic-2,2,3,3 acid sodium salt-*d*₄ was used as external standard. When DMSO-*d*₆ was used, spectra were recorded at 30°C. Shifts are given in ppm relative to the external standard (in ³¹P-NMR) or relative to the remaining protons of the deuterated solvents used as internal standard (¹H, ¹³C-NMR) (*Table 6.1*). Coupling constants are given in Hertz (Hz). The designation used to assign the peaks in the spectra is as follows: singlet (s), doublet (d), triplet (t), quartet (q), multiplet (m), broad (br).

Table 6.1: NMR internal standards. Shifts are given in ppm relative to the remaining protons of the deuterated solvents used as internal standard (¹H, ¹³C NMR).

Solvent	¹ H	¹³ C
(CD ₃) ₂ SO	$\delta = 2.49$	$\delta = 39.7$
CD ₃ OD	$\delta = 3.35$	$\delta = 49.3$

Melting points were determined on a *Buchi 530* melting point apparatus and are uncorrected.

Absorption spectra were recorded on a *Varian Cary 50 Bio* (Agilant Technologies, USA). Absorbance was measured compared to a blank from 300 to 800 nm. The 10 mm stock solutions were prepared in water.

Fluorescence spectra were recorded on a *flx safas monaco* (Monaco, Monaco) spec-

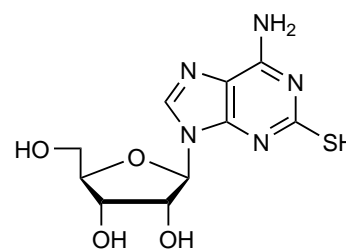
trofluorometer. Adjusted band widths were 5 nm for excitation and emission wavelength, and the emission was recorded from 300 to 800 nm. The excitation wavelength was set corresponding to the absorbance maxima of the corresponding compound.

Absorption and fluorescence spectra were recorded in H₂O, PBS, and sodium acetate buffer pH 4. The final concentrations were 100 μM and 10 μM for the recording of absorption and emission spectra, respectively.

6.3 Experimental procedures

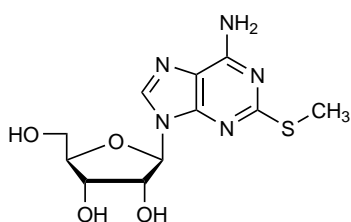
6.3.1 2-Thioadenosine (4), CAS 43157-50-2

To a solution of adenosine (5.0 g, 3.7 mmol, 1.0 eq) in glacial acetic acid (50 ml), a 35% solution of hydrogen peroxide in water (5 ml) was added. The mixture was stirred at 50°C overnight. Active carbon (10.0 g) was added and the mixture was stirred at 50°C until the reaction mixture was free of peroxide as detected by MQuantTM peroxide test strips. The active carbon was removed by filtration followed by evaporation of the filtrate to dryness. The remaining residue was co-evaporated with water repeatedly and finally dissolved in water. The resulting precipitate was collected by filtration and dissolved in refluxed 5 M NaOH (45 ml). The mixture was refluxed for 15 min, cooled to room temperature and adjusted to pH 9.0 with concentrated hydrochloric acid. After evaporation to a small volume, formed sodium chloride salt was removed by filtration and washed with methanol. This process was repeated followed by evaporation to dryness which afforded an amber-coloured gum. The residue was dissolved in a mixture of H₂O/CH₃OH/CS₂ 1:7:2 (150 ml) and was autoclaved at 120°C. After 5 h, the reaction mixture was allowed to cool down and the resulting precipitate was filtered and washed with H₂O and CH₃OH yielding the desired product as yellow powder (1.40 g, 26%). ¹H-NMR (500 MHz, DMSO-d₆) δ 11.90 (br s, 1H, CSH) 8.21 (s, 1H, N=CHN) 5.75 (d, 1H, J = 5.92 Hz, CHN), 4.45 (t, 1H, J = 5.10 Hz, CHOH) 4.09 (br s, 1H, CHOH) 3.92 (br s, 1H, CHCH₂) 3.64-3.52 (dd, 2H, J = 11.97, 64.49 Hz, CHCH₂). ¹³C-NMR (125 MHz, DMSO-d₆) δ 173.91, 161.60, 155.94, 139.82, 112.79, 87.20, 85.93, 73.80, 70.59, 61.58. LC/ESI-MS (m/z): positive



mode 300.0 $[M+H]^+$. Purity determined by HPLC-UV (254 nm)-ESI-MS: 82%. mp: 207°C (*lit.* 196–199°C).¹⁷⁹

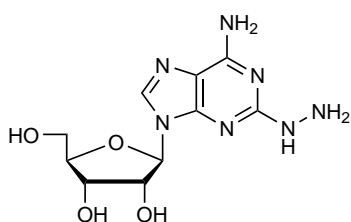
6.3.2 2-Methylthioadenosine (5), CAS 4105-39-9



2-Thioadenosine (0.5 g, 1.7 mmol, 1.0 eq) was resuspended in a mixture of $H_2O/EtOH$ (1:1). The solution was adjusted to basic pH with 0.5 M NaOH (5 ml). Methylsulfide (0.3 ml, 5.0 mmol, 3.0 eq) was added and the reaction was stirred at rt for 20 min. Addition of ethylacetate resulted in precipitation.

Filtration yielded the desired product as white powder (0.50 g, 100%). 1H -NMR (500 MHz, $DMSO-d_6$) δ 8.21 (s, 1H, $NCH=N$) 7.31 (s, 2H, NH_2) 6.09 (d, 1H, $J=5.89$ Hz, CHN) 4.55 (t, 1H, $J=5.48$ Hz, $CHCH_2$) 4.13 (dd, 1H, $J=3.72, 4.90$ Hz, $CHOH$) 3.90 (q, 1H, $J=4.14$ Hz, $CHOH$) 3.63–3.51 (d m, 2H, $CHCH_2$) 2.46 (s, 3H, SCH_3). ^{13}C -NMR (125 MHz, $DMSO-d_6$) δ 164.28, 155.58, 150.31, 138.39, 117.01, 87.55, 85.64, 73.63, 70.57, 61.78, 13.80. LC-MS (m/z): positive mode 314.2 $[M+H]^+$. Purity determined by HPLC-UV (254 nm)-ESI-MS: 90%. mp: 247°C (*lit.* 225°C).¹⁷⁹

6.3.3 2-Hydrazinyladenosine (7), CAS 15763-11-8

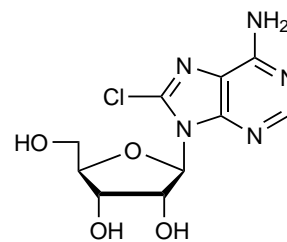


2-Chloroadenosine (0.5 g, 1.7 mmol) was dissolved in hydrazine hydrate (7.5 ml) and the reaction was stirred for 8 h. The reaction mixture was diluted with 2-propanol (10 ml). After evaporation, the residue was taken up in water followed by lyophilization. Purification by column chromatography (CH_3OH/DCM 1:3) yielded the desired product (0.49 g, 100%).

1H -NMR (500 MHz, $DMSO-d_6$) δ 7.93 (s, 1H, $N=CHN$) 7.21 (s, 1H, NH) 6.82 (s, 2H, NH_2) 5.77 (d, 1H, $J=6.29$ Hz, CHN) 5.31 (br s, 1H, CH_2OH) 5.17 (br s, 1H, $CHOH$) 5.11 (br s, 1H, $CHOH$) 4.58 (t, 1H, $J=5.63$ Hz, $CHCH_2$) 4.13 (m, 1H, $CHOH$) 3.91 (q, 1H, $J=3.76$ Hz, $CHOH$) 3.65–3.52 (d m, 2H, $CHCH_2$). ^{13}C -NMR (125 MHz, $DMSO-d_6$) δ 162.07, 156.4, 151.31, 136.76, 114.27, 87.27, 85.56, 73.23, 70.85, 61.85. LC/ESI-MS (m/z): positive mode 298.2 $[M+H]^+$. Purity determined by HPLC-UV (254 nm)-ESI-MS: 99.5%. mp: 162°C.

6.3.4 8-Chloroadenosine (8), CAS 34408-14-5

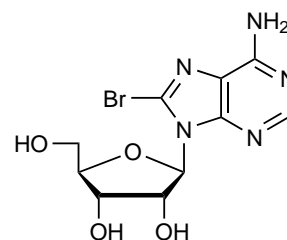
To a solution of adenosine (0.5 g, 1.9 mmol, 1.0 eq) in DMF (4 ml), benzoyl chloride (0.2 ml, 2.0 mmol, 1.1 eq) was added. mCPBA (0.45 g, 2.6 mmol, 1.4 eq) was dissolved in DMF (2 ml) and the solution was added to the reaction mixture. The reaction was stirred for 30 min and then poured into cold water.



The resulting precipitate was filtered and washed with water. The combined filtrate was washed with diethyl ether (3x20 ml) and evaporated to dryness. The resulting yellow syrup was submitted to column chromatography and the desired product was eluted with 10% CH₃OH in DCM. Appropriate fractions were combined and evaporated, followed recrystallization with ethylacetate yielding the desired compound as white solid (0.20 g, 40%). ¹H-NMR (500 MHz, DMSO-d₆) δ 8.20 (s, 1H, N=CHN) 7.80 (br s, 2H, NH₂) 5.85 (d, 1H, *J* = 6.59 Hz, CHN) 5.03 (dd, 1H, *J* = 5.20, 6.61 Hz, CHCH₂) 4.19 (dd, 1H, *J* = 2.69, 5.24 Hz, CHOH) 3.97 (m, 1H, CHOH) 3.67-3.52 (d m, 2H, CHCH₂). ¹³C-NMR (125 MHz, DMSO-d₆) δ 154.44, 151.67, 149.67, 137.55, 118.05, 89.46, 86.77, 71.35, 70.83, 62.10. LC/ESI-MS (*m/z*): positive mode 302.1 [M+H]⁺. Purity determined by HPLC-UV (254 nm)-ESI-MS: 97.4%. mp: 138°C (*lit.* 189-191°C).¹⁸⁰

6.3.5 8-Bromoadenosine (9), CAS 2946-39-6

To a solution of adenosine (3 g, 11.2 mmol, 1.0 eq) in 0.1 M sodium acetate buffer pH 4.0 (15 ml) bromine (1.4 ml, 5.0 eq) was added. The reaction was stirred at rt overnight and regularly checked by TLC. The solution was decolorized by the addition of a 40% solution of NaHSO₃, and the pH of



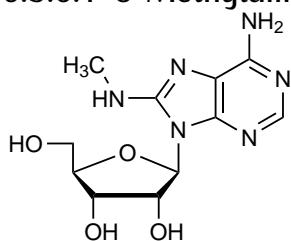
the solution was then adjusted to 7 with concentrated NaOH. The precipitate was filtered off and washed with water. The compound was isolated as slightly yellow colored solid (1.20 g, 31%). ¹H-NMR (500 MHz, DMSO-d₆) δ 8.11 (s, 1H, N=CHN) 7.52 (br s, 2H, NH₂) 5.83 (d, 1H, *J* = 6.74 Hz, CHN) 5.45 (dd, 1H, *J* = 3.91, 8.59 Hz, CHOH) 5.42 (d, 1H, *J* = 6.24 Hz, CHOH) 5.18 (d, 1H, *J* = 4.47 Hz, CH₂OH) 5.08 (q, 1H, *J* = 6.24 Hz, CHCH₂) 4.19 (t, 1H, *J* = 5.97 Hz, CHOH) 3.97 (m, 1H, CHOH) 3.67-3.51 (d m, 2H, CHCH₂). ¹³C-NMR (125 MHz, DMSO-d₆) δ 155.29, 152.55, 150.02, 127.26, 119.82, 90.55, 86.83, 71.24, 71.00, 62.25. LC/ESI-MS (*m/z*): positive mode 346.2

$[M+H]^+$. Purity determined by HPLC-UV (254 nm)-ESI-MS: 89.8%. mp: 225°C (*lit.* 210–212°C).¹⁸¹

6.3.6 General procedure for the synthesis of compounds 10–12

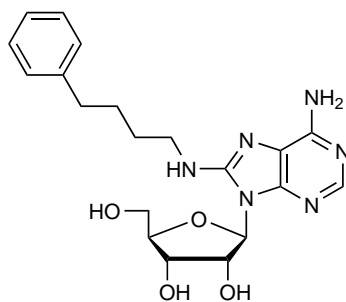
8-Bromoadenosine (**9**, 0.5 g, 1.4 mmol, 1.0 eq) was dissolved in H₂O/absolute EtOH (1:3, 15 ml). The corresponding alkylamine and triethylamine (0.4 ml, 2.9 mmol, 2.0 eq) were added. The reaction was refluxed for 6–36 h followed by evaporation. The crude product was submitted to silica gel column chromatography (CH₃OH/DCM).

6.3.6.1 8-Methylaminoadenosine (**10**), CAS 13389-13-4



The compound was synthesized using 33 wt% methylamine in absolute ethanol (1 ml, 24.3 mmol, 24.0 eq). Purification by column chromatography (CH₃OH/DCM 1:4) yielding the desired compound as a white powder (0.30 g, 89%). ¹H-NMR (500 MHz, DMSO-d₆) δ 7.88 (s, 1H, NCH=N) 6.88 (d, 1H, *J* = 4.80 Hz, NHCH₃) 6.42 (d, 2H, NH₂) 5.84 (d, 1H, *J* = 7.21 Hz, CHN) 5.19 (d, 1H, *J* = 5.52 Hz, CHO_H) 5.08 (d, 1H, *J* = 3.38 Hz, CHO_H) 4.66 (d, 1H, *J* = 6.30 Hz, CHCH₂) 4.12 (br s, 1H, CHO_H) 3.95 (d, 1H, *J* = 2.24 Hz, CHO_H) 3.63 (m, 2H, CHCH₂) 2.87 (d, 3H, *J* = 4.53 Hz, NHCH₃). ¹³C-NMR (125 MHz, DMSO-d₆) δ 152.68, 152.18, 149.95, 148.48, 117.32, 86.65, 85.79, 71.07, 70.87, 61.79, 29.24. LC/ESI-MS (*m/z*): positive mode 297.2 $[M+H]^+$. Purity determined by HPLC-UV (254 nm)-ESI-MS: 94.4%. mp: 215°C (*lit.* 217–218°C).⁹¹

6.3.6.2 8-(4-Phenyl)butylaminoadenosine (**11**), CAS 402724-85-0

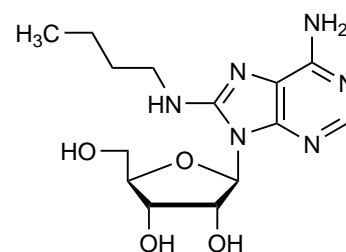


The compound was synthesized using 4-phenylbutylamine (0.3 ml, 2.2 mmol, 1.5 eq). Purification by column chromatography (CH₃OH/DCM 1:4) yielding the desired compound as a white powder (0.27 g, 54%). ¹H-NMR (500 MHz, DMSO-d₆) δ 7.87 (s, 1H, N=CHN) 7.25 (t, 2H, *J* = 7.6 Hz, aryl) 7.19 (d, 2H, *J* = 7.1 Hz, aryl) 7.15 (t, 1H, *J* = 7.3 Hz, aryl) 6.89 (t, 1H, *J* = 5.5 Hz, NHCH₂) 6.44 (s,

2H, NH₂) 5.88 (d, 1H, *J* = 7.4 Hz, CHN) 5.85 (t, 1H, *J* = 4.9 Hz, CH₂OH) 5.20 (d, 1H, *J* = 6.8 Hz, CHOH) 5.12 (d, 1H, *J* = 4.0 Hz, CHOH) 4.63 (q, 1H, *J* = 6.9 Hz, CHCH₂) 4.10 (m, 1H, CHOH) 3.95 (d, 1H, *J* = 2.1 Hz, CHOH) 3.61 (m, 2H, CHCH₂) 2.60 (t, 2H, *J* = 7.0 Hz, CH₂-aryl) 1.61 (m, 4H, (CH₂)₂). ¹³C-NMR (125 MHz, DMSO-d₆) δ 152.46, 151.54, 149.94, 148.60, 142.39, 128.48, 128.42, 125.82, 117.26, 86.55, 85.87, 71.16, 70.90, 61.87, 56.22, 42.27, 35.08, 28.62. LC/ESI-MS (m/z): positive mode 415.0 [M+H]⁺. Purity determined by HPLC-UV (254 nm)-ESI-MS: 95.5%. mp: 108°C.

6.3.6.3 8-Butylaminoadenosine (12), CAS 65456-84-0

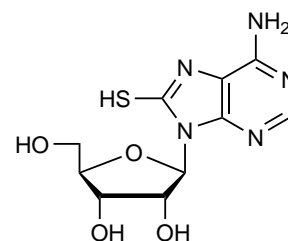
The compound was synthesized using butylamine (0.3 ml, 2.9 mmol, 2.0 eq). Purification by column chromatography (CH₃OH/ DCM 1:4) yielding the desired compound as a white powder (0.48 g, 100%). ¹H-NMR (500 MHz, DMSO-d₆) δ 7.87 (s, 1H, N=CHN) 6.83 (t, 1H, *J* = 5.4 Hz, NHCH₂) 6.44 (s, 2H, NH₂) 5.89 (d, 1H, *J* = 7.3 Hz, CHN) 5.83 (dd, 1H, *J* = 4.3, 5.7 Hz, CH₂OH) 5.19 (d, 1H, *J* = 6.7 Hz, CHOH) 5.11 (d, 1H, *J* = 4.0 Hz, CHOH) 4.62 (m, 1H, CHCH₂) 4.10 (m, 1H, CHOH) 3.95 (q, 1H, *J* = 2.3 Hz, CHOH) 3.62 (dt, 2H, *J* = 2.7, 5.8 Hz, NHCH₂) 3.37 (dd, 1H, *J* = 6.8, 12.7 Hz, overlapping with H₂O, 1x CHCH₂) 3.28 (dd, 1H, *J* = 6.9, 12.7 Hz, overlapping with H₂O, 1x CHCH₂) 1.56 (m, 2H, CH₂) 1.34 (m, 2H, CH₂) 0.9 (t, 3H, *J* = 7.3 Hz, CH₃). ¹³C-NMR (125 MHz, DMSO-d₆) δ 152.43, 151.51, 149.94, 148.56, 117.23, 86.50, 85.81, 71.13, 70.85, 61.80, 42.19, 31.03, 19.83, 13.95. LC/ESI-MS (m/z): positive mode 339.1 [M+H]⁺. Purity determined by HPLC-UV (254 nm)-ESI-MS: 94.7%. mp: 168°C.



6.3.7 8-Thioadenosine (13), CAS 3001-45-4

Method A: To a solution of 8-bromoadenosine (**9**, 0.5 g, 1.4 mmol, 1.0 eq) in absolute ethanol (3 ml), thiourea (0.2 g, 2.6 mmol, 1.8 eq) was added. After 5 h of refluxing the solution was allowed to cool down and the resulting precipitate was removed by filtration. Evaporation of the filtrate yielded crude 8-thioadenosine (**13**) as a yellow-coloured oil.

Method B: To **9** (0.5 g, 1.4 mmol, 1.0 eq) in DMF (5 ml) was added NaHS (0.8 g,

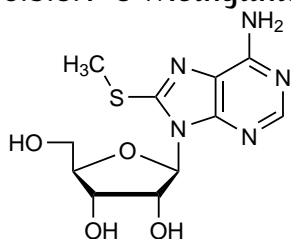


14.4 mmol, 10.0 eq). The mixture was stirred at 100°C for 5 h until TLC analysis indicated that the reaction was complete. The mixture was cooled down to rt and treated with methanol followed by filtration. The filtrate was evaporated and co-evaporated with methanol. The remaining residue was taken up in water, neutralized with 1 M HCl and lyophilized. The crude product was taken up in water and extracted with ethyl acetate. The organic layers were combined, dried over MgSO₄ and reduced *in vacuo* yielding the desired product as brown solid (0.26 g, 59%). ¹H-NMR (500 MHz, DMSO-d₆) δ 12.52 (s, 1H, SH) 8.11 (s, 1H, N=CHN) 6.95 (br s, 2H, NH₂) 6.33 (d, 1H, *J* = 6.3 Hz, CHN) 5.22 (d, 1H, *J* = 6.1 Hz, CHOH) 5.18 (dd, 1H, *J* = 4.1, 8.2 Hz, CH₂OH) 5.08 (d, 1H, *J* = 4.7 Hz, CHOH) 4.99 (q, 1H, *J* = 5.9 Hz, CHCH₂) 4.21 (m, 1H, CHOH) 3.89 (q, 1H, *J* = 3.9 Hz, CHOH) 3.65–3.49 (d m, 2H, CHCH₂). ¹³C-NMR (125 MHz, DMSO-d₆) δ 168.21, 152.20, 148.44, 148.18, 107.33, 88.95, 85.90, 71.01, 70.95, 62.44. LC/ESI-MS (m/z): positive mode 300.0 [M+H]⁺. Purity determined by HPLC-UV (254 nm)-ESI-MS: 99%. mp: 216°C.

6.3.8 General procedure for the synthesis of compounds 14–16

Compound 13 was used without further purification and was resuspended in a mixture of H₂O/EtOH 1:1. The solution was adjusted to basic pH with 1 M NaOH. The corresponding alkylhalide was added and the reaction was stirred at rt for or refluxed.

6.3.8.1 8-Methylthioadenosine (14), CAS 29836-01-9



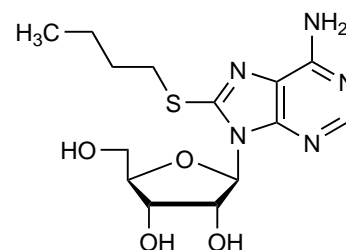
The compound was synthesized using methyl iodide (0.3 ml, 4.3 mmol, 3.0 eq). The reaction was stirred at rt for 15 min. The precipitate was filtered off and was washed with ethanol yielding the desired compound as white solid (0.36 g, 80 %).

¹H-NMR (500 MHz, DMSO-d₆) δ 8.04 (s, 1H, NCH=N) 7.21 (s, 2H, NH₂) 5.72 (d, 1H, *J* = 6.86 Hz, CHN) 5.56 (dd, 1H, *J* = 3.70, 8.65 Hz, CHOH) 5.36 (d, 1H, *J* = 5.07 Hz, CHOH) 5.15 (br s, 1H, CHOH) 4.98 (m, 1H, CHCH₂) 4.15 (br s, 1H, CHOH) 3.95 (m, 1H, CHOH) 3.52–3.66 (d m, 2H, CHCH₂) 2.71 (s, 3H, SCH₃). ¹³C-NMR (125 MHz, DMSO-d₆) δ 154.58, 151.32, 150.85, 149.84, 119.70, 88.89, 88.72, 71.43, 71.07, 62.34, 14.77. LC/ESI-MS (m/z): positive mode 314.1 [M+H]⁺. Purity

determined by HPLC-UV (254 nm)-ESI-MS: 96.8%. mp: 234°C (*lit.* 235-237°C).¹⁸²

6.3.8.2 8-Butylthioadenosine (15), CAS 68807-84-1

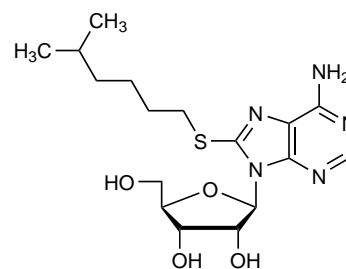
The compound was synthesized using butyliodide (0.5 ml, 4.32 mmol, 3.0 eq). The reaction was stirred at room temperature for 2 h. After extraction with ethyl acetate, the organic phase was evaporated. Purification by column chromatography (CH₃OH/DCM 2:23) afforded the product as a white solid (0.39 g, 76%).



¹H-NMR (500 MHz, DMSO-d₆) δ 8.04 (s, 1H, NCH=N) 7.23 (s, 2H, NH₂) 5.77 (d, 1H, *J* = 7.21 Hz, CHN) 5.59 (dd, 1H, *J* = 3.47, 8.81 Hz, CHOH) 5.36 (d, 1H, *J* = 6.14 Hz, CHOH) 5.14 (d, 1H, *J* = 4.54 Hz, CH₂OH) 4.98 (dd, 1H, *J* = 6.14, 11.88 Hz, CHCH₂) 4.16 (m, 1H, CHOH) 3.96 (m, 1H, CHOH) 3.68-3.50 (d m, 2H, CHCH₂) 3.32-3.27 (d m, 2H overlapping with H₂O peak, SCH₂) 1.68 (m, 2H, CH₂) 1.41 (m, 2H, CH₂) 0.90 (t, 3H, *J* = 7.27 Hz, CH₂CH₃). ¹³C-NMR (126 MHz, DMSO-d₆) δ 184.05, 154.67, 151.39, 150.56, 148.83, 119.74, 89.01, 86.72, 71.40, 71.12, 62.36, 32.22, 31.03, 21.32, 13.56. LC/ESI-MS (*m/z*): positive mode 356.2 [M+H]⁺. Purity determined by HPLC-UV (254 nm)-ESI-MS: 60.9% (rest injection peak). mp: 105°C (*lit.* 171.5°C).¹⁸³

6.3.8.3 8-(5-Methyl)hexylthioadenosine (16)

The compound was synthesized using 1-bromo-5-methylhexane (0.17 ml, 1 mmol, 2.0 eq). The reaction was refluxed for 30 h followed by evaporation. The resulting residue was extracted with ethyl acetate and water. The organic phases were combined, washed with brine, dried over MgSO₄, and reduced *in vacuo*. The crude product



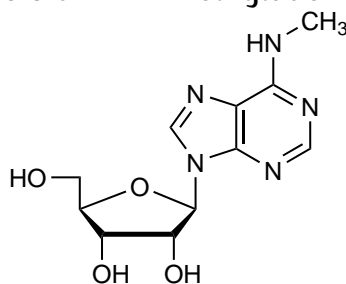
was purified by column chromatography (CH₃OH/DCM 3:47) yielding the desired product as white solid (0.08 g, 30%). ¹H-NMR (500 MHz, DMSO-d₆) δ 8.04 (s, 1H, N=CHN) 7.22 (s, 2H, NH₂) 5.77 (d, 1H, *J* = 6.9 Hz, CHN) 5.59 (dd, 1H, *J* = 3.7, 8.9 Hz, CH₂OH) 5.35 (d, 1H, *J* = 6.2 Hz, CHOH) 5.14 (d, 1H, *J* = 4.3 Hz, CHOH) 4.99 (q, 1H, *J* = 6.2 Hz, CHCH₂) 4.15 (m, 1H, CHOH) 3.95 (td, 1H, *J* = 2.2, 3.8 Hz, CHOH) 3.66-3.51 (d m, 2H, CHCH₂) 3.28 (m, 2H, SCH₂ overlapping with H₂O) 1.67 (m, 2H, CH₂) 1.49 (m, 1H, CH(CH₃)₂) 1.39 (m, 2H, CH₂) 1.16 (m, 2H, CH₂) 0.84 (s, 3H, CHCH₃) 0.83 (s, 3H,

CHCH₃). ¹³C-NMR (126 MHz, DMSO-d₆) δ 154.69, 151.41, 150.56, 148.86, 119.76, 89.03, 86.74, 71.43, 71.14, 62.37, 37.95, 32.58, 29.25, 27.47, 25.98, 22.58. LC/ESI-MS (m/z): positive mode 398.0 [M+H]⁺. Purity determined by HPLC-UV (254 nm)-ESI-MS: 99%. mp: 180°C.

6.3.9 General procedure for the synthesis of 21-38

To 6-chloro-9-(β-D-ribofuranosyl)purine (0.5 g, 1.7 mmol, 1.0 eq) in absolute ethanol (15 ml) the corresponding alkylamine and Et₃N (0.1 ml, 1.6 mmol, 0.9 eq) were added. The reaction mixture was refluxed for 6-36 h followed by evaporation of the solvent.

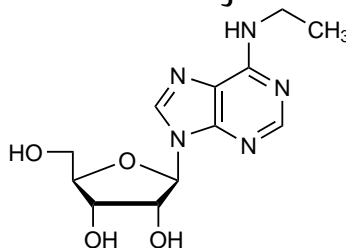
6.3.9.1 N⁶-Methyladenosine (21), CAS 1867-73-8



The compound was synthesized using 33 wt% methylamine in absolute ethanol (0.1 ml, 2.4 mmol, 1.4 eq) yielding a white solid (0.70 g). ¹H-NMR (500 MHz, DMSO-d₆) δ 8.32 (s, 1H, NCH=N) 8.21 (br s, 1H, NCH=N) 7.77 (br s, 1H, NHCH₃) 5.87 (d, 1H, *J* = 6.17 Hz, CHN) 5.40 (br s, 1H, CHOH) 5.14 (br s, 1H, CHOH) 4.59 (t, 1H, *J* = 5.33 Hz, CHOH) 4.14 (dd, 1H, *J* = 3.21, 4.75 Hz, CHOH) 3.95 (q, 1H, *J* = 3.51 Hz, CHCH₂) 3.66-3.54 (d m, 2H, CHCH₂) 3.05 (m, 3H, NHCH₃).

¹³C-NMR (125 MHz, DMSO-d₆) δ 156.52, 152.46, 148.22, 139.74, 119.98, 88.05, 86.02, 73.65, 70.77, 61.79, 24.44. LC/ESI-MS (m/z): positive mode 282.3 [M+H]⁺. Purity determined by HPLC-UV (254 nm)-ESI-MS: 99.3%. mp: 132°C (*lit.* 130-132°C).¹⁸⁴

6.3.9.2 N⁶-Ethyladenosine (22), CAS 14357-08-5

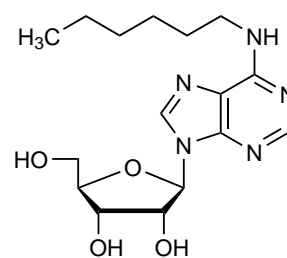


The compound was synthesized using 70% ethylamine in H₂O (0.1 ml, 1.76 mmol, 1.0 eq) yielding a white solid (0.60 g). ¹H-NMR (500 MHz, DMSO-d₆) δ 8.32 (s, 1H, NCH=N) 8.18 (br s, 1H, NCH=N) 7.81 (br s, 1H, NHCH₂) 5.87 (d, 1H, *J* = 6.16 Hz, CHN) 5.40 (d, 1H, *J* = 6.22 Hz, CHOH) 5.14 (d, 1H, *J* = 4.55 Hz, CHOH) 4.59 (q, 1H, *J* = 5.97 Hz, CHOH) 4.14 (q, 1H, *J* = 4.40 Hz, CHOH) 3.95 (q, 1H, *J* = 3.50 Hz, CHCH₂) 3.66-3.55 (d m, 2H, CHCH₂)

3.04 (m, 2H, CH_2CH_3) 1.16 (m, 3H, CH_2CH_3). ^{13}C -NMR (125 MHz, DMSO-d_6) δ 154.67, 152.47, 148.57, 139.72, 119.82, 88.07, 86.02, 73.63, 70.78, 61.80, 34.24, 12.63. LC/ESI-MS (m/z): positive mode 296.1 $[\text{M}+\text{H}]^+$. Purity determined by HPLC-UV (254 nm)-ESI-MS: 97.4%. mp: 159°C (*lit.* 191–192°C).¹⁸⁵

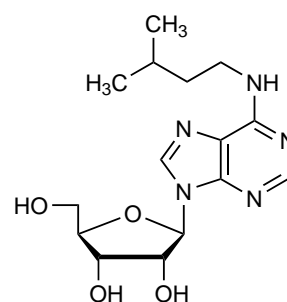
6.3.9.3 N^6 -Hexyladenosine (23), CAS 15824-83-6

The compound was synthesized using *N*-hexylamine (0.25 ml, 1.9 mmol, 1.0 eq) and purified by silica gel column chromatography ($\text{CH}_3\text{OH}/\text{DCM}$ 2:23) yielding a white powder (0.66 g, 99%). ^1H -NMR (500 MHz, DMSO-d_6) δ 8.31 (s, 1H, $\text{N}=\text{CHN}$) 8.19 (s, 1H, $\text{N}=\text{CHN}$) 7.80 (s, 1H, NHCH_2) 5.86 (d, 1H, $J=6.2$ Hz, CHN) 5.39 (m, 2H, overlapping 2x CHOH) 5.14 (d, 1H, $J=4.6$ Hz, CH_2OH) 4.60 (q, 1H, $J=6.0$ Hz, CHCH_2) 4.14 (t, 1H, $J=4.7$ Hz, CHOH) 3.95 (q, 1H, $J=3.4$ Hz, CHOH) 3.66–3.54 (d m, 2H, CHCH_2OH) 3.46 (br s, 2H, NHCH_2) 1.57 (m, 2H, $\text{NHCH}_2\text{CH}_2\text{CH}_2$) 1.28 (m, 4H, $\text{CH}_2(\text{CH}_2)_2\text{CH}_2$) 1.18 (t, 2H, $J=7.0$ Hz, CH_2CH_3) 0.85 (t, 3H, $J=6.7$ Hz, CH_2CH_3). ^{13}C -NMR (126 MHz, DMSO-d_6) δ 154.83, 152.50, 148.36, 139.69, 119.89, 88.10, 86.04, 73.61, 70.81, 61.83, 48.73, 45.77, 31.18, 26.20, 22.21, 14.04. LC/ESI-MS (m/z): positive mode 351.9 $[\text{M}+\text{H}]^+$. Purity determined by HPLC-UV (254 nm)-ESI-MS: 98.0%. mp: 116°C.



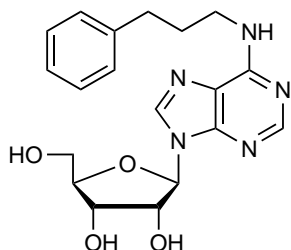
6.3.9.4 N^6 -*iso*-Pentyladenosine (24), CAS 17659-78-8

The compound was synthesized using isopentylamine (1 ml, 8.6 mmol, 4.6 eq) and purified by silica gel column chromatography ($\text{CH}_3\text{OH}/\text{DCM}$ 2:23) yielding a white powder (0.60 g, 95%). ^1H -NMR (500 MHz, DMSO-d_6) δ 8.31 (s, 1H, $\text{N}=\text{CHN}$) 8.19 (s, 1H, $\text{N}=\text{CHN}$) 7.80 (s, 1H, NHCH_2) 5.86 (d, 1H, $J=6.2$ Hz, CHN) 5.39 (m, 2H, 2x CHOH) 5.14 (d, 1H, $J=4.6$ Hz, CH_2OH) 4.60 (q, 1H, $J=6.0$ Hz, CHCH_2) 4.14 (t, 1H, $J=4.7$ Hz, CHOH) 3.95 (q, 1H, $J=3.4$ Hz, CHOH) 3.66–3.54 (d m, 2H, CHCH_2) 3.49 (br s, 2H, NHCH_2) 1.62 (m, 1H, $\text{CH}(\text{CH}_3)_2$) 1.48 (q, 2H, $J=7.0$ Hz, $\text{CH}_2\text{CH}_2\text{CH}$) 0.89 (d, 6H, $J=6.6$ Hz, $\text{CH}(\text{CH}_3)_2$). ^{13}C -NMR (126 MHz, DMSO-d_6) δ 154.81, 152.55, 148.35, 139.74, 119.91, 88.12, 86.06, 73.61, 70.83, 61.85, 38.16, 25.45, 22.66 (missing: NHCH_2). LC/ESI-MS (m/z): positive mode 338.1 $[\text{M}+\text{H}]^+$. Purity determined by



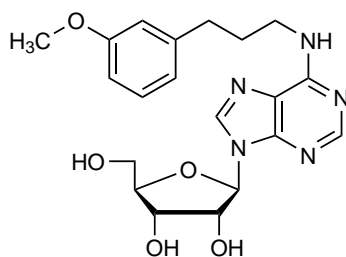
HPLC-UV (254 nm)-ESI-MS: 97%. mp: 158°C.

6.3.9.5 *N*⁶-(3-Phenyl)propyladenosine (25), CAS 101565-57-5



The compound was synthesized using 3-phenylpropylamine (0.25 ml, 1.8 mmol, 1.0 eq) yielding the product as white powder (1.1 g). ¹H-NMR (500 MHz, DMSO-d₆) δ 8.33 (s, 1H, NCH=N) 8.19 (br s, 1H, NCH=N) 7.89 (d, 2H, *J* = 29.21 Hz, aryl) 7.28 (dt, 3H, *J* = 7.52, 21.51 Hz, aryl) 5.87 (d, 1H, *J* = 6.16 Hz, CHN) 5.41 (d, 1H, *J* = 6.24 Hz, CHOH) 5.38 (m, 1H, CHOH) 5.15 (d, 1H, *J* = 4.59 Hz, CH₂OH) 4.60 (q, 1H, *J* = 5.92 Hz, CHOH) 4.14 (q, 1H, *J* = 4.65 Hz, CHOH) 3.95 (q, 1H, *J* = 3.34 Hz, CHCH₂) 3.66-3.55 (d m, 2H, CHCH₂) 3.50 (m, 2H, NHCH₂CH₂) 2.63 (t, 2H, *J* = 7.71 Hz, CH₂CH₂Ph) 1.87 (m, 2H, CH₂CH₂CH₂). ¹³C-NMR (125 MHz, DMSO-d₆) δ 154.84, 152.50, 141.98, 140.97, 139.78, 128.58, 128.44, 128.40, 126.19, 125.83, 119.96, 88.08, 86.03, 73.63, 70.80, 61.82, 45.66, 31.97, 28.88. LC/ESI-MS (*m/z*): positive mode 386.2 [M+H]⁺. Purity determined by HPLC-UV (254 nm)-ESI-MS: 91.0%. mp: 103°C.

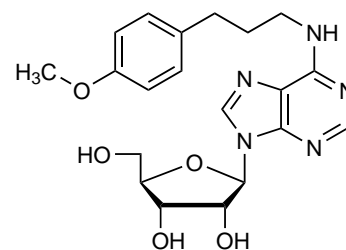
6.3.9.6 *N*⁶-(3-(3-Methoxy)phenyl)propyladenosine (26)



The compound was synthesized using 3-methoxybenzene-propanamine (43, 0.29 g, 1.75 mmol, 1.0 eq) and purified by silica gel column chromatography (CH₃OH/DCM 1:9) yielding white powder (0.34 g, 47%). ¹H-NMR (500 MHz, DMSO-d₆) δ 8.33 (s, 1H, NCH=N) 8.19 (br s, 1H, NCH=N) 7.94 (s, 1H, NHCH₂) 7.17 (t, 1H, *J* = 8.05 Hz, aryl) 6.78-6.71 (m, 3H, aryl) 5.87 (d, 1H, *J* = 6.19 Hz, CHN) 5.41 (overlapping d and t, 2H, CHOH & CHOH) 5.16 (d, 1H, *J* = 4.62 Hz, CH₂OH) 4.60 (q, 1H, *J* = 6.09 Hz, CHCH₂) 4.13 (td, 1H, *J* = 3.11, 4.75 Hz, CHOH) 3.95 (q, 1H, CHOH) 3.71 (s, 3H, OCH₃) 3.68-3.52 (m, 2H, CHCH₂) 3.16 (d, 1H, *J* = 5.24 Hz, NHCH₂CH₂) 2.61 (m, 2H, CH₂Ph) 1.89 (m, 2H, CH₂CH₂CH₂). ¹³C-NMR (125 MHz, DMSO-d₆) δ 159.44, 154.86, 152.52, 148.39, 143.60, 139.82, 129.42, 120.73, 119.94, 114.06, 111.39, 88.11, 86.08, 7.63, 70.84, 61.85, 55.04, 48.77, 32.83, 30.82. LC/ESI-MS (*m/z*): positive mode 416.0 [M+H]⁺. Purity determined by HPLC-UV (254 nm)-ESI-MS: 94%. mp: 132°C.

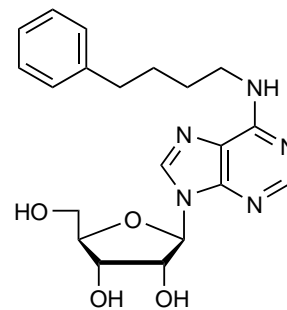
6.3.9.7 *N*⁶-(3-(4-Methoxy)phenyl)propyladenosine (27), CAS 157640-48-7

The compound was synthesized using 4-methoxybenzene-propanamine (44, 0.29 g, 1.75 mmol, 1.0 eq) and purified by silica gel column chromatography (CH₃OH/DCM 1:9) yielding a white powder (0.31 g, 43%). ¹H-NMR (500 MHz, DMSO-d₆) δ 8.33 (s, 1H, NCH=N) 8.19 (br s, 1H, NCH=N) 7.92 (br s, 1H, NH) 7.12 (d, 2H, *J* = 8.17 Hz, aryl) 6.82 (d, 2H, *J* = 8.25 Hz, aryl) 5.88 (s, 1H, CHN) 5.42 (s, 2H, overlapping CHO_H & CHO_H) 5.17 (s, 1H, CH₂OH) 4.60 (s, 1H, CHCH₂) 4.13 (s, 1H, CHOH) 3.95 (s, 1H, CHOH) 3.70 (s, 3H, OCH₃) 3.65-3.55 (d m, 2H, CHCH₂) 3.48 (br s, 2H, NHCH₂) 2.57 (s, 2H, CH₂-aryl) 1.85 (s, 2H, CH₂). ¹³C-NMR (125 MHz, DMSO-d₆) δ 157.55, 154.91, 152.55, 148.42, 139.83, 133.84, 129.39, 120.01, 113.08, 88.14, 86.10, 73.64, 70.86, 61.88, 55.14, 48.79, 31.91, 31.19. LC/ESI-MS (*m/z*): positive mode 416.0 [M+H]⁺. Purity determined by HPLC-UV (254 nm)-ESI-MS: 98.0%. mp: 130°C.

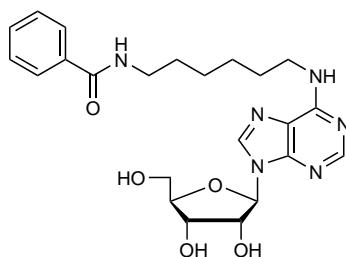


6.3.9.8 *N*⁶-(4-Phenyl)butyladenosine (28), CAS 101565-58-6

The compound was synthesized using 4-phenylbutylamine (0.28 ml, 1.75 mmol, 1.0 eq) yielding the product as white powder (0.60 g, 88%). ¹H-NMR (500 MHz, DMSO-d₆) δ 8.31 (s, 1H, NCH=N) 8.18 (br s, 1H, NCH=N) 7.86 (s, 1H, NHCH₂) 7.19 (m, 5H, aryl) 5.87 (d, 1H, *J* = 6.16 Hz, NCH=N) 5.38 (m, 1H, CHO_H) 5.36 (m, 1H, CHO_H) 5.13 (d, 1H, *J* = 4.64 Hz, CH₂OH) 4.60 (q, 1H, *J* = 6.13 Hz, CHOH) 4.14 (m, 1H, CHOH) 3.95 (q, 1H, *J* = 3.47 Hz, CHCH₂) 3.68-3.52 (d m, 2H, CHCH₂) 2.60 (m, 2H, CH₂CH₂Ph) 1.61 (br s, 4H, CH₂(CH₂)CH₂) 1.16 (t, 2H, *J* = 7.27 Hz, NHCH₂CH₂). ¹³C-NMR (125 MHz, DMSO-d₆) δ 154.88, 152.44, 148.33, 142.31, 139.68, 128.39, 128.29, 125.69, 119.81, 88.06, 86.00, 73.57, 70.76, 61.79, 45.76, 28.53, 27.72, 26.70. LC/ESI-MS (*m/z*): positive mode 400.2 [M+H]⁺. Purity determined by HPLC-UV (254 nm)-ESI-MS: 94.3%. mp: 106°C.



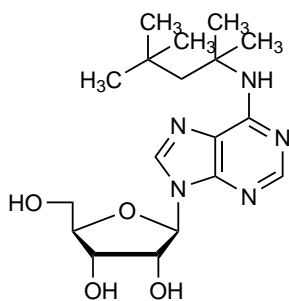
6.3.9.9 *N*⁶-(6-Benzamide)hexyladenosine (29), CAS 1582751-81-2



The compound was synthesized using **19** (1.1 g, 5.2 mmol, 1.5 eq) and purified by RP-HPLC (20 → 100% CH₃OH in water in 20 min, 20 ml/min) yielding the product as white powder (0.30 g, 17%). ¹H-NMR (500 MHz, DMSO-d₆) δ 8.38 (t, 1H, *J* = 5.62 Hz, NHCH₂) 8.31 (s, 1H, N=CHN) 8.18 (s, 1H, N=HN) 7.81 (m, 2H, aryl) 7.48 (m, 1H, aryl)

7.43 (m, 2H, aryl) 5.87 (d, *J* = 6.14 Hz, 1H, CHN) 5.38 (d, 2H, *J* = 6.13 Hz, 2x CHOH) 5.13 (d, 1H, *J* = 4.61 Hz, CH₂OH) 4.60 (q, 1H, *J* = 5.85 Hz, CHCH₂) 4.14 (td, 1H, *J* = 3.01, 4.76 Hz, CHOH) 3.95 (q, 1H, *J* = 3.46 Hz, CHOH) 3.66–3.55 (d m, 2H, CHCH₂) 3.46 (br s, 2H, NHCH₂) 3.23 (m, 2H, NHCH₂) 1.59 (m, 2H, CH₂) 1.51 (m, 2H, CH₂) 1.34 (m, 4H, (CH₂)₂). ¹³C-NMR (125 MHz, DMSO-d₆) δ 166.21, 154.82, 152.49, 148.38, 145.29, 139.71, 134.90, 131.05, 128.31, 127.23, 119.86, 88.10, 86.04, 73.60, 70.80, 61.83, 45.94, 39.29, 29.27, 29.20, 26.44, 26.32. LC/ESI-MS (*m/z*): positive mode 471.0 [M+H]⁺. Purity determined by HPLC-UV (254 nm)-ESI-MS: 95.7%. mp: 114°C.

6.3.9.10 *N*⁶-(1,1,3,3-Tetramethyl)butyladenosine (30), CAS 37676-69-0

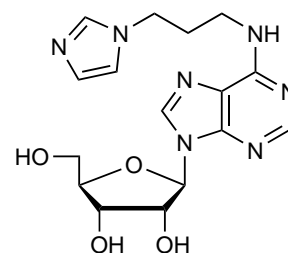


The compound was synthesized using 2,4,4-trimethylpentan-2-amine (0.4 ml, 2.6 mmol, 1.5 eq) and purified by silica gel column chromatography (CH₃OH/DCM 1:24), yielding the product as white powder (0.22 g, 34%). ¹H-NMR (500 MHz, DMSO-d₆) δ 8.31 (s, 1H, N=CHN) 8.21 (s, 1H, N=CHN) 6.69 (s, 1H, NHCH₂) 5.86 (d, 1H, *J* = 6.2 4 Hz, CHN) 5.41 (br s, 1H, CHOH) 5.37 (dd, 1H, *J* = 4.6, 7.2 Hz, CHOH) 5.16 (d,

1H, *J* = 3.3 Hz, CH₂OH) 4.62 (br s, 1H, CHOH) 4.13 (br s, 1H, CHOH) 3.95 (q, 1H, *J* = 3.5 Hz, CHCH₂) 3.66–3.54 (d m, 2H, CHCH₂) 2.00 (s, 2H, CH₂) 1.54 (s, 6H, (CH₃)₂) 0.92 (s, 9H, C(CH₃)₃). ¹³C-NMR (125 MHz, DMSO-d₆) δ 154.78, 151.89, 148.22, 139.77, 120.43, 88.13, 86.12, 73.57, 70.86, 61.88, 55.56, 50.23, 31.65, 31.40, 29.97. LC/ESI-MS (*m/z*): positive mode 379.9 [M+H]⁺. Purity determined by HPLC-UV (254 nm)-ESI-MS: 92.0%. mp: 110°C.

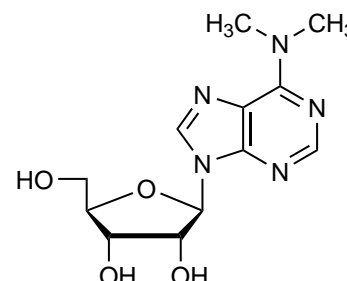
6.3.9.11 *N*⁶-(3-(Imidazol-1-yl)propyl)adenosine (31)

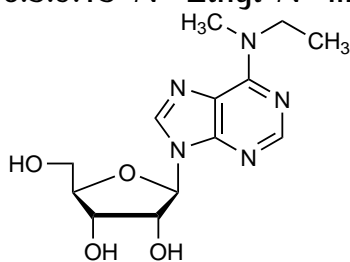
The compound was synthesized using 3-(1H-imidazol-1-yl)propan-1-amine (0.3 ml, 2.6 mmol, 1.5 eq). The crude product was extracted with water from ethyl acetate. Lyophilization of the water layer yielding the product as brown solid (0.60 g, 95%). ¹H-NMR (500 MHz, DMSO-d₆) δ 8.35 (s, 1H, N=CHN) 8.20 (s, 1H, N=CHN) 7.98 (s, 1H, NHCH₂) 7.71 (d, 1H, *J* = 27.30 Hz, imidazole) 7.21 (d, 1H, *J* = 21.59 Hz, imidazole) 6.91 (s, 1H, imidazole) 5.88 (d, 1H, *J* = 6.14 Hz, CHN) 5.40 (br s, 1H, CHOH) 5.18 (br s, 1H, CHOH) 4.59 (t, 1H, *J* = 5.51 Hz, CHCH₂) 4.14 (m, 1H, CHOH) 4.07 (t, 2H, *J* = 6.86 Hz, NHCH₂) 4.04 (t, 2H, *J* = 6.94 Hz, NCH₂) 3.95 (q, 1H, *J* = 3.40 Hz, CHOH) 3.66–3.54 (dm, 2H, CHCH₂) 2.69 (m, 2H, CH₂). ¹³C-NMR (125 MHz, DMSO-d₆) δ 154.87, 152.50, 148.52, 139.93, 137.43, 128.03, 119.70, 119.51, 88.09, 86.07, 73.70, 70.82, 61.63, 43.23, 36.32, 28.84. LC/ESI-MS (*m/z*): positive mode 376.0 [M+H]⁺. Purity determined by HPLC-UV (254 nm)-ESI-MS: 97.2%. mp: 100°C.



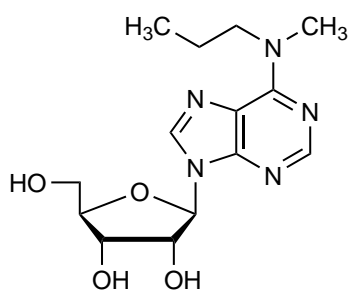
6.3.9.12 *N*⁶-Dimethyladenosine (32), CAS 2620-62-4

The compound was synthesized using *N*-dimethylamine (0.1 ml, 1.75 mmol, 1.0 eq) and purified by silica gel column chromatography (CH₃OH/DCM 1:49) yielding a white powder (0.52 g). ¹H-NMR (500 MHz, DMSO-d₆) δ 8.35 (s, 1H, N=CHN) 8.20 (s, 1H, N=CHN) 5.90 (d, 1H, *J* = 5.97 Hz, CHN) 5.39 (d, 1H, *J* = 6.17 Hz, CHOH) 5.32 (dd, 1H, *J* = 4.62, 6.95 Hz, CHOH) 5.13 (d, 1H, *J* = 4.78 Hz, CHOH) 4.56 (q, 1H, *J* = 5.99 Hz, CHOH) 4.14 (m, 1H, CHCH₂) 3.95 (q, 1H, *J* = 3.55 Hz, CHOH) 3.66–3.55 (dm, 2H, CHCH₂) 3.45 (br s, 6H, N(CH₃)₂). ¹³C-NMR (125 MHz, DMSO-d₆) δ 154.46, 151.82, 150.05, 138.69, 119.94, 87.94, 85.88, 73.64, 70.65, 61.68, 11.57. LC/ESI-MS (*m/z*): positive mode 296.0 [M+H]⁺. Purity determined by HPLC-UV (254 nm)-ESI-MS: 98%. mp: 186°C (*lit.* 184°C).¹⁸⁶



6.3.9.13 *N*⁶-Ethyl-*N*⁶-methyladenosine (33), CAS 402724-55-4

The compound was synthesized using *N*-ethylmethylamine (0.2 ml, 1.75 mmol, 1.0 eq) yielding a white powder (0.93 g). ¹H-NMR (500 MHz, DMSO-*d*₆) δ 8.35 (s, 1H, N=CHN) 8.20 (s, 1H, N=CHN) 5.90 (d, 1H, *J* = 6.00 Hz, CHN) 5.39 (d, 1H, *J* = 6.19 Hz, CHOH) 5.32 (dd, 1H, *J* = 4.61, 6.96 Hz, CH₂OH) 5.13 (d, 1H, *J* = 4.76 Hz, CHOH) 4.57 (q, 1H, *J* = 5.99 Hz, CHOH) 4.14 (m, 1H, CHCH₂) 4.04 (br s, 2H, NCH₂) 3.95 (q, 1H, *J* = 3.51 Hz, CHOH) 3.66-3.54 (d m, 2H, CHCH₂) 3.39 (br s, 3H, NCH₃) 1.17 (t, 3H, *J* = 7.00 Hz, CH₃). ¹³C-NMR (125 MHz, DMSO-*d*₆) δ 153.82, 151.89, 150.02, 138.82, 119.69, 87.91, 85.88, 73.59, 70.66, 61.69, 44.78, 35.47, 12.56. LC/ESI-MS (*m/z*): positive mode 310.0 [M+H]⁺. Purity determined by HPLC-UV (254 nm)-ESI-MS: 98.0%. mp: 101°C.

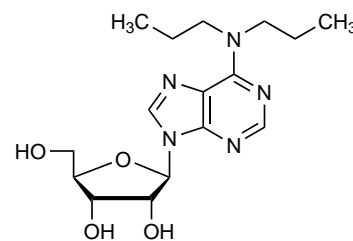
6.3.9.14 *N*⁶-Methyl-*N*⁶-propyladenosine (34), CAS 402724-38-3

The compound was synthesized using *N*-methylpropylamine (0.18 ml, 1.75 mmol, 1.0 eq) and purified by silica gel column chromatography (CH₃OH/DCM 1:9) yielding a white powder (0.66 g). ¹H-NMR (500 MHz, DMSO-*d*₆) δ 8.35 (s, 1H, N=CHN) 8.19 (s, 1H, N=CHN) 5.89 (d, 1H, *J* = 5.97 Hz, CHN) 5.41 (d, 1H, *J* = 6.16 Hz, CHOH) 5.33 (m, 1H, CH₂OH) 5.14 (d, 1H, *J* = 4.64 Hz, CHOH) 4.57 (q, 1H, *J* = 5.76 Hz, CHOH) 4.14 (d, 1H, *J* = 3.62 Hz, CHOH) 3.95 (d, 1H, *J* = 3.13 Hz, CHCH₂) 3.66-3.54 (d m, 2H, CHCH₂) 3.16 (br s, 2H, NCH₂) [bulb underneath previous peaks: NCH₃] 1.64 (q, 2H, *J* = 7.30 Hz, CH₂) 0.87 (t, 3H, *J* = 7.34 Hz, CH₃). ¹³C-NMR (125 MHz, DMSO-*d*₆) δ 154.16, 151.88, 150.10, 138.79, 119.71, 87.92, 85.92, 73.62, 70.71, 61.74, 51.32, 48.75, 21.58, 11.06. LC/ESI-MS (*m/z*): positive mode 324.1 [M+H]⁺. Purity determined by HPLC-UV (254 nm)-ESI-MS: 97.7%. mp: 178°C.

6.3.9.15 *N*⁶-Dipropyladenosine (35), CAS 17270-24-5

The compound was synthesized using *N*-dipropylamine (0.25 ml, 1.75 mmol, 1.0 eq) and purified by silica gel column chromatography (CH₃OH/DCM 1:19) yielding a white powder (0.65 g).

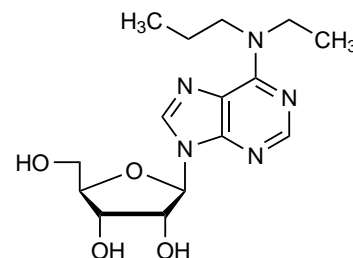
¹H-NMR (500 MHz, DMSO-d₆) δ 8.35 (s, 1H, N=CHN) 8.18 (br s, 1H, N=CHN) 5.89 (d, 1H, *J* = 6.05 Hz, CHN) 5.40 (d, 1H, *J* = 5.91 Hz, CHOH) 5.33 (dd, 1H, *J* = 4.63, 6.97 Hz, CH₂OH) 5.14 (d, 1H, *J* = 4.60 Hz, CHOH) 4.58 (q, 1H, *J* = 5.66 Hz, CHOH) 4.13 (q, 1H, *J* = 4.53 Hz, CHOH) 4.06 (m, 4H, N(CH₂)₂) 3.95 (q, 1H, *J* = 3.50 Hz, CHCH₂) 3.65-3.54 (d m, 2H, CHCH₂) 1.64 (m, 4H, (CH₂)₂) 0.89 (t, 6H, *J* = 7.37 Hz, (CH₃)₂). ¹³C-NMR (125 MHz, DMSO-d₆) δ 153.80, 151.88, 150.10, 138.89, 119.50, 87.92, 85.92, 73.56, 70.73, 61.92, 56.17, 48.74, 18.70, 11.18. LC/ESI-MS (*m/z*): positive mode 352.1 [M+H]⁺. Purity determined by HPLC-UV (254 nm)-ESI-MS: 98.3%. mp: 145°C.



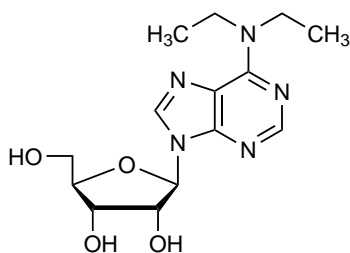
6.3.9.16 *N*⁶-Ethyl-*N*⁶-propyladenosine (36)

The compound was synthesized using *N*-ethylpropylamine (0.2 ml, 1.75 mmol, 1.0 eq) and purified by silica gel column chromatography (CH₃OH/DCM 1:9) yielding a white powder (0.38 g, 65%).

¹H-NMR (500 MHz, CD₃OD) δ 8.15 (d, 2H, *J* = 2.01 Hz, 2x N=CHN) 5.93 (d, 1H, *J* = 6.55 Hz, CHN) 4.74 (dd, 1H, *J* = 5.15, 6.48 Hz, CHOH) 4.30 (dd, 1H, *J* = 2.45, 5.09 Hz, CHCH₂) 4.16 (q, 1H, *J* = 2.40 Hz, CHOH) 3.88-3.72 (d m, 2H, CHCH₂) overlapping with 4.10-3.72 (br s, 4H, 2x NCH₂) 1.73 (m, 2H, CH₂CH₂CH₃) 1.25 (t, 3H, *J* = 7.04 Hz, CH₂CH₃) 0.95 (t, 3H, *J* = 7.39 Hz, (CH₂)₂CH₃). ¹³C-NMR (151 MHz, CD₃OD) δ 155.40, 152.72, 150.70, 140.17, 121.60, 91.21, 88.17, 75.17, 72.77, 63.58, 51.25, 44.72, 22.52, 13.90, 11.36. LC/ESI-MS (*m/z*): positive mode 310.0 [M+H]⁺. Purity determined by HPLC-UV (254 nm)-ESI-MS: 97.2%. mp: 160°C.



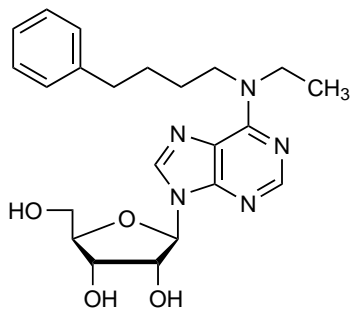
6.3.9.17 *N*⁶-Diethyladenosine (37), CAS 2139-60-8



The compound was synthesized using *N*-diethylamine (0.3 ml, 3.4 mmol, 2.0 eq) and purified by silica gel column chromatography (CH₃OH/DCM 2:23) yielding a white powder (0.50 g, 100%). ¹H-NMR (500 MHz, DMSO-*d*₆) δ 8.34 (s, 1H, NCH=N) 8.19 (s, 1H, NCH=N) 5.89 (d, 1H, *J* = 6.04 Hz, CHN) 5.39 (d, 1H, *J* = 6.19 Hz, CHO_H)

5.33 (dd, 1H, *J* = 4.59, 7.02 Hz, CH₂OH) 5.13 (d, 1H, *J* = 4.61 Hz, CHO_H) 4.58 (q, 1H, *J* = 6.04 Hz, CHOH) 4.14 (td, 1H, *J* = 3.36, 4.82 Hz, CHOH) 4.03 (br s, 4H, N(CH₂CH₃)₂) 3.95 (q, 1H, *J* = 3.54 Hz, CHCH₂) 3.66–3.54 (d m, 2H, CHCH₂) 1.19 (t, 6H, *J* = 6.95 Hz, N(CH₂CH₃)₂). ¹³C-NMR (125 MHz, DMSO-*d*₆) δ 153.27, 151.95, 150.06, 138.96, 119.47, 87.94, 85.91, 73.57, 70.70, 61.73, 42.56, 13.48. LC/ESI-MS (*m/z*): positive mode 324.1 [M+H]⁺. Purity determined by HPLC-UV (254 nm)-ESI-MS: 99.2%. mp: 180°C.

6.3.9.18 *N*⁶-Ethyl-*N*⁶-(4-Phenyl)butyladenosine (38)

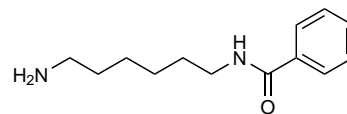


The compound was synthesized using *N,N*-ethyl(4-phenylbutyl)amine (0.68 g, 3.82 mmol, 1.0 eq) and purified by silica gel column chromatography (CH₃OH/DCM 2:23) yielding a white powder (0.93 g, 58%). ¹H-NMR (500 MHz, DMSO-*d*₆) δ 8.35 (s, 1H, N=CHN) 8.18 (s, 1H, N=CHN) 7.24–7.15 (m, 5H, aryl) 5.89 (d, 1H, *J* = 6.03 Hz, CHN) 5.39 (d, 1H, *J* = 6.19 Hz, CHO_H) 5.32 (dd, 1H, *J* = 4.61, 6.99 Hz, CHO_H) 5.13 (d, 1H, *J* = 4.74 Hz, CH₂OH) 4.58 (q, 1H, *J* = 6.04 Hz, CHOH) 4.14 (m, 1H, CHOH) 4.06 (br s, 2H, NCH₂) 3.95 (q, 1H, *J* = 3.52 Hz, CHCH₂) 3.75 (br s, 2H, NCH₂) 3.66–3.55 (d m, 2H, CHCH₂) 2.62 (t, 2H, *J* = 7.29 Hz, CH₂-aryl) 1.62 (m, 4H, (CH₂)₂) 1.16 (t, 3H, *J* = 6.81 Hz, CH₂CH₃).

¹³C-NMR (125 MHz, DMSO-*d*₆) δ 153.52, 151.92, 150.09, 142.24, 138.92, 128.41, 125.77, 119.49, 87.94, 85.92, 75.59, 70.71, 61.74, 48.74, 47.45, 35.07, 28.37, 13.90. LC/ESI-MS (*m/z*): positive mode 428.1 [M+H]⁺. Purity determined by HPLC-UV (254 nm)-ESI-MS: 97.4%. mp: 60.5°C.

6.3.10 *N*-(6-Aminohexyl)benzamide (**19**), CAS 66095-34-9

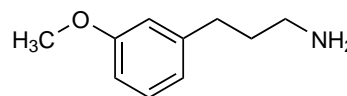
To benzoic acid (0.48 g, 3.95 mmol, 1.0 eq) in anhydrous THF (20 ml), HOBt (0.5 g, 3.95 mmol, 1.0 eq) and DCC (0.8 g, 3.95 mmol, 1.0 eq) were added. After activation, *N*-



Boc-hexandiamine (**17**, 1.0 g, 3.95 mmol, 1.0 eq) dissolved in THF (10 ml) was added and the reaction was stirred overnight at rt. DCU was filtered off and the filtrate was evaporated. The intermediate **18** was purified by silica gel column chromatography (CH₃OH/DCM 1:19) yielding a colorless oil (1.15 g, 91%). LC/ESI-MS (m/z): positive mode 321.3 [M+H]⁺. Purity determined by HPLC-UV (254 nm)-ESI-MS: 90.4%. **18** was taken up in DCM (10 ml) and TFA (0.6 ml, 6%_{w/w}) was added. The reaction was stirred at rt for 2 days. TFA and DCM were added on a regular basis since both chemicals evaporated quickly due to the hot weather and high temperatures in the lab. The reaction was carefully monitored by TLC analysis. Evaporation followed by extraction with ethyl acetate afforded the compound as oil (2.4 g, 100%). ¹H-NMR (500 MHz, DMSO-d₆) δ 8.42 (t, 1H, *J* = 5.42 Hz, NHCH₂) 7.81 (d, 2H, *J* = 7.08 Hz, aryl) 7.64 (br s, 2H, CH₂NH₂) 7.50 (t, 1H, *J* = 7.89 Hz, aryl) 7.44 (t, 2H, *J* = 7.49 Hz, aryl) 3.25 (q, 2H, *J* = 6.86 Hz, NH₂CH₂) 2.76 (dd, 2H, *J* = 6.68, 14.07 Hz, CH₂NH) 1.51 (m, 4H, (CH₂)₂) 1.32 (m, 4H, (CH₂)₂). ¹³C-NMR (125 MHz, DMSO-d₆) δ 134.87, 131.77, 128.39, 127.26, 116.65, 114.73, 33.50, 29.12, 27.17, 26.13, 25.67, 24.62, 21.20. LC/ESI-MS (m/z): positive mode 220.8 [M+H]⁺. Purity determined by HPLC-UV (254 nm)-ESI-MS: 90.4%.

6.3.11 3-Methoxybenzenepropanamine (**43**), CAS 18655-52-2

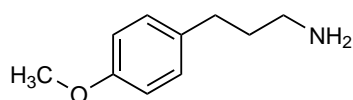
A solution of 3-(3-methoxyphenyl)propionic acid (2.0 g, 11.08 mmol, 1.0 eq) and 4-methylmorpholine (1.3 ml, 12.2 mmol, 1.1 eq) in THF (20 ml) was cooled to 0°C, and



iso-butyl chloroformate (1.58 ml, 12.2 mmol, 1.1 eq) was added slowly. After 30 min of stirring at 0°C, a 7 M solution of NH₃ in CH₃OH (3.2 ml, 22.16 mmol, 2.0 eq) was added dropwise. The mixture was allowed to warm up to rt and stirred for 2 h. The reaction was quenched with 10% *aq* K₂CO₃. The crude product was extracted with ethyl acetate. The organic layers were combined, washed with water and brine and dried over MgSO₄, followed by filtration and evaporation to dryness. LC/ESI-MS (m/z): positive mode 179.9 [M+H]⁺. Purity determined by HPLC-UV (254 nm)-ESI-MS:

95%. The intermediate **41** was dissolved in THF (50 ml) at 0°C and lithium aluminium hydride (0.84 g, 22.16 mmol, 2.0 eq) was added carefully. The reaction mixture was heated to reflux. After 30 min no starting material was detected anymore by TLC (CH₃OH/DCM 1:3). The reaction was quenched carefully with sequential addition of H₂O (10 ml), 15% *aq* NaOH, and H₂O (40 ml), followed by extraction with diethyl ether (3x50 ml). The organic layers were combined, dried over NaSO₄ and concentrated *in vacuo*. Purification by silica gel column chromatography (CH₃OH/DCM 1:9) yielded a yellow liquid (0.69 g, 5.11 mmol, 38%). ¹H-NMR (500 MHz, DMSO-d₆) δ 7.16 (m, 1H, aryl) 6.73 (m, 3H, aryl) 3.72 (s, 3H, OCH₃) 2.54 (dt, 4H, *J* = 7.25, 11.65 Hz, (CH₂)₂) 1.62 (m, 2H, CH₂). ¹³C-NMR (125 MHz, DMSO-d₆) δ 159.40, 144.06, 129.30, 120.7, 114.08, 111.12, 55.00, 41.27, 35.07, 32.76. LC/ESI-MS (*m/z*): positive mode 166.0 [M+H]⁺. Purity determined by HPLC-UV (254 nm)-ESI-MS: 100%.

6.3.12 4-Methoxybenzenepropanamine (**44**), CAS 36397-23-6

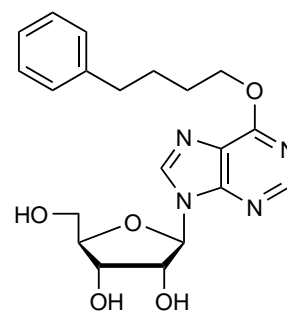


A solution of 3-(4-methoxyphenyl)propionic acid (2.0 g, 11.08 mmol, 1.0 eq) and 4-methylmorpholine (1.3 ml, 12.2 mmol, 1.1 eq) in THF (20 ml) was cooled to 0°C, and *iso*-butyl chloroformate (1.6 ml, 12.2 mmol, 1.1 eq) was added slowly. After 30 min of stirring at 0°C, a 7 M solution of NH₃ in CH₃OH (3.2 ml, 22.16 mmol, 2.0 eq) was added dropwise. The mixture was allowed to warm up to rt and stirred for 2 h. The reaction was quenched with 10% *aq* K₂CO₃. The crude product was extracted with ethyl acetate. The organic layers were combined, washed with water and brine and dried over MgSO₄, followed by filtration and evaporation to dryness. LC/ESI-MS (*m/z*): positive mode 189.9 [M+H]⁺. Purity determined by HPLC-UV (254 nm)-ESI-MS: 94.0%. The intermediate **42** was dissolved in THF (50 ml) at 0°C and lithium aluminium hydride (0.84 g, 22.16 mmol, 2.0 eq) was added carefully. The reaction mixture was heated to reflux. After 30 min no starting material was detected anymore by TLC (CH₃OH/DCM 1:3). The reaction was quenched carefully with sequential addition of H₂O (10 ml), 15% *aq* NaOH, and H₂O (40 ml), followed by extraction with diethyl ether (3x50 ml). The organic layers were combined, dried over NaSO₄ and concentrated *in vacuo*. Purification by silica gel column chromatography (CH₃OH/DCM 1:9) yielded a colorless liquid (0.84 g, 46%). ¹H-NMR (500 MHz, DMSO-d₆) δ 7.08 (d, 2H, *J* = 8.63 Hz, aryl) 6.81 (d, 2H, *J* = 8.63 Hz, aryl) 3.69 (s, 3H,

OCH₃) 2.50 (m, 4H, (CH₂)₂) 1.57 (dt, 2H, $J = 6.94, 14.15$ Hz, CH₂). ¹³C-NMR (125 MHz, DMSO-d₆) δ 157.40, 134.29, 129.26, 113.27, 55.08, 48.72, 41.26, 33.57, 31.79, 18.69. LC/ESI-MS (m/z): positive mode 165.9 [M+H]⁺. Purity determined by HPLC-UV (254 nm)-ESI-MS: 98.1%.

6.3.13 6-(4-Phenyl)butoxypurine riboside (45)

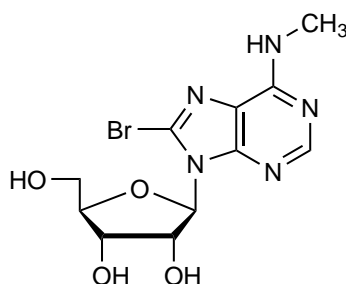
To 4-phenylbutanol (7 ml) small pieces of sodium were carefully added until a milky solution was generated. The sodium alkoxide was added to a suspension of **20** (0.5 g, 1.74 mmol, 1.0 eq) in 4-phenylbutanol (5 ml). The reaction was refluxed for 2 h and the solvent was evaporated. Purification by silica gel column chromatography (CH₃OH/DCM 1:9), yielding the product as white solid (0.2 g, 31%). ¹H-NMR (500 MHz, dimethylsulfoxide (DMSO)-d₆) δ 8.59 (s, 1H, N=CHN) 8.51 (s, 1H, N=CHN) 7.21 (m, 5H, aryl) 5.97 (d, 1H, $J = 5.75$ Hz, CHN) 5.47 (d, 1H, $J = 5.76$ Hz, CHOH) 5.19 (d, 1H, $J = 4.82$ Hz, CHOH) 5.11 (t, 1H, $J = 5.62$ Hz, CH₂OH) 4.58 (m, 3H, overlapping OCH₂ & CHCH₂) 4.16 (m, 1H, CHOH) 3.96 (q, 1H, $J = 3.78$ Hz, CHOH) 3.66-3.54 (d m, 2H, CHCH₂OH) 2.65 (t, 2H, $J = 7.58$ Hz, OCH₂CH₂) 1.81 (m, 2H, CH₂CH₂CH₂) 1.72 (m, 2H, CH₂CH₂-phenyl). ¹³C-NMR (126 MHz, DMSO-d₆) δ 160.31, 151.95, 151.74, 142.43, 142.03, 128.42, 128.37, 125.82, 121.25, 87.92, 85.83, 73.88, 70.47, 66.57, 61.46, 34.85, 28.09, 27.47. LC/ESI-MS (m/z): positive mode 401.1 [M+H]⁺. Purity determined by HPLC-UV (254 nm)-ESI-MS: 95%. mp: 90°C.



6.3.14 General procedure for the synthesis of 46-49

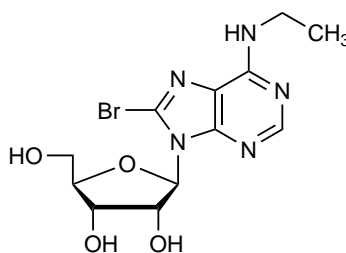
To a solution of *N*⁶-substituted adenosine (1 eq) in 0.1 M sodium acetate buffer pH 4.0 (15 ml) bromine (5.0 eq) was added. The reaction was stirred at rt overnight and monitored by TLC. The solution was decolorized by the addition of a 40% solution of NaHSO₃, and the pH of the solution was then adjusted to 7 with concentrated NaOH. The precipitate was filtered off and washed with water.

6.3.14.1 8-Bromo-*N*⁶-methyladenosine (46), CAS 37116-71-5



The compound was synthesized starting from **21** (1.96 g, 7.0 mmol, 1.0 eq) and afforded a white solid (0.60 g, 25%). ¹H-NMR (500 MHz, DMSO-*d*₆) δ 8.20 (s, 1H, NCH=N) 8.02 (s, 1H, NH) 5.84 (d, 1H, *J* = 7.08 Hz, CHN) 5.45 (q, 1H, *J* = 4.07 Hz, CHOH) 5.41 (d, 1H, *J* = 6.77 Hz, CHOH) 5.19 (d, 1H, *J* = 4.60 Hz, CH₂OH) 5.07 (dd, 1H, *J* = 6.55, 11.33 Hz, CHCH₂) 4.20 (m, 1H, CHOH) 3.97 (dd, 1H, *J* = 4.07, 5.66 Hz, CHOH) 3.69-3.49 (d m, 2H, CHCH₂) 2.94 (s, 3H, NHCH₃). ¹³C-NMR (125 MHz, DMSO-*d*₆) δ 154.12, 152.58, 149.04, 126.87, 120.40, 90.57, 86.84, 71.34, 70.99, 62.24, 27.10. LC/ESI-MS (*m/z*): positive mode 346.1 [M+H]⁺. Purity determined by HPLC-UV (254 nm)-ESI-MS: 95.6%. mp: 228°C.

6.3.14.2 8-Bromo-*N*⁶-ethyladenosine (47)



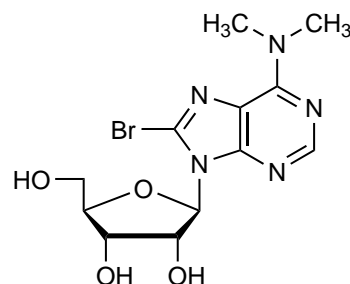
The compound was synthesized starting from **22** (2.0 g, 7.0 mmol, 1.0 eq) and purification by silica gel chromatography (CH₃OH/DCM 1:9) afforded the desired product as white solid (0.38 g, 14%). ¹H-NMR (500 MHz, DMSO-*d*₆) δ 8.18 (s, 1H, N=CHN) 8.10 (s, 1H, NHCH₂) 5.82 (d, 1H, *J* = 6.71 Hz, CHN) 5.49 (dd, 1H, *J* = 3.91, 8.68 Hz, CH₂OH) 5.43 (d, 1H, *J* = 6.29 Hz, CHOH) 5.21 (d, 1H, *J* = 4.45 Hz, CHOH) 5.07 (td, 1H, *J* = 5.15, 6.54 Hz, CHOH) 4.19 (td, 1H, *J* = 2.41, 4.89 Hz, CHOH) 3.7 (td, 1H, *J* = 2.25, 3.94 Hz, CHCH₂) 3.67-3.52 (d m, 2H, CHCH₂) 3.49 (m, 2H, NHCH₂) 1.15 (t, 3H, *J* = 7.13 Hz, CH₃). ¹³C-NMR (125 MHz, DMSO-*d*₆) δ 153.57, 152.62, 149.25, 126.96, 120.32, 90.32, 86.92, 71.39, 71.06, 62.30, 34.81, 14.79. LC/ESI-MS (*m/z*): positive mode 373.8 [M+H]⁺. Purity determined by HPLC-UV (254 nm)-ESI-MS: 95.4%.

6.3.14.3 8-Bromo-*N*⁶-dimethyladenosine (48), CAS 35665-66-8

The compound was synthesized starting from **32** (2.0 g, 7.0 mmol, 1.0 eq) and afforded a white solid (0.60 g, 21%).

¹H-NMR (500 MHz, DMSO-*d*₆) δ 8.18 (s, 1H, NCH=N) 5.84 (d, 1H, *J* = 6.47 Hz, CHN) 5.41 (overlapping q and d, 2H, 2x CHOH) 5.19 (d, 1H, *J* = 4.68 Hz, CH₂OH) 5.08 (dd, 1H, *J* = 6.48, 11.80 Hz, CHCH₂) 4.21 (m, 1H, CHOH)

3.97 (m, 1H, CHOH) 3.70-3.49 (d m, 2H, CHCH₂) 3.41 (br s, 6H, N(CH₃)₂). ¹³C-NMR (125 MHz, DMSO-*d*₆) δ 153.29, 151.72, 150.88, 126.06, 120.37, 90.68, 86.80, 71.12, 70.96, 62.25, 56.16, 18.68. LC/ESI-MS (*m/z*): positive mode 374.2 [M+H]⁺. Purity determined by HPLC-UV (254 nm)-ESI-MS: 96.6%. mp: 152°C.

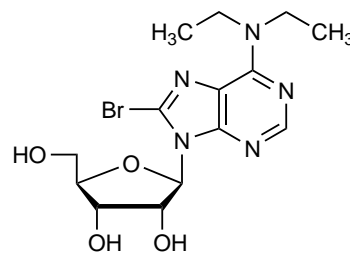


6.3.14.4 8-Bromo-*N*⁶-diethyladenosine (49)

The compound was synthesized starting from **37** (1.919 g, 5.9 mmol, 1.0 eq) and afforded a white solid (0.52 g, 23%). ¹H-NMR (500 MHz, DMSO-*d*₆) δ 8.17 (s, 1H, N=CHN) 5.84 (d, 1H, *J* = 6.75 Hz, CHN) 5.45 (dd, 1H, *J* = 3.87, 8.57 Hz, CHOH) 5.42 (d, 1H, *J* = 5.89 Hz, CHOH)

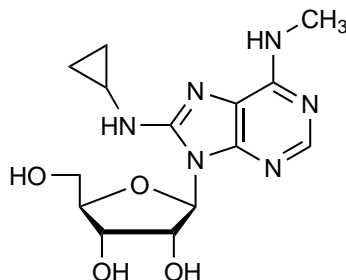
5.20 (d, 1H, *J* = 4.40 Hz, CH₂OH) 5.09 (q, 1H, *J* = 5.92 Hz, CHCH₂) 4.19 (td, 1H, *J* = 2.45, 4.76 Hz, CHOH) 3.97 (td, 1H, *J* = 2.97, 4.04 Hz, CHOH)

4.19-3.7 (br s, 4H, overlapping with previous peaks N(CH₂CH₃)₂) 3.67-3.51 (d m, 2H, CHCH₂) 1.18 (t, 6H, *J* = 6.89 Hz, N(CH₂CH₃)₂). ¹³C-NMR (125 MHz, DMSO-*d*₆) δ 152.14, 151.88, 150.94, 126.35, 119.92, 90.70, 86.85, 71.08, 62.29, 56.19, 42.87, 18.70, 13.65. LC/ESI-MS (*m/z*): positive mode 402.0 [M+H]⁺. Purity determined by HPLC-U-V (254 nm)-ESI-MS: 97.6%.

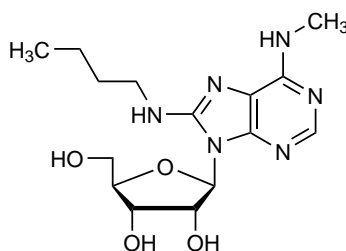


6.3.15 General procedure for the synthesis of 50-56

To the 8-bromo-*N*⁶-substituted adenosine derivatives **46-49** in absolute ethanol (15 ml) the corresponding alkylamine and Et₃N (0.1 ml, 1.6 mmol, 0.9 eq) were added. The reaction mixture was refluxed for 6-36 h followed by evaporation of the solvent.

6.3.15.1 8-Cyclopropylamino-*N*⁶-methyladenosine (50)

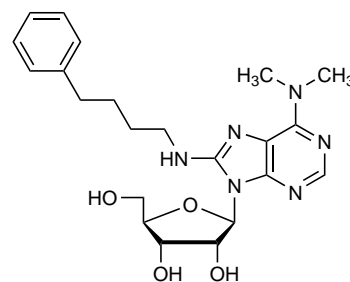
The compound was synthesized starting from **46** (0.5 g, 1.4 mmol, 1.0 eq), using cyclopropylamine (0.3 ml, 4.2 mmol, 3.0 eq). Purification by column chromatography (CH₃OH/DCM 1:49) afforded the desired product as a yellow waxy residue (0.18 g, 37%). ¹H-NMR (500 MHz, DMSO-d₆) δ 7.98 (s, 1H, N=CHN) 7.05 (d, 1H, *J* = 2.63 Hz, NHCH₃) 6.86 (q, 1H, *J* = 4.66 Hz, NHCH) 5.87 (d, 1H, *J* = 7.29 Hz, CHN) 5.82 (dd, 1H, *J* = 4.35, 6.07 Hz, NHCH) 5.15 (d, 1H, *J* = 6.68 Hz, CHOH) 5.08 (d, 1H, *J* = 4.35 Hz, CHOH) 4.58 (q, 1H, *J* = 6.98, 12.55 Hz, CH₂OH) 4.32 (t, *J* = 4.96 Hz, 1H, CHCH₂) 4.09 (m, 1H, CHOH) 3.94 (q, 1H, *J* = 2.52 Hz, CHOH) 3.61 (m, 2H, CHCH₂) 2.93 (d, 3H, *J* = 4.66 Hz, NHCH₃) 0.66 (m, 2H, CH₂) 0.45 (m, 2H, CH₂). ¹³C-NMR (125 MHz, DMSO-d₆) δ 152.26, 151.58, 148.87, 137.05, 117.62, 86.49, 85.75, 71.03, 70.84, 61.75, 25.01, 18.67, 6.83, 6.19. LC/ESI-MS (*m/z*): positive mode 337.1 [M+H]⁺. Purity determined by HPLC-UV (254 nm)-ESI-MS: 89.4 %. mp: 219°C.

6.3.15.2 8-Butylamino-*N*⁶-methyladenosine (51)

The compound was synthesized starting from **46** (0.4 g, 1.1 mmol, 1.0 eq) using *N*-butylamine (0.3 ml, 4.2 mmol, 3.0 eq). Purification by column chromatography (CH₃OH/DCM 1:9) afforded the desired product as slightly yellow solid (0.36 g, 93%). ¹H-NMR (500 MHz, DMSO-d₆) δ 7.95 (s, 1H, N=CHN) 6.83 (t, 1H, *J* = 5.51 Hz, NHCH₂) 6.77 (q, 1H, *J* = 4.74 Hz, NHCH₃) 5.89 (d, 1H, *J* = 7.69 Hz, CHN) 5.84 (br s, 1H, CH₂OH) 5.19 (br s, 1H, CHOH) 5.11 (br s, 1H, CHOH) 4.62 (br s, 1H, CHCH₂) 4.11 (br s, 1H, CHOH) 3.95 (br d, 1H, *J* = 1.98 Hz, CHOH) 3.62 (br s, 2H, CHCH₂) 3.36 (m overlapping with H₂O, 2H, NHCH₂) 2.92 (d, 3H, *J* = 4.78 Hz, NHCH₃) 1.56 (m, 2H, CH₂) 1.33 (m, 2H, CH₂) 0.89 (t, 3H, *J* = 7.38 Hz, CH₂CH₃). ¹³C-NMR (125 MHz, DMSO-d₆) δ 152.01, 151.35, 148.86, 148.59, 117.62, 86.45, 85.78, 71.09, 70.87, 61.79, 42.17, 31.00, 29.44, 27.44, 19.78, 13.19. LC/ESI-MS (*m/z*): positive mode 353.0 [M+H]⁺. Purity determined by HPLC-UV (254 nm)-ESI-MS: 91.4%. mp: 202°C.

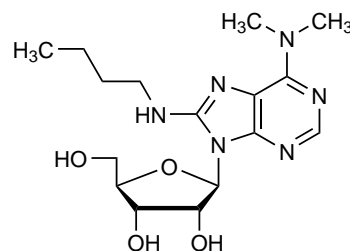
6.3.15.3 8-(4-Phenyl)butylamino-*N*⁶-dimethyladenosine (52)

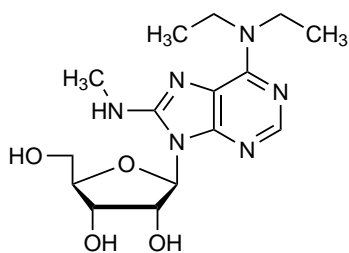
The compound was synthesized starting from **48** (0.35 g, 0.93 mmol, 1.0 eq) using (4-phenyl)butylamine (0.15 ml, 0.94 mmol, 1.0 eq). Purification by column chromatography (CH₃OH/DCM 2:23) afforded the desired product as white powder (0.16 g, 36%). ¹H-NMR (500 MHz, DMSO-d₆) δ 7.95 (s, 1H, N=CHN) 7.24-7.16 (d m, 5H, aryl) 6.88 (t, 1H, *J* = 5.39 Hz, NHCH₂) 5.91 (d, 1H, *J* = 7.42 Hz, CHN) 5.83 (t, 1H, *J* = 4.93 Hz, CHOH) 5.18 (d, 1H, *J* = 6.82 Hz, CHOH) 5.10 (d, 1H, *J* = 4.10 Hz, CH₂OH) 4.61 (m, 2H, 2x CHOH) 4.10 (q, 2H, *J* = 4.50 Hz, NCH₂) 3.95 (m, 1H, CHCH₂) 3.62 (d, 2H, *J* = 4.54 Hz, CHCH₂) 3.34 (s, 6H, N(CH₃)₂) 2.60 (t, 2H, *J* = 6.89 Hz, CH₂-aryl) 1.62 (m, 4H, CH₂(CH₂)₂CH₂). ¹³C-NMR (125 MHz, DMSO-d₆) δ 151.64, 150.63, 150.17, 148.09, 142.34, 128.41, 128.36, 125.76, 117.82, 86.48, 85.79, 71.11, 70.82, 61.78, 42.09, 40.24, 37.91, 34.97, 28.53, 28.45. LC/ESI-MS (*m/z*): positive mode 443.2 [M+H]⁺. Purity determined by HPLC-UV (254 nm)-ESI-MS: 94%. mp: 164.2°C.



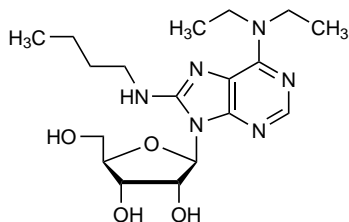
6.3.15.4 8-Butylamino-*N*⁶-dimethyladenosine (53), CAS 84758-18-9

The compound was synthesized starting from **48** (0.5 g, 1.3 mmol, 1.0 eq) using butylamine (0.4 ml, 4.3 mmol, 3.2 eq). Purification by column chromatography (CH₃OH/DCM 1:24) afforded the desired product as slightly yellow solid (0.16 g, 33%). ¹H-NMR (500 MHz, CD₃OD) δ 8.00 (s, 1H, NCH=N) 6.04 (d, 1H, *J* = 8.08 Hz, CHN) 4.76 (dd, 1H, *J* = 5.57, 7.43 Hz, CHCH₂) 4.32 (dd, 1H, *J* = 1.80, 5.60 Hz, CHOH) 4.16 (br d, 1H, *J* = 1.80 Hz, CHOH) 3.88-3.81 (m, 2H, CHCH₂) 3.47 (s, 6H, N(CH₃)₂) 2.97 (t, 2H, *J* = 7.47 Hz, NHCH₂) 1.71 (m, 2H, CH₂) 1.46 (m, 2H, CH₂) 1.02 (m, 3H, CH₃). ¹³C-NMR (125 MHz, CD₃OD) δ 152.09, 150.65, 150.06, 147.41, 118.20, 87.05, 86.16, 71.42, 71.36, 61.69, 42.00, 37.40, 31.16, 19.78, 12.79. LC/ESI-MS (*m/z*): positive mode 235.2, 366.9 [M+H]⁺. Purity determined by HPLC-UV (254 nm)-ESI-MS: 85.9%. mp: 119°C.



6.3.15.5 *N*⁶-Diethyl-8-methylaminoadenosine (54)

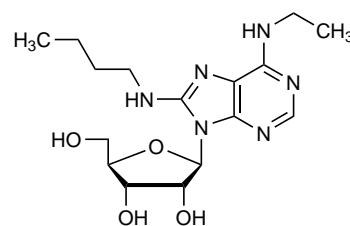
The compound was synthesized starting from **49** (0.52 g, 1.30 mmol, 1.0 eq) using methylamine (0.06 ml, 1.31 mmol, 1.0 eq) were added. Purification by column chromatography (CH₃OH/DCM 2:23) afforded the desired product as white powder (0.30 g, 67%). ¹H-NMR (500 MHz, DMSO-*d*₆) δ 7.94 (d, 1H, *J* = 0.97 Hz, N=CHN) 6.81 (q, 1H, *J* = 4.38 Hz, NHCH₃) 5.87 (d, 1H, *J* = 7.23 Hz, CHN) 5.85 (m, 2H, CH₂OH) 5.17 (d, 1H, *J* = 6.63 Hz, CHOH) 5.05 (m, 1H, CHOH) 4.65 (q, 1H, *J* = 6.71 Hz, CHCH₂) 4.11 (br s, 1H, CHOH) 3.95 (d, 1H, *J* = 1.96 Hz, CHOH) 3.87 (q, 4H, *J* = 6.09 Hz, N(CH₂)₂) 3.62 (m, 2H, CHCH₂) 3.08 (q, 3H, *J* = 7.26 Hz, NCH₃) 1.16 (m, 6H, N(CH₂CH₃)₂). ¹³C-NMR (125 MHz, DMSO-*d*₆) δ 151.00, 150.62, 150.51, 148.30, 117.27, 86.55, 85.77, 71.08, 70.81, 61.78, 45.90, 42.07, 28.98, 14.04, 8.74. LC/ESI-MS (*m/z*): positive mode 352.9 [M+H]⁺. Purity determined by HPLC-UV (254 nm)-ESI-MS: 98%. mp: 115°C.

6.3.15.6 8-Butylamino-*N*⁶-diethyladenosine (55)

The compound was synthesized starting from **49** (0.74 g, 1.83 mmol, 1.0 eq) using butylamine (0.4 ml, 3.65 mmol, 2.0 eq). Purification by column chromatography (CH₃OH/DCM 1:9) afforded the desired product as slightly yellow solid (0.70 g, 100%). ¹H-NMR (500 MHz, DMSO-*d*₆) δ 7.93 (s, 1H, N=CHN) 6.83 (t, 1H, *J* = 5.46 Hz, NHCH₂) 5.90 (d, 1H, *J* = 7.46 Hz, CHN) 5.84 (t, 1H, *J* = 5.00 Hz, CH₂OH) 5.18 (d, 1H, *J* = 6.84 Hz, CHOH) 5.10 (d, 1H, *J* = 4.08 Hz, CHOH) 4.10 (m, 1H, CHOH) 4.08 (m, 1H, CHOH) 3.95 (q, 1H, *J* = 1.99 Hz, CHCH₂) 3.85 (m, 4H, N(CH₂CH₃)₂) 3.61 (m, 2H, CHCH₂) 3.16 (d, 2H, *J* = 5.21 Hz, NHCH₂) 1.57 (q, 2H, *J* = 7.16 Hz, CH₂) 1.33 (m, 2H, CH₂) 1.15 (t, 6H, *J* = 6.94 Hz, N(CH₂CH₃)₂) 0.88 (t, 3H, *J* = 7.35 Hz, CH₂CH₃). ¹³C-NMR (125 MHz, DMSO-*d*₆) δ 150.56, 150.43, 150.39, 148.27, 117.22, 86.44, 85.80, 71.14, 70.82, 61.82, 56.20, 48.77, 42.19, 41.95, 30.95, 19.74, 18.72, 14.08, 13.87. LC/ESI-MS (*m/z*): positive mode 395.1 [M+H]⁺. Purity determined by HPLC-UV (254 nm)-ESI-MS: 94%. mp: 88°C.

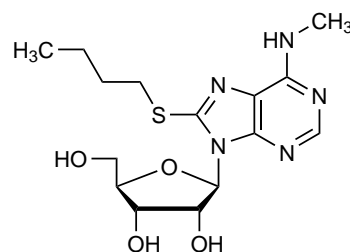
6.3.15.7 8-Butylamino-*N*⁶-ethyladenosine (56)

The compound was synthesized starting from **47** (0.38 g, 1.0 mmol, 1.0 eq) using butylamine (0.2 ml, 2.0 mmol, 2.0 eq). Purification by column chromatography (CH₃OH/DCM 1:9) afforded the desired product as slightly yellow solid (0.23 g, 64%). ¹H-NMR (500 MHz, DMSO-*d*₆) δ 7.93 (s, 1H, N=CHN) 6.82 (t, 1H, *J* = 5.41 Hz, NHCH₂) 6.78 (t, 1H, *J* = 5.93 Hz, NHCH₂) 5.88 (d, 1H, *J* = 7.44 Hz, CHN) 5.84 (t, 1H, *J* = 4.98 Hz, CH₂OH) 5.18 (d, 1H, *J* = 6.64 Hz, CHOH) 5.11 (d, 1H, *J* = 3.87 Hz, CHOH) 4.62 (q, 1H, *J* = 6.27 Hz, CHCH₂) 4.10 (br s, 1H, CHOH) 3.95 (d, 1H, *J* = 2.08 Hz, CHOH) 3.61 (m, 2H, CHCH₂) 3.48 (m, 2H, NHCH₂) 2.76 (m, 2H, NHCH₂) 1.32 (m, 4H, (CH₂)₂) 1.13 (t, 3H, *J* = 7.09 Hz, CH₂CH₃) 0.87 (m, 3H, (CH₂)₃CH₃). ¹³C-NMR (125 MHz, DMSO-*d*₆) δ 151.43, 151.37, 149.14, 148.60, 117.42, 86.48, 85.83, 71.13, 70.90, 61.82, 56.20, 42.19, 31.03, 19.82, 15.51, 13.64. LC/ESI-MS (*m/z*): positive mode 366.8 [M+H]⁺. Purity determined by HPLC-UV (254 nm)-ESI-MS: 94%. mp: 192°C.



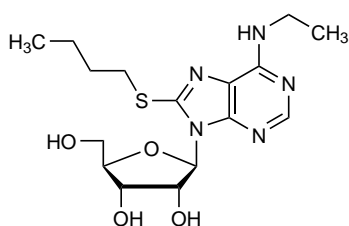
6.3.16 8-Butylthio-*N*⁶-methyladenosine (57)

To a solution of **46** (0.5 g, 1.4 mmol, 1.0 eq) in absolute ethanol, thiourea (0.2 g, 2.49 mmol, 1.8 eq) was added. After 7 h of refluxing the solution was evaporated yielding a yellow oil that was resuspended in a mixture of H₂O/EtOH 1:1. The solution was adjusted to basic pH with 2 M NaOH. 1-Iodobutane (0.5 ml, 4.32 mmol, 3.0 eq) was added and the reaction was stirred at rt for 5 h. After extraction with ethyl acetate, the organic phase was evaporated. Purification by column chromatography (CH₃OH/DCM 1:24) afforded a white solid. (0.21 g, 42%). ¹H-NMR (500 MHz, DMSO-*d*₆) δ 8.13 (br s, 1H, NCH=N) 7.63 (br s, 1H, NHCH₃) 5.77 (d, 1H, *J* = 6.89 Hz, CHN) 5.62 (dd, 1H, *J* = 3.61, 8.93 Hz, CH₂OH) 5.37 (d, 1H, *J* = 6.42 Hz, CHOH) 5.16 (d, 1H, *J* = 4.29 Hz, CHOH) 4.98 (q, 1H, *J* = 6.50 Hz, CHCH₂) 4.15 (m, 1H, CHOH) 3.96 (q, 1H, *J* = 3.70 Hz, CHOH) 3.68–3.49 (d m, 2H, CHCH₂) 3.26 (m, 2H, SCH₂CH₂) 2.96 (br s, 3H, NHCH₃) 1.67 (m, 2H, CH₂CH₂CH₂) 1.40 (m, 2H, CH₂CH₂CH₃) 0.89 (t, 3H, *J* = 7.38 Hz, CH₂CH₃). ¹³C-NMR (125 MHz, DMSO-*d*₆) δ 153.80, 151.47, 148.49, 128.29, 127.32, 89.04, 86.79, 71.54, 71.17, 62.41, 32.27, 31.11, 27.17, 21.37, 13.59.



LC/ESI-MS (m/z): positive mode 370.1 [M+H]⁺. Purity determined by HPLC-UV (254 nm)-ESI-MS: 90.1%. mp: 144°C.

6.3.17 8-Butylthio-*N*⁶-diethyladenosine (58)

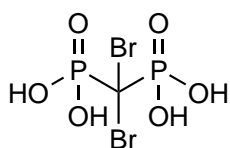


Compound **49** (0.74 g, 1.83 mmol, 1.0 eq) was suspended in absolute ethanol (5 ml) and the solution was basified with 2 M NaOH. Butanethiol (0.4 ml, 3.7 mmol, 2.0 eq) was added and the reaction mixture was stirred at rt for 5 days. After evaporation, the crude product was subjected

silica gel chromatography. However, separation of starting material and product was not possible. Therefore, the mixture was subjected to purification by RP-HPLC (20→100% CH₃OH in H₂O in 15 min, 20 ml/min) yielding the desired product as white powder (0.09 g, 12%). ¹H-NMR (500 MHz, DMSO-*d*₆) δ 8.10 (s, 1H, N=CHN) 5.72 (t, 1H, *J* = 6.89 Hz, CHN) 5.60 (dd, 1H, *J* = 3.43, 8.71 Hz, CH₂OH) 5.36 (d, 1H, *J* = 5.22 Hz, CHOH) 5.16 (m, 1H, CHOH) 4.98 (d, 1H, *J* = 5.24 Hz, CHCH₂) 4.15 (s, 1H, CHOH) 3.95 (m, 1H, CHOH) 4.15-3.65 (large bulb, 4H, underneath other peaks, N(CH₂)₂) 3.65-3.51 (d m, 2H, CHCH₂) 3.25 (m, 2H, SCH₂) 1.72 (m, 2H, CH₂) 1.40 (m, 2H, CH₂) 1.19 (t, 6H, *J* = 6.69 Hz, N(CH₂CH₃)₂) 0.89 (t, 3H, *J* = 7.39 Hz, S(CH₂)₃CH₃). ¹³C-NMR (125 MHz, DMSO-*d*₆) δ 151.78, 151.54, 150.81, 147.96, 119.80, 88.99, 86.78, 71.31, 71.16, 62.44, 42.61, 31.88, 31.39, 21.56, 13.60 (missing: N(CH₂CH₃)₂). LC/ESI-MS (m/z): positive mode 412.0 [M+H]⁺. Purity determined by HPLC-UV (254 nm)-ESI-MS: 98.5%. mp: 147°C.

6.3.18 *P,P'*-(Dibromomethylene)bisphosphonic acid (63),

CAS 10596-26-6



A solution of sodium hydroxide (4.3 g, 0.1 mol) in water (80 ml) was cooled to 0°C in an ice-salt bath, and bromine (2.6 ml, 0.05 mol) was added slowly with stirring. Tetraisopropyl methylenebisphosphonate (3.7 ml, 11.6 mmol) was then added and stirring was

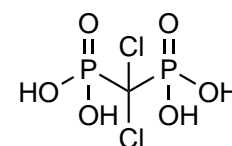
continued for 30 min at 0°C followed by an additional 15 min at room temperature. Chloroform extracts (4x50 ml) were dried over MgSO₄ and the solvent was removed *in vacuo*, leaving tetraisopropyl dibromomethanebisphosphonate as oil. It was dis-

solved in aqueous 6 M HCl (50 ml) and refluxed for 24 h. Afterwards the mixture was concentrated *in vacuo*, methanol (5x10 ml) was added, and the mixture was then evaporated again, before deionized water was added and the product was lyophilized to yield a white solid (3.6 g, 94%). $^1\text{H-NMR}$ (600 MHz, DMSO- d_6) δ 5.08 (br s, 4H, 4x OH). $^{31}\text{P-NMR}$ (202 MHz, DMSO- d_6) δ 8.21. LC/ESI-MS (m/z): positive mode 334.7 $[\text{M}+\text{H}]^+$. Purity determined by HPLC-UV (254 nm)-ESI-MS: 100%. mp: 263°C.

6.3.19 *P,P'*-(Dichloromethylene)bisphosphonic acid (**64**),

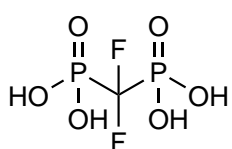
CAS 10596-23-3

(Tetraisopropylmethylene)bisphosphonate (**59**, 3.0 ml, 9.4 mmol, 1.0 eq) was added dropwise to a solution of sodium hypochlorite (12% Cl, 80 ml) at 0°C. The reaction was stirred until a white precipitate was formed (*ca.* 20 min) followed by extraction with hexane (5x50 ml). The organic phases were combined, dried over MgSO_4 and reduced *in vacuo*. Purification by column chromatography ($\text{CH}_3\text{OH}/\text{DCM}$ 1:19) yielded the desired product as colourless oil (0.70 g, 18%) [*product loss due to technical problems*]. The TLC sheets were stained with potassium permanganate in order to make the spots visible. LC/ESI-MS (m/z): positive mode 412.9 $[\text{M}+\text{H}]^+$. Purity could not be determined by HPLC-UV (254 nm)-ESI-MS due to missing UV activity. The intermediate **61** was dissolved in *aqueous* HCl (50 ml, 6 M) and refluxed for 24 h. Afterwards the mixture was concentrated *in vacuo*, methanol was added, and the mixture was then evaporated again, before deionized water was added and the product was lyophilized to yield a white solid (0.42 g, 18%). $^1\text{H-NMR}$ (600 MHz, DMSO- d_6) δ 5.29 (br s, 4H, 4x OH). $^{13}\text{C-NMR}$ (126 MHz, DMSO- d_6) δ 74.99. $^{31}\text{P-NMR}$ (202 MHz, DMSO- d_6) δ 7.69. LC/ESI-MS (m/z): positive mode 244.9 $[\text{M}+\text{H}]^+$. Purity determined by HPLC-UV (254 nm)-ESI-MS: 97%. mp: 254°C (*lit.* 250°C).¹⁸⁷



6.3.20 *P,P'*-(Difluoromethylene)bisphosphonic acid (65),

CAS 10596-32-4



(Tetraisopropylmethylene)bisphosphonate (**59**, 0.9 ml, 2.9 mmol, 1.0 eq) was put into a flask under argon with a reflux condenser attached. A 1 M solution of NaHMDS in THF (0.9 ml, 0.9 mmol, 0.3 eq) and a 1 M solution of NFSi in THF (0.9 ml, 0.9 mmol, 0.3 eq)

were added simultaneously. The mixture was stirred for approximately two minutes until the exothermic reaction is over. Then another 0.3 eq of both reagents were added. This process was repeated ten times in total until 3 eq were added. The resulting suspension was filtered and the filter cake was washed with hexane. LC/ESI-MS (*m/z*): positive mode 380.9 [M+H]⁺. It was dissolved in *aqueous* 6 M HCl (50 ml) and refluxed for 24 h. Afterwards the mixture was concentrated *in vacuo*, methanol (5x10 ml) was added, and the mixture was then evaporated again, before deionized water was added and the product was lyophilized to yield a white solid (1.2 g, 95%). ³¹P-NMR (202 MHz, DMSO-d₆) δ 3.49. ¹⁹F-NMR (202 MHz, DMSO-d₆) δ -122.73. LC/ESI-MS (*m/z*): negative mode 210.9317 [M-H]⁻.

6.3.21 Preparation of tri-*N*-butylammonium dihalogenmethylenebis-phosphonate solutions

Dihalogenmethylenebisphosphonic acids (**63-65**) were dissolved in 50% aqueous ethanol (100 ml) and tri-*N*-butylamine was dropped into the solution with stirring at room temperature until the pH reached 7.8–8.0. The resulting solutions were evaporated and lyophilized to yield white semisolids. After lyophilization, the salts were sealed immediately by a septum to avoid contact with moisture. The salts were flushed with argon and anhydrous argon flushed DMF was added yielding 0.5 M solutions. The solutions were stored sealed and cooled at 4°C until use.

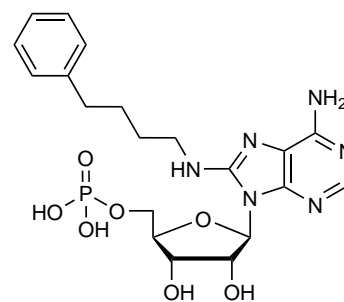
6.3.22 General procedure for the triphosphorylation

Lyophilized adenosine derivatives and proton sponge (1.5 eq) were dissolved in 5 ml of trimethyl phosphate under argon atmosphere at room temperature. The mixture was cooled to 0°C and phosphoryl chloride (0.1 ml, 1.3 mmol) was added dropwise.

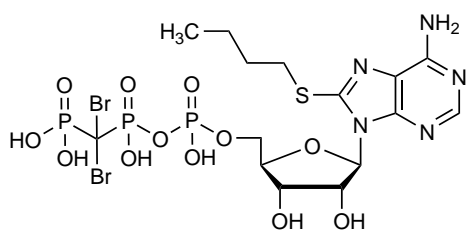
After 5 h of stirring at 0°C, tributylamine (4 eq) and 0.5 M tri-*N*-butylammonium di-bromomethylenebisphosphonate (**63**) solution in DMF (2.5 eq) were added to the mixture simultaneously. After 30 min a cold 0.5 M *aqueous* TEAC solution (20 ml, pH 7.4–7.6) was added to the mixture and stirring was continued at room temperature for one hour. Trimethyl phosphate was extracted with *tert*-butylmethylether (3x 200 ml) and the *aqueous* solution was lyophilized to yield white semisolids. The crude nucleoside triphosphates were purified by FPLC. After equilibration of the column with deionized water, the crude product was dissolved in deionized water and injected into the column. The column was firstly washed with 5% 0.5 M NH₄HCO₃ buffer to remove unbound components. Elution started with a solvent gradient of 5→80% 0.5 M NH₄HCO₃ buffer over 8 column volumes followed by an isocratic phase at 80% 0.5 M NH₄HCO₃ buffer. Fractions were collected, appropriate fractions were pooled and lyophilized several times. The monophosphate and the triphosphate were each purified by preparative HPLC (0%→30% acetonitrile in 50 mM NH₄HCO₃ buffer in 15 min, 20 ml/min). Fractions were collected and appropriate fractions pooled and lyophilized.

6.3.22.1 8-(4-Phenyl)butylamino-AMP (67b)

The compound was synthesized starting from **11** (0.27 g, 0.63 mmol, 1.0 eq) and afforded a white solid (0.01 g, 3%). ¹H-NMR (500 MHz, D₂O) δ 8.03 (s, 1H, N=CHN) 7.16 (m, 4H, aryl) 7.05 (t, 1H, *J*=6.60 Hz, aryl) 5.99 (d, 1H, *J*=7.64 Hz, CHN) 4.67 (m, 1H, CHOH) 4.43 (dd, 1H, *J*=2.01, 5.65 Hz, CHOH) 4.33 (s, 1H, CHCH₂) 4.15 (d m, 2H, CHCH₂) 3.46 (d m, 2H, NHCH₂) 2.58 (m, 2H, CH₂-aryl) 1.66 (m, 4H, (CH₂)₂). ¹³C-NMR (125 MHz, D₂O) δ 154.83, 152.86, 152.03, 150.36, 145.74, 131.34, 131.10, 128.41, 118.79, 89.23, 87.25, 73.55, 73.04, 67.56, 45.01, 37.51, 30.41, 29.88. ³¹P-NMR (202 MHz, D₂O) δ 0.36. LC/ESI-MS (*m/z*): positive mode 495.1741 [M+H]⁺ and negative mode 493.1621 [M+H]⁻ (calc. 494.17). Purity determined by HPLC-UV (254 nm)-ESI-MS: 98.7%. mp: decomposition > 170°C.

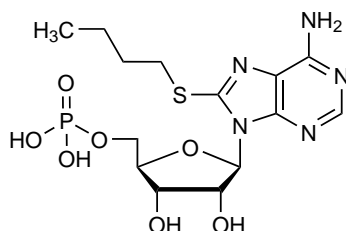


6.3.22.2 8-Butylthio- P_{β},P_{γ} -dibromomethylene-ATP (68a)



The compound was synthesized starting from **15** (0.27 g, 0.76 mmol, 1.0 eq) and afforded a white solid (0.014 g, 2.5%). $^1\text{H-NMR}$ (500 MHz, D_2O) δ 8.17 (s, 1H, $\text{N}=\text{CHN}$) 6.10 (d, 1H, $J=6.23$ Hz, CHN) 5.19 (t, 1H, $J=6.19$ Hz, CHOH) 4.61 (m, 1H, CHOH) 4.39 (dd, 1H, $J=6.34, 10.22$ Hz, CHCH_2) 4.33 (m, 2H, CHCH_2) 3.29 (m, 2H, SCH_2CH_2) 1.73 (m, 2H, $\text{SCH}_2\text{CH}_2\text{CH}_2$) 1.44 (m, 2H, $\text{CH}_2\text{CH}_2\text{CH}_3$) 0.90 (t, 3 H, $J=7.39$ Hz, CH_2CH_3). $^{13}\text{C-NMR}$ (125 MHz, D_2O) δ 155.14, 154.91, 153.42, 152.48, 121.74, 90.88, 86.35, 79.70, 72.54, 68.28, 57.53, 35.40, 33.48, 24.09, 15.69. $^{31}\text{P-NMR}$ (202 MHz, D_2O) δ 7.46 (d, 1P, $J=14.53$ Hz, P_{γ}) -0.69 (dd, 1 P, $J=14.69, 29.01$ Hz, P_{β}) -10.62 (d, 1P, $J=28.16$ Hz, P_{α}). LC/ESI-MS (m/z): positive mode 751.8752 $[\text{M}+\text{H}]^+$ and negative mode 749.8619 $[\text{M}-\text{H}]^-$ (calc. 751.17). Purity determined by HPLC-UV (254 nm)-ESI-MS: 99%. mp: 167°C.

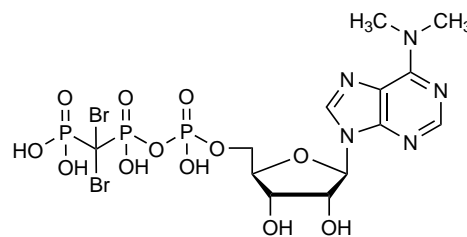
6.3.22.3 8-Butylthio-AMP (68b), CAS 344402-39-7



The compound was synthesized starting from **15** (0.27 g, 0.76 mmol, 1.0 eq) and afforded a white solid (0.04 g, 10%). $^1\text{H-NMR}$ (500 MHz, D_2O) δ 8.10 (s, 1H, $\text{N}=\text{CHN}$) 6.06 (d, 1H, $J=6.14$ Hz, 1H, CHN) 5.13 (t, 1H, $J=6.14$ Hz, CHOH) 4.53 (m, 1H, CHOH) 4.26 (q, 1H, $J=4.76$ Hz, CHCH_2) 4.17 (m, 2H, CHCH_2) 3.23 (m, 2H, SCH_2CH_2) 1.70 (m, 2H, $\text{SCH}_2\text{CH}_2\text{CH}_2$) 1.43 (m, 2H, $\text{S}(\text{CH}_2)_2\text{CH}_2\text{CH}_3$) 0.90 (t, 3H, $J=7.39$ Hz, $\text{S}(\text{CH}_2)_3\text{CH}_3$). $^{13}\text{C-NMR}$ (125 MHz, D_2O) δ 155.88, 154.45, 153.90, 153.36, 121.65, 90.90, 86.33, 73.63, 72.55, 67.38, 57.58, 35.42, 33.38, 24.08, 15.66. $^{31}\text{P-NMR}$ (202 MHz, D_2O) δ 0.88. LC/ESI-MS (m/z): positive mode 436.1031 $[\text{M}+\text{H}]^+$ and negative mode 434.0901 $[\text{M}-\text{H}]^-$ (calc. 435.39) Purity determined by HPLC-UV (254 nm)-ESI-MS: 98.6%. mp: 152°C.

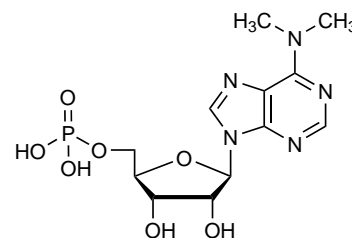
6.3.22.4 *N*⁶,*N*⁶-Dimethyl-*P*_β,*P*_γ-dibromomethylene-ATP (69a)

The compound was synthesized starting from 32 (0.29 g, 1.0 mmol, 1.0 eq) and afforded a white solid (0.01 g, 1%). ¹H-NMR (500 MHz, D₂O) δ 8.45 (s, 1H, N=CHN) 8.17 (s, 1H, N=CHN) 6.12 (d, 1H, *J* = 5.92 Hz, CHN) 4.78 (m, 1H overlapping with H₂O, CHCH₂) 4.61 (dd, 1H, *J* = 3.60, 4.99 Hz, CHOH) 4.41 (m, 1H, CHOH) 4.31 (m, 2H, CHCH₂) 3.42 (br s, 6H, N(CH₃)₂). ¹³C-NMR (125 MHz, D₂O) δ 156.66, 154.25, 152.05, 140.97, 121.92, 89.56, 86.89, 77.12, 73.26, 68.16, 51.04, 48.52, 41.92. ³¹P-NMR (202 MHz, D₂O) δ 7.48 (d, 1P, *J* = 14.23 Hz, P_γ) -0.73 (dd, 1P, *J* = 14.24, 27.90 Hz, P_β) -10.65 (d, 1P, *J* = 28.38 Hz, P_α). LC/ESI-MS (*m/z*): positive mode 691.8745 [M+H]⁺ and negative mode 689.8587 [M-H]⁻ (calc. 691.06). Purity determined by HPLC-UV (254 nm)-ESI-MS: 87.1%. mp: 184°C.



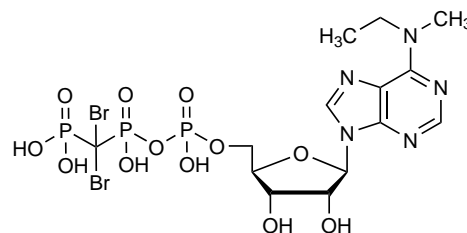
6.3.22.5 *N*⁶,*N*⁶-Dimethyl-AMP (69b), CAS 13484-65-6

The compound was synthesized starting from 32 (0.29 g, 1.0 mmol, 1.0 eq) and afforded a white solid (0.011 g, 3%). ¹H-NMR (500 MHz, D₂O) δ 8.38 (s, 1H, N=CHN) 8.11 (s, 1H, N=CHN) 6.09 (d, 1H, *J* = 5.54 Hz, CHN) 4.71 (t, 1H, *J* = 5.30 Hz, CHOH) 4.49 (t, 1H, *J* = 4.37 Hz, CHOH) 4.38 (br s, 1H, CHCH₂) 4.13 (m, 2H, CHCH₂) 3.37 (s, 6H, N(CH₃)₂). ¹³C-NMR (125 MHz, D₂O) δ 156.42, 154.11, 151.72, 140.60, 121.64, 89.69, 86.61, 77.10, 73.05, 67.09, 50.64, 41.54. ³¹P-NMR (202 MHz, D₂O) δ 0.59. LC/ESI-MS (*m/z*): positive mode 376.1016 [M+H]⁺ and negative mode 374.0882 [M-H]⁻ (calc. 375.28). Purity determined by HPLC-UV (254 nm)-ESI-MS: 95.8 %. mp: 87°C (*lit.* 223°C (decomposition)).¹⁸⁸



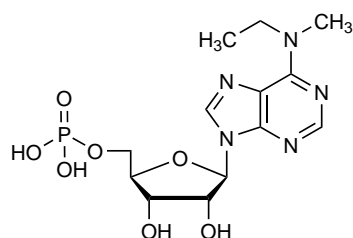
6.3.22.6 *N*⁶-Ethyl-*N*⁶-methyl-*P*_β,*P*_γ-dibromomethylene-ATP (70a)

The compound was synthesized starting from 33 (0.3 g, 1.0 mmol, 1.0 eq) and afforded a white solid (0.08 g, 12%). ¹H-NMR (500 MHz, D₂O) δ 8.41 (s, 1H, N=CHN) 8.11 (s, 1H, N=CHN) 6.10 (d, 1H, *J* = 5.79 Hz, CHN) 4.76 (t, 1H, *J* = 4.99 Hz, CHOH)



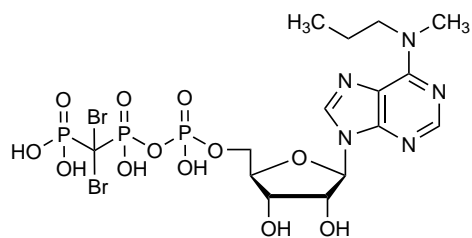
4.61 (t, 1H, $J = 3.49$ Hz, CHOH) 4.40 (br s, 1H, CHCH_2) 4.31 (m, 2H, CHCH_2) 3.88 (br s, 2H, NCH_2) 3.30 (br s, 3H, NCH_3) 1.20 (t, 3H, $J = 7.10$ Hz, NCH_2CH_3). ^{13}C -NMR (125 MHz, D_2O) δ 156.57, 155.00, 152.16, 140.60, 121.57, 89.49, 86.73, 77.08, 73.13, 68.11, 59.78, 48.81, 39.25, 14.75. ^{31}P -NMR (202 MHz, D_2O) δ 7.58 (d, 1P, $J = 14.50$ Hz, $\text{P}\gamma$) 0.22 (q, 1P, $J = 14.29, 29.14$ Hz, $\text{P}\beta$) -10.62 (d, 1P, $J = 29.27$ Hz, $\text{P}\alpha$). LC/ESI-MS (m/z): positive mode 705.8896 $[\text{M}+\text{H}]^+$ and negative mode 703.8737 $[\text{M}-\text{H}]^-$ (calc. 705.08). Purity determined by HPLC-UV (254 nm)-ESI-MS: 100%. mp: 199°C

6.3.22.7 N^6 -Ethyl- N^6 -methyl-AMP (70b)



The compound was synthesized starting from 33 (0.3 g, 1.0 mmol, 1.0 eq) and afforded a white solid (0.05 g, 14%). ^1H -NMR (500 MHz, D_2O) δ 8.40 (s, 1H, $\text{N}=\text{CHN}$) 8.07 (s, 1H, $\text{N}=\text{CHN}$) 6.07 (d, 1H, $J = 5.46$ Hz, CHN) 4.72 (t, 1H, $J = 5.30$ Hz, CHOH) 4.49 (t, 1H, $J = 4.52$ Hz, CHOH) 4.36 (m, 1H, CHCH_2) 4.08 (m, 2H, CHCH_2) 3.83 (s, 2H, NCH_2) 3.25 (s, 3H, NCH_3) 1.18 (t, 3H, $J = 7.11$ Hz, NCH_2CH_3). ^{13}C -NMR (125 MHz, D_2O) δ 156.38, 154.87, 151.93, 140.62, 121.43, 89.68, 80.40, 77.23, 73.21, 66.74, 48.78, 39.23, 14.73. ^{31}P -NMR (202 MHz, D_2O) δ 2.06. LC/ESI-MS (m/z): positive mode 390.1165 $[\text{M}+\text{H}]^+$ and negative mode 388.1029 $[\text{M}-\text{H}]^-$ (calc. 389.3). Purity determined by HPLC-UV (254 nm)-ESI-MS: 98.2%. mp: 173°C

6.3.22.8 N^6 -Methyl- N^6 -propyl- P_{β},P_{γ} -dibromomethylene-ATP (71a)



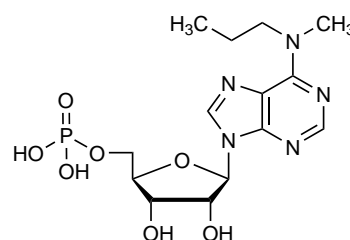
The compound was synthesized starting from 34 (0.32 g, 1.0 mmol, 1.0 eq) and afforded a white solid (0.06 g, 9%). ^1H -NMR (500 MHz, D_2O) δ 8.43 (s, 1H, $\text{N}=\text{CHN}$) 8.15 (s, 1H, $\text{N}=\text{CHN}$) 6.12 (d, 1H, $J = 5.96$ Hz, CHN) 4.77 (d, 1H, $J = 5.58$ Hz, CHOH) 4.63 (t, 1H, $J = 4.23$ Hz, CHOH) 4.41 (br s, 1H, CHCH_2) 4.36-4.24 (d m, 2H, CHCH_2) 3.90 (br s, 2H, NCH_2) 3.55 (br s, 3H, NCH_3) 1.69 (m, 2H, NCH_2CH_2) 0.89 (t, 3H, $J = 7.40$ Hz, CH_2CH_3). ^{13}C -NMR (125 MHz, D_2O) δ 157.07, 155.07, 152.33, 140.55, 121.69, 89.60, 86.82, 77.06, 73.22, 68.19, 58.70, 55.17, 39.98, 23.18, 12.99. ^{31}P -NMR (202 MHz, D_2O) δ 7.56 (d, 1P, $J = 13.84$ Hz, $\text{P}\gamma$) -0.23 (dd, 1P, $J = 14.43, 29.03$ Hz, $\text{P}\beta$) -10.62 (d, 1P, $J = 28.61$ Hz, $\text{P}\alpha$). LC/ESI-MS (m/z): positive mode 719.9047 $[\text{M}+\text{H}]^+$

and negative mode 717.8896 $[M-H]^-$ (calc. 719.11). Purity determined by HPLC-UV (254 nm)-ESI-MS: 95.6%. mp: 101°C.

6.3.22.9 *N*⁶-Methyl-*N*⁶-propyl-AMP (71b)

The compound was synthesized starting from **34** (0.32 g, 1.0 mmol, 1.0 eq) and afforded a white solid (0.07 g, 17%).

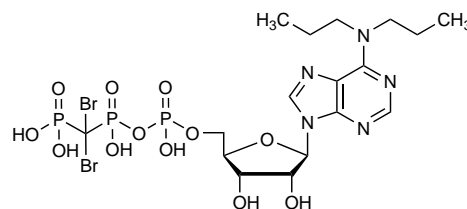
¹H-NMR (500 MHz, D₂O) δ 8.44 (s, 1H, N=CHN) 8.09 (s, 1H, N=CHN) 6.09 (d, 1H, *J* = 5.57 Hz, CHN) 4.74 (t, 1H, *J* = 5.32 Hz, CHOH) 4.50 (t, 1H, *J* = 4.43 Hz, CHOH) 4.36 (br s, 1H, CHCH₂) 4.06 (m, 2H, CHCH₂) 3.82 (br s, 2H, NCH₂) 3.28 (br s, 3H, CH₃) 1.64 (m, 2H, NCH₂CH₂) 0.87 (t, 3H, *J* = 7.39 Hz, CH₂CH₃). ¹³C-NMR (125 MHz, D₂O) δ 156.83, 154.90, 157.07, 140.60, 121.55, 89.63, 87.1, 77.24, 73.29, 66.58, 55.19, 39.97, 23.19, 12.97. ³¹P-NMR (202 MHz, D₂O) δ 2.66. LC/ESI-MS (m/z): positive mode 404.1316 $[M+H]^+$ and negative mode 402.1187 $[M-H]^-$ (calc. 403.33). Purity determined by HPLC-UV (254 nm)-ESI-MS: 99.5%. mp: 148°C.

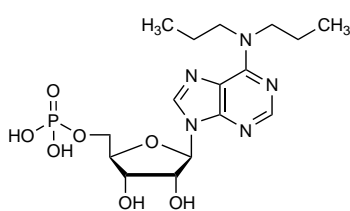


6.3.22.10 *N*⁶,*N*⁶-Dipropyl-*P*_β,*P*_γ-dibromomethylene-ATP (72a)

The compound was synthesized starting from **35** (0.35 g, 1.0 mmol, 1.0 eq) and afforded a white solid (0.06 g, 8%).

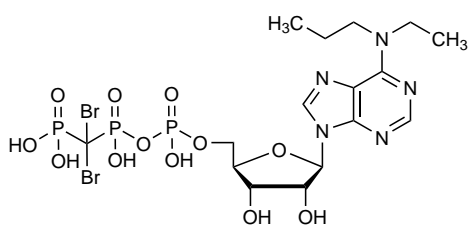
¹H-NMR (500 MHz, D₂O) δ 8.43 (s, 1H, N=CHN) 8.15 (s, 1H, N=CHN) 6.12 (d, 1H, *J* = 5.88 Hz, CHN) 4.76 (d, 1H, *J* = 5.53 Hz, CHOH) 4.64 (m, 1H, CHOH) 4.40 (m, 1H, CHCH₂) 4.36 (m, 1H, CHCH₂) 4.26 (m, 1H, CHCH₂) 3.81 (br s, 4H, N(CH₂CH₂CH₃)₂) 1.68 (m, 4H, N(CH₂CH₂CH₃)₂) 0.91 (t, 6H, *J* = 7.40 Hz, N(CH₂CH₂CH₃)₂). ¹³C-NMR (125 MHz, D₂O) δ 156.76, 155.12, 152.44, 140.49, 121.54, 89.36, 86.77, 77.06, 73.10, 68.12, 53.51, 50.89, 23.47, 13.12. ³¹P-NMR (202 MHz, D₂O) δ 7.64 (d, 1P, *J* = 13.87 Hz, P_γ) 0.78 (q, 1P, *J* = 13.82, 29.45 Hz, P_β) -10.59 (d, 1P, *J* = 29.59 Hz, P_α). LC/ESI-MS (m/z): positive mode 747.9349 $[M+H]^+$ and negative mode 745.9222 $[M-H]^-$ (calc. 747.16). Purity determined by HPLC-UV (254 nm)-ESI-MS: 97%. mp: 189°C



6.3.22.11 *N*⁶,*N*⁶-Dipropyl-AMP (72b)

The compound was synthesized starting from **35** (0.35 g, 1.0 mmol, 1.0 eq) and afforded a white solid (0.18 g, 43%). ¹H-NMR (500 MHz, D₂O) δ 8.41 (s, 1H, N=CHN) 8.10 (s, 1H, N=CHN) 6.09 (d, 1H, *J* = 5.59 Hz, CHN) 4.72 (t, 1H, *J* = 5.32 Hz, CHOH) 4.49 (t, 1H, *J* = 4.49 Hz, CHOH)

4.36 (s, 1H, CHCH₂) 4.09 (m, 2H, CHCH₂) 3.73 (s, 4H, N(CH₂CH₂CH₃)₂) 1.60 (m, 4H, N(CH₂CH₂CH₃)₂) 0.87 (t, *J* = 7.37 Hz, 6H, N(CH₂CH₂CH₃)₂). ¹³C-NMR (125 MHz, D₂O) δ 156.50, 154.93, 152.21, 140.48, 121.43, 89.61, 86.95, 77.24, 73.25, 66.78, 53.53, 50.88, 23.44, 13.09. ³¹P-NMR (202 MHz, D₂O) δ 1.91. LC/ESI-MS (*m/z*): positive mode 432.1640 [M+H]⁺ and negative mode 430.1502 [M-H]⁻ (calc. 431.39). Purity determined by HPLC-UV (254 nm)-ESI-MS: 99.2%. mp: 178°C

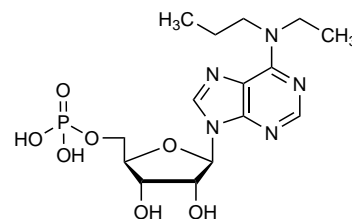
*N*⁶-Ethyl-*N*⁶-propyl-*P*_β,*P*_γ-dibromomethylene-ATP (73a)

The compound was synthesized starting from **36** (0.33 g, 1.0 mmol, 1.0 eq) and afforded a white solid (0.05 g, 6%). ¹H-NMR (500 MHz, D₂O) δ 8.42 (s, 1H, N=CHN) 8.14 (s, 1H, N=CHN) 6.10 (d, 1H, *J* = 5.70 Hz, CHN) 4.75 (t, 1H, *J* = 5.41 Hz, CHOH) 4.63 (m, 1H, CHOH) 4.39 (s, 1H, CHCH₂) 4.33 (m, 2H, CHCH₂) 3.78 (br d, 4H, *J* = 56.7 Hz, N(CH₂)₂) 1.68 (m, 2H, NCH₂CH₂CH₃) 1.20 (t, 3H, *J* = 7.05 Hz, CH₂CH₃) 0.91 (t, 3H, *J* = 7.39 Hz, CH₂CH₂CH₃).

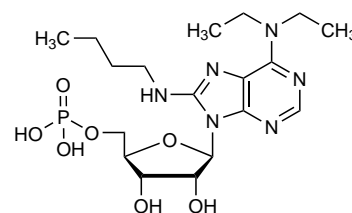
¹³C-NMR (125 MHz, D₂O) δ 156.41, 155.11, 152.37, 140.54, 121.41, 89.36, 86.32, 77.05, 73.16, 68.13, 61.65, 53.08, 47.05, 23.53, 15.39, 13.13. ³¹P-NMR (202 MHz, D₂O) δ 7.68 (d, 1P, *J* = 7.68 Hz, P_γ) 1.10 (dd, 1P, *J* = 13.61, 29.77 Hz, P_β) -10.59 (d, 1P, *J* = 29.75 Hz, P_α). LC/ESI-MS (*m/z*): positive mode 734.1371 [M+H]⁺ and negative mode 731.9086 [M-H]⁻ (calc. 733.14). Purity determined by HPLC-UV (254 nm)-ESI-MS: 97.1%. mp: 128°C.

***N*⁶-Ethyl-*N*⁶-propyl-AMP (73b)**

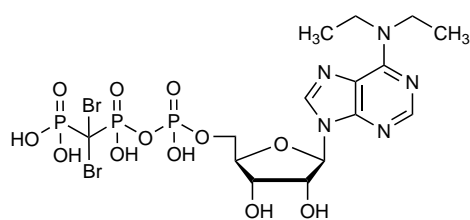
The compound was synthesized starting from **36** (0.33 g, 1.0 mmol, 1.0 eq) and afforded a white solid (0.1 g, 14%). ¹H-NMR (500 MHz, D₂O) δ 8.44 (s, 1H, N=CHN) 8.10 (s, 1H, N=CHN) 6.09 (d, 1H, *J* = 5.60 Hz, CHN) 4.73 (t, 1H, *J* = 5.34 Hz, CHOH) 4.49 (m, 1H, CHOH) 4.36 (m, 1H, CHCH₂) 4.06 (m, 2H, CHCH₂) 3.76 (br d, 4H, *J* = 65.6 Hz, N(CH₂)₂) 1.63 (m, 2H, NCH₂CH₂CH₃) 1.19 (t, 3H, *J* = 7.08 Hz, NCH₂CH₃) 0.89 (t, 3H, *J* = 7.40 Hz, NCH₂CH₂CH₃). ¹³C-NMR (125 MHz, D₂O) δ 156.26, 154.99, 152.19, 140.65, 121.33, 89.60, 87.09, 77.40, 73.28, 66.56, 53.12, 47.03, 23.53, 15.37, 13.11. ³¹P-NMR (202 MHz, D₂O) δ 2.58. LC/ESI-MS (*m/z*): positive mode 418.1479 [M+H]⁺ and negative mode 416.1320 [M-H]⁻ (calc. 417.36). Purity determined by HPLC-UV (254 nm)-ESI-MS: 97%. mp: 165°C

**6.3.22.12 8-Butylamino-*N*⁶,*N*⁶-diethyl-AMP (74b)**

The compound was synthesized starting from **55** (0.1 g, 0.3 mmol, 1.0 eq) and afforded a white powder (0.03 g, 25%). ¹H-NMR (500 MHz, D₂O) δ 7.99 (s, 1H, N=CHN) 6.04 (d, 1H, *J* = 7.84 Hz, CHN) 4.69 (dd, 1H, *J* = 5.92, 7.74 Hz, CHCH₂) 4.44 (dd, 1H, *J* = 2.29, 5.78 Hz, CHOH) 4.34 (m, 1H, CHOH) 4.19 (d m, 2H, NHCH₂) 3.83 (q, 4H, *J* = 7.06 Hz, N(CH₂)₂) 3.54-3.42 (d m, 2H, CHCH₂) 1.65 (m, 2H, CH₂) 1.34 (m, 2H, CH₂) 1.19 (t, 6H, *J* = 7.06 Hz, (CH₃)₂) 0.90 (t, 3H, *J* = 7.40 Hz, CH₃). ¹³C-NMR (125 MHz, D₂O) δ 154.17, 152.53, 152.39, 150.42, 119.72, 88.92, 87.21, 73.42, 73.03, 67.44, 46.27, 45.16, 33.65, 22.31, 16.02, 15.69. ³¹P-NMR (202 MHz, D₂O) δ 0.72. LC/ESI-MS (*m/z*): positive mode 475.2070 [M+H]⁺ and negative mode 473.1916 [M-H]⁻ (calc. 474.45). Purity determined by HPLC-UV (254 nm)-ESI-MS: 98.6%. mp: 192°C.

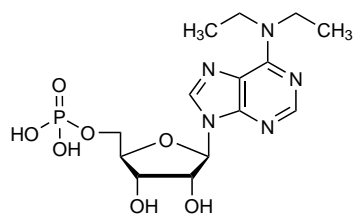


6.3.22.13 *N*⁶,*N*⁶-Diethyl-*P*_β,*P*_γ-dibromomethylene-ATP (75a), CAS 160928-38-1



The compound was synthesized starting from **37** (0.32 g, 1.0 mmol, 1.0 eq) and afforded a white solid (0.03 g, 4%). ¹H-NMR (500 MHz, D₂O) δ 8.43 (s, 1H, N=CHN) 8.14 (s, 1H, N=CHN) 6.11 (d, 1H, *J* = 5.83 Hz, CHN) 4.76 (d, 1H, *J* = 5.53 Hz, CHOH) 4.63 (m, 1H, CHOH) 4.40 (m, 1H, CHCH₂) 4.33 (m, 2H, CHCH₂) 3.85 (br s, 4H, N(CH₂CH₃)₂) 1.24 (t, 6H, *J* = 7.07 Hz, N(CH₃)₂). ¹³C-NMR (125 MHz, D₂O) δ 156.09, 155.13, 152.30, 140.63, 121.34, 89.38, 86.70, 77.05, 73.12, 68.09, 57.61, 46.64, 15.47. ³¹P-NMR (202 MHz, D₂O) δ 7.61 (d, 1P, *J* = 13.94 Hz, P_γ) 0.40 (dd, 1P, *J* = 13.66, 29.09 Hz, P_β) -10.61 (d, 1P, *J* = 29.33 Hz, P_α). LC/ESI-MS (*m/z*): positive mode 719.9052 [M+H]⁺ and negative mode 717.8904 [M-H]⁻ (calc. 719.11). Purity determined by HPLC-UV (254 nm)-ESI-MS: 95.8%. mp: 127°C.

6.3.22.14 *N*⁶,*N*⁶-Diethyl-AMP (75b), CAS 1620028-29-6



The compound was synthesized starting from **37** (0.32 g, 1.0 mmol, 1.0 eq) and afforded a white solid (0.15 g, 36%). ¹H-NMR (500 MHz, D₂O) δ 8.53 (s, 1H, N=CHN) 8.13 (s, 1H, N=CHN) 6.11 (d, 1H, *J* = 5.63 Hz, CHN) 4.76 (t, 1H, *J* = 5.36 Hz, CHOH) 4.51 (t, 1H, *J* = 4.49 Hz, CHOH) 4.35 (br s, 1H, CHCH₂) 4.01 (m, 2H, CHCH₂) 3.84 (br s, 4H, N(CH₂)₂) 1.23 (t, 6H, *J* = 7.09 Hz, N(CH₂CH₃)₂). ¹³C-NMR (125 MHz, D₂O) δ 156.10, 155.11, 152.24, 140.95, 121.33, 89.54, 87.43, 77.26, 73.37, 66.16, 46.64, 15.46. ³¹P-NMR (202 MHz, D₂O) δ 4.03. LC/ESI-MS (*m/z*): positive mode 404.1321 [M+H]⁺ and negative mode 402.1185 [M-H]⁻ (calc. 403.03). Purity determined by HPLC-UV (254 nm)-ESI-MS: 99.3%. mp: 194°C.

6.3.22.15 8-Cyclopropylamino-*N*⁶-methyl-*P*_β,*P*_γ-dibromomethylene-ATP (76a)

The compound was synthesized starting from **50**

(0.14 g, 0.41 mmol, 1.0 eq) and afforded a white solid (7.0 mg, 2%).

¹H-NMR (500 MHz, D₂O) δ 8.16 (s, 1H, N=CHN) 5.96 (d, 1H, *J* = 7.36 Hz,

CHN) 4.63 (dd, 1H, *J* = 2.7, 5.7 Hz, CHCH₂) 4.41

(m, 1H, CHOH) 4.35 (br s, 1H, CHOH) 4.24 (d, 2H, *J* = 11.92 Hz, CHCH₂) 3.10 (s,

3H, NHCH₃) 2.76 (m, 1H, NHCH) 0.88 (m, 2H, CHCH₂) 0.8-0.72 (d m, 2H, CHCH₂).

¹³C-NMR (125 MHz, D₂O) δ 155.34, 152.79, 150.67, 150.23, 117.66, 89.45, 87.11,

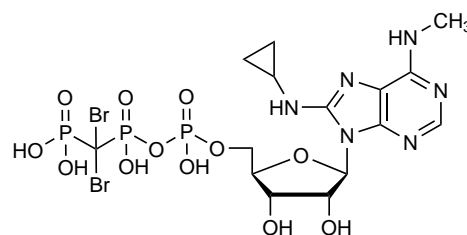
73.81, 72.65, 63.36, 50.90, 30.49, 27.18, 9.67. ³¹P-NMR (202 MHz, D₂O) δ 7.51 (d,

1P, *J* = 14.60 Hz, P_γ) -0.84 (dd, 1P, *J* = 14.74, 27.48 Hz, P_β) -11.16 (d, 1P, *J* = 27.67 Hz,

P_α). LC/ESI-MS (*m/z*): positive mode 732.8970 [M+H]⁺ and negative mode 730.8852

[M-H]⁻ (calc. 732.11). Purity determined by HPLC-UV (254 nm)-ESI-MS: 100%. mp:

232°C.

**6.3.22.16 8-Butylamino-*N*⁶-methyl-*P*_β,*P*_γ-dibromomethylene-ATP (77a)**

The compound was synthesized starting from **51**

(0.32 g, 1.0 mmol, 1.0 eq) and afforded a white solid (0.017 g, 2.3%).

¹H-NMR (500 MHz, D₂O) δ 8.13 (s, 1H, N=CHN) 6.04 (d, 1H, *J* = 7.76 Hz,

CHN) 4.78 (t, 1H, *J* = 7.82 Hz, CHOH) 4.66 (dd,

1H, *J* = 2.16, 5.70 Hz, CHOH) 4.45 (m, 1H, 1x

CHCH₂) 4.38 (br s, 1H, CHCH₂) 4.24 (m, 1H, 1x CHCH₂) 3.50 (m, 2H, NHCH₂) 3.04 (s,

3H, NHCH₃) 1.67 (m, 2H, NHCH₂CH₂CH₂) 1.39 (q, 2H, *J* = 7.48 Hz, CH₂CH₂CH₃) 0.93

(t, 3H, *J* = 7.40 Hz, CH₂CH₃). ¹³C-NMR (125 MHz, D₂O) δ 154.90, 152.87, 150.47,

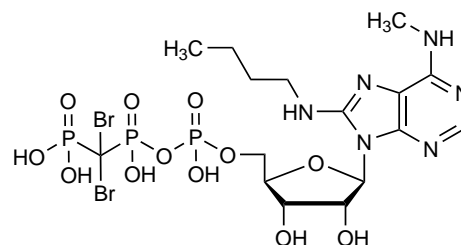
150.25, 118.58, 89.15, 87.28, 73.33, 72.84, 68.44, 57.70, 45.31, 33.43, 30.46, 22.31,

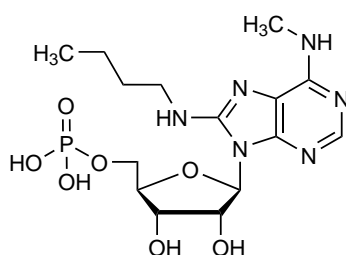
16.07. ³¹P-NMR (202 MHz, D₂O) δ 7.48 (d, 1P, *J* = 16.02 Hz, P_γ) -0.87 (dd, 1P,

J = 14.47, 26.89 Hz, P_β) -11.26 (d, 1P, *J* = 27.48 Hz, P_α). LC/ESI-MS (*m/z*): positive

mode 748.9324 [M+H]⁺ and negative mode 746.9163 [M-H]⁻ (calc. 748.15). Purity

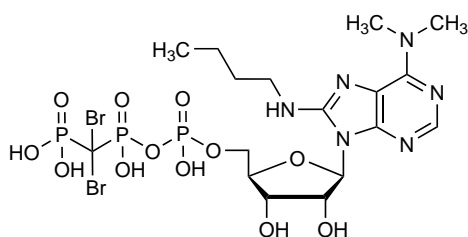
determined by HPLC-UV (254 nm)-ESI-MS: 97.0%. mp: 178°C.



6.3.22.17 8-Butylamino-*N*⁶-methyl-AMP (77b)

The compound was synthesized starting from **51** (0.32 g, 1.0 mmol, 1.0 eq) and afforded a white solid (0.09 g, 22%). ¹H-NMR (500 MHz, D₂O) δ 7.99 (s, 1H, N=CHN) 5.97 (d, 1H, *J* = 7.68 Hz, CHN) 4.69 (dd, 1H, *J* = 5.95, 7.53 Hz, CHOH) 4.44 (dd, 1H, *J* = 2.51, 5.79 Hz, CHOH) 4.34 (m, 1H, CHCH₂) 4.17 (d m, 2H, CHCH₂) 3.42 (m, 2H, NHCH₂) 3.01

(s, 3H, NHCH₃) 1.63 (m, 2H, NHCH₂CH₂CH₂) 1.37 (m, 2H, CH₂CH₂CH₃) 0.92 (t, 3H, *J* = 7.40 Hz, CH₂CH₃). ¹³C-NMR (125 MHz, D₂O) δ 154.66, 153.51, 150.97, 150.34, 118.72, 89.18, 87.10, 73.42, 72.91, 67.45, 45.25, 33.49, 30.30, 22.35, 16.05. ³¹P-NMR (202 MHz, D₂O) δ 0.38. LC/ESI-MS (*m/z*): positive mode 433.1587 [M+H]⁺ and negative mode 431.1456 [M-H]⁻ (calc. 432.37). Purity determined by HPLC-UV (254 nm)-ESI-MS: 99.2%. mp: 157°C.

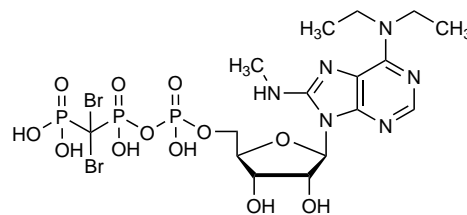
6.3.22.18 8-Butylamino-*N*⁶,*N*⁶-dimethyl-*P*_β,*P*_γ-dibromomethylene-ATP (78a)

The compound was synthesized starting from **53** (0.1 g, 0.27 mmol, 1.0 eq) and afforded a white solid (6.0 mg, 1.8%). ¹H-NMR (500 MHz, D₂O) δ 8.07 (s, 1H, N=CHN) 6.06 (d, 1H, *J* = 7.83 Hz, CHN) 4.71 (m, 2H, NCH₂) 4.45 (m, 1H, CHOH)

4.38 (br s, 1H, CHOH) 4.24 (d, 1H, *J* = 11.78 Hz, CHCH₂) 3.54 (d m, 2H, CHCH₂) 3.42 (s, 6H, N(CH₃)₂) 1.68 (m, 2H, NHCH₂CH₂CH₂) 1.38 (m, 2H, CH₂CH₂CH₃) 0.93 (t, 3H, *J* = 7.40 Hz, CH₂CH₃). ¹³C-NMR (125 MHz, D₂O) δ 163.50, 154.52, 152.23, 149.19, 119.98, 89.00, 87.24, 73.35, 72.84, 68.47, 56.93, 45.12, 41.61, 33.75, 22.88, 16.03. ³¹P-NMR (202 MHz, D₂O) δ 6.15 (d, 1P, *J* = 14.67 Hz, P_γ) -2.22 (dd, 1P, *J* = 14.72, 27.57 Hz, P_β) -12.61 (d, 1P, *J* = 27.71 Hz, P_α). LC/ESI-MS (*m/z*): positive mode 762.9478 [M+H]⁺ and negative mode 760.9331 [M+H]⁻ (calc. 762.18). Purity determined by HPLC-UV (254 nm)-ESI-MS: 98%. mp: 193°C.

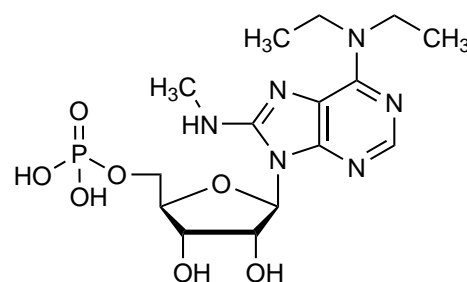
6.3.22.19 *N*⁶,*N*⁶-Diethyl-8-methylamino-*P*_β,*P*_γ-dibromomethylene-ATP (79a)

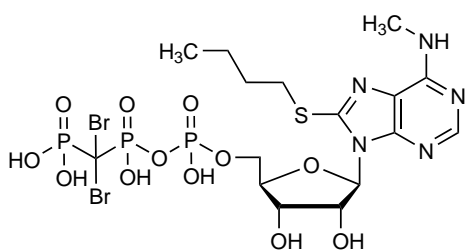
The compound was synthesized starting from **54** (0.08 g, 0.23 mmol, 1.0 eq) and afforded a white solid (9.0 mg, 4%). ¹H-NMR (500 MHz, D₂O) δ 8.04 (s, 1H, N=CHN) 6.06 (d, 1H, *J* = 7.82 Hz, CHN) 4.72 (m, 1H, CHOH) 4.60 (dd, 1H, *J* = 1.99, 5.68 Hz, CHOH) 4.45 (dd, 1H, *J* = 6.43, 10.55 Hz, CHCH₂) 4.33 (d m, 2H, CHCH₂) 3.88 (m, 4H, N(CH₂CH₃)₂) 3.09 (s, 3H, NHCH₃) 1.24 (t, 6H, *J* = 7.06 Hz, N(CH₂CH₃)₂). ¹³C-NMR (125 MHz, D₂O) δ 155.08, 152.57, 151.93, 149.89, 119.72, 89.05, 87.04, 73.36, 72.91, 68.66, 57.89, 46.34, 31.89, 15.61. ³¹P-NMR (202 MHz, D₂O) δ 7.14 (s, 1P, P_γ) 0.27 (br s, 1P, P_β) -10.77 (d, 1P, *J* = 26.2 Hz, P_α). LC/ESI-MS (m/z): positive mode 748.9295 [M+H]⁺ and negative mode 746.9181 [M+H]⁻ (calc. 748.15). Purity determined by HPLC-UV (254 nm)-ESI-MS: 93.7%. mp: 249°C.



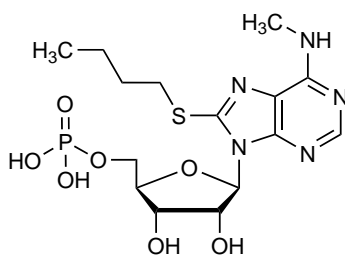
6.3.22.20 *N*⁶,*N*⁶-Diethyl-8-methylamino-AMP (79b)

The compound was synthesized starting from **54** (0.08 g, 0.23 mmol, 1.0 eq) and afforded a white solid (6.0 mg, 5%). ¹H-NMR (500 MHz, D₂O) δ 8.0 (s, 1H, N=CHN) 6.05 (d, 1H, *J* = 7.86 Hz, CHN) 4.66 (dd, 1H, *J* = 5.91, 7.72 Hz, CHOH) 4.43 (dd, 1H, *J* = 2.17, 5.77 Hz, CHOH) 4.35 (m, 1H, CHCH₂) 4.16 (d m, 2H, CHCH₂) 3.85 (m, 4H, N(CH₂CH₃)₂) 3.05 (s, 3H, NHCH₃) 1.21 (t, 6H, *J* = 7.08 Hz, N(CH₂CH₃)₂). ¹³C-NMR (125 MHz, D₂O) δ 155.88, 154.45, 153.90, 153.36, 121.65, 90.90, 86.33, 73.63, 72.55, 67.38, 46.40, 31.76, 15.61. ³¹P-NMR (202 MHz, D₂O) δ 0.65. LC/ESI-MS (m/z): positive mode 433.1592 [M+H]⁺ and negative mode 431.1480 [M+H]⁻ (calc. 432.15). Purity determined by HPLC-UV (254 nm)-ESI-MS: 97.9%. mp: degradation >219°C.



6.3.22.21 8-Butylthio-*N*⁶-methyl-*P*_β,*P*_γ-dibromomethylene-ATP (80a)

The compound was synthesized starting from **57** (0.2 g, 0.54 mmol, 1.0 eq) and afforded a white solid (13.0 mg, 3%). ¹H-NMR (500 MHz, D₂O) δ 8.19 (s, 1H, N=CHN) 6.11 (d, 1H, *J* = 6.70 Hz, CHN) 5.20 (q, 1H, *J* = 6.30 Hz, CHOH) 4.62 (dd, 1H, *J* = 4.10, 6.09 Hz, CHOH) 4.37 (m, 1 H, CHCH₂) 4.32 (d m, 2H, CHCH₂) 3.26 (m, 2H, SCH₂CH₂) 3.08 (s, 3H, NCH₃) 1.71 (m, 2H, CH₂CH₂CH₂) 1.44 (m, 2H, CH₂CH₂CH₃) 0.91 (t, 3H, *J* = 7.40 Hz, CH₂CH₃). ¹³C-NMR (125 MHz, D₂O) δ 156.01, 154.39, 153.99, 152.30, 122.21, 90.78, 86.17, 73.53, 72.52, 68.30, 50.37, 35.76, 33.60, 30.30, 24.06, 15.69. ³¹P-NMR (202 MHz, D₂O) δ 7.49 (d, 1P, *J* = 14.51 Hz, P_γ) 0.70 (dd, 1 P, *J* = 14.28, 27.73 Hz, P_β) -10.64 (d, 1P, *J* = 28.37 Hz, P_α). LC/ESI-MS (*m/z*): positive mode 765.8919 [M+H]⁺ and negative mode 763.8787 [M-H]⁻ (calc. 765.20). Purity determined by HPLC-UV (254 nm)-ESI-MS: 95.4%. mp: 172°C.

6.3.22.22 8-Butylthio-*N*⁶-methyl-AMP (80b)

The compound was synthesized starting from **57** (0.2 g, 0.54 mmol, 1.0 eq) and afforded a white solid (0.13 g, 51%). ¹H-NMR (500 MHz, D₂O) δ 8.09 (s, 1H, N=CHN) 6.04 (d, 1H, *J* = 6.22 Hz, CHN) 5.12 (t, 1H, *J* = 6.22 Hz, CHOH) 4.59 (m, 1H, CHOH) 4.25 (q, 1H, *J* = 4.98 Hz, CHCH₂) 4.14 (m, 2H, CHCH₂) 3.20 (m, 2H, SCH₂CH₂) 3.01 (s, 3H, NCH₃) 1.68 (m, 2H, CH₂CH₂CH₂) 1.42 (m, 2H, CH₂CH₂CH₃) 0.89 (t, 3H, *J* = 7.39 Hz, CH₂CH₃). ¹³C-NMR (125 MHz, D₂O) δ 156.07, 154.55, 153.08, 152.08, 122.10, 90.84, 86.38, 73.58, 72.62, 67.22, 35.68, 33.45, 30.19, 24.07, 15.66. ³¹P-NMR (202 MHz, D₂O) δ 1.33. LC/ESI-MS (*m/z*): positive mode 450.1195 [M+H]⁺ and negative mode 448.1047 [M-H]⁻ (calc. 449.42). Purity determined by HPLC-UV (254 nm)-ESI-MS: 97.8%. mp: 162°C.

6.3.22.23 8-Butylthio-*N*⁶-diethyl-*P*_β,*P*_γ-dibromomethylene-ATP (81a)

The compound was synthesized starting from **58**

(0.1 g, 0.24 mmol, 1.0 eq) and afforded a white solid (7.0 mg, 4%).

¹H-NMR (500 MHz, D₂O) δ 8.18 (s, 1H, N=CHN) 6.13 (d, 1H, *J* = 6.41 Hz,

CHN) 5.16 (t, 1H, *J* = 6.26 Hz, CHCH₂) 4.63 (m,

1H, CHOH) 4.38 (dd, 1H, *J* = 4.92, 10.90 Hz, CHOH) 4.32 (m, 2H, CHCH₂) 3.92 (br s,

4H, N(CH₂)₂) 3.30-3.22 (d m, 2H, SCH₂) 1.72 (m, 2H, CH₂) 1.42 (m, 2H, CH₂CH₃) 1.26

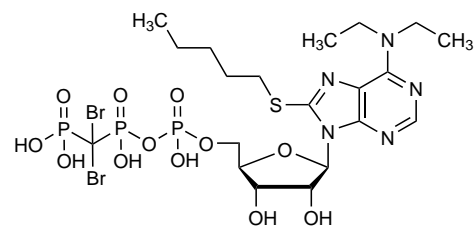
(t, 6H, *J* = 7.03 Hz, N(CH₂CH₃)₂) 0.89 (t, 3H, *J* = 7.39 Hz, CH₂CH₃).

¹³C-NMR (125 MHz, D₂O) δ 153.66, 153.37, 152.57, 151.90, 122.31, 90.78, 86.33, 73.72, 72.61, 68.29,

50.92, 47.16, 36.19, 34.10, 24.22, 15.75, 15.38.

³¹P-NMR (202 MHz, D₂O) δ 7.48 (d, 1P, *J* = 13.83 Hz, P_γ) -0.74 (dd, 1P, *J* = 12.88, 25.51 Hz, P_β) -10.64 (d, 1P, *J* = 28.45 Hz,

P_α). LC/ESI-MS (*m/z*): positive mode 807.9381 [M+H]⁺ and negative mode 805.9304 [M+H]⁻ (calc. 807.28). Purity determined by HPLC-UV (254 nm)-ESI-MS: 92%. mp: 190°C.



6.3.22.24 8-Butylthio-*N*⁶-diethyl-AMP (81b)

The compound was synthesized starting from **58** (0.1 g,

0.24 mmol, 1.0 eq) and afforded a white solid (0.05 g, 41%).

¹H-NMR (500 MHz, D₂O) δ 8.11 (s, 1H, N=CHN) 6.12 (d, 1H, *J* = 6.40 Hz, CHN) 5.12 (t, 1H, *J* = 6.28 Hz, CHCH₂)

4.52 (m, 1H, CHOH) 4.25 (q, 1H, *J* = 4.95 Hz, CHOH) 4.15

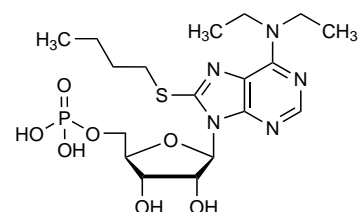
(d m, 2H, CHCH₂) 3.87 (br s, 4H, N(CH₂)₂) 3.22 (d m, 2H, SCH₂) 1.70 (m, 2H, CH₂) 1.40

(m, 2H, CH₂CH₃) 1.22 (t, 6H, *J* = 7.01 Hz, N(CH₂CH₃)₂) 0.87 (t, 3H, *J* = 7.38 Hz, CH₃).

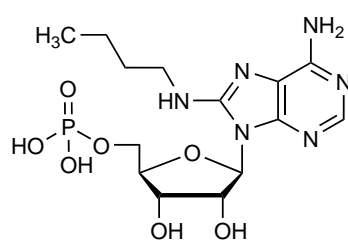
¹³C-NMR (125 MHz, D₂O) δ 154.65, 154.06, 153.94, 151.08, 122.28, 90.69, 86.35,

73.57, 72.62, 67.32, 46.69, 30.25, 34.08, 24.20, 15.71, 15.52.

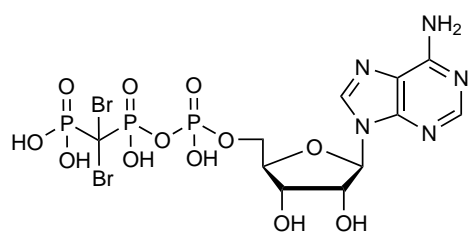
³¹P-NMR (202 MHz, D₂O) δ 1.00. LC/ESI-MS (*m/z*): positive mode 492.1673 [M+H]⁺ and negative mode 490.1527 [M+H]⁻ (calc. 491.50). Purity determined by HPLC-UV (254 nm)-ESI-MS: 96%. mp: 167°C.



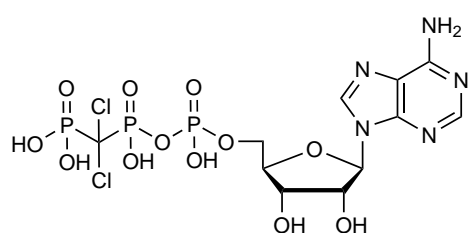
6.3.22.25 8-Butylamino-AMP (82b), CAS 344402-40-0



The compound was synthesized starting from **12** (0.1 g, 0.3 mmol, 1.0 eq) and afforded a white solid (5.0 mg, 4%). $^1\text{H-NMR}$ (500 MHz, D_2O) δ 7.99 (d, 1H, $J=1.08$ Hz, $\text{N}=\text{CHN}$) 6.00 (d, 1H, $J=7.70$ Hz, CHN) 4.73 (dd, 1H, $J=5.94, 7.82$ Hz, CHOH) 4.45 (dd, 1H, $J=2.50, 5.86$ Hz, CHOH) 4.33 (t, 1H, $J=2.41$ Hz, CHCH_2) 4.13 (m, 2H, CHCH_2) 3.45 (m, 2H, NCH_2) 1.65 (m, 2H, CH_2) 1.37 (q, 2H, $J=7.51$ Hz, CH_2) 0.91 (m, 3H, CH_3). $^{13}\text{C-NMR}$ (125 MHz, D_2O) δ 155.20, 153.89, 152.36, 151.55, 119.14, 89.14, 87.33, 73.34, 73.02, 67.33, 45.24, 33.52, 22.37, 16.12. $^{31}\text{P-NMR}$ (202 MHz, D_2O) δ 1.14. LC/ESI-MS (m/z): positive mode 419.1438 $[\text{M}+\text{H}]^+$ and negative mode 417.1295 $[\text{M}+\text{H}]^-$ (calc. 418.14). Purity determined by HPLC-UV (254 nm)-ESI-MS: 100%. mp: 180°C.

6.3.22.26 P_β, P_γ -Dibromomethylene-ATP (83), CAS 116751-21-4

The compound was synthesized starting from **1** (0.2 g, 0.75 mmol, 1.0 eq) and afforded a white powder (0.12 g, 24%). $^1\text{H-NMR}$ (500 MHz, D_2O) δ 8.53 (s, 1H, $\text{N}=\text{CHN}$) 8.25 (s, 1H, $\text{N}=\text{CHN}$) 6.14 (d, 1H, $J=6.0$ Hz, CHN) 4.79 (s, 1H, CHOH) 4.62 (m, 1H, CHOH) 4.41 (m, 1H, CHCH_2) 4.30 (d m, 2H, CHCH_2). $^{13}\text{C-NMR}$ (125 MHz, D_2O) δ 158.49, 155.69, 152.04, 142.81, 121.51, 89.63, 86.95, 77.21, 73.33, 68.20, 57.26. $^{31}\text{P-NMR}$ (202 MHz, D_2O) δ 7.56 (d, 1P, $J=14.45$ Hz, P_γ) -0.50 (dd, 1P, $J=14.40, 28.55$ Hz, P_β) -10.58 (d, 1P, $J=28.56$ Hz, P_α). LC/ESI-MS (m/z): positive mode 663.8407 $[\text{M}+\text{H}]^+$ and negative mode 661.8256 $[\text{M}+\text{H}]^-$ (calc. 663.00). Purity determined by HPLC-UV (254 nm)-ESI-MS: 100%. mp: degradation > 250°C.

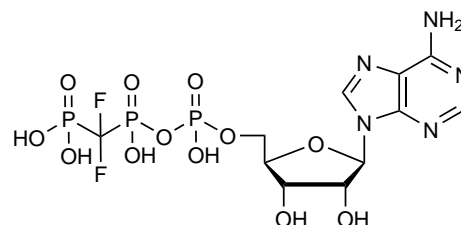
6.3.23 P_β, P_γ -Dichloromethylene-ATP (84), CAS 81336-74-5

Adenosine (**1**, 0.2 g, 0.75 mmol, 1.0 eq) and proton sponge (0.24 g, 1.13 mmol, 1.5 eq) were dissolved in 5.0 ml of trimethyl phosphate under argon atmosphere at room temperature. The mixture was cooled to 0°C and phosphoryl chlo-

ride (0.1 ml, 1.3 mmol, 1.7 eq) was added dropwise. After 5 h of stirring at 0°C, tributylamine (4.0 eq) and 0.5 M tri-*N*-butylammonium dichloromethylenebisphosphonate (**64**) solution in DMF (2.5 eq) were added to the mixture simultaneously. After 30 min a cold 0.5 M *aqueous* TEAC solution (20 ml, pH 7.4–7.6) was added to the mixture and stirring was continued at room temperature for one hour. Trimethyl phosphate was extracted with *tert.*-butylmethylether (3x 200 ml) and the *aqueous* solution was lyophilized to yield white semisolids. The crude nucleoside triphosphates were purified by FPLC. After equilibration of the column with deionized water, the crude product was dissolved in deionized water and injected into the column. The column was firstly washed with 5% 0.5 M NH₄HCO₃ buffer to remove unbound components. Elution started with a solvent gradient of 5→80% 0.5 M NH₄HCO₃ buffer over 8 column volumes followed by an isocratic phase at 80% 0.5 M NH₄HCO₃ buffer. Fractions were collected, appropriate fractions were pooled and lyophilized several times. The triphosphate was further purified by preparative HPLC (0%→30% acetonitrile in 50 mM NH₄HCO₃ buffer in 15 min, 20 ml/min). Fractions were collected and appropriate fractions pooled and lyophilized yielding a white solid (0.05 g, 8%). ¹H-NMR (500 MHz, D₂O) δ 8.53 (s, 1H, N=CHN) 8.25 (s, 1H, N=CHN) 6.14 (d, 1H, *J* = 5.95 Hz, CHN) 4.78 (s, 1H, CHOH) 4.61 (m, 1H, CHOH) 4.41 (br s, 1H, CHCH₂) 4.28 (d m, 2H, CHCH₂). ¹³C-NMR (125 MHz, D₂O) δ 158.54, 155.74, 152.05, 142.79, 121.52, 89.62, 86.99, 77.21, 73.26, 68.16, 37.53. ³¹P-NMR (202 MHz, D₂O) δ 7.83 (d, 1P, *J* = 18.36 Hz, P_γ) 0.16 (dd, 1P, *J* = 18.58, 29.06 Hz, P_β) -10.55 (d, 1P, *J* = 29.64 Hz, P_α). LC/ESI-MS (*m/z*): positive mode 573.9446 [M+H]⁺ and negative mode 571.9304 [M+H]⁻ (calc. 572.94). Purity determined by HPLC-UV (254 nm)-ESI-MS: 98.1%. mp: 205°C.

6.3.24 P_β,P_γ-Difluoromethylene-ATP (**85**), CAS 81336-78-9

Adenosine (**1**, 0.2 g, 0.75 mmol, 1.0 eq) and proton sponge (0.24 g, 1.13 mmol, 1.5 eq) were dissolved in 5.0 ml of trimethyl phosphate under argon atmosphere at room temperature. The mixture was cooled to 0°C and phosphoryl chloride (0.1 ml, 1.3 mmol, 1.7 eq) was added dropwise. After 5 h of stirring at 0°C, tributylamine (4.0 eq) and 0.5 M tri-*N*-butylammonium difluoromethylenebisphosphonate



(65) solution in DMF (2.5 eq) were added to the mixture simultaneously. After 30 min a cold 0.5 M *aqueous* TEAC solution (20 ml, pH 7.4–7.6) was added to the mixture and stirring was continued at room temperature for one hour. Trimethyl phosphate was extracted with *tert.*-butylmethylether (3x 200 ml) and the *aqueous* solution was lyophilized to yield white semisolids. The crude nucleoside triphosphates were purified by FPLC. After equilibration of the column with deionized water, the crude product was dissolved in deionized water and injected into the column. The column was firstly washed with 5% 0.5 M NH_4HCO_3 buffer to remove unbound components. Elution started with a solvent gradient of 5→80% 0.5 M NH_4HCO_3 buffer over 8 column volumes followed by an isocratic phase at 80% 0.5 M NH_4HCO_3 buffer. Fractions were collected, appropriate fractions were pooled and lyophilized several times. The triphosphate was further purified by preparative HPLC (0%→30% acetonitrile in 50 mM NH_4HCO_3 buffer in 15 min, 20 ml/min). Fractions were collected and appropriate fractions pooled and lyophilized yielding a white solid (0.025 g, 6%). $^1\text{H-NMR}$ (500 MHz, D_2O) δ 8.52 (s, 1H, N=CHN) 8.25 (s, 1H, N=CHN) 6.14 (d, 1H, $J=6.02$ Hz, CHN) 4.78 (d, 1H, $J=5.60$ Hz, CHCH₂) 4.57 (m, 1H, CHOH) 4.41 (br s, 1H, CHOH) 4.25 (d m, 2H, CHCH₂). $^{13}\text{C-NMR}$ (125 MHz, D_2O) δ 158.39, 155.55, 152.01, 142.77, 121.48, 89.58, 86.87, 71.17, 73.24, 68.07. $^{31}\text{P-NMR}$ (202 MHz, D_2O) δ 3.40 (td, 1P, $J=58.87, 79.05$ Hz, P γ) -4.56 (tdd, 1P, $J=28.07, 56.21, 84.20$ Hz, P β) -10.68 (d, 1P, $J=30.49$ Hz, P α). $^{19}\text{F-NMR}$ (202 MHz, D_2O) δ -119.76 (t, 2F, $J=82.12$ Hz). LC/ESI-MS (m/z): positive mode 542.0017 $[\text{M}+\text{H}]^+$ and negative mode 539.9888 $[\text{M}+\text{H}]^-$ (calc. 541.00). Purity determined by HPLC-UV (254 nm)-ESI-MS: 100%. mp: decomposition > 231°C.

6.3.25 General procedure for the synthesis of compounds 87-103

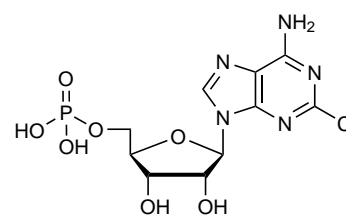
Lyophilized nucleosides (1.0 eq) were dissolved in trimethyl phosphate (5 ml) under argon. The solution was cooled to 0–4°C and dry proton sponge (1.5 eq) was added. After 5 min of stirring, phosphoryl chloride (0.1 ml, 1.1 mmol) was added and the reaction mixture was stirred at 0–4°C under argon. After 4–5 h the reaction was quenched with 0.5 M TEAC buffer pH 7.4–7.6 (10 ml). After 10 min of stirring at 0–4°C under argon, the argon was removed, and the reaction mixture was allowed to warm up to room temperature. Trimethyl phosphate was extracted with *tert.*-butylmethylether (500 ml) and the crude product was dried by lyophilisation. The

crude product was purified by preparative HPLC (0%→50% acetonitrile in 50 mM NH_4HCO_3 buffer in 20 min, 20 ml/min). Fractions were collected and appropriate fractions pooled and lyophilized multiple times to remove the TEAC buffer, yielding the desired nucleoside 5'-*O*-monophosphates as white powders.

6.3.25.1 2-Chloro-AMP (87), CAS 21466-01-3

The compound was synthesized starting from **6** (0.1 g, 0.33 mmol, 1.0 eq) and afforded a white solid (0.1 g, 84%).

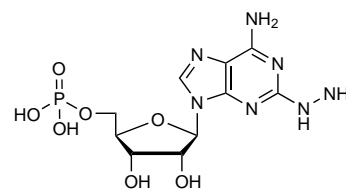
$^1\text{H-NMR}$ (600 MHz, D_2O) δ 8.57 (s, 1H, $\text{NCH}=\text{N}$) 6.04 (d, 1H, $J = 5.60$ Hz, CHN) 4.50 (m, 1H, CHOH) 4.36 (br s, 1H, CHOH) 4.01 (br s, 2H, CHCH_2) 3.59 (d, 1H, $J = 10.69$ Hz, CHCH_2). $^{13}\text{C-NMR}$ (150 MHz, D_2O) δ 163.08, 159.07, 153.07, 143.24, 120.46, 89.81, 87.62, 77.48, 73.48, 66.30. $^{31}\text{P-NMR}$ (202 MHz, D_2O) δ 3.99. LC/ESI-MS (m/z): positive mode 382.0313 $[\text{M}+\text{H}]^+$ and negative mode 380.0172 $[\text{M}-\text{H}]^-$ (calc. 381.02). Purity determined by HPLC-UV (254 nm)-ESI-MS: 99.9%. mp: 185°C.



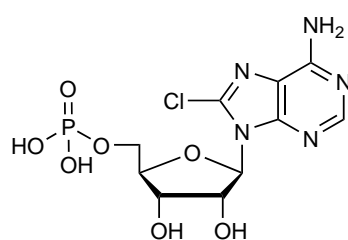
6.3.25.2 2-Hydrazinyl-AMP (88)

The compound was synthesized starting from **7** (0.1 g, 0.3 mmol, 1.0 eq) and afforded a white solid (0.07 g, 58%).

$^1\text{H-NMR}$ (600 MHz, D_2O) δ 8.23 (s, 1H, $\text{N}=\text{CHN}$) 6.03 (d, 1H, $J = 5.98$ Hz, CHN) 4.86 (t, 1H, $J = 5.25$ Hz, CHCH_2) 4.51 (t, 1H, $J = 4.23$ Hz, CHOH) 4.34 (d, 1H, $J = 2.97$ Hz, CHOH) 4.03 (t, 2H, $J = 4.23$ Hz, CHCH_2). $^{13}\text{C-NMR}$ (125 MHz, D_2O) δ 158.74, 154.08, 140.90, 132.50, 116.32, 89.47, 87.22, 76.66, 73.51, 66.63. $^{31}\text{P-NMR}$ (202 MHz, D_2O) δ 5.33. LC/ESI-MS (m/z): positive mode 378.0911 $[\text{M}+\text{H}]^+$ and negative mode 376.0774 $[\text{M}+\text{H}]^-$ (calc. 377.08). Purity determined by HPLC-UV (254 nm)-ESI-MS: 100.0%. mp: 77°C.

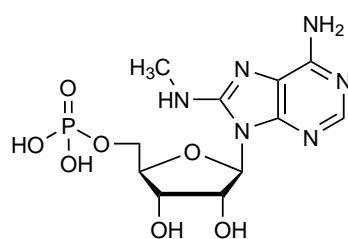


6.3.25.3 8-Chloro-AMP (89), CAS 37676-40-7



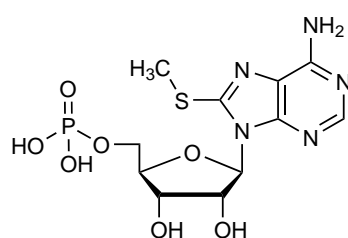
The compound was synthesized starting from **8** (0.1 g, 0.33 mmol, 1.0 eq) and afforded a white solid (0.09 g, 69%). $^1\text{H-NMR}$ (600 MHz, D_2O) δ 8.23 (s, 1H, $\text{NCH}=\text{N}$) 6.12 (d, 1H, $J=5.47$ Hz, CHN) 5.25 (br s, 1H, CHOH) 4.59 (br s, 1H, CHOH) 4.29 (br s, 1H, CHCH_2) 4.12 (d m, 2H, CHCH_2). $^{13}\text{C-NMR}$ (150 MHz, D_2O) δ 157.21, 155.79, 152.85, 141.97, 120.49, 91.06, 86.56, 73.64, 72.50, 61.75. $^{31}\text{P-NMR}$ (202 MHz, D_2O) δ 1.76. LC/ESI-MS (m/z): positive mode 382.0383 $[\text{M}+\text{H}]^+$ and negative mode 380.0162 $[\text{M}-\text{H}]^-$ (calc. 381.02). Purity determined by HPLC-UV (254 nm)-ESI-MS: 100.0 %. mp: 150°C.

6.3.25.4 8-Aminomethyl-AMP (90), CAS 61370-73-8



The compound was synthesized starting from **10** (0.1 g, 0.34 mmol, 1.0 eq) and afforded a white solid (0.03 g, 23%). $^1\text{H-NMR}$ (600 MHz, D_2O) δ 8.05 (s, 1H, $\text{NCH}=\text{N}$) 6.08 (d, 1H, $J=7.86$ Hz, CHN) 4.69 (dd, 1H, $J=5.93, 7.69$ Hz, CHOH) 4.44 (dd, 1H, $J=2.04, 5.73$ Hz, CHOH) 4.36 (br s, 1H, CHCH_2) 4.17 (d m, 2H, CHCH_2) 3.06 (s, 3H, NHCH_3). $^{13}\text{C-NMR}$ (150 MHz, D_2O) δ 155.87, 153.59, 152.44, 151.33, 118.88, 89.16, 87.31, 73.31, 73.08, 67.50, 31.80. $^{31}\text{P-NMR}$ (202 MHz, D_2O) δ 3.35. LC/ESI-MS (m/z): positive mode 377.0966 $[\text{M}+\text{H}]^+$ and negative mode 375.0813 $[\text{M}-\text{H}]^-$ (calc. 376.09). Purity determined by HPLC-UV (254 nm)-ESI-MS: 99.5 %. mp: 197°C.

6.3.25.5 8-Methylthio-AMP (91), CAS 54503-66-1



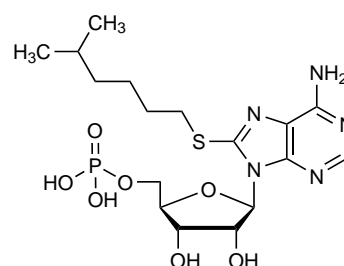
The compound was synthesized starting from **14** (0.1 g, 0.32 mmol, 1.0 eq) and afforded a white solid (0.1 g, 81%). $^1\text{H-NMR}$ (600 MHz, D_2O) δ 8.16 (s, 1H, $\text{NCH}=\text{N}$) 6.06 (d, 1H, $J=4.75$ Hz, CHN) 5.13 (br s, 1H, CHOH) 4.52 (br s, 1H, CHOH) 4.27 (br s, 1H, CHCH_2) 4.13 (d, 2H, $J=20.08$ Hz, CHCH_2) 2.74 (br s, 3H, SCH_3). $^{13}\text{C-NMR}$ (150 MHz, D_2O) δ 156.34, 155.56, 154.51, 153.90, 121.76, 90.56, 86.69, 73.41, 72.57, 66.87, 17.23. $^{31}\text{P-NMR}$ (202 MHz, D_2O) δ 2.78. LC/ESI-MS (m/z): positive mode 394.0582 $[\text{M}+\text{H}]^+$ and neg-

ative mode 392.0446 [M-H]⁻ (calc. 393.05). Purity determined by HPLC-UV (254 nm)-ESI-MS: 100.0%. mp: 145°C.

6.3.25.6 8-(5-Methyl)hexylthio-AMP (92)

The compound was synthesized starting from **16** (0.1 g, 0.25 mmol, 1.0 eq) and afforded a white solid (0.03 g, 24%).

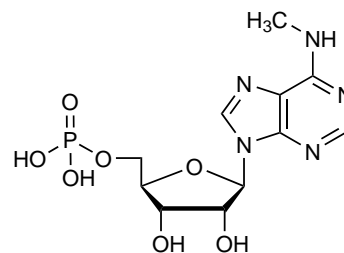
¹H-NMR (600 MHz, D₂O) δ 8.15 (s, 1H, N=CHN) 6.09 (d, *J* = 6.15 Hz, 1H, CHN) 5.17 (t, 1H, *J* = 6.13 Hz, CHOH) 4.54 (m, 1H, CHOH) 4.26 (q, 1H, *J* = 4.91 Hz, CHCH₂) 4.16 (m, 2H, CHCH₂) 3.27 (m, 2H, SCH₂) 1.71 (m, 2H, CH₂) 1.46 (m, 1H, CH) 1.40 (m, 2H, CH₂) 1.15 (q, 2H, *J* = 7.11 Hz, CH₂) 0.81 (d, 6H, *J* = 6.60 Hz, CH(CH₃)₂). ¹³C-NMR (150 MHz, D₂O) δ 156.46, 154.58, 154.36, 153.54, 121.87, 90.94, 86.44, 73.59, 72.64, 67.30, 40.39, 35.88, 31.63, 29.98, 28.40, 24.67, 21.83. ³¹P-NMR (202 MHz, D₂O) δ 1.43. LC/ESI-MS (*m/z*): positive mode 478.1504 [M+H]⁺ and negative mode 476.1402 [M+H]⁻ (calc. 505.18). Purity determined by HPLC-UV (254 nm)-ESI-MS: 95.5%. mp: degradation >180°C.

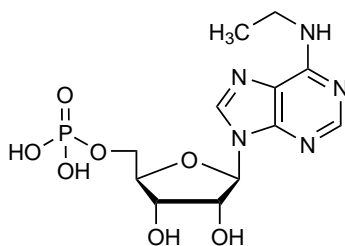


6.3.25.7 N⁶-Methyl-AMP (93), CAS 4229-50-9

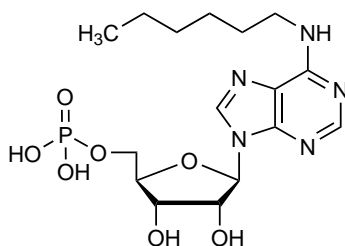
The compound was synthesized starting from **21** (0.1 g, 0.36 mmol, 1.0 eq) and afforded a white powder (0.09 g, 74%).

¹H-NMR (600 MHz, D₂O) δ 8.55 (s, 1H, NCH=N) 8.23 (s, 1H, NCH=N) 6.12 (d, 1H, *J* = 5.92 Hz, CHN) 4.51 (m, 1H, CHOH) 4.36 (d, 1H, *J* = 3.42 Hz, CHOH) 4.00 (d, 2H, *J* = 4.04 Hz, CHCH₂) 3.59 (d, 1H, *J* = 10.69 Hz, CHCH₂) 3.08 (br s, 3H, NHCH₃). ¹³C-NMR (150 MHz, D₂O) δ 163.11, 158.00, 155.67, 142.29, 121.82, 89.51, 87.68, 77.29, 73.29, 73.56, 66.52, 30.17. ³¹P-NMR (202 MHz, D₂O) δ 4.22. LC/ESI-MS (*m/z*): positive mode 362.0864 [M+H]⁺ and negative mode 360.0713 [M-H]⁻ (calc. 361.08). Purity determined by HPLC-UV (254 nm)-ESI-MS: 99.9%. mp: 105°C.



6.3.25.8 N⁶-Ethyl-AMP (94), CAS 30419-48-8

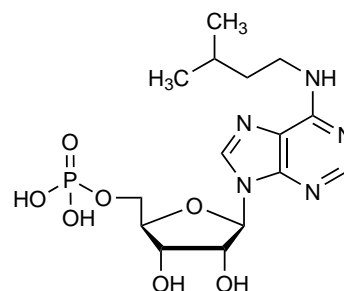
The compound was synthesized starting from 22 (0.1 g, 0.35 mmol, 1.0 eq) and afforded a white powder (0.08 g, 65%). ¹H-NMR (600 MHz, D₂O) δ 8.50 (s, 1H, NCH=N) 8.21 (s, 1H, NCH=N) 6.12 (d, 1H, *J* = 5.93 Hz, CHN) 4.78 (d, 1H, *J* = 5.46 Hz, CHCH₂) 4.50 (m, 1H, CHOH) 4.37 (s, 1H, CHOH) 4.05 (s, 2H, CHCH₂) 3.83 (d, 1H, CHCH₂) 3.59 (br s, 2H, NHCH₂CH₃) 1.28 (overlapping m, NHCH₂CH₃ & TEAC: N(CH₂CH₃)₃). ¹³C-NMR (150 MHz, D₂O) δ 163.13, 158.01, 155.70, 142.30, 121.72, 89.51, 87.69, 77.30, 73.57, 66.26, 55.59, 16.54. ³¹P-NMR (202 MHz, D₂O) δ 2.80. LC/ESI-MS (*m/z*): positive mode 376.1020 [M+H]⁺ and negative mode 374.0859 [M-H]⁻ (calc. 375.09). Purity determined by HPLC-UV (254 nm)-ESI-MS: 97.2%. mp: 125°C.

6.3.25.9 N⁶-Hexyl-AMP (95), CAS 1053739-19-7

The compound was synthesized starting from 23 (0.1 g, 0.28 mmol, 1.0 eq) and afforded a white solid (0.03 g, 22%). ¹H-NMR (500 MHz, D₂O) δ 8.40 (s, 1H, N=CHN) 8.16 (s, 1H, N=CHN) 6.09 (d, *J* = 5.80 Hz, 1H, CHN) 4.73 (t, 1H, *J* = 5.46 Hz, CHOH) 4.49 (m, 1H, CHOH) 4.37 (br s, 1H, CHCH₂) 4.12 (q, 2H, *J* = 3.70, 4.12 Hz, CHCH₂) 3.47 (br s, 2H, NHCH₂) 1.62 (m, 2H, NHCH₂CH₂) 1.35 (m, 2H, CH₂CH₃) 1.25 (m, 4H, CH₂(CH₂)₂CH₂) 0.82 (t, 3H, *J* = 6.94 Hz, NH(CH₂)₅CH₃). ¹³C-NMR (125 MHz, D₂O) δ 157.15, 155.41, 150.58, 141.80, 121.58, 89.69, 86.83, 77.23, 73.28, 72.42, 67.15, 33.64, 31.24, 28.57, 24.75, 16.11. ³¹P-NMR (202 MHz, D₂O) δ 0.92. LC/ESI-MS (*m/z*): positive mode 432.1643 [M+H]⁺ and negative mode 430.1497 [M+H]⁻ (calc. 431.39). Purity determined by HPLC-UV (254 nm)-ESI-MS: 96.0%. mp: 109°C.

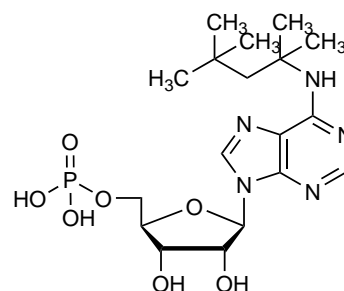
6.3.25.10 *N*⁶-*iso*-Pentyl-AMP (96), CAS 125186-39-2

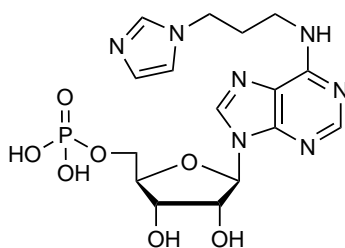
The compound was synthesized starting from **24** (0.1 g, 0.30 mmol, 1.0 eq) and afforded a white solid (0.02 g, 18%). ¹H-NMR (500 MHz, D₂O) δ 8.42 (s, 1H, N=CHN) 8.16 (s, 1H, N=CHN) 6.09 (d, *J* = 5.85 Hz, 1H, CHN) 4.74 (t, 1H, *J* = 5.48 Hz, CHOH) 4.49 (m, 1H, CHOH) 4.37 (br s, 1H, CHCH₂) 4.09 (br s, 2H, CHCH₂) 3.50 (br s, 2H, NHCH₂) 1.69 (m, 1H, CH(CH₃)₂) 1.54 (q, 2H, *J* = 7.12 Hz, CH₂CH₂CH) 0.92 (d, 6H, *J* = 6.65 Hz, CH(CH₃)₂). ¹³C-NMR (125 MHz, D₂O) δ 157.23, 155.58, 150.59, 141.84, 121.59, 89.62, 87.00, 77.23, 73.34, 66.94, 41.93, 40.16, 28.02, 24.56. ³¹P-NMR (202 MHz, D₂O) δ 1.64. LC/ESI-MS (*m/z*): positive mode 418.1479 [M+H]⁺ and negative mode 416.1338 [M+H]⁻ (calc. 417.36). Purity determined by HPLC-UV (254 nm)-ESI-MS: 96.0%. mp: 114°C.



6.3.25.11 *N*⁶-(1,1,3,3-Tetramethyl)butyl-AMP (97)

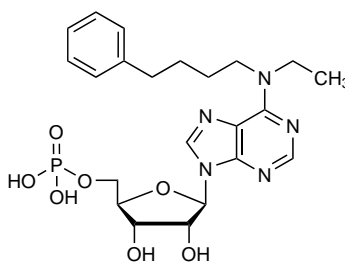
The compound was synthesized starting from **30** (0.1 g, 0.26 mmol, 1.0 eq) and afforded a white powder (0.02 g, 13%). ¹H-NMR (500 MHz, D₂O) δ 8.44 (s, 1H, N=CHN) 8.22 (s, 1H, N=CHN) 6.10 (d, 1H, *J* = 5.95 Hz, CHN) 4.75 (t, 1H, *J* = 5.55 Hz, CHCH₂) 4.49 (m, 1H, CHOH) 4.37 (m, 1H, CHOH) 4.07 (dd, 2H, *J* = 2.89, 4.80 Hz, CHCH₂) 1.97 (s, 2H, CH₂) 1.56 (s, 6H, C(CH₃)₂) 0.91 (s, 9H, C(CH₃)₃). ¹³C-NMR (125 MHz, D₂O) δ 157.23, 155.37, 150.39, 141.66, 122.35, 89.34, 87.20, 87.15, 77.25, 73.45, 66.96, 58.73, 52.52, 33.76, 33.67, 33.48, 32.12, 32.09. ³¹P-NMR (202 MHz, D₂O) δ 1.93. LC/ESI-MS (*m/z*): positive mode 460.1875 [M+H]⁺ and negative mode 458.1786 [M+H]⁻ (calc. 459.19). Purity determined by HPLC-UV (254 nm)-ESI-MS: 98%. mp: 183°C.



6.3.25.12 *N*⁶-(3-(Imidazol-1-yl)propyl)-AMP (98)

The compound was synthesized starting from **31** (0.1 g, 0.26 mmol, 1.0 eq) and afforded a white powder (0.02 g, 17%). ¹H-NMR (500 MHz, D₂O) δ 8.52 (s, 1H, N=CHN) 8.44 (s, 1H, N=CHN) 8.16 (s, 1H, NCH=N) 7.38 (s, 1H, NCH=CH) 7.21 (s, 1H, NCH=CH) 6.09 (m, 1H, CHN) 4.83 (br s, 1H, CHCH₂) 4.53 (m, 1H, CHOH) 4.38 (s, 1H, CHOH)

4.34 (m, 2H, CHCH₂) 4.07 (m, 2H, NHCH₂) 3.69 (br s, 2H, NCH₂) 2.31 (m, 2H, CH₂). ¹³C-NMR (125 MHz, D₂O) δ 157.11, 155.47, 142.36, 142.20, 137.55, 124.24, 122.97, 89.75, 87.44, 87.38, 77.29, 73.54, 66.68, 49.91, 40.62, 30.91. ³¹P-NMR (202 MHz, D₂O) δ 2.27. LC/ESI-MS (m/z): positive mode 456.1390 [M+H]⁺ and negative mode 454.1248 [M+H]⁻ (calc. 455.13). Purity determined by HPLC-UV (254 nm)-ESI-MS: 98.7%. mp: 196°C.

6.3.25.13 *N*⁶-Ethyl-*N*⁶-(4-phenyl)butyl)-AMP (99)

The compound was synthesized starting from **38** (0.1 g, 0.23 mmol, 1.0 eq) and afforded a white solid (0.03 g, 28%). ¹H-NMR (500 MHz, D₂O) δ 8.33 (s, 1H, N=CHN) 8.06 (s, 1H, N=CHN) 7.09 (m, 5H, aryl) 6.03 (d, 1H, *J* = 5.40 Hz, CHN) 4.63 (t, 1H, *J* = 5.23 Hz, CHOH) 4.45 (t, 1H, *J* = 4.52 Hz, CHOH) 4.33 (s, 1H, CHCH₂) 4.09 (br s, 2H, CHCH₂) 3.70 (br s, 4H, N(CH₂)₂) 2.47 (s, 2H, NHCH₂CH₂) 1.53 (br s, 4H, (CH₂)₂-aryl) 1.11 (t, 3H, *J* = 7.01 Hz, CH₂CH₃).

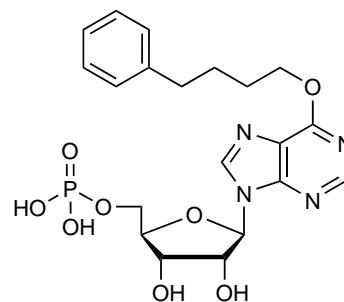
¹³C-NMR (125 MHz, D₂O) δ 156.13, 154.81, 152.07, 145.29, 140.38, 131.14, 131.09, 128.50, 121.39, 89.67, 86.63, 77.18, 73.10, 66.98, 51.21, 47.06, 37.63, 30.43, 29.52, 15.41. ³¹P-NMR (202 MHz, D₂O) δ 1.34. LC/ESI-MS (m/z): positive mode 508.1940 [M+H]⁺ and negative mode 506.1846 [M+H]⁻ (calc. 507.48). Purity determined by HPLC-UV (254 nm)-ESI-MS: 97.9%. mp: 187°C.

6.3.25.14 6-(4-Phenyl)butoxide-AMP (100)

The compound was synthesized starting from **45** (0.1 g, 0.25 mmol, 1.0 eq) and afforded a white solid (0.01 g, 7%).

$^1\text{H-NMR}$ (500 MHz, D_2O) δ 8.67 (s, 1H, N=CHN) 8.39 (s, 1H, N=CHN) 7.15 (m, 5 H, aryl) 6.19 (d, 1H, $J=5.77$ Hz, CHN) 4.53 (m, 4H, overlapping peaks: 2x CHOH & CHCH₂) 4.39 (br s, 1H, CHCH₂) 4.08 (m, 2H, OCH₂) 2.66 (t, 2H, $J=7.05$ Hz, OCH₂CH₂) 1.89 (m, 4H, (CH₂)₂-aryl).

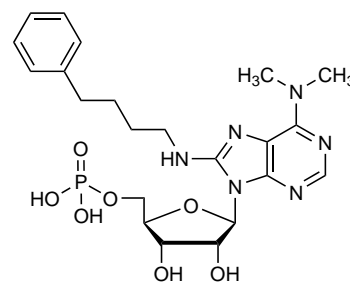
$^{13}\text{C-NMR}$ (125 MHz, D_2O) δ 163.99, 154.84, 154.11, 145.56, 144.63, 131.31, 131.12, 128.51, 123.63, 90.02, 87.37, 77.38, 73.45, 70.80, 66.70, 37.31, 30.18, 29.37. $^{31}\text{P-NMR}$ (202 MHz, D_2O) δ 2.56. LC/ESI-MS (m/z): positive mode 481.1477 [M+H]⁺ and negative mode 479.1366 [M+H]⁻ (calc. 480.41). Purity determined by HPLC-UV (254 nm)-ESI-MS: 96.0%. mp: 180°C.

**6.3.25.15 8-(4-Phenyl)butylamino-*N*⁶,*N*⁶-dimethyl AMP (101)**

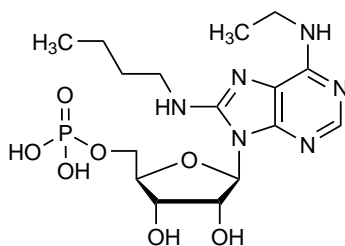
The compound was synthesized starting from **52** (0.1 g, 0.23 mmol, 1.0 eq) and afforded a white solid (0.03 g, 22%).

$^1\text{H-NMR}$ (500 MHz, D_2O) δ 7.90 (s, 1H, N=CHN) 7.05 (m, 5H, aryl) 5.99 (d, $J=7.80$ Hz, 1H, CHN) 4.67 (m, 1 H, CHOH) 4.44 (dd, 1H, $J=1.82, 5.61$ Hz, CHOH) 4.30 (br s, 1H, CHCH₂) 4.16 (d m, 2H, CHCH₂) 3.45 (d m, 2H, NHCH₂) 3.14 (s, 6H, N(CH₃)₂) 2.52 (m, 2H, NHCH₂CH₂) 1.63 (m, 4H, overlapping peaks (CH₂)₂-aryl).

$^{13}\text{C-NMR}$ (125 MHz, D_2O) δ 154.15, 153.47, 152.19, 150.91, 145.61, 131.14, 121.00, 128.29, 119.88, 88.92, 87.21, 73.49, 73.12, 67.31, 44.93, 41.17, 41.13, 37.40, 30.28, 30.21. $^{31}\text{P-NMR}$ (202 MHz, D_2O) δ 1.31. LC/ESI-MS (m/z): positive mode 523.2049 [M+H]⁺ and negative mode 521.1933 [M+H]⁻ (calc. 522.50). Purity determined by HPLC-UV (254 nm)-ESI-MS: 97.0%. mp: 163°C.



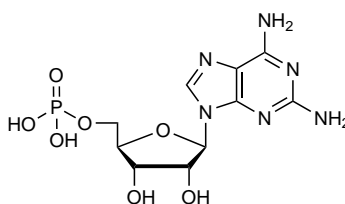
6.3.25.16 8-Butylamino-*N*⁶-ethyl-AMP (102)



The compound was synthesized starting from **56** (0.08 g, 0.22 mmol, 1.0 eq) and afforded a white solid (0.06 g, 56%). ¹H-NMR (500 MHz, D₂O) δ 7.48 (s, 1H, N=CHN) 5.99 (d, 1H, *J* = 7.77 Hz, CHN) 4.70 (m, 1H, CHOH) 4.44 (dd, 1H, *J* = 2.37, 5.78 Hz, CHOH) 4.33 (br s, 1H, CHCH₂) 4.15 (m, 2H, CHCH₂) 3.43 (m, 4H, 2x NHCH₂) 1.64 (m, 2H, CH₂)

1.37 (m, 2H, CH₂) 1.26 (m, 3H, CH₃) 0.91 (d, 3H, *J* = 7.36 Hz, CH₃). ¹³C-NMR (125 MHz, D₂O) δ 154.72, 153.32, 151.47, 151.32, 150.65, 118.90, 89.09, 87.24, 87.18, 73.34, 72.99, 67.47, 45.26, 38.74, 33.52, 22.37, 16.62, 16.17. ³¹P-NMR (202 MHz, D₂O) δ 0.29. LC/ESI-MS (*m/z*): positive mode 447.1739 [M+H]⁺ and negative mode 445.1617 [M+H]⁻ (calc. 446.17). Purity determined by HPLC-UV (254 nm)-ESI-MS: 95%. mp: 186°C.

6.3.25.17 2-Amino-AMP (103), CAS 7561-54-8



The compound was synthesized starting from **86** (0.1 g, 0.35 mmol, 1.0 eq) and afforded a white powder (0.06 g, 45%). ¹H-NMR (600 MHz, D₂O) δ 8.20 (s, 1H, NCH=N) 5.95 (d, 1H, *J* = 5.89 Hz, CHN) 4.49 (br s, 1H, CHOH) 4.34 (s, 1H, CHOH) 4.05 (s, 2H, CHCH₂) 3.59 (d, 1H,

J = 10.56 Hz, CHCH₂). ¹³C-NMR (150 MHz, D₂O) δ 162.63, 158.77, 154.03, 140.47, 115.79, 89.18, 87.19, 76.78, 73.46, 66.78. ³¹P-NMR (202 MHz, D₂O) δ 2.62. LC/ESI-MS (*m/z*): positive mode 363.0812 [M+H]⁺ and negative mode 361.0666 [M-H]⁻ (calc. 362.07). Purity determined by HPLC-UV (254 nm)-ESI-MS: 99.5%. mp: 228°C.

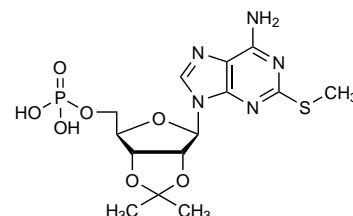
6.3.26 General procedure for the synthesis of 104-109

Nucleosides (1.0 eq) were dissolved in dry acetone (45 ml), and 2,2-dimethoxypropane (5.3 eq) and concentrated H₂SO₄ (1.7 eq) were added. The reaction was stirred for 15 min and followed by TLC (CH₃OH/DCM 1:9). After completion of the reaction, Et₃N was added dropwise until the color of the solution turned white. After evaporation of the solvent, the crude product was purified by column chromatography

over silica gel (CH₃OH/DCM 1:49) yielding the desired compound.

6.3.26.1 2',3'-*O*-Isopropylidene-2-methylthioadenosine (104), CAS 32976-08-2

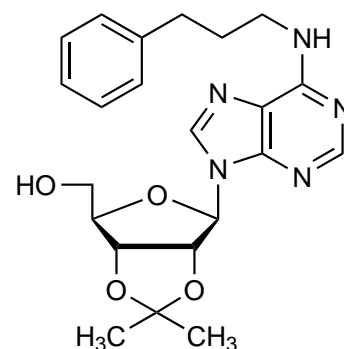
The compound was synthesized starting from **5** (0.5 g, 1.67 mmol, 1.0 eq) and afforded an orange–yellow oil (0.64 g). ¹H-NMR (500 MHz, DMSO-d₆) δ 8.18 (s, 1H, N=CHN) 7.35 (br s, 2H, NH₂) 6.09 (d, 1H, *J* = 2.70 Hz, CHN) 5.41 (dd, 1H, *J* = 2.70 6.22 Hz, CH₂OH) 4.96 (m, 1H, CHOH) 4.15 (m, 1H, CHO) 4.05 (q, 1H, *J* = 5.26 Hz, CHCH₂) 3.54 (m, 2H, CHCH₂) 2.47 (s, 3H, SCH₃) 1.53 (s, 3H, CCH₃) 1.32 (s, 3H, CCH₃).



¹³C-NMR (125 MHz, DMSO-d₆) δ 164.53, 155.58, 149.66, 138.98, 116.88, 113.11, 89.21, 86.72, 83.24, 81.46, 61.57, 27.11, 25.26. LC/ESI-MS (m/z): positive mode 354.0 [M+H]⁺. Purity determined by HPLC-UV (254 nm)–ESI-MS: 98.4%.

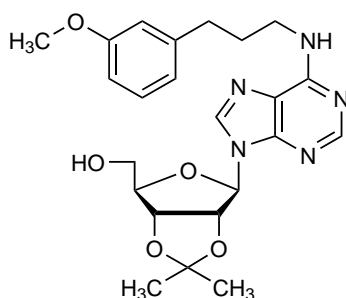
6.3.26.2 2',3'-*O*-Isopropylidene-*N*⁶-(3-phenyl)propyladenosine (105)

The compound was synthesized starting from **25** (0.5 g, 1.74 mmol, 1.0 eq) and afforded a colourless oil (0.47 g, 68% yield). ¹H-NMR (500 MHz, DMSO-d₆) δ 8.32 (s, 1H, NCH=N) 8.21 (s, 1H, NCH=N) 7.90 (s, 1H, NH) 7.22 (m, 5H, aryl) 6.12 (d, 1H, *J* = 3.07 Hz, CHN) 5.33 (dd, 1H, *J* = 3.06, 6.13 Hz, CH₂OH) 5.19 (t, 1H, *J* = 5.34 Hz, CHO) 4.96 (dd, 1H, *J* = 2.51, 6.16 Hz, CHO) 4.21 (m, 1H, CHCH₂) 3.53 (d m, 2H, CHCH₂) 2.64 (m, 2H, NHCH₂) 1.90 (m, 2H, CH₂) 1.54 (s, 3H, CH₃) 1.32 (s, 3H, CH₃) 1.05 (t, 2H, *J* = 6.99 Hz, CH₂–aryl).



¹³C-NMR (125 MHz, DMSO-d₆) δ 154.77, 152.71, 148.17, 141.93, 139.52, 128.39, 128.37, 125.79, 119.25, 113.18, 89.74, 86.50, 83.37, 81.49, 62.72, 56.14, 32.76, 30.86, 27.22, 25.34. LC/ESI-MS (m/z): positive mode 426.2 [M+H]⁺. Purity determined by HPLC-UV (254 nm)–ESI-MS: 84.2%.

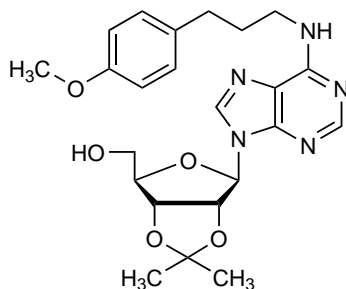
6.3.26.3 2',3'-*O*-Isopropylidene-*N*⁶-(3-(3-methoxyphenyl)propyl)adenosine (106)



The compound was synthesized starting from **26** (0.6 g, 1.45 mmol, 1.0 eq) and afforded a colourless oil (0.3 g, 86%). ¹H-NMR (500 MHz, DMSO-*d*₆) δ 8.32 (s, 1H, NCH=N) 8.21 (br s, 1H, NCH=N) 7.89 (br s, 1H, NH) 7.17 (t, 1H, *J* = 8.03 Hz, aryl) 6.78 (br m, 2H, aryl) 6.71 (d m, 1H, aryl) 6.12 (d, 1H, *J* = 3.08 Hz, CHN) 5.33 (dd, 1H, *J* = 3.09, 6.15 Hz, CH₂OH) 5.19 (t, 1H, *J* = 4.94 Hz, CHO)

4.96 (dd, 1H, *J* = 2.50, 6.19 Hz, CHO) 4.20 (d m, 1H, CHCH₂) 3.71 (s, 3H, OCH₃) 3.58-3.48 (br m, 4H, overlapping CH₂OH & NHCH₂) 2.68 (t, 2H, NHCH₂CH₂) 1.89 (m, 2H, CH₂-aryl) 1.54 (s, 3H, OCH₃) 1.32 (s, 3H, OCH₃). ¹³C-NMR (125 MHz, DMSO-*d*₆) δ 159.41, 154.82, 152.78, 143.54, 139.53, 129.35, 120.67, 114.02, 113.16, 111.35, 89.77, 86.53, 83.40, 81.50, 61.73, 55.00, 32.78, 30.74, 27.22, 25.34. LC/ESI-MS (*m/z*): positive mode 456.1 [M+H]⁺. Purity determined by HPLC-UV (254 nm)-ESI-MS: 92.8%.

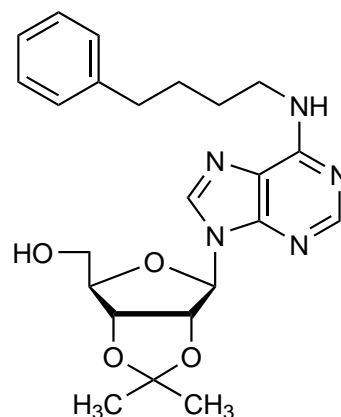
6.3.26.4 2',3'-*O*-Isopropylidene-*N*⁶-(3-(4-methoxy)phenyl)propyl)adenosine (107)



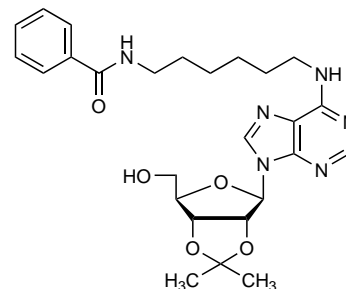
The compound was synthesized starting from **27** (0.3 g, 0.75 mmol, 1.0 eq) and afforded a colourless oil (0.11 g, 30%). ¹H-NMR (500 MHz, DMSO-*d*₆) δ 8.32 (s, 1H, NCH=N) 8.21 (br s, 1H, NCH=N) 7.88 (br s, 1H, NH) 7.12 (d, 2H, *J* = 8.61 Hz, aryl) 6.82 (d, 2H, *J* = 8.63 Hz, aryl) 6.11 (d, 1H, *J* = 3.08 Hz, CHN), 5.33 (dd, 1H, *J* = 3.12, 6.16 Hz, CH₂OH) 5.19 (t, 1H, *J* = 5.60 Hz, CHO) 4.95 (dd, 1H, *J* = 2.53, 6.17 Hz, CHO) 4.20 (m, 1H, CHCH₂) 3.70 (s, 3H, OCH₃) 3.57-3.49 (br m, 4H, overlapping CH₂OH & NHCH₂) 2.57 (m, 2H, NHCH₂CH₂) 1.86 (m, 2H, CH₂Ph) 1.54 (s, 3H, OCH₃) 1.32 (s, 3H, OCH₃). ¹³C-NMR (125 MHz, DMSO-*d*₆) δ 157.52, 154.80, 152.74, 139.53, 133.70, 129.35, 113.84, 113.84, 113.18, 89.78, 86.54, 83.41, 81.51, 61.74, 59.87, 55.10, 35.10, 31.86, 27.23, 25.35. LC/ESI-MS (*m/z*): positive mode 456.1 [M+H]⁺. Purity determined by HPLC-UV (254 nm)-ESI-MS: 90.4%.

6.3.26.5 2',3'-*O*-Isopropylidene-*N*⁶-(4-phenyl)butyladenosine (108)

The compound was synthesized starting from **28** (0.69 g, 1.74 mmol, 1.0 eq) and afforded a yellow oil (0.99 g). ¹H-NMR (500 MHz, DMSO-*d*₆) δ 8.31 (s, 1H, NCH=N) 8.21 (s, 1H, NCH=N) 7.86 (br s, 1H, NHCH₂) 7.26-7.12 (m, 5H, aryl) 6.11 (d, 1H, *J* = 3.08 Hz, CHN) 5.34 (q, 1H, *J* = 2.99, 6.08 Hz, CHCH₂) 5.19 (t, 1H, *J* = 5.51 Hz, CHO) 4.96 (q, 1H, *J* = 2.56, 6.15 Hz, CH₂OH) 4.21 (m, 1H, CHO) 3.58-3.49 (overlapping m, 4H, CH₂OH & NHCH₂) 2.61 (br t, 2H, *J* = 4.97 Hz, CH₂Ph) 1.61 (br s, 4H, (CH₂)₂) 1.54 (s, 3H, CH₃) 1.32 (s, 3H, CH₃). ¹³C-NMR (125 MHz, DMSO-*d*₆) δ 158.74, 152.81, 145.22, 142.92, 139.50, 128.41, 128.40, 125.71, 113.15, 89.78, 86.53, 83.39, 81.49, 62.72, 56.41, 34.99, 28.45, 27.21, 25.33. LC/ESI-MS (*m/z*): positive mode 440.1 [M+H]⁺. Purity determined by HPLC-UV (254 nm)-ESI-MS: 84.5%.

**6.3.26.6 2',3'-*O*-Isopropylidene-*N*⁶-(*N*-benzamide)hexyladenosine (109)**

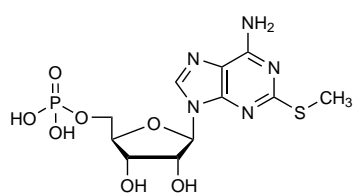
The compound was synthesized starting from **29** (0.2 g, 0.43 mmol, 1.0 eq) and afforded a colourless oil (0.19 g, 84%). ¹H-NMR (500 MHz, DMSO-*d*₆) δ 8.39 (t, 1H, *J* = 5.45 Hz, N=CHN) 8.30 (s, 1H, N=CHN) 8.20 (br s, 1H, NHCH₂) 7.84 (br s, 1H, NHCH₂) 7.80 (m, 2H, aryl) 7.46 (m, 3H, aryl) 6.10 (d, 1H, *J* = 3.07 Hz, CHN) 5.32 (dd, 1H, *J* = 2.99, 5.98 Hz, CHO) 5.23 (br s, 1H, CH₂OH) 4.95 (dd, 1H, *J* = 2.47, 6.13 Hz, CHO) 4.20 (m, 1H, CHCH₂) 3.51 (m, 2H, CHCH₂) 3.23 (d, 2H, *J* = 6.20 Hz, NHCH₂) 3.16 (d, 2H, *J* = 4.94 Hz, NHCH₂) 1.59 (m, 2H, CH₂) 1.53 (s, 3H, CCH₃) 1.51 (m, 2H, CH₂) 1.33 (m, 4H, (CH₂)₂) 1.31 (s, 3H, CCH₃). ¹³C-NMR (125 MHz, DMSO-*d*₆) δ 166.33, 154.82, 152.85, 148.15, 139.57, 134.91, 131.15, 128.40, 127.28, 119.68, 113.26, 89.84, 86.57, 83.45, 81.55, 61.79, 56.23, 56.00, 29.31, 29.20, 27.27, 26.48, 26.37, 25.38. LC/ESI-MS (*m/z*): positive mode 511.1 [M+H]⁺. Purity determined by HPLC-UV (254 nm)-ESI-MS: 96.8%.



6.3.27 General procedure for the synthesis of 110-115

Lyophilized nucleosides (1.0 eq) were dissolved in trimethyl phosphate (5 ml) under argon. The solution was cooled to 0–4°C and dry proton sponge (1.5 eq) was added. After 5 min of stirring, phosphoryl chloride (0.1 ml, 1.0 mmol) was added and the reaction mixture was stirred at 0–4°C under argon. After 6–7 h the reaction was quenched with 0.5 M TEAC buffer pH 7.4–7.6 (10 ml). After 10 min of stirring at 0–4°C under argon, the argon was removed, and the reaction mixture was allowed to warm up to room temperature. Trimethyl phosphate was extracted with *tert*-butylmethylether (500 ml) and the crude product was dried by lyophilisation. The crude product was purified by preparative HPLC (0%→75% acetonitrile in 50 mM NH₄HCO₃ buffer in 20 min, 20 ml/min). Fractions were collected and appropriate fractions pooled and lyophilized multiple times to remove the TEAC buffer, yielding the desired 2',3'-*O*-protected nucleoside 5'-*O*-monophosphates as white powders. The protected nucleoside monophosphates were dissolved in 8% TFA in H₂O/DCM 1:9 (5.0 ml) and the reaction mixture was stirred at room temperature for 2 h. The solvents were evaporated and precipitation was induced by the addition of diethyl ether. After decantation of the ether, the crude product was purified by preparative HPLC (0%→50% acetonitrile in 50 mM ammonium bicarbonate (NH₄HCO₃) buffer in 20 min, 20 ml/min). Lyophilization afforded the desired nucleoside 5'-*O*-monophosphates.

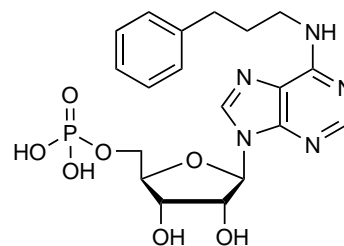
6.3.27.1 2-Methylthio-AMP (110), CAS 22140-20-1



The compound was synthesized starting from **104** (0.2 g, 0.67 mmol, 1.0 eq) and afforded a white powder (0.02 g; 8%). ¹H-NMR (500 MHz, D₂O) δ 8.44 (s, 1H, NCH=N) 6.12 (d, 1H, *J* = 5.78 Hz, CHN) 4.53 (m, 1H, CHOH) 4.34 (br s, 1H, CHOH) 3.99 (d, 2H, *J* = 3.77 Hz, CHCH₂) 3.59 (d, 1H, *J* = 10.69 Hz, CHCH₂) 2.58 (s, 3H, SCH₃). ¹³C-NMR (125 MHz, D₂O) δ 169.08, 163.28, 153.23, 142.25, 119.07, 87.61, 87.38, 77.03, 73.59, 66.43, 16.53. ³¹P-NMR (202 MHz, D₂O) δ 4.09. LC/ESI-MS (*m/z*): positive mode 394.0582 [M+H]⁺ and negative mode 392.0425 [M-H]⁻ (calc. 393.31). Purity determined by HPLC-UV (254 nm)-ESI-MS: 100.0%. mp: 85°C.

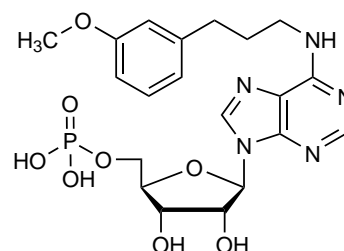
6.3.27.2 *N*⁶-(3-Phenyl)propyl-AMP (111)

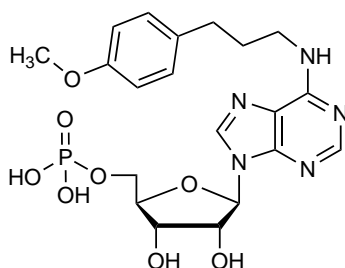
The compound was synthesized starting from **105** (0.2 g, 0.47 mmol, 1.0 eq) and afforded a white powder (0.04 g; 18%). ¹H-NMR (500 MHz, D₂O) δ 8.45 (s, 1H, NCH=N) 8.14 (s, 1H, NCH=N) 7.18 (br s, 4H, aryl) 7.10 (br s, 1H, aryl) 6.07 (s, 1H, CHN) 4.75 (s, 2H, NHCH₂) 4.49 (s, 1H, CHOH) 4.36 (s, 1H, CHOH) 4.04 (s, 2H, CH₂OH) 3.55 (br s, 1H, CHCH₂) 2.72 (s, 2H, CH₂) 2.01 (s, 2H, CH₂-aryl). ¹³C-NMR (125 MHz, D₂O) δ 157.32, 155.45, 144.86, 141.87, 131.2, 131.18, 128.51, 121.65, 89.52, 87.29, 77.30, 73.44, 72.42, 66.61, 35.28, 32.57. ³¹P-NMR (202 MHz, D₂O) δ 2.95 LC/ESI-MS (m/z): positive mode 466.1487 [M+H]⁺ and negative mode 464.1360 [M-H]⁻ (calc. 465.40). Purity determined by HPLC-UV (254 nm)-ESI-MS: 97.6%. mp: 142°C.



6.3.27.3 *N*⁶-(3-(3-Methoxy)phenyl)propyl-AMP (112)

The compound was synthesized starting from **106** (0.25 g, 0.60 mmol, 1.0 eq) and afforded a white solid (0.1 g, 34%). ¹H-NMR (600 MHz, D₂O) δ 8.50 (s, 1H, NCH=N) 8.27 (s, 1H, NCH=N) 7.08 (s, 1H, aryl) 6.81-6.57 (m, 3H, aryl) 6.13 (d, 1H, *J* = 4.38 Hz, CHN) 4.75 (t, 1H, *J* = 5.37 Hz, CHOH) 4.51 (t, 1H, *J* = 3.89 Hz, CHOH) 4.40 (br s, 1H, CHCH₂) 4.15 (br m, 2H, NHCH₂) 3.69 (s, 3H, OCH₃) 3.60 (m, 2H, CHCH₂) 2.76 (br s, 2H, CH₂-aryl) 2.15 (br t, 2H, *J* = 6.21 Hz, CH₂CH₂CH₂). ¹³C-NMR (125 MHz, D₂O) δ 165.75, 161.45, 149.40, 146.08, 143.59, 132.50, 123.95, 120.15, 118.21, 116.69, 113.61, 90.35, 87.16, 77.52, 73.26, 67.21, 57.89, 44.31, 35.28, 31.03. ³¹P-NMR (202 MHz, D₂O) δ 0.41. LC/ESI-MS (m/z): positive mode 496.1557 [M+H]⁺ and negative mode 494.1417 [M-H]⁻ (calc. 495.15) Purity determined by HPLC-UV (254 nm)-ESI-MS: 96.5%.

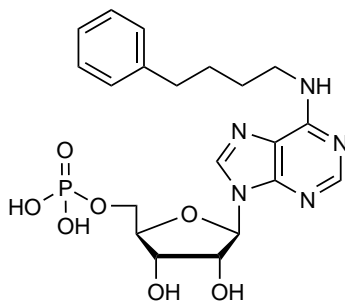


6.3.27.4 *N*⁶-(3-(4-Methoxy)phenyl)propyl-AMP (113)

The compound was synthesized starting from **107** (0.2 g, 0.44 mmol, 1.0 eq) and afforded a white solid (0.02 g; 10%).

¹H-NMR (600 MHz, D₂O) δ 8.43 (s, 1H, NCH=N) 8.11 (s, 1H, NCH=N) 7.05 (d, 2H, *J* = 7.81 Hz, aryl) 6.71 (d, 2H, *J* = 7.81 Hz, aryl) 6.05 (d, 1H, *J* = 5.80 Hz, CHN) 4.72 (t, 1H, *J* = 5.76 Hz, CHOH) 4.49 (t, 1H, *J* = 4.43 Hz, CHOH)

4.35 (br s, 1H, CHCH₂) 4.05 (br s, 2H, NHCH₂) 3.70 (s, 3H, OCH₃) 3.60 (m, 2H, CHCH₂) 2.65 (t, 2H, *J* = 7.06 Hz, CH₂-aryl) 1.98 (m, 2H, CH₂CH₂CH₂). ¹³C-NMR (125 MHz, D₂O) δ 159.42, 157.14, 155.40, 146.53, 141.70, 137.34, 132.21, 132.01, 116.39, 89.65, 86.97, 77.29, 73.28, 66.95, 58.15, 43.14, 34.52, 32.63. ³¹P-NMR (202 MHz, D₂O) δ 1.21. LC/ESI-MS (*m/z*): positive mode 496.1572 [M+H]⁺ and negative mode 494.1434 [M-H]⁻ (calc. 495.15) Purity determined by HPLC-UV (254 nm)-ESI-MS: 92.7%. mp: 95°C.

6.3.27.5 *N*⁶-(4-Phenyl)butyl-AMP (114)

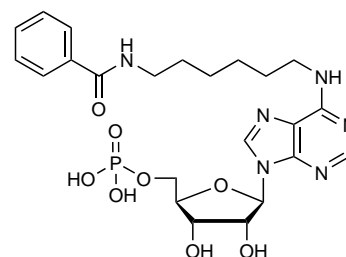
The compound was synthesized starting from **108** (0.2 g, 0.44 mmol, 1.0 eq) and afforded a white powder (0.03 g; 14%).

¹H-NMR (500 MHz, D₂O) δ 8.45 (s, 1H, NCH=N) 8.15 (s, 1H, NCH=N) 7.22-7.11 (d m, 5H, aryl) 6.10 (d, 1H, *J* = 5.90 Hz, CHN) 4.75 (m, 1H, CHOH) 4.49 (m, 1H, CHOH) 4.38 (s, 1H, CHCH₂) 4.10 (s, 2H, CHCH₂) 3.55 (br s, 1H, NHCH₂) 2.63 (br s, 2H, CH₂-aryl) 1.70 (m, 4H, (CH₂)₂).

¹³C-NMR (125 MHz, D₂O) δ 157.30, 155.51, 145.64, 141.87, 131.34, 131.14, 128.52, 109.55, 89.58, 87.11, 77.25, 73.36, 72.43, 67.01, 37.45, 30.43, 30.23. ³¹P-NMR (202 MHz, D₂O) δ 1.57 LC/ESI-MS (*m/z*): positive mode 480.1640 [M+H]⁺ and negative mode 478.1490 [M-H]⁻ (calc. 479.43). Purity determined by HPLC-UV (254 nm)-ESI-MS: 98.1%. mp: 120°C.

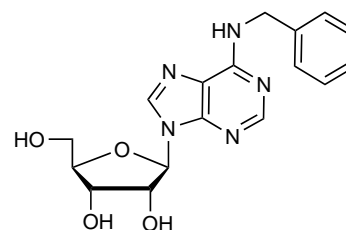
6.3.27.6 *N*⁶-(*N*-benzamide)hexyl-AMP (115)

The compound was synthesized starting from **109** (0.18 g, 0.35 mmol, 1.0 eq) and afforded a white powder (0.03 g, 15%). ¹H-NMR (500 MHz, D₂O) δ 8.38 (s, 1H, N=CHN) 8.12 (s, 1H, N=CHN) 7.60 (d, 2H, *J* = 8.23 Hz, aryl) 7.49 (t, 1H, *J* = 7.44 Hz, aryl) 7.37 (t, 2H, *J* = 7.37 Hz, aryl) 6.07 (d, 1H, *J* = 5.80 Hz, CHN) 4.71 (t, 1H, *J* = 5.43 Hz, CHCH₂) 4.48 (m, 1H, CHOH) 4.38 (br s, 1H, CHOH) 4.12 (m, 2H, CHCH₂) 3.50 (br s, 2H, NHCH₂) 3.37 (t, 2H, *J* = 6.62 Hz, NHCH₂) 1.69 (m, 2H, CH₂) 1.63 (m, 2H, CH₂) 1.44 (m, 4H, (CH₂)₂). ¹³C-NMR (125 MHz, D₂O) δ 173.54, 157.23, 155.39, 155.35, 141.78, 136.45, 134.68, 131.38, 129.57, 89.69, 89.92, 86.86, 77.23, 73.32, 67.11, 42.57, 42.56, 30.93, 30.75, 28.42, 28.34. ³¹P-NMR (202 MHz, D₂O) δ 0.86. LC/ESI-MS (*m/z*): positive mode 551.2001 [M+H]⁺ and negative mode 549.1846 [M+H]⁻ (calc. 550.19). Purity determined by HPLC-UV (254 nm)-ESI-MS: 98.1%. mp: 111°C.

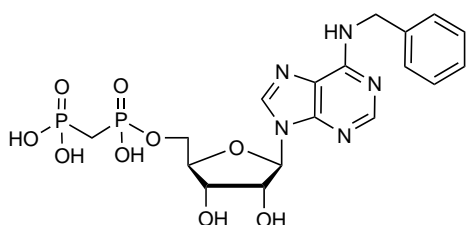


6.3.28 *N*⁶-Benzyladenosine (122), CAS 4294-16-0

A mixture of 6-chloro-9-(β-D-ribofuranosyl)purine (2.0 g, 7.0 mmol, 1 eq), *N*-benzylamine (1.5 ml, 14 mmol, 2 eq), and Et₃N (2 ml, 14 mmol, 2 eq) in absolute ethanol (20 ml) was refluxed for 3 h. After completion of reaction it was evaporated under high *vacuo*. Purification by silica gel column chromatography (1:19 CH₃OH/DCM) followed by precipitation with acetone yielded the title compound (2.48 g, 100%). ¹H-NMR (500 MHz, DMSO-*d*₆) δ 8.36 (s, 1H, N=CHN) 8.19 (s, 1H, N=CHN) 7.45-7.18 (br m, 5H, aryl) 5.89 (d, *J* = 6.10 Hz, 1H, CHN) 4.60 (t, 1H, *J* = 5.38 Hz, CHCH₂) 4.15 (q, *J* = 3.04, 5.03 Hz, 1H, CHOH) 3.95 (overlapping peak, 3H, CHOH & NHCH₂) 3.68-3.53 (d dd, *J* = 3.74, 12.16, 58.93 Hz, 2H, CH₂OH). ¹³C-NMR (126 MHz, DMSO-*d*₆) δ 154.79, 152.42, 140.00, 135.97, 128.67, 128.61, 128.31, 128.15, 127.24, 126.72, 88.07, 88.01, 73.64, 70.76, 61.78, 48.72, 42.90. LC/ESI-MS (*m/z*): positive mode 358.1 [M+H]⁺. Purity determined by HPLC-UV (254 nm)-ESI-MS: 97.9%. mp: 144°C (*lit.* 167-169°C).¹⁸⁹

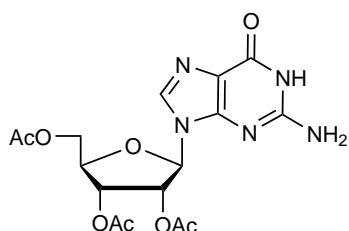


6.3.29 *N*⁶-Benzyladenosine-5'-*O*-[(phosphonomethyl)phosphonic acid] (123), CAS 1802226-78-3



A solution of methylenebis(phosphonic dichloride) (0.34 g, 1.4 mmol, 5 eq) in trimethyl phosphate (3 ml), cooled to 0–4°C was added to a suspension 122 (0.1 g, 0.3 mmol, 1 eq) in trimethyl phosphate (2 ml) at 0–4°C. The reaction mixture was stirred at 0–4°C and samples were withdrawn at 10 min interval for TLC to check the disappearance of nucleosides. After 30 min, on disappearance of nucleoside, 5 ml of cold 0.5 M aqueous TEAC solution (pH 7.4–7.6) was added. It was stirred at 0–4°C for 15 min followed by stirring at room temperature for 2 h. Trimethyl phosphate was extracted using *tert.*-butylmethylether (2 x 100 ml) and the aqueous layer was lyophilized. The crude product was then purified by semi-preparative RP-HPLC (10–40% MeCN/50 mM NH₄HCO₃ buffer in 30 min, 15 ml/min) to get final product (0.72 g, 50%). ¹H-NMR (600 MHz, D₂O) δ 8.50 (s, 1H, N=CHN) 8.20 (s, 1H, N=CHN) 7.40–7.29 (br m, 5H, aryl) 6.11 (d, *J* = 6.05 Hz, 1H, CHN) 4.77 (t, 2H, overlapping with H₂O, NHCH₂) 4.54 (t, *J* = 4.34 Hz, 1H, CHOH) 4.38 (br s, 1H, CHOH) 4.17 (br s, 1H, CH₂O) 3.80 (dd, 1H, *J* = 0.80, 11.06 Hz, CHCH₂) 2.21 (m, 2H, PCH₂P). ¹³C-NMR (151 MHz, D₂O) δ 163.13, 157.37, 155.70, 142.27, 141.22, 135.50, 131.88, 131.57, 130.18, 129.77, 121.84, 89.74, 86.70, 77.02, 73.01, 66.26, 45.86, 31.52, 30.69, 29.88. ³¹P-NMR (243 MHz, D₂O) δ 19.12 (d, 1P, *J* = 9.3 Hz, Pβ), 14.53 (d, 1P, *J* = 9.6 Hz, Pα). LC/ESI-MS (*m/z*): positive mode 516.1029 [M+H]⁺ and negative mode 514.0896 [M-H]⁻ (calc. 515.10). Purity determined by HPLC-UV (254 nm)-ESI-MS: 96.4%. mp: 180°C.

6.3.30 2',3',5'-Tri-*O*-acetyl-2-amininosine (125), CAS 6979-94-8

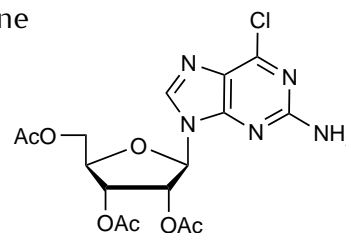


Guanosine (10 g, 35.3 mmol, 1 eq) and DMAP (0.2 g, 1.8 mmol, 0.05 eq) were suspended in acetonitrile (100 ml). *N,N*-dimethylethylamine (7 ml, 141 mmol, 4 eq) and acetic anhydride (10 ml, 105.8 mmol, 3 eq) were added and the reaction was stirred at room temperature for 10 min until a clear solution was obtained. The excess of acetic anhydride was quenched by the addition of methanol (30 ml). The mixture was stirred at room temperature for 15 min followed by evaporation. Recrystallization from isopropanol,

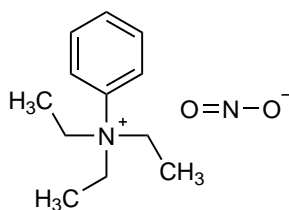
followed by acetone gave the desired product as white powder (11.8 g, 82%). $^1\text{H-NMR}$ (500 MHz, DMSO-d_6) δ 10.72 (s, 1H, NH) 7.91 (s, 1H, N=CHN) 6.51 (br s, 2H, NH_2) 5.98 (d, $J = 6.24$ Hz, 1H, CHN) 5.78 (t, $J = 6.02$ Hz, 1H, CHCH_2) 5.48 (dd, $J = 4.38$ Hz, 1H, CHO) 4.38–4.29 (d m, 2H, CH_2O) 4.24 (dd, 1H, $J = 6.00, 11.80$ Hz, CHO) 2.10 (s, 3H, COCH_3) 2.03 (d, $J = 3.70$ Hz, 6H, 2x COCH_3). $^{13}\text{C-NMR}$ (151 MHz, DMSO-d_6) δ 170.17, 169.52, 156.72, 153.99, 151.20, 135.71, 116.94, 84.53, 79.64, 72.15, 70.41, 63.17, 25.59, 20.62, 20.47, 20.28. LC/ESI-MS (m/z): positive mode 410.2 $[\text{M}+\text{H}]^+$. Purity determined by HPLC-UV (254 nm)-ESI-MS: 94.6%. mp: 228°C (*lit.* 224–225°C).¹⁹⁰

6.3.31 2',3',5'-Tri-*O*-acetyl-2-amino-6-chlorinosine (126), CAS 1348645-55-5

Compound 125 (10.0 g, 24.4 mmol, 1 eq), *N,N*-dimethylaniline (3.4 ml, 26.9 mmol, 1.1 eq), and tetraethylammonium chloride (8.1 g, 48.9 mmol, 2 eq) were dissolved in phosphorus oxychloride (45.5 ml) and the reaction was stirred at room temperature under argon. After 7 min, the reaction mixture was placed in a preheated oil bath and was refluxed for 13 min at 90°C followed by evaporation. The resulting oil was stirred in DCM (100 ml) and ice (100 ml). The product was extracted with DCM (2x 100 ml). The organic layers were combined, washed with 2 M HCl (4x 100 ml) and brine (2x 100 ml), and dried over magnesium sulfate. Evaporation yielded a dark brown oil. Purification by column chromatography ($\text{CH}_3\text{OH}/\text{DCM}$ 1:49) yielded the desired product as brown solid (6.5 g, 62%). $^1\text{H-NMR}$ (500 MHz, DMSO-d_6) δ 8.34 (s, 1H, N=CHN) 7.01 (br s, 2H, NH_2) 6.10 (d, $J = 5.84$ Hz, 1H, CHN) 5.86 (t, 1H, $J = 5.80$ Hz, CHO) 5.53 (dd, 1H, $J = 4.11, 5.80$ Hz, CHO) 4.41–4.33 (m, 2H, CHCH_2) 4.28 (q, $J = 5.56$ Hz, 1H, CHCH_2) 2.11 (s, 3H, COCH_3) 2.03 (s, 3H, COCH_3) 2.02 (s, 3H, COCH_3). $^{13}\text{C-NMR}$ (126 MHz, DMSO-d_6) δ 170.18, 169.51, 169.37, 160.01, 153.79, 150.03, 141.39, 123.65, 85.08, 79.83, 72.03, 70.38, 63.06, 20.62, 20.49, 20.30. LC/ESI-MS (m/z): positive mode 259.1, 428.0 $[\text{M}+\text{H}]^+$. Purity determined by HPLC-UV (254 nm)-ESI-MS: 92.7%. mp: 141°C.



6.3.32 Benzyltriethylammonium nitrite (BETA-NO₂, 128)



A column was packed with DOWEX 1X8 (chloride form, 20 g) and washed with 1 M sodium nitrite (300 ml) until no chloride could be detected anymore. Chloride was detected using 2% AgNO₃/EtOH and a drop of nitric acid to prevent false positive results from AgNO₂ precipitation. After that, it was eluted with 1 M benzyltriethylammoniumchlorid solution (20 ml) twice. Fractions containing the desired compound were combined and dried by lyophilization. The content of NO₂ was detected by centrimetric titration. A solution of 0.1 M aqueous Cer(IV) sulfate (2.0 ml) and 1 M H₂SO₄ (20 ml) was titrated with an the compound (0.2 g, 0.892 mmol) dissolved in water (100 ml). When the yellow color became less intense, a few drops of ferroin solution were added. The titration was continued until the color changed from slightly blue to rose.

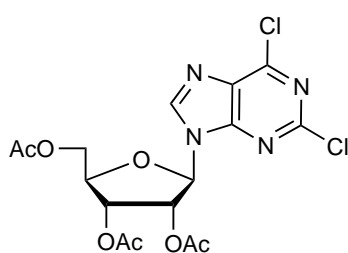
Calculation: 0.2 mmol Cer(IV) 0.1 mmol NO₂

Theoretical volume: 0.1 mmol / 0.892 mmol = 0.112 → 11,2 ml

Content: (11,2 ml/10.1 ml)*(200 mg:206 mg) = 106.5%

6.3.33 2',3',5'-Tri-*O*-acetyl-2,6-dichloropurine riboside (127),

CAS 3056-18-6



Method A: To **126** (7.6 g, 17.8 mmol, 1 eq) in anhydrous DCM (50 ml), acetyl chloride (10 ml, 143 mmol, 8 eq) was added under argon. Under ice-cooling, BETA-NO₂ (10 g, 44.6 mmol, 2.5 eq) in anhydrous DCM (30 ml) was added dropwise to the reaction mixture within an hour. The reaction was further stirred at 0-4°C under argon for 5 h.

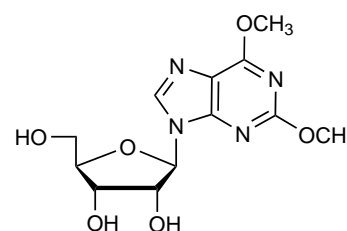
The reaction mixture was extracted with water (3x 500 ml) and the organic phase was dried over MgSO₄ and reduced *in vacuo*. Purification by column chromatography (EtOAc/DCM 1:4) yielded the desired compound as orange solid (3.5 g, 43%). ¹H-NMR (500 MHz, DMSO-d₆) δ 8.90 (s, 1H, NCH=N) 6.31 (d, 1H, J = 4.63 Hz, CHN) 5.90 (t, 1H, J = 5.45 Hz, CHO) 5.61 (t, 1H, J = 5.39 Hz, CHO) 4.41 (m, 1H, CHCH₂) 4.38-4.27 (d dd, 2H, J = 5.47, 12.31, 49.95 Hz, CHCH₂) 2.11 (s, 3H, COCH₃) 2.04 (s, 3H, COCH₃) 2.00 (s, 3H, COCH₃). ¹³C-NMR (126 MHz, DMSO-d₆) δ 170.10, 169.45, 169.31, 152.90, 151.44, 150.39, 146.95, 131.36, 86.37, 79.99, 72.49, 69.90, 62.74, 20.58,

20.46, 20.32. LC/ESI-MS (m/z): positive mode 447.0 [M+H]⁺. Purity determined by HPLC-UV (254 nm)-ESI-MS: 86.7%. mp: 162°C (*lit.* 161-163°C).¹⁹¹

Method B: Tetraacetylribose (5 g, 16.0 mmol, 1 eq) was melted at 85°C and 2,6-dichloropurine (3.0 g, 16.0 mmol, 1 eq) was added while stirring. To the reaction mixture, trifluoromethane sulfonic acid (70 μL, 0.8 mmol, 0.05 eq) was added to catalyze the reaction. The reaction mixture was stirred at 85°C under reduced pressure for 1 h. TLC analysis showed that the reaction was over and the mixture was allowed to cool down to rt to allow solidification. The desired product was recrystallized from absolute ethanol yielding the desired product as white solid (4.84 g, 69%). ¹H-NMR (600 MHz, DMSO-d₆) δ 8.89 (s, 1H, NCH=N) 6.31 (d, 1H, *J* = 5.0 Hz, CHN) 5.90 (q, 1H, *J* = 5.2 Hz, CHO) 5.61 (t, 1H, *J* = 5.5 Hz, CHO) 4.43 (m, 1H, CHCH₂) 4.39 (dd, 1H, *J* = 3.6, 12.1 Hz, CHCH₂O) 4.29 (m, 1H, CHCH₂O) 2.11 (s, 3H, COCH₃) 2.05 (s, 3H, COCH₃) 2.01 (s, 3H, COCH₃). ¹³C-NMR (151 MHz, DMSO-d₆) δ 170.12, 169.47, 169.33, 152.92, 151.46, 150.41, 146.98, 131.38, 86.38, 80.01, 72.51, 69.92, 62.76, 20.61, 20.48, 20.34. LC/ESI-MS (m/z): positive mode 447.1 [M+H]⁺. Purity determined by HPLC-UV (254 nm)-ESI-MS: 93.4%. mp: 160°C (*lit.* 161-163°C).¹⁹¹

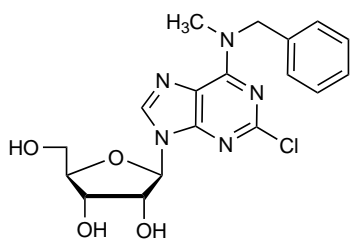
6.3.34 2,6-Methoxy-9-β-D-ribofuranosylpurine (133), CAS 88508-72-9

To **127** (0.3 g, 0.67 mmol, 1 eq) in methanol (7 ml), 30% NaOMe (0.5 ml) were added. After 10 min of stirring, the solution was evaporated and the crude product was purified by column chromatography (CH₃OH/DCM 1:9) yielding not the desired product (**132**) but instead compound



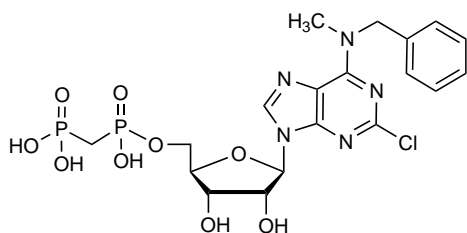
133 as colorless oil (0.1 g, 53%). ¹H-NMR (600 MHz, D₂O) δ 8.17 (s, 1H, NCH=N) 5.98 (d, 1H, *J* = 5.61 Hz, CHN) 4.87 (t, 1H, *J* = 5.03 Hz, CHOH) 4.51 (t, 1H, *J* = 4.45 Hz, CHOH) 4.23 (q, 1H, *J* = 3.87 Hz, CHCH₂) 4.06 (s, 3H, COCH₃) 3.99 (s, 3H, COCH₃) 3.93 (dd, 1H, *J* = 3.29, 13.35 Hz, CHCH₂) 3.84 (dd, 1H, *J* = 4.45, 12.38 Hz, CHCH₂). ¹³C-NMR (151 MHz, D₂O) δ 164.47, 164.36, 154.58, 144.60, 119.43, 91.36, 87.81, 76.00, 73.12, 64.16, 58.12, 57.50. LC/ESI-MS (m/z): positive mode 313.1 [M+H]⁺. Purity determined by HPLC-UV (254 nm)-ESI-MS: 98.3%.

6.3.35 *N*⁶-Benzyl-2-chloro-*N*⁶-methyladenosine (134)



A mixture of **127** (0.2 g, 0.6 mmol, 1 eq), *N*-benzylmethylamine (0.2 ml, 1.3 mmol, 2 eq), and Et₃N (2 ml, 1.3 mmol, 2 eq) in absolute ethanol (10 ml) was refluxed at 60°C for 18 h. After completion of reaction it was evaporated *in vacuo*. To the intermediate product in methanol (5 ml), 0.5% NaOCH₃ in methanol (10 ml) were added. After 18 h at room temperature, the solution was evaporated and the crude was purified by silica chromatography (1:24 CH₃OH/DCM). Additional purification by preparative RP-HPLC (20%–90% MeOH/H₂O in 20 min followed by 5 min at 90% methanol, 15 ml/min) was required, followed by evaporation of methanol and lyophilization yielding the desired product as white solid (0.2 g, 76%). ¹H-NMR (500 MHz, DMSO-*d*₆) δ 8.42 (s, 1H, N=CHN) 7.34–7.26 (m, 5H, aryl) 5.85 (d, *J* = 5.95 Hz, 1H, CHN) 5.46 (d, *J* = 6.29 Hz, 1H, CHO) 5.17 (d, *J* = 5.27 Hz, 1H, CHOH) 5.01 (t, 1H, *J* = 5.78 Hz, CH₂OH) 4.52 (q, 1H, *J* = 5.63, 11.07 Hz, CHCH₂) 4.14 (q, 1H, *J* = 4.70, 8.19 Hz, CHOH) 3.95 (q, 1H, *J* = 3.83, 7.41 Hz, CHOH) 3.67–3.52 (d m, 2H, CH₂OH) 3.16 (d, 2H, NCH₂) 3.10 (br s, 3H, NCH₃). ¹H-NMR (600 MHz, DMSO-*d*₆ with D₂O exchange) δ 8.29 (s, 1H, N=CHN) 7.31–7.22 (m, 5H, aryl) 5.82 (d, 1H, *J* = 6.03 Hz, CHN) 4.49 (t, 1H, *J* = 5.50 Hz, CHCH₂) 4.11 (dd, 1H, *J* = 3.43, 4.95 Hz, CHOH) 3.95 (q, 1H, *J* = 3.55 Hz, CHOH) 3.64–3.52 (d dd, 2H, *J* = 3.67, 12.25, 45.31 Hz, CH₂OH) 3.14 (s, 2H, NCH₂) 3.06 (br s, 3H, NCH₃). ¹³C-NMR (126 MHz, DMSO-*d*₆) δ 154.63, 152.76, 139.18, 128.75, 127.44, 118.60, 87.46, 85.82, 73.83, 70.43, 61.42, 56.16, 18.67. LC/ESI-MS (*m/z*): positive mode 406.2 [M+H]⁺. Purity determined by HPLC-UV (254 nm)-ESI-MS: 97.3%. mp: 178°C (*lit.* 207–208°C).⁸⁵

6.3.36 *N*⁶-Benzyl-2-chloro-*N*⁶-methyladenosine-5'-*O*-[(phosphonomethyl)phosphonic acid] (135)



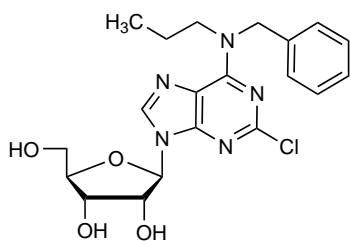
A solution of methylenebis(phosphonic dichloride) (0.25 g, 5 mmol, 5 eq) in trimethyl phosphate (2 ml), cooled to 0–4°C was added to a suspension of **134** (0.35 g, 1 mmol, 1 eq) in trimethyl phosphate (4 ml) at 0–4°C. The reaction mixture was stirred at 0–4°C and samples were withdrawn at 15 min interval for TLC to check the disappearance of nucleosides. After

90 min, on disappearance of nucleoside, 10 ml of cold 0.5 M aqueous TEAC solution (pH 7.4–7.6) was added. It was stirred at 0–4°C for 15 min followed by stirring at room temperature for 1 h. Trimethyl phosphate was extracted using (2x 100 ml) of *tert.*-butylmethylether and the aqueous layer was lyophilized. The crude product was then purified by semi-preparative RP-HPLC (0–50% MeCN/50 mM NH₄HCO₃ buffer in 20 min, 20 ml/min) to get final product as white powder (0.07 g, 52%). ¹H-NMR (600 MHz, D₂O) δ 8.40 (s, 1H, N=CHN) 7.32 (m, 5H, aryl) 6.05 (d, *J* = 5.4 Hz, 1H, CHN) 5.31 (br s, 2H, NCH₂) 4.73 (t, 1H, *J* = 5.2 Hz, CHO) 4.53 (t, 1H, *J* = 4.5 Hz, CHO) 4.38 (m, 1H, CHCH₂) 4.17 (br s, 2H, CHCH₂) 3.19 (br m, 3H, NCH₃) 2.20 (t, 2H, *J* = 19.3 Hz, PCH₂P). ¹³C-NMR (151 MHz, D₂O) δ 157.85, 156.50, 153.86, 141.12, 139.58, 131.67, 130.48, 130.11, 120.96, 89.74, 86.74, 77.08, 73.04, 66.41, 49.49, 31.00, 30.18, 29.35, 11.06. ³¹P-NMR (243 MHz, D₂O) δ 18.46 (s, 1P, Pβ) 15.47 (s, 1P, Pα). LC/ESI-MS (*m/z*): positive mode 564.0803 [M+H]⁺ and negative mode 562.0667 [M-H]⁻ (calc. 563.82). Purity determined by HPLC-UV (254 nm)-ESI-MS: 99.6%. mp: 213°C.

6.3.37 General procedure for the synthesis of 136–138

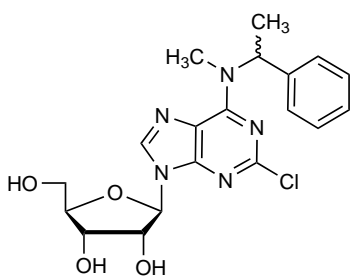
A mixture of 2,6-dichloro-9-(β-D-ribofuranosyl)purine (**127**, 0.2 g, 0.6 mmol, 1.0 eq), *N*-dialkylamine (1.3 mmol, 2.0 eq), and Et₃N (2 ml, 1.3 mmol, 2.0 eq) in absolute ethanol (10 ml) was refluxed at 60°C for 36 h. After completion of reaction it was evaporated under high *vacuo*. Purification using silica chromatography (CH₃OH/DCM 1:49) yielded the protected intermediate. To the intermediate product in methanol (5 ml), 0.5% NaOCH₃ in methanol (10 ml) were added. After 18 h at room temperature, the solution was evaporated and the crude was purified by silica chromatography (1:24 CH₃OH/DCM) and precipitation using diethyl ether yielded the desired nucleoside analogs. In some cases, disubstitution at the C2- and C6-position was observed. In these cases, additional purification by preparative RP-HPLC (20%–90% MeOH/H₂O in 20 min followed by 5 min at 90% methanol, 15 ml/min) was required, followed by evaporation of methanol and lyophilization.

6.3.37.1 *N*⁶-Benzyl-2-chloro-*N*⁶-propyladenosine (136)



The compound was synthesized using *N*-benzylpropylamine (0.6 mL, 4.4 mmol, 2.0 eq) yielding a white solid (0.64 g, 66%). ¹H-NMR (600 MHz, CD₃OD) δ 8.21 (s, 1H, N=CHN) 7.37 - 7.27 (m, 5H, aryl) 5.96 (d, 1H, *J* = 6.1 Hz, CHN) 5.61 (br s, 1H, 1x NCH₂) 5.04 (br s, 1H, 1x NCH₂) 4.73 (m, 1H, CHCH₂) 4.36 (dd, 1H, *J* = 5.0, 3.0 Hz, CHOH) 4.19 (q, 1H, *J* = 2.7 Hz, CHOH) 4.13 (br s, 1H, 1x NCH₂) 3.93-3.79 (d m, 2H, CHCH₂) 3.64 (br s, 1H, 1x NCH₂) 1.72 (br s, 2H, CH₂CH₂CH₃) 0.95 (t, 3H, *J* = 7.4 Hz, CH₂CH₃). ¹³C-NMR (151 MHz, CD₃OD) δ 156.45, 154.86, 152.80, 140.85, 139.38, 129.90, 129.17, 128.74, 120.79, 91.23, 88.12, 75.57, 72.70, 63.67, 22.83, 21.58, 15.73, 11.48. LC/ESI-MS (*m/z*): positive mode 434.2 [M+H]⁺. Purity determined by HPLC-UV (254 nm)-ESI-MS: 96%. mp: 92°C.

6.3.37.2 2-Chloro-*N*⁶-ethyl-(1-benzyl)-*N*⁶-methyladenosine (137)

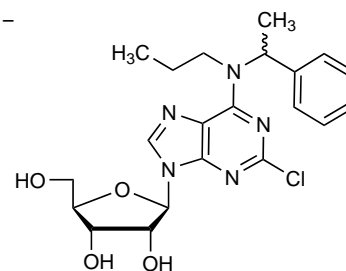


The compound was synthesized using *N,N*-methyl-(1-phenyl)ethanamine (0.7 mL, 4.5 mmol, 2.0 eq) yielding a white solid (0.54 g, 58%). ¹H-NMR (600 MHz, DMSO-*d*₆) δ 8.44 (s, 1H, N=CHN) 7.36-7.27 (m, 5H, aryl) 5.87 (d, 1H, *J* = 5.7 Hz, CHN) 5.48 (d, 1H, *J* = 6.0 Hz, CHOH) 5.19 (d, 1H, *J* = 5.1 Hz, CHOH) 5.03 (m, 1H, CH₂OH) 4.52 (m, 1H, CHOH) 4.14 (m, 1H, CHOH) 3.95 (q, *J* = 3.8 Hz, 1H, CHCH₂), 3.68-3.53 (d m, 2H, CHCH₂) 3.37 (q, *J* = 7.0 Hz, 1H, NCH) 2.84 (br s, 2H, NCH₃), 1.62 (s, 3H, CHCH₃) 1.08 (t, 1H, *J* = 7.0 Hz, NCH₃). ¹³C-NMR (151 MHz, DMSO-*d*₆) δ 154.52, 152.77, 151.22, 140.44, 139.00, 128.70, 127.49, 127.02, 118.65, 87.47, 85.80, 73.89, 70.42, 65.04, 54.33, 29.60, 16.50. LC/ESI-MS (*m/z*): positive mode 420.2 [M+H]⁺. Purity determined by HPLC-UV (254 nm)-ESI-MS: 91%. mp: 120°C.

6.3.37.3 2-Chloro-*N*⁶-ethyl-(1-benzyl)-*N*⁶-propyladenosine (138)

The compound was synthesized using *N,N*-(1-phenylethyl)-

1-propanamine HCl (0.9 g, 4.4 mmol, 2.0 eq) yielding a white solid (0.13 g, 13%). ¹H-NMR (500 MHz, DMSO-*d*₆) δ 8.43 (s, 1H, N=CHN) 7.38-7.26 (m, 5H, aryl) 5.87 (d, 1H, *J* = 5.6 Hz, CHN) 5.45 (br s, 1H, CH₂OH) 5.20 (br s, 1H, CHOH) 5.02 (br s, 1H, CHOH) 4.52 (dd, 1H, *J* = 5.3,

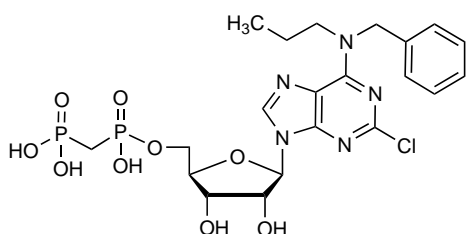


6.2 Hz, CHOH) 4.13 (m, 1H, CHOH) 3.95 (q, *J* = 3.5 Hz, 1H, CHCH₂), 3.66-3.53 (d m, 1H, CHCH₂), 3.13 (br s, 1H, NCH), 1.64 (d, 3H, *J* = 6.5 Hz, CHCH₃), 1.39 (br d, *J* = 90.3 Hz, 2H, CH₂CH₃) 0.74 (br s, 3H, CH₂CH₃). ¹³C-NMR (126 MHz, DMSO-*d*₆) δ 154.16, 152.71, 151.80, 140.88, 139.39, 128.60, 127.55, 127.32, 118.61, 87.42, 85.81, 73.88, 70.50, 61.46, 54.87, 23.27, 21.12, 17.06, 11.22. LC/ESI-MS (*m/z*): positive mode 448.1 [M+H]⁺. Purity determined by HPLC-UV (254 nm)-ESI-MS: 98%. mp: 105°C.

6.3.38 General procedure for the synthesis of 139-141

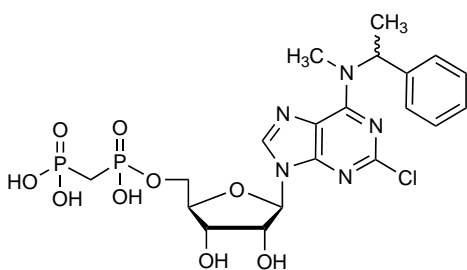
A solution of methylenebis(phosphonic dichloride) (5.0 eq) in trimethyl phosphate (5 ml), cooled to 0°C was added to a suspension of adenosine derivative (0.1 g, 1.0 eq) in trimethyl phosphate (3 ml) at 0°C. The reaction mixture was stirred at 0°C and samples were withdrawn at 15 min interval for TLC to check the disappearance of nucleosides. After 40 min, on disappearance of nucleoside, 10 ml of cold 0.5 M aqueous TEAC solution (pH 7.4-7.6) was added. It was stirred at 0°C for 15 min followed by stirring at room temperature for 1 h. Trimethyl phosphate was extracted using (2x 100 ml) of *tert.*-butylmethylether and the aqueous layer was lyophilized. The crude product was then purified by preparative RP-HPLC (0-50% MeCN/50 mM NH₄HCO₃ buffer in 20 min, 20 ml/min) to get final product.

6.3.38.1 *N*⁶-Benzyl-2-chloro-*N*⁶-propyladenosine-5'-*O*-[(phosphonomethyl)phosphonic acid] (139)



White powder (0.12 g, 91%). ¹H-NMR (600 MHz, D₂O) δ 8.37 (s, 1H, N=CHN) 7.30–7.23 (m, 5H, aryl) 6.01 (d, 1H, *J* = 5.3 Hz, CHN) 5.27 (br s, 2H, NCH₂) 4.69 (t, 1H, *J* = 5.0 Hz, CHOH) 4.52 (m, 1H, CHOH) 4.35 (br s, 1H, CHCH₂) 4.16 (br s, 2H, CHCH₂) 3.93 (br s, 2H, NCH₂) 2.16 (t, 2H, *J* = 19.0 Hz, PCH₂P) 1.61 (br s, 2H, CH₂CH₂CH₃) 0.84 (t, 3H, *J* = 7.1 Hz, CH₂CH₃). ¹³C-NMR (151 MHz, D₂O) δ 157.65, 156.45, 153.99, 140.97, 140.02, 131.50, 130.26, 130.12, 120.78, 89.71, 86.64, 77.09, 72.97, 66.36, 55.64, 55.60, 30.37, 27.95, 13.10. ³¹P-NMR (243 MHz, D₂O) δ 19.15 (s, 1P, Pβ) 14.63 (s, 1P, Pα). LC/ESI-MS (*m/z*): positive mode 592.1115 [M+H]⁺ and negative mode 590.0978 [M-H]⁻ (calc. 591.88). Purity determined by HPLC-UV (254 nm)-ESI-MS: 97.6%. mp: 220°C.

6.3.38.2 2-Chloro-*N*⁶-(α-methyl)benzyl-*N*⁶-methyladenosine-5'-*O*-[(phosphonomethyl)phosphonic acid] (140)

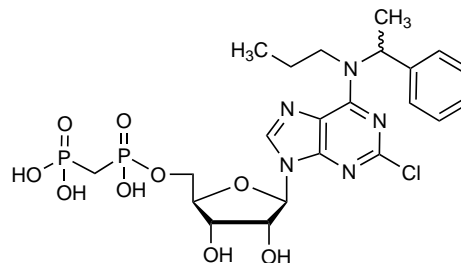


White powder (0.07 g, 51%). ¹H-NMR (600 MHz, D₂O) δ 8.43 (s, 1H, N=CHN) 7.39–7.31 (m, 5H, aryl) 6.06 (d, 1H, *J* = 5.5 Hz, CHN) 4.75 (t, 1H, *J* = 5.3 Hz, CHOH) 4.54 (t, 1H, *J* = 4.5 Hz, CHOH) 4.38 (m, 1H, CHCH₂) 4.18 (br s, 2H, CHCH₂) 3.19 (q, 1H, *J* = 7.3 Hz, NCH) 3.02 (br s, 3H, NCH₃) 2.21 (m, 2H, PCH₂P) 1.67 (br s, 3H, CHCH₃). ¹³C-NMR (151 MHz, D₂O) δ 157.83, 156.55, 153.94, 142.90, 140.87, 131.48, 130.44, 129.91, 121.08, 89.67, 86.80, 77.05, 73.06, 66.39, 57.83, 30.19, 18.70, 11.07. ³¹P-NMR (243 MHz, D₂O) δ 17.14 (d, 1P, *J* = 8.0 Hz, Pβ) 14.07 (d, 1P, *J* = 8.4 Hz, Pα). LC/ESI-MS (*m/z*): positive mode 578.0940 [M+H]⁺ and negative mode 576.0858 [M-H]⁻ (calc. 577.85). Purity determined by HPLC-UV (254 nm)-ESI-MS: 95.4%. mp: 202°C.

6.3.38.3 2-Chloro-*N*⁶-(α -methylbenzyl)-*N*⁶-propyladenosine-5'-*O*-[(phosphonomethyl)phosphonic acid] (141)

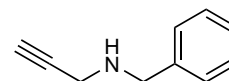
White powder (0.03 g, 20%). ¹H-NMR (600 MHz, D₂O) δ 8.36 (s, 1H, N=CHN) 7.21 (m, 5H, aryl) 6.01 (s, 1H, CHN) 4.66 (m, 1H, CHOH) 4.49 (br s, 1H, CHOH) 4.33 (br s, 1H, CHCH₂) 4.15 (br s, 2H, CHCH₂) 3.81-3.02 (br s, 1H, N(CH)CH₂) 2.26 (t, 2H, *J* = 9.7 Hz, PCH₂P) 1.57 (br s, 3H, CHCH₃)

1.28 (br s, 2H, CH₂CH₂CH₃) 0.63 (br s, 3H, CH₂CH₃). ¹³C-NMR (151 MHz, D₂O) δ 157.27, 156.41, 154.04, 143.17, 140.75, 131.25, 130.35, 130.18, 120.95, 89.77, 86.47, 77.13, 73.00, 66.57, 49.10, 29.85, 22.16, 19.13, 13.34, 11.04. ³¹P-NMR (243 MHz, D₂O) δ 17.92 (s, 1P, P β) 16.84 (s, 1P, P α). LC/ESI-MS (*m/z*): positive mode 606.1279 [M+H]⁺ and negative mode 604.1183 [M-H]⁻ (calc. 605.91). Purity determined by HPLC-UV (254 nm)-ESI-MS: 96%. mp: 149°C.



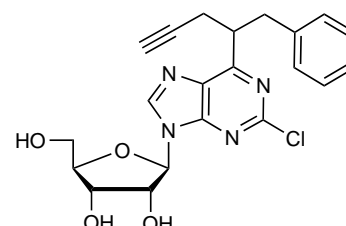
6.3.38.4 *N*-Benzylprop-2-yn-1-amine (144), CAS 1197-51-9

Propargylic bromide (80% in toluene, 3 ml, 0.035 mmol, 1.0 eq) was added to benzylamine (21 ml, 0.21 mmol, 6.0 eq) and the reaction was stirred at rt *o/n* followed by evaporation. Purification by column chromatography (petroleum ether/ethyl acetate 1:9 \rightarrow 1:3) yielded the desired product as colorless oil (4.2 g, 85%). ¹H-NMR (500 MHz, DMSO-*d*₆) δ 7.32-7.19 (m, 5H, aryl) 3.73 (s, 2H, NHCH₂) 3.26 (d, 2H, *J* = 2.4 Hz, NHCH₂) 2.40 (s, 1H, CCH). ¹³C-NMR (125 MHz, DMSO-*d*₆) δ 140.19, 128.19, 128.11, 126.71, 82.91, 73.73, 51.38, 36.74, 24.20. LC/ESI-MS (*m/z*): positive mode 146.0 [M+H]⁺. Purity determined by HPLC-UV (254 nm)-ESI-MS: 95.7%.



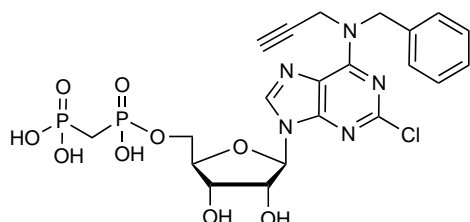
6.3.38.5 *N*⁶-Benzyl-2-chloro-*N*⁶-propargyladenosine (145)

Compound **127** (1.0 g, 2.2 mmol, 1.0 eq) was suspended in absolute ethanol. To the suspension, Et₃N (0.6 ml, 4.4 mmol, 2.0 eq) and **144** (0.65 g, 4.4 mmol, 2.0 eq) were added and the reaction mixture was refluxed overnight. The crude product was purified by silica gel column chro-



matography (CH₃OH/DCM 1:19) yielding the protected intermediate (1.2 g). To the intermediate product in methanol (5 ml), 0.5% NaOMe in methanol (2 ml) were added. After 18 h at room temperature, the solution was evaporated and the crude product was extracted with diethyl ether yielded the desired product as yellow waxy substance (0.9 g, 97%). ¹H-NMR (600 MHz, DMSO-d₆) δ 8.50 (s, 1H, N=CHN) 7.3 (m, 5H, aryl) 5.88 (d, 1H, *J* = 5.7 Hz, CHN) 5.6 (br s, 1H, 1x N(CH₂)₂) 5.49 (d, 1H, *J* = 6.0 Hz, CHOH) 5.19 (d, 1H, *J* = 5.1 Hz, CHOH) 5.02 (t, 1H, *J* = 5.5 Hz, CH₂OH) 4.51 (q, 1H, *J* = 5.6 Hz, CHOH) 4.39 (br s, 1H, 1x N(CH₂)₂), 4.13 (q, 1H, *J* = 4.8 Hz, CHOH) 3.95 (q, 1H, *J* = 3.8 Hz, CHCH₂), 3.72 (s, 1H, C≡CH) 3.67-3.52 (d m, 2H, CHCH₂) 3.26 (d, 1H, *J* = 2.3 Hz, 1x N(CH₂)₂) 3.22 (br s, 1H, 1x N(CH₂)₂). ¹³C-NMR (151 MHz, DMSO-d₆) δ 153.94, 152.62, 151.96, 140.23, 139.88, 128.72, 128.25, 128.16, 127.60, 126.77, 118.65, 87.53, 85.84, 82.96, 73.89, 73.85, 70.40, 61.36, 51.41, 40.79, 36.77. LC/ESI-MS (*m/z*): positive mode 430.0 [M+H]⁺. Purity determined by HPLC-UV (254 nm)-ESI-MS: 95.3%.

6.3.38.6 *N*⁶-Benzyl-2-chloro-*N*⁶-propargyladenosine-5'-*O*-[(phosphonomethyl)phosphonic acid (146)]

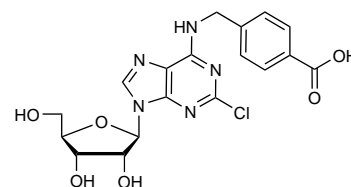


A solution of methylenebis(phosphonic dichloride) (5.0 eq) in trimethyl phosphate (5 ml), cooled to 0°C was added to a suspension of **145** (0.1 g, 0.22 mmol, 1.0 eq) in trimethyl phosphate (3 ml) at 0°C. The reaction mixture was stirred at 0°C and samples were withdrawn at 15 min interval for TLC to check the disappearance of nucleosides. After 40 min, on disappearance of nucleoside, 10 ml of cold 0.5 M aqueous TEAC solution (pH 7.4-7.6) was added. It was stirred at 0°C for 15 min followed by stirring at room temperature for 1 h. Trimethyl phosphate was extracted using (2x 100 ml) of *tert.*-butylmethylether and the aqueous layer was lyophilized. The crude product was then purified by preparative RP-HPLC using a gradient of 50 mM ammoniumbicarbonate/acetonitrile from 100:0 to 50:50 in 20 min (20 ml/min) followed by lyophilization to get final product a white powder (0.05 g, 37%). ¹H-NMR (600 MHz, D₂O) δ 8.46 (s, 1H, N=CHN) 7.36 (m, 5H, aryl) 6.08 (d, 1H, *J* = 5.5 Hz, CHN) 5.30 (br s, 2H, NCH₂) 4.75 (t, 1H, *J* = 5.3 Hz, CHOH) 4.65 (br s, 2H, NCH₂) 4.54 (m, 1H, CHOH) 4.38 (m, 1H, CHCH₂) 4.17 (m, 2H, CHCH₂) 2.64 (s, 1H, C≡CH) 2.19 (t, 2H, *J* = 19.7 Hz, PCH₂P). ¹³C-NMR (151 MHz, D₂O) δ 157.42, 156.44, 154.50, 141.88,

139.25, 131.66, 130.68, 130.57, 121.88, 89.81, 86.88, 86.84, 82.06, 77.13, 76.18, 73.09, 66.41, 54.39, 49.54, 30.32, 11.11. ^{31}P -NMR (243 MHz, D_2O) δ 18.7 (d, 1P, $J = 9.9$ Hz, $\text{P}\beta$) 15.02 (d, 1P, $J = 9.9$ Hz, $\text{P}\alpha$). LC/ESI-MS (m/z): positive mode 588.0787 $[\text{M}+\text{H}]^+$ and negative mode 586.0669 $[\text{M}-\text{H}]^-$ (calc. 587.07). Purity determined by HPLC-UV (254 nm)-ESI-MS: 97.7%. mp: degradation $>260^\circ\text{C}$.

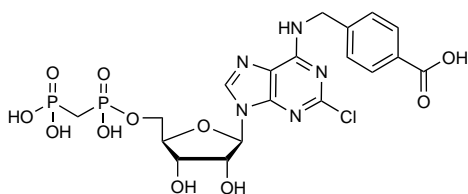
6.3.39 4-(((2-Chloro-9- β -D-ribofuranosyl-9H-purin-6-yl)amino)-methyl)benzoic acid (147), CAS 722508-74-9

Compound **127** (1.0 g, 2.2 mmol, 1.0 eq) was suspended in absolute ethanol. To the suspension, triethylamine (0.6 ml, 4.4 mmol, 2.0 eq) and 4-(aminobenzyl)benzoic acid (0.7 g, 4.5 mmol, 2.0 eq) were added and the reaction



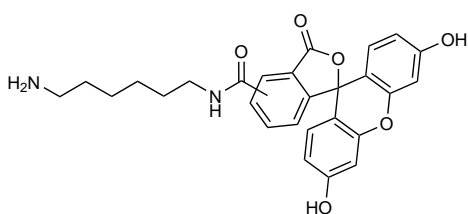
mixture was refluxed overnight. The solvent was evaporated followed by purification by silica gel column chromatography ($\text{CH}_3\text{OH}/\text{DCM}$ 1:4) yielding the protected intermediate. To the intermediate product in methanol (5 ml), NaOMe (0.05 g) was added. After 18 h at room temperature, the solution was evaporated and the crude product was purified by silica gel column chromatography ($\text{CH}_3\text{OH}/\text{DCM}$ 1:3 plus some acetic acid) (0.9 g, 100%). ^1H -NMR (600 MHz, $\text{DMSO}-d_6$) δ 8.86 (br s, 1H, NHCH_2) 8.40 (s, 1H, $\text{N}=\text{CHN}$) 7.79 (d, 2H, $J = 7.7$ Hz, aryl) 7.23 (d, 2H, $J = 7.7$ Hz, aryl) 5.81 (d, 1H, $J = 5.7$ Hz, CHN) 4.64 (br s, 1H, NCH_2) 4.48 (br s, 1H, CHOH) 4.13 (br s, 1H, CHOH) 3.93 (br s, 1H, CHCH_2) 3.64 (m overlapping with H_2O , 2H, CHCH_2). ^{13}C -NMR (151 MHz, $\text{DMSO}-d_6$) δ 169.58, 155.15, 153.34, 149.85, 140.23, 140.16, 138.25, 129.26, 126.32, 118.76, 87.77, 85.91, 74.00, 70.49, 61.53, 43.24. LC-MS (m/z): positive mode 430.0 $[\text{M}+\text{H}]^+$. Purity determined by HPLC-UV (254 nm)-ESI-MS: 95.3%. mp: 219°C .

6.3.40 4-(((2-Chloro-9-((2*R*,3*R*,4*S*,5*R*)-3,4-dihydroxy-5-(((hydroxy-(phosphonomethyl)phosphoryl)oxy)methyl)tetrahydrofuran-2-yl)-9*H*-purin-6-yl)amino)methyl)benzoic acid (**148**)



A solution of methylenebis(phosphonic dichloride) (0.6 g, 2.3 mmol, 5.0 eq) in trimethyl phosphate (7 ml), cooled to 0–4°C was added to a suspension of **147** (0.2 g, 0.46 mmol, 1.0 eq) in trimethyl phosphate (3 ml) at 0–4°C. The reaction mixture was stirred at 0–4°C and samples were withdrawn at 15 min interval for TLC to check the disappearance of nucleosides. After 40 min, on disappearance of nucleoside, cold 0.5 M aqueous TEAC solution (pH 7.4–7.6, 20 ml) was added. It was stirred at 0°C for 15 min followed by stirring at room temperature for 1 h. Trimethyl phosphate was extracted using (2 × 100 ml) of *tert.*-butylmethylether and the aqueous layer was lyophilized. The crude product was then purified by RP-HPLC (0 → 30% MeCN/50 mM NH₄HCO₃ buffer in 15 min, 20 ml/min) followed by lyophilization to get final product (0.08 g, 29%). ¹H-NMR (600 MHz, D₂O) δ 8.45 (s, 1H, N=CHN) 7.81 (d, 2H, *J* = 8.1 Hz, aryl) 7.43 (d, 2H, *J* = 8.1 Hz, aryl) 6.03 (d, 1H, *J* = 5.3 Hz, CHN) 4.73 (t, 1H, *J* = 5.2 Hz, CHOH) 4.53 (t, 1H, *J* = 4.6 Hz, CHOH) 4.36 (d, 1H, *J* = 3.4 Hz, CHCH₂) 4.16 (m, 2H, CHCH₂) 2.13 (t, 2H, *J* = 19.7 Hz, PCH₂P). ¹³C-NMR (126 MHz, D₂O) δ 178.24, 163.14, 158.04, 157.08, 152.12, 143.98, 142.45, 138.13, 132.03, 129.80, 89.89, 86.71, 77.14, 72.98, 66.25, 46.57, 30.77. ³¹P-NMR (202 MHz, D₂O) δ 20.28 (s, 1P, Pβ) 13.65 (s, 1P, Pα). LC-MS (m/z): positive mode 594.0 [M+H]⁺. Purity determined by HPLC-UV (254 nm)-ESI-MS: 100%. mp: 205°C.

6.3.41 *N*-(6-Aminohexyl)-3',6'-dihydroxy-3-oxo-3*H*-spiro-[isobenzofuran-1,9'-xanthene]-5(6)-carboxamide (**151a**)

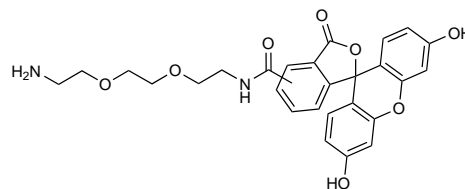


To 5(6)-carboxyfluorescein (**150**, 0.5 g, 1.0 mmol, 1.0 eq) in anhydrous THF (10 ml), HOBt (0.18 g, 1.3 mmol, 1.0 eq) and DCC (0.27 g, 1.3 mmol, 1.0 eq) were added. After 20 min of activation, *N,N*-*boc*-hexanediamine (**149a**, 0.33 g, 1.3 mmol, 1.0 eq) was added and the reaction was stirred overnight at rt. DCU was filtered off

and the filtrate was evaporated. The crude product was purified by column chromatography (CH₃OH/DCM 1:9). LC-MS (m/z): positive mode 575.5 [M+H]⁺. Purity determined by HPLC-UV (254 nm)-ESI-MS: 93.9%. The intermediate was taken up in DCM (10 ml) and TFA (0.3 ml) and a drop of water were added. The reaction mixture was stirred at rt for 2 h followed by evaporation. ¹H-NMR (600 MHz, DMSO-d₆) δ 8.80 + 8.65 (2x t, 1H, *J* = 5.5 Hz, C=CH) 8.44 + 7.65 (2x s, 1H, CH=CCO or CH=CH) 8.22 + 8.15 (2x d, 1H, *J* = 8.1 Hz, CH=CCO) 7.68 (br s, 2H, NH₂) 6.69 (dd, 2H, *J* = 2.2, 4.7 Hz, 2x C=CH) 6.56 (m, 4H, 4x CHCOH) 3.31 + 3.19 (2x q, 2H, *J* = 6.7 Hz, NHCH₂) 2.76 (m, 2H, NH₂CH₂) 1.55 (q, 2H, *J* = 7.0 Hz, CH₂) 1.46 (m, 2H, CH₂) 1.35 (m, 2H, CH₂) 1.26 (m, 2H, CH₂). ¹³C-NMR (151 MHz, DMSO-d₆) δ 168.39, 164.73, 159.83, 158.56, 158.22, 152.01, 154.78, 152.90, 140.98, 136.59, 134.81, 129.40, 126.63, 124.40, 123.38, 118.92, 116.98, 115.04, 112.94, 109.34, 102.48, 83.56, 55.22, 48.76, 39.46, 38.99, 28.99, 27.16, 26.15, 25.70. LC-MS (m/z): positive mode 475.5 [M+H]⁺. Purity determined by HPLC-UV (254 nm)-ESI-MS: 95.3%. mp: 114°C.

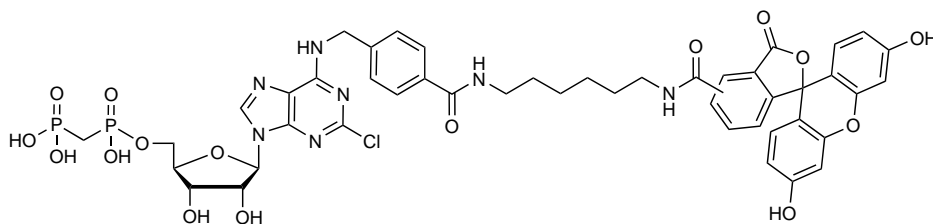
6.3.42 *N*-(2-(2-(2-Aminoethoxy)ethoxy)ethyl)-3',6'-dihydroxy-3-oxo-3H-spiro[isobenzofuran-1,9'-xanthene]-5(6)-carboxamide (151b)

To 5(6)-carboxyfluorescein (**150**, 0.5 g, 1.3 mmol, 1.0 eq) in anhydrous THF (10 ml), HOBt (0.18 g, 1.3 mmol, 1.0 eq) and DCC (0.27 g, 1.3 mmol, 1.0 eq) were added. After 20 min of activation, *N*-Boc-2,2'-(ethylenedioxy)-diethylamine (**149b**, 0.3 ml, 1.3 mmol, 1.0 eq) was added and the reaction was stirred overnight at rt. DCU was filtered off and the filtrate was evaporated. The crude product was purified by column chromatography (CH₃OH/DCM 1:9). LC-MS (m/z): positive mode 607.1 [M+H]⁺. Purity determined by HPLC-UV (254 nm)-ESI-MS: 92%. The intermediate was taken up in DCM (10 ml) and TFA (0.8 ml) and a drop of water were added. The reaction mixture was stirred at rt overnight followed by evaporation. ¹H-NMR (600 MHz, DMSO-d₆) δ 10.20 (s, 2H, 2x OH) 8.87 + 8.73 (t, 1H, *J* = 5.6 Hz, C=CH) 8.43 + 7.66 (s, 1H, NHCH₂) 8.22 + 8.15 (dd, 1H, *J* = 1.4, 8.0 Hz, CH=CO) 8.07 + 7.36 (d, 1H, *J* = 8.0 Hz, CH=CCO or CH=CH) 7.76 (br s, 2H, NH₂) 6.69 (dd, 2H, *J* = 2.3, 4.5 Hz, 2x C=CH) 6.56 (m, 4H, 4x CH=COH) 3.58 (m, 4H, 2x CH₂O) 3.50 (m, 6H, 2x CH₂O + NH₂CH₂) 2.97 + 2.91 (m, 2H, NHCH₂).



^{13}C -NMR (151 MHz, DMSO-d_6) δ 168.39, 165.06, 159.83, 158.24, 154.93, 152.98, 152.02, 140.71, 136.37, 134.85, 129.57, 129.42, 126.67, 125.12, 124.47, 123.49, 122.43, 112.96, 109.32, 102.51, 83.51, 69.90, 69.63, 68.95, 66.88, 39.42, 38.85. LC-MS (m/z): positive mode 507.3 $[\text{M}+\text{H}]^+$. Purity determined by HPLC-UV (254 nm)-ESI-MS: 98.9%. mp: 143°C.

6.3.43 (((((2*R*,3*S*,4*R*,5*R*)-5-(2-Chloro-6-((4-((6-(3',6'-dihydroxy-3-oxo-3*H*-spiro[isobenzofuran-1,9'-xanthene]-5(6)-carboxamido)hexyl)carbamoyl)benzyl)amino)-9*H*-purin-9-yl)-3,4-dihydroxytetrahydrofuran-2-yl)methoxy)(hydroxy)-phosphoryl)methyl)phosphonic acid (152a)



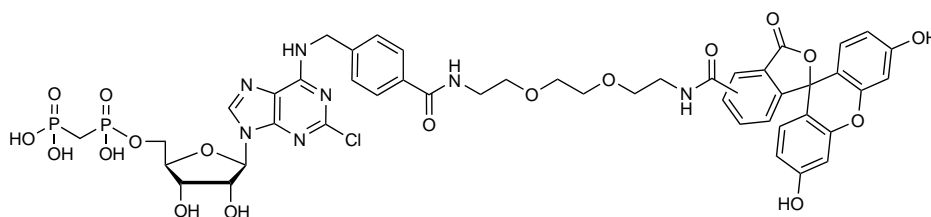
Method A: To **148** (0.04 g, 0.07 mmol, 1.0 eq) in THF (1 ml), HOBt (9 mg, 0.07 mmol, 1.0 eq) and DCC (14 mg, 0.07 mmol, 1.0 eq) were added. After 20 min of activation, **151a** (0.03 g, 0.7 mmol, 1.0 eq) was added and the reaction was stirred overnight at rt. DCU was filtered off and the filtrate was evaporated. LC-MS analysis, however, showed that the desired reaction did not occur.

Method B: A solution of methylenebis(phosphonic dichloride) (0.14 g, 0.6 mmol, 5.0 eq) in trimethyl phosphate (5 ml), cooled to 0–4°C was added to a suspension **153a** (0.1 g, 0.1 mmol, 1.0 eq) in trimethyl phosphate (3 ml) at 0–4°C. The reaction mixture was stirred at 0–4°C and samples were withdrawn at 15 min interval for TLC to check the disappearance of nucleosides. After 30 min, on disappearance of nucleoside, 10 ml of cold 0.5 M aqueous TEAC solution (pH 7.4–7.6) was added. It was stirred at 0–4°C for 15 min followed by stirring at room temperature for 1 h. Trimethyl phosphate was extracted using (2 x 250 ml) of *tert*-butylmethylether and the aqueous layer was lyophilized. The crude product was then purified by RP-HPLC (0→50% MeCN/50 mM NH_4HCO_3 buffer in 15 min, 20 ml/min) followed by lyophilization. Unfortunately, only starting material was isolated as indicated by LC-MS analysis.

Method C: To **150** (0.013 g, 0.03 mmol, 1.0 eq) in THF (2 ml), HOBt (0.004 g, 0.03 mmol,

1.0 eq) and DCC (0.007 g, 0.03 mmol, 1.0 eq) were added. After 10 min of pre-activation (solution became clear), **155a** (0.02 g, 0.03 mmol, 1.0 eq) in water (2 ml) was added. The reaction was stirred at rt overnight followed by evaporation and lyophilisation. The crude product was purified by preparative RP-HPLC (0%→50% MeCN/50 mM NH₄HCO₃ buffer in 15 min, 20 ml/min). Fractions were collected and appropriate fractions pooled and lyophilized. LC/ESI-MS analysis, however, revealed, that the desired product was not formed.

6.3.44 (((((2*R*,3*S*,4*R*,5*R*)-5-(2-Chloro-6-((4-((2-(2-(2-(2-(3',6'-dihydroxy-3-oxo-3*H*-spiro[isobenzofuran-1,9'-xanthene]-5(6)-carboxamido)ethoxy)ethoxy)ethyl)carbonyl)benzyl)-amino)-9*H*-purin-9-yl)-3,4-dihydroxytetrahydrofuran-2-yl)methoxy)(hydroxy)phosphoryl)methyl)phosphonic acid (152b**))**

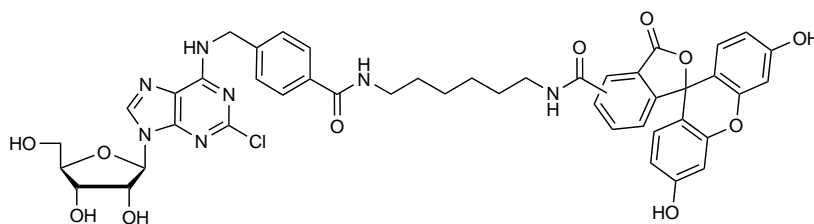


Method A: To **148** (0.04 g, 0.07 mmol, 1.0 eq) in THF (1 ml), HOBT (9 mg, 0.07 mmol, 1.0 eq) and DCC (14 mg, 0.07 mmol, 1.0 eq) were added. After 20 min of activation, **151b** (0.03 g, 0.7 mmol, 1.0 eq) was added and the reaction was stirred overnight at rt. DCU was filtered off and the filtrate was evaporated. LC/ESI-MS analysis, however, showed that the desired reaction did not occur.

Method B: A solution of methylenebis(phosphonic dichloride) (0.18 g, 0.7 mmol, 5.0 eq) in trimethyl phosphate (5 ml), cooled to 0–4°C was added to a suspension **153b** (0.14 g, 0.15 mmol, 1.0 eq) in trimethyl phosphate (3 ml) at 0–4°C. The reaction mixture was stirred at 0–4°C and samples were withdrawn at 15 min interval for TLC to check the disappearance of nucleosides. After 30 min, on disappearance of nucleoside, 10 ml of cold 0.5 M aqueous TEAC solution (pH 7.4–7.6) was added. It was stirred at 0–4°C for 15 min followed by stirring at room temperature for 1 h. Trimethyl phosphate was extracted using (2 x 250 ml) of *tert*-butylmethylether and the aqueous layer was lyophilized. The crude product was then purified by RP-HPLC (0→50%

MeCN/50 mM NH₄HCO₃ buffer in 15 min, 20 ml/min) followed by lyophilization. Unfortunately, only starting material was isolated as indicated by LC/ESI-MS analysis. **Method C:** To **150** (0.03 g, 0.08 mmol, 1.0 eq) in THF (2 ml), HOBt (0.011 g, 0.08 mmol, 1.0 eq) and DCC (0.016 g, 0.08 mmol, 1.0 eq) were added. After 10 min of pre-activation (solution became clear), **155b** (0.06 g, 0.08 mmol, 1.0 eq) in water (2 ml) was added. The reaction was stirred at rt overnight followed by evaporation and lyophilisation. The crude product was purified by preparative RP-HPLC (0%→50% MeCN/50 mM NH₄HCO₃ buffer in 15 min, 20 ml/min). Fractions were collected and appropriate fractions pooled and lyophilized. LC/ESI-MS analysis, however, revealed, that the desired product was not formed.

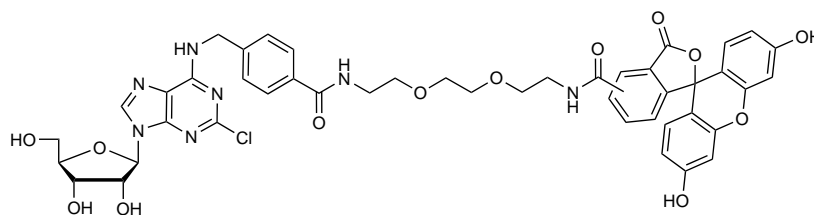
6.3.45 N-(6-(4-(((2-Chloro-9-((2R,3R,4S,5R)-3,4-dihydroxy-5-(hydroxymethyl)tetrahydrofuran-2-yl)-9H-purin-6-yl)-amino)methyl)benzamido)hexyl)-3',6'-dihydroxy-3-oxo-3H-spiro[isobenzofuran-1,9'-xanthene]-5(6)-carboxamide (153a)



To **147** (0.16 g, 0.36 mmol, 1.0 eq) in THF (2 ml), HOBt (0.05 g, 0.36 mmol, 1.0 eq) and DCC (0.07 g, 0.36 mmol, 1.0 eq) were added. After 20 min of activation, **151a** (0.17 g, 0.36 mmol, 1.0 eq) was added and the reaction was stirred overnight at rt. DCU was filtered off and the filtrate was evaporated. The crude product was purified twice by preparative RP-HPLC (20 → 100% MeOH in H₂O in 30 min, 20 ml/min) followed by lyophilisation, yielding the desired product as yellow solid (0.1 g, 30%). ¹H-NMR (600 MHz, DMSO-d₆) δ 8.99 + 6.62 (m, 1H, CH=CCO) 8.94 + 8.76 (d, 1H, J = 5.6 Hz, C=CH) 8.43 8.41 (s, 1H, NHCH₂) 8.20 + 7.76 (d, 1H, J = 8.1 Hz, CH=CO or CH=CCO) 7.65 (s, 1H, NHCH₂) 7.36 (m, 4H, 4x CHCOH) 6.66 (br s, 2H, 2x C=CH) 6.55 (m, 4H, aryl) 5.82 (d, 1H, J = 5.8 Hz, CHN) 5.56 (d, 2H, J = 7.9 Hz, NHCH₂-aryl) 5.45 (d, 1H, J = 6.9 Hz, OH) 5.18 (d, 1H, J = 3.7 Hz, OH) 5.03 (br s, 1H, OH) 4.68 (br s, 1H, OH) 4.51 (br s, 1H, OH) 4.43 (d, 1H, J = 5.9 Hz, CHCH₂) 4.12 (br s, 1H, CHOH), 3.93 (br s, 1H, CHOH) 3.65–3.54 (d m, 2H, CHCH₂OH) 3.21 (m, 2H, NHCH₂) 1.49 (m, 4H, (CH₂)₂)

1.35 (m, 2H, CH_2) 1.13 (m, 2H, CH_2). ^{13}C -NMR (151 MHz, DMSO-d_6) δ 168.42, 168.27, 166.19, 166.16, 164.78, 164.59, 160.08, 155.15, 154.42, 153.32, 152.14, 149.91, 142.38, 140.90, 140.36, 136.61, 134.73, 133.59, 129.52, 129.45, 129.37, 127.40, 127.17, 126.92, 125.16, 124.48, 123.52, 122.51, 118.82, 113.14, 113.05, 109.48, 109.40, 102.49, 87.67, 85.93, 73.91, 70.56, 69.98, 61.54, 54.29, 54.25, 45.88, 43.18, 29.32, 29.22, 29.14, 29.05, 26.42, 26.34, 11.31. LC/ESI-MS (m/z): positive mode 892.6 $[\text{M}+\text{H}]^+$. Purity determined by HPLC-UV (254 nm)-ESI-MS: 83%. mp: 201°C.

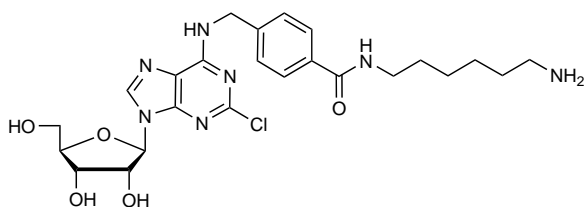
6.3.46 *N*-(2-(2-(2-(4-(((2-Chloro-9-((2*R*,3*R*,4*S*,5*R*)-3,4-dihydroxy-5-(hydroxymethyl)tetrahydrofuran-2-yl)-9*H*-purin-6-yl)amino)methyl)benzamido)ethoxy)ethoxy)ethyl)-3',6'-dihydroxy-3-oxo-3*H*-spiro[isobenzofuran-1,9'-xanthene]-5(6)-carboxamide (153b)



To **147** (0.15 g, 0.35 mmol, 1.0 eq) in THF (2 ml), HOBt (0.05 g, 0.35 mmol, 1.0 eq) and DCC (0.07 g, 0.35 mmol, 1.0 eq) were added. After 20 min of activation, **151b** (0.18 g, 0.35 mmol, 1.0 eq) was added and the reaction was stirred overnight at rt. DCU was filtered off and the filtrate was evaporated. The crude product was purified twice by preparative HPLC (20 → 100% MeOH in H_2O in 30 min, 20 ml/min) followed by lyophilisation, yielding the desired product as yellow solid (0.14 g, 42%). ^1H -NMR (600 MHz, DMSO-d_6) δ 8.92 (t, 1H, $J = 6.2$ Hz, NHCH_2) 8.85 (t, 1H, $J = 5.5$ Hz, NHCH_2) 8.72 (t, 1H, $J = 5.6$ Hz, NHCH_2) 8.44 + 7.67 (s, 1H, $\text{CH}=\text{CCO}$ or $\text{CH}=\text{CH}$) 8.41 (s, 1H, $\text{N}=\text{CHN}$) 8.22 + 8.14 (d, 1H, $J = 9.2$ Hz, $\text{C}=\text{CH}$) 8.05 + 7.35 (d, 1H, $J = 8.0$ Hz, $\text{CH}=\text{CO}$) 7.76 (t, 2H, $J = 8.6$ Hz, aryl) 7.38 (d, 2H, $J = 6.2$ Hz, aryl) 6.67 (m, 2H, 2x $\text{C}=\text{CH}$) 6.55 (m, 4H, 4x $\text{CH}=\text{COO}$) 5.82 (d, 1H, $J = 5.7$ Hz, CHN) 5.46 (br s, 1H, OH) 5.19 (br s, 1H, OH) 5.04 (br s, 1H, OH) 4.67 (br s, 1H, CHOH) 4.51 (br s, 1H, CHOH) 4.11 (br s, 1H, OH) 3.93 (br s, 1H, OH) 3.64 (d, 1H, $J = 11.5$ Hz, CHCH_2) 3.55–3.45 (m, overlapping with H_2O , 16H, $\text{CHCH}_2 + \text{NHCH}_2 + 6x \text{CH}_2\text{O}$). ^{13}C -NMR (151 MHz, DMSO-d_6) δ 168.37, 168.25, 166.37, 165.00, 164.85, 160.09, 155.15, 153.31, 152.13,

149.91, 142.55, 140.61, 140.36, 136.34, 134.73, 133.26, 129.56, 129.46, 129.38, 127.44, 127.19, 126.97, 125.18, 124.52, 123.62, 122.60, 118.83, 113.12, 113.05, 109.46, 109.39, 102.49, 102.47, 87.67, 85.93, 73.91, 70.56, 69.77, 69.68, 69.12, 69.05, 68.94, 68.82, 61.54, 43.18. LC/ESI-MS (m/z): positive mode 924.8 [M+H]⁺. Purity determined by HPLC-UV (254 nm)-ESI-MS: 90%. mp: 188°C.

6.3.47 *N*-(6-Aminoethyl)-4-(((2-chloro-9-((2*R*,3*R*,4*S*,5*R*)-3,4-dihydroxy-5-(hydroxymethyl)tetrahydrofuran-2-yl)-9H-purin-6-yl)amino)methyl)benzamide (154a)



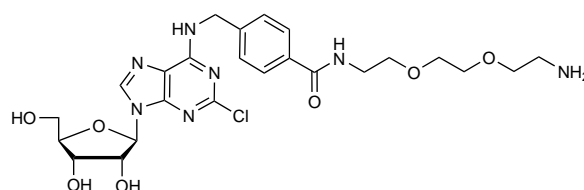
To a solution of 2',3',5'-tri-*O*-acetyl protected **147** (0.6 g, 1.1 mmol, 1.0 eq) in THF (10ml), HOBt (0.15 g, 1.1 mmol, 1.0 eq) and DCC (0.23 g, 1.1 mmol, 1.0 eq) were added. After 20 min of pre-

activation, *N*-Boc-hexanediamine (0.23 g, 1.1 mmol, 1.0 eq) was added and the reaction was stirred overnight at rt. DCU was filtered off followed by evaporation of the filtrate. Next, the crude product was taken up in 0.5% NaOMe in methanol (10 ml) and the reaction was stirred at rt overnight followed by evaporation. The crude product was purified by column chromatography (10% MeOH/DCM) yielding the desired intermediate as yellow oil. LC/ESI-MS (m/z): positive mode 666.7 [M+H]⁺. Purity determined by HPLC-UV (254 nm)-ESI-MS: 92.4%. To remove the Boc group, the intermediate was taken up in 6% TFA in DCM and a catalytical drop of water was added. The reaction was stirred at rt for 24h followed by evaporation. The crude product was purified by RP-HPLC (50→100% MeOH/H₂O in 15 min, 20 ml/min) followed by lyophilisation to get the desired product as white solid (0.5 g, 88%). ¹H-NMR (600 MHz, DMSO-*d*₆) δ 8.41 (s, 1H, N=CHN) 8.36 (s, 2H, NH₂) 8.01 (s, 1H, NHCH₂) 7.90 (s, 1H, NH) 7.75 (t, 2H, *J* = 6.48 Hz, aryl) 7.39 (t, 2H, *J* = 7.84 Hz, aryl) 5.82 (d, 1H, *J* = 5.79 Hz, CHN) 4.68 (br s, 2H, 2x CHOH) 4.51 (s, 1H, CH₂OH) 4.12 (s, 1H, CHOH) 3.93 (s, 1H, CHOH) 3.75 (s, 1H, CHCH₂) 3.54 (overlapping with H₂O peak: CH₂OH) 3.21 (m, 2H, NH₂CH₂) 2.88 (br s, 2H, NHCH₂) 2.58 (br s, 2H, NHCH₂) 1.48 (br s, 2H, CH₂) 1.37 (br s, 2H, CH₂) 1.27 (br s, 4H, (CH₂)₂). ¹³C-NMR (151 MHz, DMSO-*d*₆) δ 166.19, 161.93, 158.17, 155.16, 153.33, 152.14, 149.93, 142.89, 140.38, 133.49, 127.35, 118.84, 87.84, 85.96, 72.94, 70.57, 61.56, 53.39, 61.56, 53.99, 42.20,

30.90, 29.91, 29.27, 26.43, 26.10. LC/ESI-MS (m/z): positive mode 534.4 [M+H]⁺. Purity determined by HPLC-UV (254 nm)-ESI-MS: 98%. mp: 116°C.

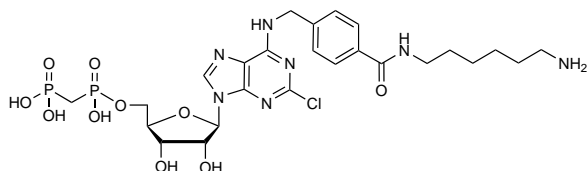
6.3.48 *N*-(2-(2-(2-Aminoethoxy)ethoxy)ethyl)-4-(((2-chloro-9-((2*R*,3*R*,4*S*,5*R*)-3,4-dihydroxy-5-(hydroxymethyl)-tetrahydrofuran-2-yl)-9*H*-purin-6-yl)amino)methyl)-benzamide (154b)

To a solution of 2',3',5'-tri-*O*-acetyl protected **147** (0.6 g, 1.1 mmol, 1.0 eq) in THF (10ml), HOBT (0.15 g, 1.1 mmol, 1.0 eq) and DCC (0.23 g, 1.1 mmol, 1.0 eq)



were added. After 20 min of pre-activation, *N*-Boc-2,2'-(ethylenedioxy)-diethylamine (0.26 ml, 1.1 mmol, 1.0 eq) was added and the reaction was stirred overnight at rt. DCU was filtered off followed by evaporation of the filtrate. Next, the crude product was taken up in 0.5% NaOMe in methanol (10 ml) and the reaction was stirred at rt overnight followed by evaporation. The crude product was purified by column chromatography (10% MeOH/DCM) yielding the desired intermediate as yellow oil. LC/ESI-MS (m/z): positive mode 666.7 [M+H]⁺. Purity determined by HPLC-UV (254 nm)-ESI-MS: 92.4%. To remove the Boc group, the intermediate was taken up in 6% TFA in DCM and a drop of water was added. The reaction was stirred at rt for 24h followed by evaporation. The crude product was purified by RP-HPLC (50→100% MeOH/H₂O in 15 min, 20 ml/min) followed by lyophilisation to get the desired product as white solid (0.27 g, 43%). ¹H-NMR (600 MHz, DMSO-*d*₆) δ 8.92 (t, 1H, *J* = 6.22 Hz, NHCH₂) 8.42 (d, 1H, *J* = 5.82 Hz, NHCH₂) 8.41 (s, 1H, N=CHN) 7.76 (d, 4H, *J* = 8.11 Hz, aryl) 7.39 (d, 2H, *J* = 8.10 Hz, CH₂NH₂) 5.82 (d, 1H, *J* = 5.92 Hz, CHN) 4.68 (d, 2H, *J* = 5.61 Hz, 2x CHOH) 4.51 (t, 1H, *J* = 5.22 Hz, CH₂OH) 4.12 (m, 1H, CHOH) 3.93 (m, 1H, CHOH) 3.65 (m, 1H, CHCH₂) 2.55 (m, 14H, 6x CH₂ and overlapping CH₂OH) 2.93 (p, 2H, *J* = 5.60 Hz, NHCH₂-aryl). ¹³C-NMR (151 MHz, DMSO-*d*₆) δ 166.44, 158.23, 157.98, 155.14, 153.30, 149.91, 142.62, 140.36, 133.22, 127.42, 127.19, 118.82, 94.74, 87.64, 85.96, 73.90, 70.56, 69.89, 69.92, 69.09, 66.83, 61.55, 43.18, 39.21, 38.86. LC/ESI-MS (m/z): positive mode 566.4 [M+H]⁺. Purity determined by HPLC-UV (254 nm)-ESI-MS: 97.8%. mp: 81°C.

6.3.49 (((((2*R*,3*S*,4*R*,5*R*)-5-(6-((4-((6-Aminohexyl)-carbamoyl)-benzyl)amino)-2-chloro-9*H*-purin-9-yl)-3,4-dihydroxy-tetrahydrofuran-2-yl)methoxy)(hydroxy)phosphoryl)-methyl)phosphonic acid (155a)

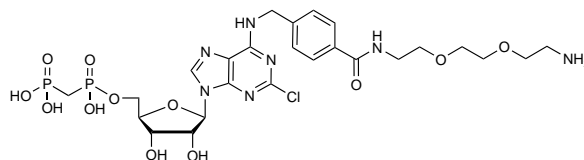


A solution of methylenebis(phosphonic dichloride) (0.22 g, 0.9 mmol, 5.0 eq) in trimethyl phosphate (5 ml), cooled to 0–4°C was added to a suspension of **154a**

(0.1 g, 0.18 mmol, 1.0 eq) in trimethyl phosphate (3 ml) at 0–4°C. The reaction mixture was stirred at 0–4°C and samples were withdrawn at 15 min interval for TLC to check the disappearance of nucleosides. After 30 min, on disappearance of nucleoside, 10 ml of cold 0.5 M aqueous TEAC solution (pH 7.4–7.6) was added. It was stirred at 0°C for 15 min followed by stirring at room temperature for 1 h. Trimethyl phosphate was extracted using (2 x 250 ml) of *tert*-butylmethylether and the aqueous layer was lyophilized. The crude product was then purified by RP-HPLC (0→50% MeCN/50 mM NH₄HCO₃ buffer in 15 min, 20 ml/min) followed by lyophilization yielding a white solid (0.02 g, 16%). ¹H-NMR (600 MHz, D₂O) δ 8.44 (s, 1H, N=CHN) 7.57 (d, 2H, *J* = 7.95 Hz, aryl) 7.34 (d, 2H, *J* = 7.91 Hz, aryl) 5.96 (d, 1H, *J* = 5.37 Hz, CHN) 4.70 (t, 1H, *J* = 5.29 Hz, CHOH) 4.52 (t, 1H, *J* = 4.55 Hz, CHOH) 4.36 (m, 1H, CHCH₂) 4.16 (m, 2H, CHCH₂) 3.83 (d, 2H, *J* = 1.44 Hz, NH₂CH₂) 3.81 (d, 2H, *J* = 1.27 Hz, NHCH₂) 3.27 (t, 2H, *J* = 6.86 Hz, NHCH₂-aryl) 2.91 (m, 2H, CH₂) 2.18 (t, 2H, *J* = 19.18 Hz, PCH₂P) 1.57 (m, 2H, CH₂) 1.49 (m, 2H, CH₂) 1.28 (m, 2H, CH₂). ¹³C-NMR (126 MHz, D₂O) δ 172.71, 164.44, 157.77, 157.02, 152.06, 144.83, 142.48, 135.37, 130.31, 130.01, 120.88, 89.83, 86.79, 77.21, 73.07, 72.45, 66.42, 57.90, 57.53, 55.63, 46.37, 42.55, 42.20, 31.04, 29.63, 29.49, 28.41, 28.12. ³¹P-NMR (202 MHz, D₂O) δ 18.92 (d, 1P, *J* = 8.13 Hz, Pβ) 14.76 (d, 1P, *J* = 9.32 Hz, Pα). LC/ESI-MS (*m/z*): positive mode 692.5 [M+H]⁺. Purity determined by HPLC-UV (254 nm)-ESI-MS: 93%. mp: 202°C.

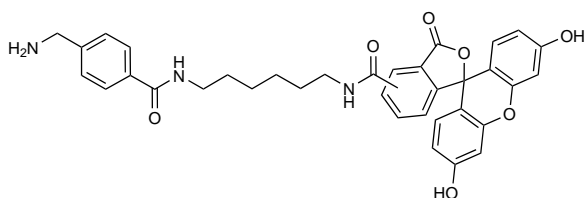
6.3.50 (((((2*R*,3*S*,4*R*,5*R*)-5-(6-((4-((2-(2-(2-Aminoethoxy)ethoxy)-ethyl)carbamoyl)benzyl)amino)-2-chloro-9*H*-purin-9-yl)-3,4-dihydroxytetrahydrofuran-2-yl)methoxy)(hydroxy)-phosphoryl)methyl)phosphonic acid (155b)

A solution of methylenebis(phosphonic dichloride) (0.22 g, 0.9 mmol, 5.0 eq) in trimethyl phosphate (5 ml), cooled to 0–4°C was added to a suspension



(0.1 g, 0.17 mmol, 1.0 eq) in trimethyl phosphate (3 ml) at 0–4°C. The reaction mixture was stirred at 0–4°C and samples were withdrawn at 15 min interval for TLC to check the disappearance of nucleosides. After 30 min, on disappearance of nucleoside, 10 ml of cold 0.5 M aqueous TEAC solution (pH 7.4–7.6) was added. It was stirred at 0°C for 15 min followed by stirring at room temperature for 1 h. Trimethyl phosphate was extracted using (2x 250 ml) of *tert*-butylmethylether and the aqueous layer was lyophilized. The crude product was then purified by RP-HPLC (0→50% MeCN/50 mM NH₄HCO₃ buffer in 15 min, 20 ml/min) followed by lyophilization yielding a white solid (0.06 g, 48%). ¹H-NMR (600 MHz, D₂O) δ 8.45 (s, 1H, N=CHN) 7.64 (d, 2H, *J* = 7.74 Hz, aryl) 7.38 (d, 2H, *J* = 7.88 Hz, aryl) 5.98 (d, 1H, *J* = 5.23 Hz, CHN) 4.72 (br s, 2H, CH₂NH₂) 4.62 (br s, 1H, CHOH) 4.53 (t, 1H, *J* = 4.48 Hz, CHOH) 4.36 (m, 1H, CHCH₂) 4.17 (m, 2H, CHCH₂) 3.70 (m, 4H, 2x CH₂O) 3.66 (q, 4H, *J* = 6.01 Hz, O(CH₂)₂) 3.56 (t, 2H, *J* = 5.19 Hz, NHCH₂-aryl) 3.08 (m, 2H, CH₂) 2.15 (m, 2H, PCH₂P). ¹³C-NMR (126 MHz, D₂O) δ 173.07, 157.79, 156.98, 152.05, 145.06, 142.52, 135.14, 130.31, 130.15, 120.92, 89.90, 86.76, 77.21, 73.01, 72.40, 71.77, 69.32, 66.37, 57.90, 46.34, 42.30, 41.84, 30.63. ³¹P-NMR (202 MHz, D₂O) δ 19.58 (d, 1P, *J* = 8.58 Hz, Pβ) 14.17 (d, 1P, *J* = 8.44 Hz Pα). LC/ESI-MS (*m/z*): positive mode 724.5 [M+H]⁺. Purity determined by HPLC-UV (254 nm)-ESI-MS: 94%. mp: 195°C.

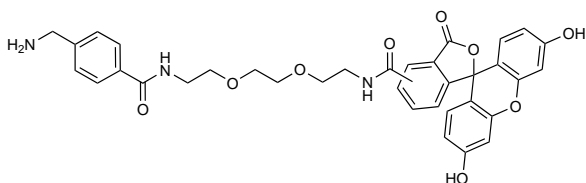
6.3.51 *N*-(6-(4-(Aminomethyl)benzamido)hexyl)-3',6'-dihydroxy-3-oxo-3H-spiro[isobenzofuran-1,9'-xanthene]-5(6)-carboxamide (156a)



To 4-(Boc-aminomethyl)benzoic acid (0.2 g, 0.63 mmol, 1.0 eq) in THF (5 ml), HOBT (0.09 g, 0.63 mmol, 1.0 eq) and DCC (0.13 g, 0.63 mmol, 1.0 eq) were added. After 20 min of pre-activation,

151a (0.3 g, 0.63 mmol, 1.0 eq) was added. The reaction was stirred at rt overnight. DCU was filtered off and the filtrate was evaporated. Deprotection was achieved by treatment 6-8% TFA in DCM and drop of water for 3 h at rt. The mixture was evaporated and purified by RP-HPLC (20%→100% methanol/water in 20 min, 20 ml/min) and lyophilization yielded the desired product (0.04 g, 6%). ¹H-NMR (600 MHz, DMSO-d₆) δ 8.45 + 7.67 (br s, 1H, CH=CCO or CH=CH) 8.19 + 8.14 (dd, 1H, *J* = 1.4, 8.1 Hz, C=CH) 8.10 + 7.34 (d, 1H, *J* = 8.0 Hz, CH=CCO) 7.91 (dd, 2H, *J* = 8.3, 24.9 Hz, aryl) 7.56 (dd, 2H, *J* = 8.3, 13.8 Hz, aryl) 6.73 (m, 4H, 4x CHCOH) 6.60 (m, 2H, 2x C=CH) 4.20 (br s, 2H, NHCH₂-aryl) 3.47 (dt, 2H, *J* = 7.0, 27.5 Hz, NHCH₂) 3.38 (m, 2H, overlapping with H₂O, NH₂CH₂) 1.72 (m, 2H, CH₂) 1.63 (m, 2H, CH₂) 1.53 (m, 2H, CH₂) 1.44 (m, 2H, CH₂). ¹³C-NMR (151 MHz, DMSO-d₆) δ 171.39, 169.65, 169.54, 168.84, 168.58, 138.24, 138.12, 136.85, 136.78, 131.13, 130.96, 130.32, 130.28, 129.36, 129.32, 103.99, 44.19, 41.24, 41.18, 41.10, 30.65, 30.62, 30.42, 29.10, 27.90, 27.83. LC/ESI-MS (*m/z*): positive mode 608.2 [M+H]⁺. Purity determined by HPLC-UV (254 nm)-ESI-MS: 94.5%. mp: 215°C.

6.3.52 *N*-(2-(2-(2-(4-(Aminomethyl)benzamido)ethoxy)ethoxy)ethyl)-3',6'-dihydroxy-3-oxo-3H-spiro[isobenzofuran-1,9'-xanthene]-5(6)-carboxamide (156b)



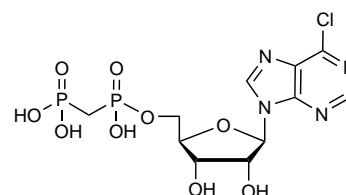
To 4-(Boc-aminomethyl)benzoic acid (0.2 g, 0.63 mmol, 1.0 eq) in THF (5 ml), HOBT (0.09 g, 0.63 mmol, 1.0 eq) and DCC (0.13 g, 0.63 mmol, 1.0 eq) were

added. After 20 min of pre-activation, **151b** (0.3 g, 0.63 mmol, 1.0 eq) was added. The

reaction was stirred at rt overnight. DCU was filtered off and the filtrate was evaporated. The crude product was purified by column chromatography (CH₃OH/DCM 1:9 → 1:4). The desired product was obtained as pure isomer (0.067 g, 14%) and as isomer mixture (0.197 g, 42%). Deprotection was achieved by treatment 6–8% TFA in DCM and drop of water for 3 h at rt. The mixture was evaporated and purified by RP-HPLC (20%→100% methanol/water in 20 min, 20 ml/min). Lyophilization yielded the desired product (pure isomer: 0.033 g, 8%; isomer mix: 0.078 g, 19%) Analysis of the pure isomer: ¹H-NMR (600 MHz, DMSO-d₆) δ 8.72 (t, 1H, *J* = 5.59 Hz, NH) 8.48 (t, 1H, *J* = 5.57 Hz, NH) 8.20 (br s, 2H, NH₂) 8.15 (dd, 1H, *J* = 1.39, 8.05 Hz, C=CH) 8.05 (d, 1H, *J* = 8.58 Hz, CH=CO) 7.86 (d, 2H, *J* = 8.40 Hz, aryl) 7.67 (s, 1H, CH=CO) 7.51 (d, 2H, *J* = 8.40 Hz, aryl) 6.69 (d, 2H, *J* = 2.23 Hz, 2x C=CH) 6.56 (m, 4H, 4x CH=COH) 4.08 (d, 2H, *J* = 5.83 Hz, NHCH₂-aryl) 3.48 (m, 8H, 4x CH₂O) 3.34 (dd, 4H, *J* = 5.89, 11.82 Hz, 2x NHCH₂). ¹³C-NMR (151 MHz, DMSO-d₆) δ 168.17, 165.88, 164.76, 159.77, 158.45, 158.16, 152.82, 151.99, 140.70, 137.03, 134.54, 129.52, 129.34, 128.73, 128.36, 127.56, 125.00, 122.42, 112.90, 109.32, 102.41, 69.64, 68.97, 68.76, 42.09. LC/ESI-MS (*m/z*): positive mode 640.3 [M+H]⁺. Purity determined by HPLC-UV (254 nm)-ESI-MS: 99.5%. mp: 86°C.

6.3.53 (((((2R,3S,4R,5R)-5-(6-chloro-9H-purin-9-yl)-3,4-dihydroxytetrahydrofuran-2-yl)methoxy)(hydroxy)phosphoryl)methyl)phosphonic acid (157), CAS 1889-6

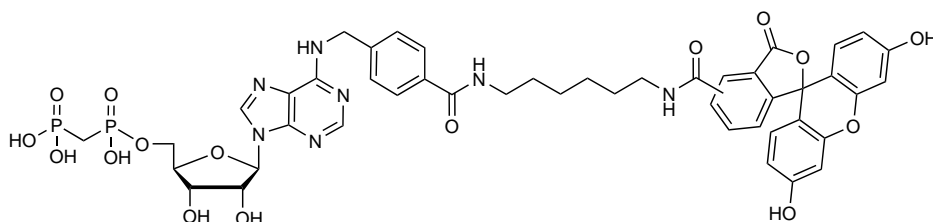
A solution of methylenebis(phosphonic dichloride) (0.87 g, 3.5 mmol, 5.0 eq) in trimethyl phosphate (5 ml), cooled to 0–4°C was added to a suspension 6-chloropurine riboside (0.2 g, 0.7 mmol, 1.0 eq) in trimethyl phosphate (5 ml) at 0–4°C. The reaction mixture was stirred at 0–4°C and



samples were withdrawn at 15 min interval for TLC to check the disappearance of nucleosides. After 30 min, on disappearance of nucleoside, 20 ml of cold 0.5 M aqueous TEAC solution (pH 7.4–7.6) was added. It was stirred at 0°C for 15 min followed by stirring at room temperature for 1 h. Trimethyl phosphate was extracted using (2x 250 ml) of *tert.*-butylmethylether and the *aqueous* layer was lyophilized. The crude product was then purified by RP-HPLC (0→30% MeCN/50 mM NH₄HCO₃ buffer

in 15 min, 20 ml/min) followed by lyophilization to get final product as white solid (0.17 g, 55%). $^1\text{H-NMR}$ (600 MHz, D_2O) δ 8.95 (s, 1H, $\text{N}=\text{CHN}$) 8.78 (s, 1H, $\text{N}=\text{CHN}$) 6.27 (d, 1H, $J = 5.00$ Hz, CHN) 4.84 (t, 1H, $J = 5.13$ Hz, CHOH) 4.59 (t, 1H, $J = 4.72$ Hz, CHOH) 4.41 (d, 1H, $J = 3.65$ Hz, CHCH_2) 4.21 (t, 2H, $J = 3.62$ Hz, CHCH_2O) 2.15 (m, 2H, PCH_2P). $^{13}\text{C-NMR}$ (126 MHz, D_2O) δ 154.79, 154.23, 152.08, 148.38, 134.17, 90.87, 86.94, 77.24, 72.95, 66.17, 30.66. $^{31}\text{P-NMR}$ (202 MHz, D_2O) δ 19.73 (d, 1P, $J = 9.47$ Hz, $\text{P}\beta$) 14.18 (d, 1P, $J = 9.73$ Hz, $\text{P}\alpha$). LC/ESI-MS (m/z): positive mode 444.9 $[\text{M}+\text{H}]^+$. Purity determined by HPLC-UV (254 nm)-ESI-MS: 94.2%. mp: 190°C.

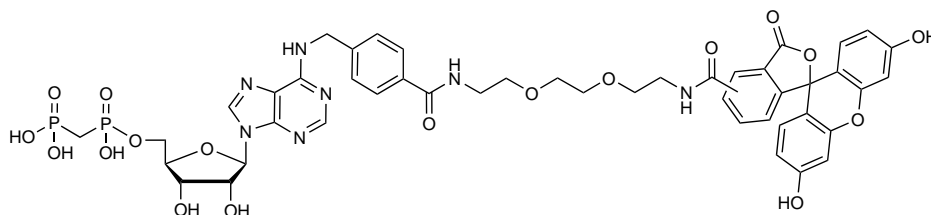
6.3.54 (((((2*R*,3*S*,4*R*,5*R*)-5-(6-((4-((6-(3',6'-Dihydroxy-3-oxo-3H-spiro[isobenzofuran-1,9'-xanthene]-5(6)-carboxamido)-hexyl)carbamoyl)benzyl)amino)-9H-purin-9-yl)-3,4-dihydroxytetrahydrofuran-2-yl)methoxy)(hydroxy)-phosphoryl)methyl)phosphonic acid (158a)



Compounds **157** (0.02 g, 0.04 mmol, 1.0 eq) and **156a** (0.03 g, 0.04 mmol, 1.0 eq) were dissolved in absolute ethanol (5 ml). Et_3N (0.1 ml, 0.65 mmol, 15.0 eq) was added and the mixture was stirred at 60°C. After 18 h the solution was evaporated followed by purification by RP-HPLC (0→50% MeCN/50 mM NH_4HCO_3 buffer in 15 min, 20 ml/min) followed by lyophilization to get final product (0.02 g, 50%). $^1\text{H-NMR}$ (600 MHz, CD_3OD) δ 8.61 (br s, 1H, $\text{N}=\text{CHN}$) 8.33 + 7.64 (s, 1H, $\text{CH}=\text{CCO}$ or $\text{CH}=\text{CH}$) 8.26 + 8.22 (d, 1H, $J = 5.71$ Hz, $\text{C}=\text{CH}$) 8.03 (s, 1H, $\text{N}=\text{CHN}$) 7.98 + 7.35 (d, 1H, $J = 7.91$ Hz, $\text{CH}=\text{CCO}$) 7.75 (dd, 2H, $J = 8.26, 24.93$ Hz, aryl) 7.50 (dd, 2H, $J = 8.31, 13.17$ Hz, aryl) 7.09 (m, 2H, 2x $\text{C}=\text{CH}$) 6.60 (m, 4H, 4x CHCOH) 6.13 (d, 1H, $J = 5.01$ Hz, CHN) 4.72 (t, 1H, $J = 5.08$ Hz, CHOH) 4.58 (t, 1H, $J = 4.63$ Hz, CHOH) 4.34 (m, 1H, CHCH_2) 4.21 (m, 2H, CHCH_2O) 3.45 (m, 2H, NHCH_2 -aryl) 3.05 + 2.87 (m, 4H, 2x NHCH_2) 2.51 (m, 1H, PCH_2P) 1.50 (m, 2H, CH_2) 1.44 (m, 2H, CH_2) 1.36 (m, 2H, CH_2) 0.97 (m, 2H, CH_2). $^{13}\text{C-NMR}$ (126 MHz, CD_3OD) δ 182.43, 174.23, 174.04, 170.89, 170.24, 169.78, 160.17, 159.73, 159.49, 154.09, 144.43, 144.06, 141.96, 141.08,

137.17, 136.48, 135.98, 134.36, 134.10, 132.44, 131.56, 130.59, 129.71, 129.20, 129.03, 128.80, 128.58, 124.44, 113.24, 104.81, 88.76, 85.41, 76.07, 71.67, 64.73, 54.11, 49.15, 47.65, 41.18, 30.16, 27.61, 27.40, 21.21. ^{31}P -NMR (243 MHz, CD_3OD) δ 20.51 (d, 1P, $J=6.03$ Hz, $\text{P}\beta$) 11.35 (d, 1P, $J=7.54$ Hz, $\text{P}\alpha$). LC/ESI-MS (m/z): positive mode 1016.2627 $[\text{M}+\text{H}]^+$ and negative mode 1014.3045 $[\text{M}+\text{H}]^-$ (calc. 1015.86). Purity determined by HPLC-UV (254 nm)-ESI-MS: 95.8%. mp: degradation $> 260^\circ\text{C}$.

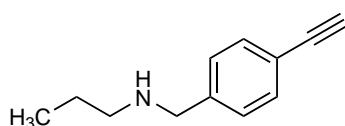
6.3.55 (((((2*R*,3*S*,4*R*,5*R*)-5-(6-(((4-((2-(2-(2-(3',6'-Di-hydroxy-3-oxo-3*H*-spiro[isobenzofuran-1,9'-xanthene]-5(6)-carboxamido)-ethoxy)ethoxy)ethyl)carbamoyl)benzyl)amino)-9*H*-purin-9-yl)-3,4-dihydroxytetrahydrofuran-2-yl)methoxy)(hydroxy)-phosphoryl)methyl)phosphonic acid (158b)



Compounds **157** (0.01 g, 0.05 mmol, 1.0 eq) and **156b** (0.03 g, 0.05 mmol, 1.0 eq) were dissolved in absolute ethanol (5 ml). Et_3N (0.2 ml, 0.15 mmol, 3.0 eq) was added and the mixture was stirred at 80°C . After 18 h the solution was evaporated followed by purification by RP-HPLC (0 \rightarrow 50% MeCN/50 mM NH_4HCO_3 buffer in 15 min, 20 ml/min) followed by lyophilization to get final product (0.02 g, 49%). ^1H -NMR (600 MHz, D_2O) δ 8.30 (s, 1H, $\text{N}=\text{CHN}$) 7.88 (s, 1H, $\text{CH}=\text{CH}$) 7.60 (s, 1H, $\text{N}=\text{CHN}$) 7.52 (d, 1H, $J=7.37$ Hz, $\text{C}=\text{CH}$) 7.48 (d, 1H, $J=7.75$ Hz, $\text{C}=\text{CH}$) 7.27 (d, 1H, $J=7.93$ Hz, $\text{CH}=\text{CO}$) 7.20 (d, 1H, $J=7.85$ Hz, $\text{CH}=\text{CO}$) 7.06 (dd, 2H, $J=2.10, 9.53$ Hz, 2x $\text{CH}=\text{COH}$) 7.03 (d, 2H, $J=9.26$ Hz, 2x $\text{CH}=\text{COH}$) 6.62 (m, 2H, aryl) 6.57 (m, 2H, aryl) 6.09 (d, 2H, $J=5.04$ Hz, CHN) 4.73 (m, 1H, CHOH) 4.53 (t, 1H, $J=4.83$ Hz, CHOH) 4.50 (br s, 2H, NHCH_2) 4.38 (q, 1H, $J=3.69$ Hz, CHCH_2) 4.18 (d, 2H, $J=4.19$ Hz, CHCH_2O) 3.73 (t, 2H, $J=5.01$ Hz, CH_2) 3.63 (m, 2H, CH_2) 3.60 (t, 2H, $J=5.01$ Hz, CH_2) 3.51 (t, 2H, $J=5.37$ Hz, CH_2) 3.45 (m, 2H, CH_2) 3.25 (t, 2H, $J=5.50$ Hz, CH_2) 2.17 (t, 2H, $J=18.47$ Hz, PCH_2P). ^{13}C -NMR (151 MHz, D_2O) δ 176.62, 172.57, 171.74, 161.19, 160.95, 160.77, 160.23, 160.11, 156.86, 155.34, 145.48, 144.76, 142.02, 139.05, 137.31, 136.89, 136.17, 134.95, 134.30, 134.11, 131.64, 131.19, 130.47, 130.32, 129.98, 125.49,

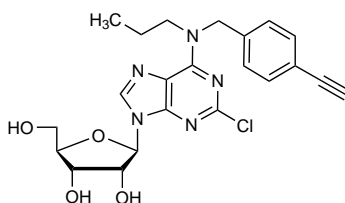
116.04, 115.55, 106.47, 106.25, 90.06, 86.48, 77.03, 73.01, 71.85, 71.67, 71.56, 71.47, 66.39, 45.31, 42.61, 42.17, 30.37. ^{31}P -NMR (202 MHz, D_2O) δ 18.88 (d, 1P, $J = 9.04$ Hz, $\text{P}\beta$) 14.96 (d, 1P, $J = 9.33$ Hz, $\text{P}\alpha$). LC/ESI-MS (m/z): positive mode 1048.2610 $[\text{M}+\text{H}]^+$ and negative mode 1046.3153 $[\text{M}+\text{H}]^-$ (calc. 1047.86). Purity determined by HPLC-UV (254 nm)-ESI-MS: 96.7%. mp: decomposition $>190^\circ\text{C}$.

6.3.56 *N,N*-(4-Ethynyl)-benzylproylamine (161), CAS 1870989-99-3



1-Bromopropane (0.34 ml, 3.8 mmol, 1.0 eq) was added to (4-ethynylphenyl)methanamine (0.5 g, 3.8 mmol, 1.0 eq) and the reaction was stirred at rt for 2 days followed by filtration yielding the desired product as white solid (0.27 g, 41%). ^1H -NMR (500 MHz, DMSO-d_6) δ 8.62 (br s, 1H, NH) 7.57 (m, 2H, aryl) 7.51 (m, 2H, aryl) 4.27 (s, 1H, $\text{C}\equiv\text{CH}$) 4.18 (s, 2H, NHCH_2 -aryl) 2.89 (m, 2H, NHCH_2) 1.63 (m, 2H, CH_2CH_3) 0.92 (t, 3H, $J = 7.44$ Hz, CH_3). ^{13}C -NMR (126 MHz, DMSO-d_6) δ 133.61, 132.82, 132.76, 131.05, 130.00, 123.22, 83.76, 82.61, 50.53, 49.21, 19.86, 11.78. LC/ESI-MS (m/z): positive mode 173.9 $[\text{M}+\text{H}]^+$. Purity determined by HPLC-UV (254 nm)-ESI-MS: 74%. mp: 157°C .

6.3.57 *N*⁶-(4-Ethynyl)benzyl-2-chloro-*N*⁶-propylpurine riboside (162)

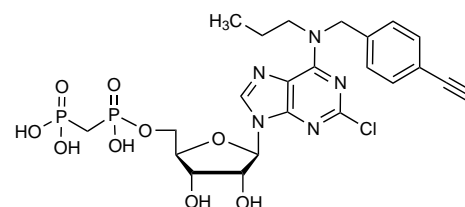


2',3',5'-tri-*O*-Acetyl-2,6-dichlororibofuranosylpurine (**127**, 0.34 g, 0.77 mmol, 1.0 eq) was suspended in absolute ethanol. To the suspension, triethylamine (0.2 ml, 1.54 mmol, 2.0 eq) and **161** (0.26 g, 1.54 mmol, 2.0 eq) were added and the reaction mixture was refluxed overnight. The solvent was evaporated followed by deprotection with 1 M NaOMe (10 ml). The crude product was purified by silica gel column chromatography ($\text{CH}_3\text{OH}/\text{DCM}$ 1:19) yielding the desired product as white solid (0.25 g, 71%). ^1H -NMR (500 MHz, DMSO-d_6) δ 8.42 (br s, 1H, $\text{N}=\text{CHN}$) 7.42 (d, 2H, $J = 8.04$ Hz, aryl) 7.28 (br s, 2H, aryl) 5.85 (d, $J = 5.83$ Hz, 1H, CHN) 5.54 (d, 1H, $J = 12.20$ Hz, 1x NCH_2) 5.45 (br s, 1H, CHOH) 5.18 (br s, 1H, CHOH) 5.00 (br s, 1H, CH_2OH) 4.92 (d, 1H, $J = 15.05$ Hz, 1x NCH_2)

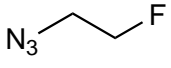
4.51 (br s, 1H, CHOH) 4.12 (s, 2H, NCH_2), 4.05 (q, 1H, $J = 5.19$ Hz, CHOH) 3.94 (q, 1H, $J = 3.92$ Hz, CHCH_2), 3.59 (d m, 2H, CHCH_2) 1.63 (br s, 2H, CH_2CH_3) 1.05 (t, 1H, $J = 7.02$ Hz, $\text{C}\equiv\text{CH}$) 0.85 (t, 3H, $J = 7.21$ Hz, CH_3). ^{13}C -NMR (126 MHz, DMSO-d_6) δ 154.38, 152.79, 151.73, 139.27, 132.03, 127.78, 120.67, 118.46, 87.47, 85.85, 83.46, 80.83, 73.84, 70.48, 61.45, 39.72, 21.88, 18.60, 11.08. LC/ESI-MS (m/z): positive mode 458.2 $[\text{M}+\text{H}]^+$. Purity determined by HPLC-UV (254 nm)-ESI-MS: 88%. mp: 110°C.

6.3.58 *N*⁶-(4-Ethynyl)benzyl-2-chloro-*N*⁶-propylpurine riboside 5'-*O*-[(phosphonomethyl)phosphonic acid] (163)

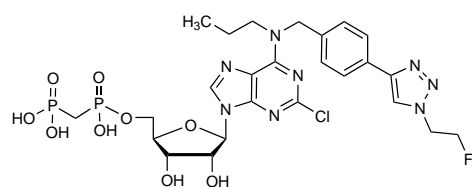
A solution of methylenebis(phosphonic dichloride) (0.27 g, 1.1 mmol, 5.0 eq) in trimethyl phosphate (3 ml), cooled to 0-4°C was added to a suspension of **162** (0.1 g, 0.2 mmol, 1.0 eq) in trimethyl phosphate (2 ml) at 0-4°C. The reaction mixture was stirred at 0-4°C and samples were withdrawn at 15 min interval for TLC to check the disappearance of nucleosides. After 30 min, on disappearance of nucleoside, 20 ml of cold 0.5 M aqueous TEAC solution (pH 7.4-7.6) was added. It was stirred at 0°C for 15 min followed by stirring at room temperature for 1 h. Trimethyl phosphate was extracted using (2x 250 ml) of *tert.*-butylmethylether and the aqueous layer was lyophilized. The crude product was then purified by RP-HPLC (0-50% MeCN/50 mM NH_4HCO_3 buffer in 20 min, 20 ml/min) to get final product as white solid (0.04 g, 28%). ^1H -NMR (600 MHz, D_2O) δ 8.37 (s, 1H, $\text{N}=\text{CHN}$) 7.30 (br s, 2H, aryl) 7.18 (d, 2H, $J = 7.83$ Hz, aryl) 6.01 (d, 1H, $J = 5.20$ Hz, CHN) 5.29 (br s, 2H, NCH_2) 4.68 (t, 1H, $J = 5.16$ Hz, CHOH) 4.52 (d, 1H, $J = 8.76$ Hz, CHOH) 4.36 (s, 1H, CHCH_2) 4.17 (br s, 2H, CHCH_2) 3.90 (br s, 2H, NCH_2) 2.17 (t, 2H, $J = 19.65$ Hz, PCH_2P) 1.62 (br s, 2H, CH_2CH_3) 1.25 (t, 1H, $J = 7.21$ Hz, $\text{C}\equiv\text{CH}$) 0.84 (t, 3H, $J = 7.49$ Hz, CH_3). ^{13}C -NMR (151 MHz, D_2O) δ 157.59, 156.41, 154.05, 147.0, 141.06, 134.97, 130.31, 123.07, 120.82, 89.78, 86.58, 85.92, 81.00, 77.15, 72.98, 66.41, 57.61, 53.51, 30.37, 23.79, 13.11. ^{31}P -NMR (243 MHz, D_2O) δ 18.94 (d, 1P, $J = 8.92$ Hz, $\text{P}\beta$) 14.89 (d, 1P, $J = 7.97$ Hz, $\text{P}\alpha$). LC/ESI-MS (m/z): positive mode 616.1130 $[\text{M}+\text{H}]^+$ and negative mode 614.0991 $[\text{M}-\text{H}]^-$ (calc. 615,90). Purity determined by HPLC-UV (254 nm)-ESI-MS: 84%. mp: 141°C.



6.3.59 2-Fluoroethylazide (165), CAS 894792-94-0

 To a solution of 2-fluoro-ethyl-4-toluenesulfonate (50.0 μ l, 0.3 mmol, 1.0 eq) in anhydrous DMF (0.5 ml) sodium azide (0.05 g, 0.9 mmol, 3.0 eq) was added. The reaction was stirred at rt for 24 h and was monitored by TLC. The crude mixture was filtered. The filtrate was used without any further purification. *WARNING: Attempts to isolate neat 2-fluoroethylazide may result in explosion.*¹⁷¹

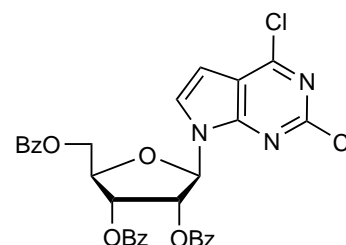
6.3.60 2-Chloro-*N*⁶-((4-(1-(2-fluoroethyl)-1H-1,2,3-triazol-4-yl)benzyl)(propyl)aminopurine riboside 5'-*O*-[(phosphonomethyl)phosphonic acid]) (166)



To a solution of **163** (15.0 mg, 0.02 mmol, 1.0 eq) in THF/H₂O/*t*-BuOH (3:1:1, 0.5 ml) crude **165** (50.0 μ l) was added. Additionally, 1 M sodium ascorbate in H₂O (0.03 ml, 0.03 mmol, 1.2 eq) was added. Finally, a premixed solution of CuSO₄ (1.0 mg, 0.009 mmol, 0.3 eq) and TBTA (4.0 mg, 0.003 mmol, 0.3 eq) in THF/H₂O/*t*-BuOH (3:1:1, 0.5 ml) was added to the reaction mixture. The reaction was stirred in the dark under argon at rt. During the reaction the color of the reaction mixture changed from a bright yellow to milky mint green. After one night of stirring the reaction mixture was evaporated and directly submitted to purification by RP-HPLC (0–70% MeCN/50 mM NH₄HCO₃ buffer in 20 min, 20 ml/min) to get final product as white solid (0.003 g, 17.5%). ¹H-NMR (600 MHz, D₂O) δ 8.40 (s, 1H, triazolyl) 8.27 (s, 1H, N=CHN) 7.67 (d, 2H, *J* = 6.91 Hz, aryl) 7.36 (d, 2H, *J* = 7.90 Hz, aryl) 6.02 (d, 1H, *J* = 4.74 Hz, CHN) 4.93–4.85 (m, 2H, NCH₂) 4.77 (m, 2H, overlapping with H₂O, NCH₂) 4.73 (s, 1H, CHOH) 4.53 (s, 1H, CHOH) 4.38 (s, 1H, CHCH₂) 4.18 (br s, 2H, CHCH₂) 3.15 (m, 2H, NCH₂) 2.18 (br s, 2H, PCH₂P) 1.67 (m, 2H, CH₂F) 1.34 (m, 2H, CH₂CH₃) 0.91 (m, 3H, CH₃). ¹³C-NMR (151 MHz, D₂O) δ 159.10, 156.48, 154.08, 152.57, 143.88, 141.04, 131.31, 130.98, 128.64, 125.38, 120.81, 89.68, 86.75, 85.48, 77.08, 73.07, 66.51, 55.52, 53.76, 53.63, 28.05, 22.14, 15.63. ³¹P-NMR (243 MHz, D₂O) δ 16.44 (s, 1P, P β) 0.39 (s, 1P, P α). ¹⁹F-NMR (202 MHz, D₂O) δ -75.62. LC/ESI-MS (*m/z*): positive mode 705.1486 [M+H]⁺ and negative mode 703.1335 [M+H]⁻ (calc. 704.97). Purity determined by HPLC-UV (254 nm)-ESI-MS: 99.9%. mp: 169°C.

6.3.61 2',3',5'-Tri-*O*-benzoyl-7-deaza-2,6-dichloropurine riboside (**169**)

To a suspension of 2,6-dichloro-7-deazapurine (**168**, 0.5 g, 1.0 eq, 2.7 mmol) in anhydrous acetonitrile (10 mL) was added BSA (0.8 mL, 1.3 eq, 3.4 mmol). When the solution became clear, 1-*O*-acetyl-2',3',5'-tri-*O*-benzoyl- β -D-ribofuranose (**167**, 2.1 g, 2.5 eq, 6.8 mmol) and trimethylsilyl trifluoromethanesulfonate (0.7 mL, 1.4 eq,



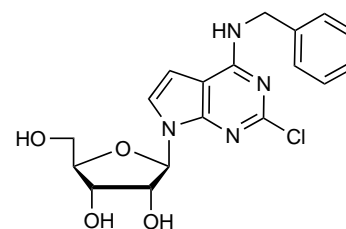
3.8 mmol) were added. The reaction mixture was stirred at 50°C for 16 h. The mixture was cooled down to rt and diluted with DCM. The organic phase was washed with saturated NaHCO₃ and reduced *in vacuo*. The crude product was purified by column chromatography (0.5% CH₃OH in DCM) but could not be isolated. LC/ESI-MS (m/z): positive mode 632.0 [M+H]⁺. Purity determined by HPLC-UV (254 nm)-ESI-MS: 29.2%.

6.3.62 General procedure for the synthesis of 170-173

To crude **169** (approx. 0.2 g, 0.38 mmol, 1.0 eq) in absolute ethanol, trimethylamine (1 mL, 7.2 mmol, 20.0 eq) and alkylamine (1.44 mmol, 4.0 eq) were added. The mixture was refluxed for 18 h followed by evaporation. The crude product was treated with a 1 M solution of NaOCH₃ in methanol for 24 h at rt to achieve full deprotection.

6.3.62.1 7-Deaza-*N*⁶-benzyl-2-chloropurine riboside (**170**)

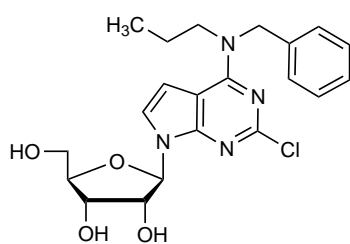
The compound was synthesized using benzylamine (0.15 mL, 1.44 mmol, 4.0 eq). Purification by column chromatography (CH₃OH/DCM 1:19 → 1:4) gave a mixture of the α - and the β -anomer (0.1 g, 67%). LC/ESI-MS (m/z): positive mode 391.1 [M+H]⁺. Purity determined by HPLC-UV (254 nm)-ESI-MS: 72.5% (α -anomer: 11.5%).



¹H-NMR (600 MHz, DMSO-d₆) δ 8.03 (t, 1H, *J* = 6.25 Hz, N=CHC) 7.33 (d, 2H, *J* = 7.40 Hz, aryl) 7.28 (t, 2H, *J* = 7.26 Hz, aryl) 7.20 (t, 1H, *J* = 7.29 Hz, aryl) 7.10 (s, 1H, CH=CH) 5.26 (t, 1H, *J* = 4.26 Hz, CHN) 4.96 (d, 1H, *J* = 6.61 Hz, CHOH) 4.91 (s, 1H, CHOH) 4.60 (d, 2H, *J* = 6.43 Hz, NHCH₂) 4.58 (d, 1H, *J* = 8.59 Hz, CH₂OH) 4.02 (br s, 1H, CHCH₂)

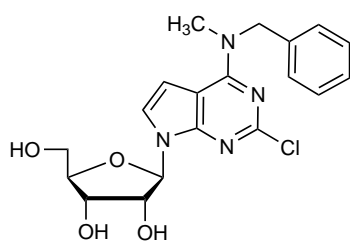
3.80 (q, 1H, $J = 2.82$ Hz, CHOH) 3.66 (br s, 1H, CHOH) 3.62 (m, 2H, CHCH_2). ^{13}C -NMR (151 MHz, DMSO-d_6) δ 156.82, 152.87, 153.11, 140.20, 128.50, 128.33, 128.27, 127.45, 127.34, 126.73, 120.88, 112.77, 99.53, 86.49, 78.54, 76.22, 69.81, 60.68, 43.17. mp: 95°C.

6.3.62.2 7-Deaza- N^6 -benzyl-2-chloro- N^6 -propylpurine riboside (171)



The compound was synthesized using benzylpropylamine (0.88 ml, 5.3 mmol, 2.0 eq). Purification by column chromatography ($\text{CH}_3\text{OH}/\text{DCM}$ 1:19 \rightarrow 1:4) gave a mixture of the α - and the β -anomer (0.1 g, 67%). LC/ESI-MS (m/z): positive mode 433.1 $[\text{M}+\text{H}]^+$. Purity determined by HPLC-UV (254 nm)-ESI-MS: 78.3% (α -anomer: 16.7%). ^1H -NMR (600 MHz, DMSO-d_6) δ 7.41 (s, 1H, $\text{N}=\text{CHC}$) 7.33 (m, 5H, aryl) 7.27 (q, 1H, $J = 3.98$ Hz, $\text{CH}=\text{CH}$) 5.04 (d, 1H, $J = 6.96$ Hz, CHN) 4.97 (d, 2H, $J = 1.67$ Hz, NCH_2) 4.22 (m, 1H, CHOH) 4.09 (dd, 1H, $J = 4.38, 5.58$ Hz, CHOH) 3.81 (q, 1H, $J = 4.18$ Hz, CHCH_2) 3.73-3.67 (d m, 2H, CHCH_2) 3.63-3.55 (d m, 2H, NCH_2) 1.71 (m, 2H, CH_2CH_3) 0.89 (t, 3H, $J = 7.35$ Hz, CH_3). ^{13}C -NMR (151 MHz, DMSO-d_6) δ 162.64, 155.30, 153.43, 139.64, 132.81, 129.99, 129.81, 129.31, 129.15, 128.52, 128.52, 123.53, 115.17, 104.62, 86.31, 79.06, 77.28, 72.71, 63.66, 54.61, 52.68, 21.90, 11.96. mp: 98°C.

6.3.62.3 7-Deaza- N^6 -benzyl-2-chloro- N^6 -methylpurine riboside (172)

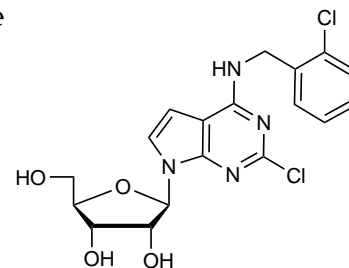


The compound was synthesized using benzylmethylamine (0.94 ml, 5.3 mmol, 2.0 eq). Purification by column chromatography ($\text{CH}_3\text{OH}/\text{DCM}$ 1:19 \rightarrow 1:4) gave a mixture of the α - and the β -anomer (0.05 g, 34%). LC/ESI-MS (m/z): positive mode 405.1 $[\text{M}+\text{H}]^+$. Purity determined by HPLC-UV (254 nm)-ESI-MS: 75.5% (α -anomer: 19%). ^1H -NMR (600 MHz, DMSO-d_6) δ 7.36 (s, 1H, $\text{N}=\text{CH}$) 7.32 (m, 1H, aryl) 7.30 (s, 1H, $\text{CH}=\text{CH}$) 7.29 (m, 2H, aryl) 7.28 (m, 2H, aryl) 4.92 (s, 1H, CHN) 4.89 (s, 1H, CHOH) 4.82 (br s, 1H, CHOH) 4.80 (s, 1H, CH_2OH) 4.02 (t, 1H, $J = 6.06$ Hz, CHOH) 3.87 (m, 1H, CHOH) 3.63 (br s, 2H, NCH_2) 3.62 (br s, 1H, CHCH_2) 3.49-3.43 (d m, 2H, CHCH_2) 2.25 (s, 3H, NCH_3). ^{13}C -NMR (151 MHz, DMSO-d_6) δ 160.09, 153.74, 151.07, 137.73, 128.57, 128.22, 128.13, 127.82, 127.19, 126.72, 122.02, 113.83, 101.69, 84.56, 77.33, 75.19, 70.78, 61.84, 54.58,

35.55. mp: 75°C.

6.3.62.4 7-Deaza-*N*⁶-(2-chloro)-benzyl-2-chloropurine riboside (173)

The compound was synthesized using 2-chlorobenzylamine (0.64 ml, 5.3 mmol, 2.0 eq). Purification by column chromatography (CH₃OH/DCM 1:19 → 1:4) gave a mixture of the α - and the β -anomer (0.07 g, 47%). LC/ESI-MS (m/z): positive mode 425.1 [M+H]⁺. Purity determined by HPLC-UV (254 nm)-ESI-MS: 80.9% (α -anomer: 13.2%).

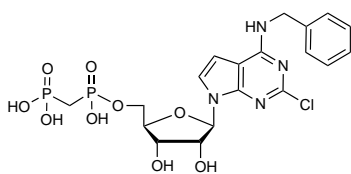


¹H-NMR (600 MHz, DMSO-d₆) δ 8.01 (s, 1H, N=CH) 7.43 (m, 1H, aryl) 7.25 (dd, 1H, *J* = 1.69, 3.00 Hz, aryl) 7.14 (m, 1H, aryl) 7.09 (s, 1H, CH=CH) 5.08 (d, 1H, *J* = 1.95 Hz, CHN) 4.69 (br s, 2H, NHCH₂) 4.64 (s, 1H, CHOH) 4.62 (s, 1H, CHOH) 4.00 (dd, 1H, *J* = 3.72, 6.38 Hz, CHCH₂) 3.80 (q, 1H, *J* = 2.89 Hz, CHOH) 3.74 (dd, 1H, *J* = 6.44, 8.46 Hz, CHOH) 3.56 (d, 2H, *J* = 2.87 Hz, CHCH₂). ¹³C-NMR (151 MHz, DMSO-d₆) δ 156.85, 152.73, 152.26, 137.08, 132.00, 129.22, 128.38, 128.00, 127.20, 121.12, 112.85, 99.67, 86.46, 78.52, 76.24, 69.92, 60.63, 41.81. mp: 151°C.

6.3.63 General procedure for the synthesis of 174-177

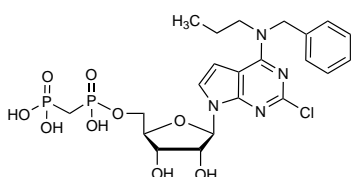
A solution of methylenebis(phosphonic dichloride) (5 eq) in trimethyl phosphate (5 mL), cooled to 0°C was added to a suspension of 7-deazaadenosine derivative (1 eq) in trimethyl phosphate (3 mL) at 0°C. The reaction mixture was stirred at 0°C and samples were withdrawn at 15 min interval for TLC to check the disappearance of nucleosides. After 40 min, on disappearance of nucleoside, 10 mL of cold 0.5 M aqueous TEAC solution (pH 7.4-7.6) was added. It was stirred at 0°C for 15 min followed by stirring at room temperature for 1 h. Trimethyl phosphate was extracted using (2x 100 mL) of *tert.*-butylmethylether and the aqueous layer was lyophilized. The crude product was then purified by preparative RP-HPLC (0-50% MeCN/50 mM NH₄HCO₃ buffer in 20 min, 20 ml/min) to get final product.

6.3.63.1 7-Deaza-*N*⁶-benzyl-2-chloropurine riboside 5'-*O*-[(phosphonomethyl)phosphonic acid] (174)



White solid (0.01 g, 15%). ¹H-NMR (600 MHz, D₂O) δ 7.43 (s, 1H, N=CH) 7.42 (m, 5H, aryl) 7.22 (s, 1H, C=CH) 4.91 (d, 1H, *J* = 8.18 Hz, CHN) 4.24 (dd, 1H, *J* = 3.69, 6.11 Hz, CHOH) 4.17 (dd, 1H, *J* = 6.18, 8.33 Hz, CHOH) 4.10 (q, 1H, *J* = 3.61 Hz, CHCH₂) 3.89 (d m, 2H, CHCH₂O) 3.70 (br s, 2H, NHCH₂) 2.06 (t, 2H, *J* = 19.90 Hz, PCH₂P). ¹³C-NMR (151 MHz, D₂O) δ 160.14, 156.10, 153.36, 141.29, 131.78, 131.66, 131.52, 130.44, 130.22, 129.88, 123.35, 114.33, 102.79, 87.20, 80.31, 77.24, 73.44, 66.48, 47.19, 30.30. ³¹P-NMR (243 MHz, D₂O) δ 18.55 (d, 1P, *J* = 8.58 Hz, Pβ) 15.14 (d, 1P, *J* = 8.48 Hz, Pα). LC/ESI-MS (*m/z*): positive mode 549.0692 [M+H]⁺ and negative mode 547.0548 [M-H]⁻ (calc. 548.81). Purity determined by HPLC-UV (254 nm)-ESI-MS: 85.4%. mp: decomposition >164°C.

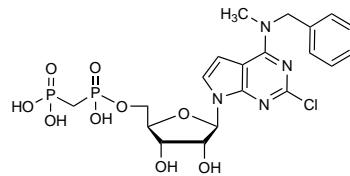
6.3.63.2 7-Deaza-*N*⁶-benzyl-2-chloro-*N*⁶-propylpurine riboside 5'-*O*-[(phosphonomethyl)phosphonic acid] (175)



White solid (0.02 g, 17%). ¹H-NMR (600 MHz, D₂O) δ 7.57 (s, 1H, N=CH) 7.33 (m, 6H, CH=C and aryl overlapping) 5.12 (d, 1H, *J* = 7.29 Hz, CHN) 4.94 (d, 1H, *J* = 15.18 Hz, CHOH) 4.73 (d, 1H, *J* = 15.19 Hz, CHOH) 4.35 (d m, 2H, NCH₂) 4.06 (m, 1H, CHCH₂) 4.02 (br s, 2H, NCH₂) 3.56-3.40 (d m, 2H, CHCH₂) 2.16 (t, 2H, *J* = 19.84 Hz, PCH₂P) 1.65 (m, 2H, CH₂) 0.78 (t, 3H, *J* = 7.26 Hz, CH₂CH₃). ¹³C-NMR (151 MHz, D₂O) δ 164.29, 155.57, 154.42, 140.40, 131.60, 131.52, 130.81, 130.34, 126.28, 114.93, 106.47, 85.82, 79.49, 77.85, 73.74, 66.64, 55.55, 54.57, 30.40, 22.96, 13.36. ³¹P-NMR (243 MHz, D₂O) δ 18.92 (d, 1P, *J* = 9.21 Hz, Pβ) 15.02 (d, 1P, *J* = 9.16 Hz, Pα). LC/ESI-MS (*m/z*): positive mode 591.1160 [M+H]⁺ and negative mode 589.1015 [M-H]⁻ (calc. 590.89). Purity determined by HPLC-UV (254 nm)-ESI-MS: 96.1%. mp: decomposition >177°C.

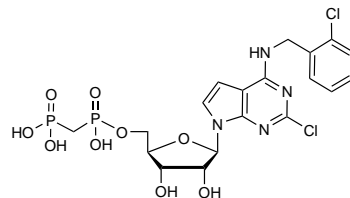
6.3.63.3 7-Deaza-*N*⁶-benzyl-2-chloro-*N*⁶-methylpurine riboside 5'-*O*-[(phosphonomethyl)phosphonic acid] (176)

White solid (0.01 g, 15%). ¹H-NMR (600 MHz, D₂O) δ 7.52 (s, 1H, N=CH) 7.42 (m, 5H, aryl) 7.32 (s, 1H, C=CH) 5.00 (d, 1H, *J* = 7.43 Hz, CHN) 4.87 (m, 2H, NCH₂) 4.35 (m, 1H, CHOH) 4.23 (m, 1H, CHOH) 4.13 (br s, 1H, CHCH₂) 3.99 (m, 2H, CHCH₂) 3.08 (s, 3H, NCH₃) 2.14 (t, 2H, *J* = 19.85 Hz, PCH₂P). ¹³C-NMR (151 MHz, D₂O) δ 163.99, 155.33, 154.44, 139.97, 133.46, 132.51, 132.43, 132.03, 131.64, 130.47, 125.82, 114.81, 105.19, 85.80, 79.34, 77.50, 73.51, 66.60, 58.85, 34.80, 30.38. ³¹P-NMR (243 MHz, D₂O) δ 18.84 (d, 1P, *J* = 9.61 Hz, Pβ) 15.08 (d, 1P, *J* = 9.48 Hz, Pα). LC/ESI-MS (*m/z*): positive mode 563.0861 [M+H]⁺ and negative mode 561.0710 [M-H]⁻ (calc. 562.84). Purity determined by HPLC-UV (254 nm)-ESI-MS: 94%. mp: decomposition >166°C.



6.3.63.4 7-Deaza-*N*⁶-(2-chloro)-benzyl-2-chloro-purine riboside 5'-*O*-[(phosphonomethyl)phosphonic acid] (177)

White solid (0.02 g, 20%). ¹H-NMR (600 MHz, D₂O) δ 7.45 (m, 1H, N=CH) 7.33 (m, 5H, aryl) 7.22 (s, 1H, C=CH) 4.90 (d, 1H, *J* = 7.75 Hz, CHN) 4.75 (s, 1H, CHOH) 4.20 (d, 1H, *J* = 5.39 Hz, CHOH) 4.09 (m, 1H, CHCH₂) 3.86 (d m, 2H, CHCH₂) 3.55 (d m, 2H, NHCH₂) 2.02 (t, 2H, *J* = 19.75 Hz, PCH₂P). ¹³C-NMR (151 MHz, D₂O) δ 160.02, 156.03, 153.38, 138.17, 135.94, 132.51, 131.86, 130.20, 123.26, 114.34, 102.88, 87.17, 80.21, 77.13, 73.59, 66.49, 45.63, 30.28. ³¹P-NMR (243 MHz, D₂O) δ 18.45 (d, 1P, *J* = 8.62 Hz, Pβ) 15.29 (d, 1P, *J* = 8.61 Hz, Pα). LC/ESI-MS (*m/z*): positive mode 583.0300 [M+H]⁺ and negative mode 581.0165 [M-H]⁻ (calc. 583.25). Purity determined by HPLC-UV (254 nm)-ESI-MS: 94.9%. mp: decomposition >160°C.



6.4 Biological experiments

6.4.1 Pharmacological evaluation of 8-BuS-AMP and ARL67156 derivatives

6.4.1.1 CD39 inhibition assay

Compound screening was carried out by Sang-Yong Lee, Xihuan Luo, and Laura Schäkel as described previously.¹¹⁵ The assay was conducted at 37°C in a final volume of 100 μ L with each compound in a concentration of 10 μ M as shown in *Table 6.2*. The reaction mixture contained 10 mM 4-(2-hydroxyethyl)piperazine-1-ethanesulfonic acid (HEPES), 1 mM MgCl₂ and 2 mM CaCl₂ (pH 7.4) and 0.5 μ M FL-6-AMP (PSB-170621A, *Jena Bioscience GmbH*, Jena, Germany) as a substrate. The enzyme reaction was started by adding 0.2 μ g human umbilical cord membrane preparation of NTPDase1, which was obtained from the working group of Prof. Sévigny. Importantly, the enzyme solution was added on ice to avoid unevenness of reaction. The enzyme mixture was incubated for 4 min at 37°C and 500 rpm. Subsequently, the enzyme reaction was stopped by heating at 90°C and 500 rpm for 5 min. After cooling the reaction samples on ice, the enzyme mixture was diluted with the assay buffer by 20-fold and the samples were then measured with the CE.

Table 6.2: Sample preparation for FFCE.

Component	Concentration	Volume	End concentration
Test compound	50 μ M in 10% DMSO	20 μ l	10 μ M
Substrate (PSB-017621A)	0.833 μ M	60 μ l	0.5 μ M
Enzyme	0.004 mg/ml	20 μ l	0.0008 mg/ml

6.4.1.2 Detection by the fast fluorescent capillary electrophoresis assay

Analysis was carried out using *P/ACE MDQ CE* system (Beckman Instruments, Fullerton, CA, USA) equipped with a LIF detection system as described previously.¹¹⁵ Data collection and peak area analysis were performed by the *P/ACE MDQ software 32 KARAT* obtained from Beckman Coulter (Fullerton, CA, USA). The electrophoretic separations were carried out using a polyacrylamide-coated capillary (30 cm, 50 μ m (id), 20 cm effective length) was purchased from *Chromatographie Service GmbH* (Langerwehe, Germany). As running buffer 50 mM phosphate buffer (pH 6.5) was used. Samples were injected electrokinetically by applying voltage of 6 kV for 30 s

in outlet-side. Finally, analytes were separated by applying separation voltage of 15 kV for 2.5 min. Between separations, the capillary was washed with 50 mM phosphate buffer (pH 6.5) for 1 min (25 psi) before each injection. The detection was done with an excitation wavelength of 488 nm and an emission wavelength of 520 nm. The % inhibition was calculated as described in (Equation Eq. 6.4.1):

B: Absorption of blank

T: Absorption of test compound

$$\% inhibition = \frac{B - T}{B} * 100 \quad (Eq. 6.4.1)$$

The results were plotted, and concentration-inhibition curves were fitted with *GraphPad Prism 5* (GraphPad Software, La Jolla, USA).

6.4.1.3 Malachite green assay

Compound screening was carried out by Laura Schäkel as described previously.¹⁹² The assay was conducted at 37°C in a final volume of 100 µL with each compound in a concentration of 10 µM as shown in *Table 6.3*.

Table 6.3: Sample preparation for malachite green assay.

Component	Concentration	Volume	End concentration
Test compound	50 µM in 10% DMSO	20 µl	10 µM
CD39	12.5 ng/µl	10 µl	5 ng/µl
Substrate ATP	125 µM	20 µl	50 µM
Malachite green solution	0.6 mM	20 µl	120 µM
Ammonium molybdate solution	20 mM	30 µl	6 mM

The reaction mixture contained 10 mM HEPES, 1 mM MgCl₂ and 2 mM CaCl₂ (pH 7.4) and 50 µM ATP as a substrate. First, CD39 and the test compound were pre-incubated for 5 min at 37°C and 500 rpm. Next, ATP was added as the substrate to the reaction mixture, which was subsequently incubated for 15 min at 37°C and 500 rpm. For the detection, the detection reagents malachite green (0.6 mM in polyvinyl alcohol) and ammonium molybdate (20 mM in 1.5 M H₂SO₄) were added and the mixture was incubated for 20 min at 25°C and 500 rpm. The absorption was measured at a wavelength of 600 nm with an *BMG PheraStar FS* plate reader (BMG Labtech GmbH, Ortenberg, Germany) equipped with a UV detection system. Quantification took place by the use of an external phosphate standard. The experiment was additionally conducted with denatured enzyme (15 min at 90°C) to subtract the free phosphate background of the substrate solutions. The results were plotted, and concentration-inhibition curves were fitted with *GraphPad Prism 5* (GraphPad

Software, La Jolla, USA).

6.4.1.4 Selectivity studies on NTPDase2, 3, and 8

The experiments were performed in triplicate ($n = 3$). The selected substrate concentration (ATP) was $50 \mu\text{M}$. The inhibitors were investigated at 50 and $100 \mu\text{M}$. The enzyme concentrations were chosen after an enzyme titration and adjusted to ensure 10–20% conversion rates. The malachite green assay was performed as described above.

6.4.1.5 Selectivity studies on NPP1

The assay procedure for the selectivity studies on hNPP1 (soluble form expressed in insect cells) is described in *Table 6.4*. The experiments were performed by Vittoria Lopez according to published procedure.¹⁹³ The assay is based on the enzymatic ester hydrolysis of *p*-nitrophenolate-5'-thymidine monophosphate (*p*-Nph-5'-TMP) that results in the formation of *p*-nitrophenolate anion which has an absorption maximum of 400 nm.

Table 6.4: Assay procedure for hNPP1 (soluble form expressed in insect cells).

	Component	Concentration	Volume	End concentration
1.	Substrate <i>p</i> -Nph-5'-TMP	$666 \mu\text{M}$	$60 \mu\text{l}$	$400 \mu\text{M}$
2.	Test compound	$100 \mu\text{M}$ in 10% DMSO	$20 \mu\text{l}$	$20 \mu\text{M}$
3.	Enzyme	$90 \text{ ng}/\mu\text{l}$	$20 \mu\text{l}$	$18 \text{ ng}/\mu\text{l}$
	Total		$100 \mu\text{l}$	

The mixture was incubated for 30 min at 37°C and 500 rpm. The enzyme reaction was terminated by the addition of $20 \mu\text{L}$ 1 M NaOH. The absorption maximum was measured at 400 nm (or optimal at 405 nm) using a *BMG PheraStar FS* plate reader (BMG Labtech GmbH, Ortenberg, Germany). The % inhibition was calculated as described in (*Equation Eq. 6.4.1*).

6.4.1.6 Selectivity studies on NPP3 and 5

The assay procedure for the selectivity studies on hNPP3 and 5 (soluble form expressed in insect cells) are described in *Table 6.5*. The experiments were performed by Salahuddin Mirza according to published procedure.¹⁹⁴ The enzymatic activity of

NPP3 and 5 was measured using 1,*N*⁶-etheno-nicotinamide adenine dinucleotide⁺ (ϵ -NAD⁺) as substrate.¹⁹⁴ NPP-mediated hydrolysis of ϵ -NAD⁺ results in the generation of fluorescent *N*⁶-ethenoadenosine-5'-*O*-diphosphoribose (ϵ -ADPR) that is detected at an emission wavelength of 420 nm after excitation at 270 nm.¹⁹⁴ The accumulation of the fluorescent reaction product over time is a measure for the enzymatic activity.¹⁹⁴

Table 6.5: Assay procedure for hNPP3 and 5 (soluble form expressed in insect cells).

Component	End concentration
1. Substrate ϵ -NAD ⁺	20 μ M
2. Test compound (100 μ M in 10% DMSO)	10 μ M
3. NPP3	90 ng/ μ l
or NPP5	400 ng/ μ l

The enzymatic reactions were performed in reaction buffer (10 mM *N*-cyclohexyl-2-aminoethanesulfonic acid (CHES), 2 mM CaCl₂, and 1 mM MgCl₂, pH 9.0 in H₂O). Briefly, purified NPP3 or NPP5 (400 ng) (soluble forms expressed in insect cells) was treated with 20 μ M of ϵ -NAD⁺ and 10 μ M or 100 μ M of the test compound for 30 min at 37°C and subsequent quenching of substrate was recorded as relative fluorescence units (at $\lambda_{270/420}$) of the samples by using a fluorescence microplate reader (Flexstation, Medical Devices LLC. USA and Softmax pro software to collect the data).¹⁹⁴

6.4.1.7 Selectivity studies on NPP4

The assay procedure for the selectivity studies on hNPP4 (soluble form expressed in insect cells) are described in *Table 6.6*. The experiments were performed by Vittoria Lopez. The assay is based on the cleavage of diadenosine tetraphosphate (AP₄A) by NPP4 which results in the formation of ATP and AMP. Firefly luciferase reacts with D-luciferin in the presence of formed ATP and Mg²⁺, which act as co-factors. The resulting luminescence is a measure of the enzymatic activity.¹⁹⁵

The reaction was carried out in white 96-well plates. The mixture was incubated for 60 min at 37°C and shaking at 500 rpm. The enzyme was inactivated at 90°C for 5 min followed by the addition of 50 μ l luciferase reaction buffer I (15 mM MgCl₂, 300 mM tris(hydroxymethyl)aminomethane (Tris)-HCl, and 450 μ g/ml D-luciferin in H₂O) and 50 μ l luciferase reaction buffer II (2 μ g/ml *firefly* luciferase in H₂O). The luminescence was measured immediately (within 10 min) at 560 nm using a *BMG*

PheraStar FS plate reader (BMG Labtech GmbH, Ortenberg, Germany).

Table 6.6: Assay procedure for hNPP4 (soluble form expressed in insect cells).

	Component	Concentration	Volume	Final concentration
1.	Substrate AP ₄ A	50 μM	20 μl	20 μM
2.	Test compound	100 μM in 10% DMSO	10 μl	20 μM
3.	Enzyme	175 ng/ μl	20 μl	70 ng/ μl
	Total		50 μl	

6.4.1.8 Selectivity studies on CD38

The assay procedure is the same as described for NPP3 and 5 (*Section 6.4.1.6*) with only small changes. The enzymatic reactions were performed in a different reaction buffer (10 mM HEPES, pH 7.2) using 8 ng CD38 (soluble form expressed in insect cells). The experiments were performed by Salahuddin Mirza.

6.4.2 Pharmacological evaluation of AOPCP derivatives at CD73

6.4.2.1 Soluble CD73 enzyme preparations

Soluble CD73 enzyme preparations were generated by Christian Renn as described in Renn *et al.* 2019.¹²⁹ Soluble rat CD73 was expressed in *Spodoptera frugiperda* 9 (Sf9) insect cells and purified as previously described.¹⁹⁶ The cDNA for the soluble human CD73 (Genbank accession no. NM_002526) was obtained from Prof. Dr. Norbert Sträter (University of Leipzig, Germany).⁸¹ In order to generate a soluble enzyme the signaling sequence for anchoring the protein to the membrane via a GPI-anchor had been omitted (N-terminal residues: 1-27, C-terminal residues: 550-574 including GPI-anchor attachment site).⁸¹ In addition, a 6xHis-Tag was fused to the C-terminus and the construct was cloned into the vector pACGP67B, which provides an N-terminal signal peptide for the secretion of the protein. Sf9 insect cells were grown in *Insect-XPRESS*TM media (#: BE12-730Q, Lonza, Switzerland) with 10 mg/l gentamicin and split at a ratio of 1:3 every fourth day. For transfection, cells were seeded into cell culture flasks (25 cm²) at 60-70% confluence. 100 μl of cell medium and 1 μl of vector DNA (1000 ng/ μl) were mixed with 2.5 μl of baculovirus genomic *ProEasy*TM vector DNA (*AB vector*, CA, USA) and combined with premixed 100 μl of cell medium and 8 μl of *Cellfectin*TM II Reagent (*Thermo Fisher Scientific*, MA, USA). The transfection mixture was left for 30 min at rt and then dropwise added to the

cells into the cell culture flasks. The cells were incubated for 30 min at rt, and for further 4 days at 27°C. Cells from the transfection procedure were detached from the bottom of the flasks and centrifuged for 5 min at 2000 *g*. 1.5 ml of the supernatant (viral stock) was added to 75 cm² cell culture flasks containing Sf9 cells (60–70% confluence), and the cells were incubated for four days at 27°C. Then 1.5 ml of the supernatant were taken and added to uninfected Sf9 cells in a 75 cm² flask. This was repeated five more times, using more cells and larger flasks after the third round of infections (175 cm² to which 3.0 ml of supernatant were added).

The final stock solution was used for infection of the cells. For protein expression, 3 ml of the virus solution were used to infect 150 ml of cell media containing 2x10⁶ cells/ml in a 500 ml Erlenmeyer flask, and they were incubated for 4 days at 27°C with shaking (150 rpm). Then, cell suspensions were transferred to 50 ml Falcon tubes and centrifuged at 15 min at 5000 *g* at 4°C. The supernatants were subjected to ultrafiltration using *Amicon*[®] *Ultra-15*, 10 kDa cut-off (*Merck Millipore*, MA, USA) at 5000g for 15–30 min at 4°C. The concentrated protein was purified with *HisPur*[™] *Ni*²⁺ *NTA* spin columns (#: 88226, *Thermo Fisher Scientific*, MA, USA). The elution of the columns was performed as recommended in the instruction manual with adjusting the incubation time for protein binding to 1 h at 4°C with an end-over-end mixer and an additional incubation step of 5 min with the elution buffer before eluting. Eluates were pooled and dialyzed (*Membra-Cel*[™], 14 kDa cut-off, 250 mm x 44 mm x 0.02 mm; *Carl Roth*, Germany) at 4°C in 25 mM Tris buffer, pH 7.4, with a volume adjusted to 40 times the volume of the elution fraction. The buffer was exchanged after 8 h. The enzyme was aliquoted and stored at -80°C until use.

6.4.2.2 Cell culture

The cells were cultured as described in Renn *et al.* 2019.¹²⁹ Triple-negative breast cancer cells (MDA-MB-231), which natively express CD73, were grown in Dulbecco's Modified Eagle Medium (DMEM, #: 41966, *Thermo Fisher Scientific*, MA, USA) and melanoma cancer cells with CRISPR-Cas9 knockout of CD73 (MaMel.65-CD73^{ko}) in *Roswell Park Memorial Institute (RPMI)* medium 1640, (#: 21875034, *Thermo Fisher Scientific*, Waltham, MA, USA) plus 2 mM L-Glutamine (#: P08-2000, *PAN Biotech*, Germany). Both media were supplemented with 100 U/ml penicillin/100 µg/ml streptomycin (#: P06-07100, *PAN Biotech*, Germany) and 10% fetal bovine serum (FBS)

(#: P30-1502, *PAN Biotech*, Germany) and were cultivated at 37°C with 5% CO₂. MDA-MB-231 and MaMel.65-CD73^{ko} cells were split 1:20, 1:5 every 72 h (at 80–90% cell confluence), respectively. To detach the adherent cells, growth media was removed, cells were washed with PBS (25 cm² flask: 2.5 ml, for larger flasks correspondingly larger amounts) and incubated with trypsin/EDTA ((0.05%/0.6 mM), #: P10-022100, *PAN Biotech*, Germany; 1 ml for 25 cm² flask) for 5 min in the incubator at 37°C. Detached cells were diluted with growth media (2 ml for 25 cm² flask) and transferred to new culture flasks containing growth media (5 ml for 25 cm² flask).

6.4.2.3 Membrane preparation of CD73 from MDA-MB-231

Membrane preparations were generated by Christian Renn as described in Renn *et al.* 2019.¹²⁹ For membrane preparations, cells were expanded in 175 cm² culture flasks to 80–90% cell confluence. After detachment by trypsin/EDTA (0.05%/ 0.6 mM), 106 cells per dish were transferred to cell culture dishes (150 cm²) and incubated for 4 days at 37°C with 5% CO₂. The culture medium was removed, cells were washed with 10 ml of PBS and frozen at 20°C. Cells were treated with 1 ml of ice-cold buffer (50 mM Tris, 2 mM EDTA, pH 7.4), scraped off, collected in a conical tube and centrifuged for 10 min at 1000 *g* (4°C). The pellet was resuspended in membrane buffer (0.5 ml/dish; 25 mM Tris, 1 mM EDTA, 320 mM sucrose, 1:1000 protease inhibitor cocktail (#: P8340, *Sigma-Aldrich*, MO, USA), pH 7.4) and homogenized three times for 30 s each (20,500 rpm, *Ultraturrax*, *IKA-Labortechnik*, Germany). After centrifugation for 10 min, at 1000 *g* (4°C), the supernatants were collected and centrifuged for 30 min at 48,000 *g* (4°C). The supernatant was discarded and the pellet was resuspended in washing puffer (0.5 ml/dish; 50 mM Tris, pH 7.4) and centrifuged again (same conditions). This step was repeated three times. Finally, the pellet was resuspended in washing buffer (0.1 ml/dish), aliquoted and stored at -80°C until use.

6.4.2.4 Radiometric assay for CD73

The assay was performed by Christian Renn or Riham Idris as described previously.^{84,129} Stock solutions (10 mM) of the compounds were prepared in demineralized water, and further dilutions were performed in assay reaction buffer (25 mM Tris, 140 mM sodium chloride, 25 mM sodium dihydrogen phosphate, pH 7.4). 10 µl of the inhibitor solution were added to 70 µl of assay reaction buffer. After the addition of

10 μl of CD73-containing solution or suspension (rat CD73: 1.63 ng; human CD73: 0.365 ng; membrane preparation of MDA-MB-231 cells expressing CD73: 7.4 ng of protein per vial), the reaction was initiated by the addition of 10 μl of [2,8- ^3H]AMP (specific activity 7.4×10^8 Bq/mmol (20 mCi/mmol)), *American Radio-labeled Chemicals*, MO, USA, distributed by *Hartman Analytic*, Germany) resulting in a final substrate concentration of 5 μM . The enzymatic reaction was performed for 25 min at 37°C in a shaking water bath. Then, 500 μl of cold precipitation buffer (100 mM lanthanum chloride, 100 mM sodium acetate, pH 4.0) were added to stop the reaction and to facilitate precipitation of free phosphate and unconverted [2,8- ^3H]AMP. After the precipitation was completed (after at least 30 min on ice), the mixture was separated by filtration through GF/B glass fiber filters using a cell harvester (*M-48*, *Brandel*, MD, USA). After washing each reaction vial three times with 400 μl of cold (4°C) demineralized water, 5 ml of the scintillation cocktail (*ULTIMA Gold XR*, *PerkinElmer*, MA, USA) were added and radioactivity was measured by scintillation counting (*TRICARB 2900 TR*, *Packard/PerkinElmer*; counting efficacy: 49-52%). Two controls were included and measured as duplicates. One reaction was performed without the inhibitor resulting in 100% enzyme activity (positive control) and one was incubated without the inhibitor and the enzyme and served as background control. The resulting data were subtracted from the background and were normalized to the positive control. The results were plotted, and concentration-inhibition curves were fitted with *GraphPad Prism 5* (*GraphPad Software*, La Jolla, USA). The mean $\text{IC}_{50} \pm \text{SEM}$ from three independent experiments was used to calculate the K_i value with the Cheng-Prusoff equation (Eq. 6.4.2).¹⁹⁷ The different K_m values of the different CD73 variants are depicted in 6.4.2.4.

Table 6.7: K_m values of different CD73 variants.

$$K_i = \frac{\text{IC}_{50}}{1 + \frac{[\text{S}]}{K_m}} \quad (\text{Eq. 6.4.2})$$

CD73 variant	K_m
rat CD73	$53.0 \pm 4.1 \mu\text{M}$
human CD73	$17.0 \pm 2.1 \mu\text{M}$
MDA-MB-231	$14.8 \pm 2.1 \mu\text{M}$

6.4.3 Flow cytometry analyses

6.4.3.1 Materials for flow cytometry

Chemical reagents and their manufacturers

Fixation buffer	Thermo Fisher Scientific, Waltham (MA), USA
Permeabilization buffer	Thermo Fisher Scientific, Waltham (MA), USA
Clean solution	Becton Dickinson, Franklin Lakes (NJ), USA
Flow sheath fluid	Becton Dickinson, Franklin Lakes (NJ), USA
Rinse solution	Becton Dickinson, Franklin Lakes (NJ), USA

Fluorochrome-conjugated antibodies and their manufacturers

PE anti-human CD73, clone AD2	BioLegend, San Diego (CA), USA
Pacific Blue anti-human CD8a, clone RPA-T8	BioLegend, San Diego (CA), USA
PE/Cy7 anti-human CD19, clone HIB19	BioLegend, San Diego (CA), USA

6.4.3.2 Blood samples

Peripheral blood was drawn from healthy volunteers visiting the UKE. All blood samples were obtained and handled according to corresponding ethics protocols (Ethikkommission der Ärztekammer Hamburg, PV5139).

6.4.3.3 Isolation of peripheral blood mononuclear cells

PBMCs were isolated by gradient density centrifugation. Diluted blood (30 mL, two- to threefold dilution in PBS) was layered on 20 mL *Biocoll* (Merck, Darmstadt, Germany) and centrifuged (800 *g*, 25 min, room temperature, without break). For smaller blood volumes, the ratio was 9 mL diluted blood and 6 mL *Biocoll*. After centrifugation (*Centrifuge 5810R*, Eppendorf, Hamburg, Germany), the interphase containing the cells was transferred into a new tube and washed two times with cold PBS (650 *g*, 10 min, 4°C and 450 *g*, 5 min, 4°C, respectively). The remaining erythrocytes were lysed by adding 2 mL purified water (ddH₂O) for 20 seconds. The reaction was stopped by washing with cold PBS (450 *g*, 5 min, 4°C). For counting, the cells were resuspended in medium or PBS. Cell counting was done with the help of the *Neubauer* counting chamber (Marienfeld-Superior, Lauda-Königshofen, Germany).

6.4.3.4 Staining of surface molecules for flow cytometric analyses

For the staining of surface molecules 0.3×10^6 – 1×10^6 cells were used. The cells were washed with PBS (450xg, 5 min) and resuspended in 100 μ l PBS. For the staining of a single surface marker 10 μ l of the diluted fluorescence-labeled antibody (0.8 μ g/ml) or fluorescent marker were added to the cells. The surface staining cocktail was added to the cells and incubated for 30 min in the dark at room temperature. After the incubation the cells were washed with 1 ml PBS (450xg, 5 min) to remove unbound antibodies and resuspended in 150–200 μ l FACS buffer (0.1% BSA, 0.02% NaN₃ in PBS). For membrane fixation prior to staining, cells were incubated with 100 μ l fixation buffer for 30 min in the dark at room temperature followed by washing with 1 ml PBS (450xg, 5 min). For co-incubation with detergent, 100 μ l of permeabilization buffer were added to the surface staining cocktail. The flow cytometry measurements were done at the *FACS Canto II* (Becton Dickinson, Franklin Lakes (NJ), USA).

7 List of abbreviations

8-BuS-AMP	8-butylthio-AMP
8-BuS-ATP	8-butylthio-ATP
ACR	apyrase-conserved region
AdeR	adenine receptor
ADP	adenosine diphosphate
ADPR	ADP-ribose
AIDS	acquired immune deficiency syndrome
AMP	adenosine monophosphate
AMPPNP	β,γ -imidoadenosine 5'-triphosphate
AOPCP	adenosine-5'-O-[(phosphonomethyl)phosphonic acid]
AP ₄ A	diadenosine tetraphosphate
AR	adenosine receptor
ARL67156	<i>N</i> ⁶ -diethyl-D- β,γ -dibromo-methylene- ATP
ATP	adenosine triphosphate
BETA-NO ₂	benzyltriethylammonium nitrite
Boc	<i>tert.</i> -butyloxycarbonyl
BODIPY	boron-dipyrrromethene
BSA	bovine serum albumin
BTSA	bis(trimethylsilyl)-acetamide
cADPR	cyclic ADP-ribose
CD38	cyclic ADP ribose hydrolase
CD39	NTPDase1
CD73	<i>ecto</i> -5'-nucleotidase
cDNA	complementary DNA
CE	capillary electrophoresis
CE-UV	CE assay coupled to a UV detector
CHES	<i>N</i> -cyclohexyl-2-aminoethanesulfonic acid
CL _{int}	internal clearance
CR	conserved region
CuAAC	copper(I)-catalyzed azide-alkyne cycloaddition

DAD	diode array detector
DCC	<i>N,N'</i> -dicyclohexylcarbodiimide
DCM	dichloromethane
DCU	<i>N,N'</i> -dicyclohexylurea
DMAP	4-dimethylaminopyridine
DMF	dimethylformamide
DMSO	dimethylsulfoxide
DNA	deoxyribonucleic acid
ϵ -ADPR	<i>N</i> ⁶ -ethenoadenosine-5'- <i>O</i> -diphosphoribose
e5NT	<i>ecto</i> -5'-nucleotidase
EDTA	ethylenediaminetetraacetic acid
ϵ -NAD ⁺	1, <i>N</i> ⁶ -etheno-nicotinamide adenine dinucleotide ⁺
FACS	fluorescence-activated cell sorting
FBS	fetal bovine serum
FFCE	fast fluorescent CE assay
FL-6-ATP	<i>N</i> ⁶ -(6-fluoresceincarbamoyl)hexyl-ATP
FL-6-AMP	<i>N</i> ⁶ -(6-fluoresceincarbamoyl)hexyl-AMP
FPIA	fluorescence polarization immunoassay
FPLC	fast protein liquid chromatography
FSC	forward scatter
GPCR	G protein-coupled receptor
GPI	glycosylphosphatidylinositol
HEPES	4-(2-hydroxyethyl)piperazine-1-ethanesulfonic acid
HER2	human epidermal growth factor receptor 2
HOBt	1-hydroxybenzotriazole
HPLC	high performance liquid chromatography
HV	high voltage source
IC ₅₀	half maximal inhibitory concentration
K_i	inhibitory constant
K_m	Michaelis constant
LC/ESI-MS	HPLC analysis coupled to electrospray ionization mass spectrometry
LGIC	ligand-gated ion channel
LIF	laser-induced fluorescence
LOD	limit of detection

LpNTPDase1	<i>L. pneumophila</i> NTPDase1
mCPBA	<i>meta</i> -chloroperoxybenzoic acid
NAADP	nicotinic acid adenine dinucleotide phosphate
NADP ⁺	nicotinamide adenine dinucleotide phosphate ⁺
NAD ⁺	nicotinamide adenine dinucleotide ⁺
NaHMDS	sodium bis(trimethylsilyl)amide
NDP	nucleoside diphosphate
NFSi	<i>N</i> -fluorobenzenesulfonimide
NMP	nucleoside monophosphate
NMR	nuclear magnetic resonance
NPP	nucleotide pyrophosphatase/phosphodiesterase
NTP	nucleoside triphosphate
NTPDase	nucleoside triphosphate diphosphohydrolase
PBMC	peripheral blood mononuclear cell
PE	phycoerythrin
PET	positron emission tomography
PBS	phosphate-buffered saline
<i>p</i> -Nph-5'-TMP	<i>p</i> -nitrophenolate-5'-thymidine monophosphate
POM	polyoxometalate
PPADS	pyridoxalphosphate-6-azophenyl-2',4'-disulfonic acids
PPB	plasma protein binding
ppm	parts per million
proton sponge	1,8-bis-(dimethylamino)naphthalene
RB2	reactive blue 2
<i>R_f</i>	retention factor
ROESY	rotating frame Overhauser effect spectroscopy
RP-HPLC	reverse phase HPLC
SAR	structure-activity relationship
SD	standard deviation
SEM	standard error of the mean
SSC	side scatter
<i>t</i> _{1/2}	half-time
TBTA	tris(benzyltriazolylmethyl)amine
TEAC	triethylammonium hydrogencarbonate buffer
TFA	trifluoroacetic acid

THF	tetrahydrofuran
TIC	total ion count
TLC	thin layer chromatography
TMSOTf	trimethylsilyl trifluoromethanesulfonate
Tris	tris(hydroxymethyl)aminomethane
UDP	uridine diphosphate
UTP	uridine triphosphate
UV	ultra-violet

8 List of Figures

1.1	Overview of purinergic receptors and their endogenous ligands	3
1.2	Pathways of extracellular nucleotide metabolism	4
1.3	Phylogenetic tree of the NTPDase family based on amino acid sequence alignment	6
1.4	Schematic representation of the postulated reaction mechanism of NTPDase-mediated NTP ($R = NMP$) or NDP ($R = \text{nucleoside}$) hydrolysis	7
1.5	Homology model of human NTPDase1	8
1.6	The role of CD39 overexpression in tumor progression	10
1.7	Known inhibitors of CD39	14
1.8	Crystal structure of human <i>ecto</i> -5'-nucleotidase	17
1.9	Binding mode of AOPCP to CD73	18
1.10	Known adenosine-based inhibitors of CD73	19
1.11	Binding modes of AOPCP analogs to human CD73	20
1.12	Other known inhibitors of CD73	21
1.13	Principle of the malachite green assay	23
1.14	Principle of the capillary electrophoresis-UV assay	24
1.15	Principle of the fluorescence polarization immunoassay	25
1.16	Principle of the fast fluorescent CE assay	26
1.17	Molecular docking with ATP (A) and FL-ATP (B)	27
1.18	Principle of the radiometric assay	28
1.19	Diphosphonylation of nucleosides using methylenebis(phosphonic dichloride)	31

1.20	Possible phosphorylation products of nucleosides using methylenebis-(phosphonic dichloride)	31
3.1	Modification places of the 8-BuS-AMP- and ARL67156-scaffolds	37
3.2	Analytical spectra of 111	59
3.3	Concentration-inhibition curves of the most potent ARL67156 derivatives	65
3.4	Selectivity of ARL67156-derived CD39 inhibitors	66
3.5	Concentration-inhibition curves of the most potent 8-BuS-AMP derivatives	73
3.6	Selectivity of 8-BuS-AMP-derived CD39 inhibitors	75
4.1	ROESY-NMR spectrum of 127	83
4.2	Potencies at rat CD73 of cold ligands	88
4.3	HPLC chromatogram after tritium labeling	93
4.4	Design of an AOPCP-derived fluorescent probe for CD73.	94
4.5	Structure of PSB-12379.	98
4.6	Absorption and emission spectra of 158a and 158b	103
4.7	Titration of 158b on PBMCs.	105
4.8	Testing of different conditions to reduce the concentration-dependent shift of the 158b peak.	106
4.9	Comparison of anti-CD73-PE antibody, 158a , and 158b	107
4.10	Co-staining of PBMCs with an anti-CD73 antibody and 158a or 158b	108
4.11	AOPCP-derived PET tracer for CD73.	110
5.1	Structure-activity relationships of single modifications of the ARL67156-scaffold at human CD39	126
5.2	Structure-activity relationships of combined modifications of the ARL67156-scaffold at human CD39	126
5.3	Structure-activity relationships of single modifications of the 8-BuS-AMP-scaffold at human CD39	127

5.4	Structure-activity relationships of combined modifications of the 8-BuS-AMP-scaffold at human CD39	127
5.5	Structures of a novel radioligand (139) for CD73 and its precursor (146)	129
5.6	Novel fluorescent markers for CD73	130
5.7	Cold version of novel PET-tracer (163) and its precursor (166)	131
5.8	Inhibitory potency of N^6 -substituted 2-chloro-7-deaza-AOPCP derivatives at human CD73	132

9 List of Schemes

1.1	The Yoshikawa procedure	28
1.2	Complex formation between trimethyl phosphate and phosphoryl chloride	29
1.3	Triphosphorylation via nucleophilic attack of phosphonato phosphate on an activated nucleoside	30
1.4	Synthesis of triphosphates containing a P_{β} - P_{γ} -dibromomethylene bridge	30
3.1	Synthesis of C2-substituted adenosine derivatives	38
3.2	Synthesis of 2-hydrazinyladenosine (7)	39
3.3	Synthesis of C8-substituted adenosine derivatives	40
3.4	Synthesis of <i>N</i> -(6-aminohexyl)-benzamide (19)	43
3.5	Synthesis of primary amines for the synthesis of 26 and 27	45
3.6	Synthesis of 6-phenylbutoxyadenosine (45)	45
3.7	Synthesis of dihalogenmethylenbisphosphonate	53
3.8	Synthesis of β,γ -dibromomethylene-ATP analogs	55
4.1	Synthesis of PSB-12379	80
4.2	Synthesis of 2,6-dichloropurine-ribofuranoside	80
4.3	Nucleoside condensation reaction	82
4.4	Synthesis of PSB-12489	84
4.5	Synthesis of α,β -methylene-2-chloro- N^6 -disubstituted-ADP derivatives	87
4.6	Synthesis of N^6 -benzyl-2-chloro- N^6 -propargyl AOPCP (146)	90
4.7	Attempted synthesis route A to obtain 152	96
4.8	Attempted synthesis routes B & C to obtain 152	97
4.9	Synthesis of 158	99
4.10	Synthesis of 2-chloro- N^6 -(4-ethynyl)-benzyl- N^6 -propyl-AOPCP (163)	112
4.11	Synthesis of 2-chloro- N^6 -(4-(1-(2-fluoroethyl)-1,2,3-triazol-4-yl)-benzyl)- N^6 -propyl AOPCP	114
4.12	Synthesis of protected 7-deaza-2,6-dichloropurine riboside (169) . . .	117
4.13	Synthesis of N^6 -substituted 2-chloro-7-deazaadenosine derivatives . .	118

4.14 Phosphonylation of N^6 -substituted 2-chloro-7-deazaadenosine derivatives	119
5.1 Optimized procedure for the synthesis of 127	129

10 List of Tables

3.1	¹ H-NMR data of C2-substituted adenosine derivatives	39
3.2	¹³ C-NMR data of C2-substituted adenosine derivatives	39
3.3	¹ H-NMR data of C8-substituted adenosine derivatives	41
3.4	¹³ C-NMR data of C8-substituted adenosine derivatives	42
3.5	Synthesis of <i>N</i> ⁶ -substituted adenosine derivatives	44
3.6	¹ H-NMR data of <i>N</i> ⁶ -substituted adenosine derivatives	46
3.7	¹³ C-NMR data of <i>N</i> ⁶ -substituted adenosine derivatives	47
3.8	Synthesis of C8, <i>N</i> ⁶ -disubstituted adenosine derivatives	49
3.9	¹ H-NMR data of C8, <i>N</i> ⁶ -disubstituted adenosine derivatives	50
3.10	¹³ C-NMR data of C8, <i>N</i> ⁶ -disubstituted adenosine derivatives	51
3.11	Synthesis of ARL67156 derivatives	54
3.12	³¹ P-NMR data of ARL67156 derivatives	55
3.13	Monophosphorylation of adenosine derivatives	57
3.14	Protection and subsequent phosphorylation of adenosine derivatives	60
3.15	³¹ P-NMR data of 8-BuS-AMP derivatives	61
3.16	Potency of ARL67156 analogs and derivatives as CD39 inhibitors	62
3.17	Potency of ARL67156 derivatives at human NTPDase2, 3, and 8, NPP1-4, CD73, and CD38.	65
3.18	Potency of C2-substituted AMP derivatives as CD39 inhibitors	67
3.19	Potency of C8-substituted AMP derivatives as CD39 inhibitors	69
3.20	Potency of <i>N</i> ⁶ -substituted AMP derivatives as CD39 inhibitors	70
3.21	Potency of <i>N</i> ⁶ -C8-disubstituted AMP derivatives as CD39 inhibitors	72

3.22 Potency of 8-BuS-AMP derivatives at human NTPDase2, 3, and 8, NPP1-4, CD73, and CD38	74
3.23 Biological evaluation of 8-BuS-AMP-derived inhibitors for metabolic stability	76
4.1 ¹ H-NMR data of PSB-12379 and PSB 12489 and the corresponding adenosine derivatives	85
4.2 ¹³ C-NMR data of PSB-12379 and PSB 12489 and the corresponding adenosine derivatives	85
4.3 ³¹ P-NMR data of PSB-12379 and PSB 12489	86
4.4 Biological evaluation of CD73 inhibitors (139-141) for their pharmacological properties	89
4.5 Inhibitory potency of 139	89
4.6 ³¹ P-NMR data of the cold ligands and the precursor	90
4.7 ¹ H-NMR data of the cold ligands, the precursor, and the corresponding adenosine derivatives	91
4.8 ¹³ C-NMR data of the cold ligands, the precursor, and the corresponding adenosine derivatives	92
4.9 ¹ H-NMR data of fluorescent CD73 probe.	100
4.10 ¹³ C-NMR data of fluorescent CD73 probe	100
4.11 ³¹ P-NMR data of fluorescent CD73 probe.	101
4.12 Inhibitory potency of 158a and 158b at different enzyme preparations.	102
4.13 Measured absorption and emission maxima and calculated <i>Stokes shift</i>	102
4.14 Half-lives of different positron-emitting radionuclides	109
4.15 ¹ H-NMR data of the PET-tracer and its precursor	113
4.16 ¹³ C-NMR data of the PET-tracer and its precursor	113
4.17 ³¹ P- and ¹⁹ F-NMR data of the PET-tracer and its precursor	114
4.18 Inhibitory potency of 163 and 166 at different enzyme preparations.	115
4.19 Optimization of the synthesis of 169	117

4.20	³¹ P-NMR data of the 7-deaza-AOPCP derivatives	119
4.21	¹ H-NMR data of the 7-deazaadenosine and 7-deaza-AOPCP derivatives	120
4.22	¹³ C-NMR data of the 7-deazaadenosine and 7-deaza-AOPCP deriva- tives	121
4.23	Inhibitory potencies of the 7-deaza AOPCP derivatives 174-177	122
6.1	NMR internal standards	134
6.2	Sample preparation for FFCE	228
6.3	Sample preparation for the malachite green assay	229
6.4	Assay procedure for hNPP1 (soluble form expressed in insect cells) .	230
6.5	Assay procedure for hNPP3 and 5 (soluble form expressed in insect cells)	231
6.6	Assay procedure for hNPP4 (soluble form expressed in insect cells) .	232
6.7	<i>K_m</i> values of different CD73 variants	235

11 Literature

- [1] Fiske, C.; SubbaRow, Y. Phosphorous compounds of muscle and liver. *Science* **1929**, *70*, 381–382.
- [2] Lohmann, K. Über die Pyrophosphatfraktion im Muskel. *Naturwissenschaften* **1929**, *17*, 624–625.
- [3] Lippman, F. In *Adv. Enzymol. - Relat. Areas Mol. Biol.*; Nord, F. F., Werkman, C., Eds.; 1941; Vol. 1; pp 99–162.
- [4] Vitiello, L.; Gorini, S.; Rosano, G.; La Sala, A. Immunoregulation through extracellular nucleotides. *Blood* **2012**, *120*, 511–518.
- [5] Burnstock, G.; Verkhratsky, A. Long-term (trophic) purinergic signalling: purinoceptors control cell proliferation, differentiation and death. *Cell Death Dis.* **2010**, *1*, 1–10.
- [6] Drury, A.; Szent-Györgyi, A. The physiological activity of adenine compounds with special reference to their action upon mamalian heart. *J. Physiol.* **1929**, *68*, 213–237.
- [7] Burnstock, G.; Campbell, G.; Satchell, D.; Smythe, A. Evidence that adenosine triphosphate or a related nucleotide is the transmitter substance released by non-adrenergic inhibitory nerves in the gut. *Br. J. Pharmacol.* **1970**, *40*, 668–688.
- [8] Burnstock, G. Purinergic nerves. *Pharmacol. Rev.* **1972**, *24*, 509–581.
- [9] Burnstock, G. Do some nerve cells release more than one transmitter? *Neuroscience* **1976**, *1*, 239–248.
- [10] Burnstock, G. Cotransmission. *Curr. Opin. Pharmacol.* **2004**, *4*, 47–52.
- [11] Burnstock, G.; Wood, J. Purinergic receptors: their role in nociception and primary afferent neurotransmission. *Curr. Opin. Neurobiol.* **1996**, *6*, 526–532.
- [12] Langley, J. N. On the reaction of cells and of nerve-endings to certain poisons, chiefly as regards the reaction of striated muscle to nicotine and to curari. *J. Physiol.* **1905**, *33*, 374–413.

- [13] Prüll, C. R. Part of a scientific master plan? Paul Ehrlich and the origins of his receptor concept. *Med. Hist.* **2003**, *47*, 332–356.
- [14] Neubig, R. R.; Spedding, M.; Kenakin, T.; Christopoulos, A. International Union of Pharmacology Committee on Receptor Nomenclature and Drug Classification. XXXVIII. Update on terms and symbols in quantitative pharmacology. *Pharmacol. Rev.* **2003**, *55*, 597–606.
- [15] Ruffolo, R. R. Important concepts of receptor theory. *J. Auton. Pharmacol.* **1982**, *2*, 277–295.
- [16] Pierce, K. L.; Premont, R. T.; Lefkowitz, R. J.; Hughes, T. H. Seven-transmembrane receptors. *Nat. Rev.* **2002**, *3*, 639–650.
- [17] Burnstock, G.; Cocks, T.; Crowe, R.; Kasakov, L. Purinergic innervation of the guinea-pig urinary bladder. *Br. J. Pharmacol.* **1978**, *63*, 125–38.
- [18] Ralevic, V.; Burnstock, G. Receptors for purines and pyrimidines. *Pharmacol. Rev.* **1998**, *50*, 413–492.
- [19] Fredholm, B. B.; Ijzerman, a. P.; Jacobson, K. a.; Klotz, K. N.; Linden, J. International Union of Pharmacology. XXV. Nomenclature and classification of adenosine receptors. *Pharmacol. Rev.* **2001**, *53*, 527–552.
- [20] Burnstock, G. Physiology and pathophysiology of purinergic neurotransmission. *Physiol. Rev.* **2007**, *87*, 659–797.
- [21] Zimmermann, H.; Zebisch, M.; Sträter, N. Cellular function and molecular structure of ecto-nucleotidases. *Purinergic Signal.* **2012**, *8*, 437–502.
- [22] Surprenant, A.; North, R. A. Signaling at purinergic P2X receptors. *Annu. Rev. Physiol.* **2009**, *71*, 333–359.
- [23] Burnstock, G. Purinergic signalling and disorders of the central nervous system. *Nat. Rev. Drug Discov.* **2008**, *7*, 575–590.
- [24] Brunschweiler, A.; Müller, C. E. P2 receptors activated by uracil nucleotides – an update. *Curr. Med. Chem.* **2006**, *13*, 289–312.
- [25] Bender, E.; Buist, A.; Jurzak, M.; Langlois, X.; Baggerman, G.; Verhasselt, P.; Ercken, M.; Guo, H.-Q.; Wintmolders, C.; Van den Wyngaert, I.; Van Oers, I.; Schoofs, L.; Luyten, W. Characterization of an orphan G protein-coupled receptor localized in the dorsal root ganglia reveals adenine as a signaling molecule.

Proc. Natl. Acad. Sci. U. S. A. **2002**, *99*, 8573–8578.

- [26] Gorzalka, S. Evidence for the functional expression and pharmacological characterization of adenine receptors in native cells and tissues. *Mol. Pharmacol.* **2004**, *67*, 955–964.
- [27] von Kügelgen, I.; Schiedel, A. C.; Hoffmann, K.; Alsdorf, B. B. A.; Abdelrahman, A.; Müller, C. E. Cloning and functional expression of a novel Gi protein-coupled receptor for adenine from mouse brain. *Mol. Pharmacol.* **2008**, *73*, 469–477.
- [28] Thimm, D.; Knospe, M.; Abdelrahman, A.; Moutinho, M.; Alsdorf, B. B. A.; von Kügelgen, I.; Schiedel, A. C.; Müller, C. E. Characterization of new G protein-coupled adenine receptors in mouse and hamster. *Purinergic Signal.* **2013**, *9*, 415–426.
- [29] Slominska, E.; Szolkiewicz, M.; Smolenski, R.; Rutkowski, B.; Swierczynski, J. High plasma adenine concentration in chronic renal failure and its relation to erythrocyte ATP. *Nephron* **2002**, *91*, 286–291.
- [30] Yegutkin, G. G. Nucleotide- and nucleoside-converting ectoenzymes: Important modulators of purinergic signalling cascade. *Biochim. Biophys. Acta - Mol. Cell Res.* **2008**, *1783*, 673–694.
- [31] Lazarowski, E. R.; Boucher, R. C.; Harden, T. Mechanisms of release of nucleotides and integration of their action as P2X- and P2Y-receptor activating molecules. *Mol. Pharmacol.* **2003**, *64*, 785–795.
- [32] Müller, C. E. Unpublished work. **2016**,
- [33] Idzko, M.; Ferrari, D.; Riegel, A.; Eltzhig, H. K. Extracellular nucleotide and nucleoside signaling in vascular and blood disease. *Blood* **2014**, *124*, 1029–1037.
- [34] Marangoni, A. *Enzyme kinetics - A modern approach*; Wiley - Interscience, 2003; pp 1–226.
- [35] Löffler, G.; Schölmerich, J. *Basiswissen Biochemie mit Pathobiochemie.*, 7th ed.; Springer Medizin Verlag, 2008; pp 33–48.
- [36] Robson, S. C.; Sévigny, J.; Zimmermann, H. The E-NTPDase family of ectonucleotidases: Structure function relationships and pathophysiological significance. *Purinergic Signal.* **2006**, *2*, 409–430.

- [37] Zebisch, M.; Krauss, M.; Schäfer, P.; Lauble, P.; Sträter, N. Crystallographic snapshots along the reaction pathway of nucleoside triphosphate diphosphohydrolases. *Structure* **2013**, *21*, 1460–1475.
- [38] Kukulski, F.; Lévesque, S. A.; Lavoie, . G.; Lecka, J.; Bigonnesse, F.; Knowles, A. F.; Robson, S. C.; Kirley, T. L.; Sévigny, J. Comparative hydrolysis of P2 receptor agonists by NTPDases 1, 2, 3 and 8. *Purinergic Signal*. **2005**, *1*, 193–204.
- [39] Zebisch, M.; Krauss, M.; Schäfer, P.; Sträter, N. Crystallographic evidence for a domain motion in rat nucleoside triphosphate diphosphohydrolase (NTPDase) 1. *J. Mol. Biol.* **2012**, *415*, 288–306.
- [40] Knowles, A. F. The GDA1_CD39 superfamily: NTPDases with diverse functions. *Purinergic Signal*. **2011**, *7*, 21–45.
- [41] Zebisch, M.; Schäfer, P.; Lauble, P.; Sträter, N. New crystal forms of NTPDase1 from the bacterium *Legionella pneumophila*. *Acta Crystallogr. Sect. F Struct. Biol. Cryst. Commun.* **2013**, *69*, 257–262.
- [42] Vivian, J. P.; Riedmaier, P.; Ge, H.; Le Nours, J.; Sansom, F. M.; Wilce, M. C. J.; Byres, E.; Dias, M.; Schmidberger, J. W.; Cowan, P. J.; D'Apice, A. J. F.; Hartland, E. L.; Rossjohn, J.; Beddoe, T. Crystal structure of a *Legionella pneumophila* ecto -triphosphate diphosphohydrolase: A structural and functional homolog of the eukaryotic NTPDases. *Structure* **2010**, *18*, 228–238.
- [43] Zebisch, M.; Baqi, Y.; Schäfer, P.; Müller, C. E.; Sträter, N. Crystal structure of NTPDase2 in complex with the sulfoanthraquinone inhibitor PSB-071. *J. Struct. Biol.* **2014**, *185*, 336–341.
- [44] Geiß, J. Homology modeling and docking studies of human ectonucleoside triphosphate diphosphohydrolase 1. Bachelor Thesis, University of Bonn, 2017.
- [45] Ramachandran, G.; Ramakrishnan, C.; Sasiskharan, V. Stereochemistry of polypeptide chain configurations. *J. Mol. Biol.* **1996**, *261*, 470–489.
- [46] Sévigny, J.; Sundberg, C.; Braun, N.; Guckelberger, O.; Csizmadia, E.; Qawi, I.; Imai, M.; Zimmermann, H.; Robson, S. C. Differential catalytic properties and vascular topography of murine nucleoside triphosphate diphosphohydrolase 1 (NTPDase1) and NTPDase2 have implications for thromboregulation. *Blood* **2002**, *99*, 2801–2809.

- [47] Robson, S. C.; Wu, Y.; Sun, X.; Knosalla, C.; Dwyer, K.; Enjyoji, K. Ectonucleotidases of CD39 family modulate vascular inflammation and thrombosis in transplantation. *Semin. Thromb. Hemost.* **2005**, *31*, 217–233.
- [48] Kukulski, F.; Bahrami, F.; Ben Yebdri, F.; Lecka, J.; Martín-Satué, M.; Lévesque, S. a.; Sévigny, J. NTPDase1 controls IL-8 production by human neutrophils. *J. Immunol.* **2011**, *187*, 644–53.
- [49] Mizumoto, N.; Kumamoto, T.; Robson, S. C.; Sévigny, J.; Matsue, H.; Enjyoji, K.; Takashima, A. CD39 is the dominant Langerhans cell-associated ecto-NTPDase: modulatory roles in inflammation and immune responsiveness. *Nat. Med.* **2002**, *8*, 358–365.
- [50] Sauer, A. V.; Brigida, I.; Carriglio, N.; Hernandez, R. J.; Scaramuzza, S.; Clavenna, D.; Sanvito, F.; Poliani, P. L.; Gagliani, N.; Carlucci, F.; Tabucchi, A.; Roncarolo, M. G.; Traggiai, E.; Villa, A.; Aiuti, A. Alterations in the adenosine metabolism and CD39/CD73 adenosinergic machinery cause loss of Treg cell function and autoimmunity in ADA-deficient SCID. *Blood* **2012**, *119*, 1428–1439.
- [51] Vongtau, H.; Lavoie, E.; Sévigny, J.; Molliver, D. Distribution of ectonucleotidases in mouse sensory circuits suggests roles for nucleoside triphosphate diphosphohydrolase-3 in nociception and mechanoreception. *Neuroscience* **2011**, *193*, 387–398.
- [52] Zimmermann, H. Nucleotide signaling in nervous system development. *Eur. J. Physiol.* **2006**, *452*, 573–588.
- [53] Massé, K.; Bhamra, S.; Eason, R.; Dale, N.; Jones, E. a. Purine-mediated signalling triggers eye development. *Nature* **2007**, *449*, 1058–1062.
- [54] Chambers, D. A.; Israel, B. Characterization of ecto-ATPase of human blood platelets. *Arch. Biochem. Biophys.* **1967**, *119*, 173–178.
- [55] Antonioli, L.; Blandizzi, C.; Pacher, P.; Haskó, G. Immunity, inflammation and cancer: a leading role for adenosine. *Nat. Rev. Cancer* **2013**, *13*, 842–57.
- [56] Tan, D. B.; Ong, N. E.; Zimmermann, M.; Price, P.; Moodley, Y. P. An evaluation of CD39 as a novel immunoregulatory mechanism invoked by COPD. *Hum. Immunol.* **2016**, *77*, 916–920.
- [57] Apostolova, P.; Zeiser, R. The role of danger signals and ectonucleotidases in

- acute graft-versus-host disease. *Hum. Immunol.* **2016**, *77*, 1037–1047.
- [58] Qawi, I.; Robson, S. C. New developments in anti-platelet therapies: potential use of CD39/vascular ATP diphosphohydrolase in thrombotic disorders. *Curr. Drug Targets* **2000**, *1*, 285–296.
- [59] Copeland, R. A. *Enzymes: A practical introduction to structure, mechanism, and data analysis.*, 2nd ed.; Wiley - Interscience, 2000; pp 1–390.
- [60] Müller-Esterl, W. *Biochemie*, 1st ed.; Spektrum Akademischer Verlag, 2004; pp 172–175.
- [61] Bültmann, R.; Wittenburg, H.; Pause, B.; Kurz, G.; Nickel, P.; Starke, K. P2-purinoceptor antagonists: III. Blockade of P2-purinoceptor subtypes and ecto-nucleotidases by compounds related to suramin. *Naunyn. Schmiedeberg's Arch. Pharmacol.* **1996**, *354*, 498–504.
- [62] Chen, B. C.; Lee, C. M.; Lin, W. W. Inhibition of ecto-ATPase by PPADS, suramin and reactive blue in endothelial cells, C6 glioma cells and RAW 264.7 macrophages. *Br. J. Pharmacol.* **1996**, *119*, 1628–1634.
- [63] Lecka, J.; Gillerman, I.; Fausther, M.; Salem, M.; Munkonda, M. N.; Brosseau, J. P.; Cadot, C.; Martín-Satué, M.; D'Orléans-Juste, P.; Rousseau, É.; Poirier, D.; Künzli, B.; Fischer, B.; Sévigny, J. 8-BuS-ATP derivatives as specific NTPDase1 inhibitors. *Br. J. Pharmacol.* **2013**, *169*, 179–196.
- [64] Crack, B. E.; Pollard, C. E.; Beukers, M. W.; Roberts, S. M.; Hunt, S. F.; In-gall, a. H.; McKechnie, K. C.; IJzerman, a. P.; Leff, P. Pharmacological and biochemical analysis of FPL 67156, a novel, selective inhibitor of ecto-ATPase. *Br. J. Pharmacol.* **1995**, *114*, 475–481.
- [65] Lévesque, S.; Lavoie, E.; Lecka, J.; Bigonnesse, F.; Sévigny, J. Specificity of the ecto-ATPase inhibitor ARL 67156 on human and mouse ectonucleotidases. *Br. J. Pharmacol.* **2007**, *152*, 141–150.
- [66] Gendron, F. P.; Halbfinger, E.; Fischer, B.; Duval, M.; D'Orléans-Juste, P.; Beau-doin, A. R. Novel inhibitors of nucleoside triphosphate diphosphohydrolases: Chemical synthesis and biochemical and pharmacological characterizations. *J. Med. Chem.* **2000**, *43*, 2239–2247.
- [67] Müller, C. E.; Iqbal, J.; Baqi, Y.; Zimmermann, H.; Röllich, A.; Stephan, H. Polyoxometalates—a new class of potent ecto-nucleoside triphosphate diphos-

- phohydrolase (NTPDase) inhibitors. *Bioorganic Med. Chem. Lett.* **2006**, *16*, 5943–5947.
- [68] Lee, S. Y.; Fiene, A.; Li, W.; Hanck, T.; Brylev, K. A.; Fedorov, V. E.; Lecka, J.; Haider, A.; Pietzsch, H. J.; Zimmermann, H.; Sévigny, J.; Kortz, U.; Stephan, H.; Müller, C. E. Polyoxometalates - Potent and selective ecto-nucleotidase inhibitors. *Biochem. Pharmacol.* **2015**, *93*, 171–181.
- [69] Baqi, Y.; Weyler, S.; Iqbal, J.; Zimmermann, H.; Müller, C. E. Structure-activity relationships of anthraquinone derivatives derived from bromaminic acid as inhibitors of ectonucleoside triphosphate diphosphohydrolases (E-NTPDases). *Purinergic Signal.* **2009**, *5*, 91–106.
- [70] Kukulski, F.; Komoszynski, M. Purification and characterization of NTPDase1 (ectoapyrase) and NTPDase2 (ecto-ATPase) from porcine brain cortex synaptosomes. *Eur. J. Biochem.* **2003**, *270*, 3447–3454.
- [71] Iqbal, J.; Vollmayer, P.; Braun, N.; Zimmermann, H.; Müller, C. E. A capillary electrophoresis method for the characterization of ecto-nucleoside triphosphate diphosphohydrolases (NTPDases) and the analysis of inhibitors by in-capillary enzymatic microreaction. *Purinergic Signal.* **2005**, *1*, 349–358.
- [72] Lecka, J.; Rana, M. S.; Sévigny, J. Inhibition of vascular ectonucleotidase activities by the pro-drugs ticlopidine and clopidogrel favours platelet aggregation. *Br. J. Pharmacol.* **2010**, *161*, 1150–1160.
- [73] Munkonda, M. N.; Kauffenstein, G.; Kukulski, F.; Lévesque, S. A.; Legendre, C.; Pelletier, J.; Lavoie, E. G.; Lecka, J.; Sévigny, J. Inhibition of human and mouse plasma membrane bound NTPDases by P2 receptor antagonists. *Biochem. Pharmacol.* **2007**, *74*, 1524–1534.
- [74] Gendron, F.; Benrezzak, O.; Krugh, B.; Kong, Q.; Weisman, G.; Beaudoin, A. Purine signaling and potential new therapeutic approach: possible outcomes of NTPDase inhibition. *Curr. Drug Targets* **2002**, *3*, 229–245.
- [75] Lecka, J.; Fausther, M.; Künzli, B.; Sévigny, J. Ticlopidine in its prodrug form is a selective inhibitor of human NTPDase1. *Mediators Inflamm.* **2014**, *2014*.
- [76] Colgan, S. P.; Eltzhig, H. K.; Eckle, T.; Thompson, L. F. Physiological roles for ecto-5'-nucleotidase (CD73). *Purinergic Signal.* **2006**, *2*, 351–360.
- [77] Sowa, N. A.; Voss, M. K.; Zylka, M. Recombinant ecto-5'-nucleotidase (CD73)

- has long lasting antinociceptive effects that are dependent on adenosine A1 receptor activation. *J. Mol. Pain* **2010**, *6*, 20.
- [78] Wang, L.; Fan, J.; Thompson, L. F.; Zhang, Y.; Shin, T.; Curiel, T. J.; Zhang, B. CD73 has distinct roles in nonhematopoietic and hematopoietic cells to promote tumor growth in mice. *J. Clin. Invest.* **2011**, *121*, 2371–2382.
- [79] Zhou, X.; Zhi, X.; Zhou, P.; Chen, S.; Zhao, F.; Shao, Z.; Ou, Z.; Yin, L. Effects of ecto-5'-nucleotidase on human breast cancer cell growth in vitro and in vivo. *Oncol. Rep.* **2007**, *17*, 1341–1346.
- [80] Loi, S.; Pommey, S.; Haibe-Kains, B.; Beavis, P. A.; Darcy, P. K.; Smyth, M. J.; Stagg, J. CD73 promotes anthracycline resistance and poor prognosis in triple negative breast cancer. *Proc. Natl. Acad. Sci.* **2013**, *110*, 11091–11096.
- [81] Knapp, K.; Zebisch, M.; Pippel, J.; El-Tayeb, A.; Müller, C. E.; Sträter, N. Crystal structure of the human ecto-5'-nucleotidase (CD73): Insights into the regulation of purinergic signaling. *Structure* **2012**, *20*, 2161–2173.
- [82] Sträter, N. Ecto-5'-nucleotidase: Structure function relationships. *Purinergic Signal.* **2006**, *2*, 343–350.
- [83] Knöfel, T.; Sträter, N. Mechanism of hydrolysis of phosphate esters by the dimetal center of 5'-nucleotidase based on crystal structures. *J. Mol. Biol.* **2001**, *309*, 239–254.
- [84] Freundlieb, M.; Zimmermann, H.; Müller, C. A new, sensitive ecto-5'-nucleotidase assay for compound screening. *Anal. Biochem.* **2014**, *446*, 53–58.
- [85] Bhattarai, S. Synthesis and structure-activity relationships of α,β -methylene-ADP derivatives: potent and selective ecto-5'-nucleotidase inhibitors. Ph.D. thesis, University of Bonn, 2015.
- [86] Lawson, K.; Jin, L.; Jeffrey, J.; Kalisiak, J.; Yin, F.; Zhang, K.; Chen, A.; Swinarski, D.; Walters, M.; Young, S.; Schindler, U.; Powers, J. Discovery and characterization of AB680, a potent and selective small-molecule CD73 inhibitor for cancer immunotherapy. Annu. Meet. Am. Assoc. Cancer Res. Chicago.
- [87] Myers, T. C.; Nakamura, K.; Danielzadeh, A. B. Phosphonic Acid Analogs of Nucleoside Phosphates. III. The Synthesis of Adenosine-5'-methylenediphosphate, a Phosphonic Acid Analog of Adenosine-S'-diphosphate. *J. Org. Chem.* **1965**, *30*, 1517–1520.

- [88] Preparation and properties of 5'-nucleotidase from smooth muscle of small intestine. *J. Biol. Chem.* **1970**, *245*, 6274–6280.
- [89] Joseph, S. M.; Pifer, M. A.; Przybylski, R. J.; Dubyak, G. R. Methylene ATP analogs as modulators of extracellular ATP metabolism and accumulation. *Br. J. Pharmacol.* **2004**, *142*, 1002–1014.
- [90] Lee, E. H. A practical guide to pharmaceutical polymorph screening & selection. *Asian J. Pharm. Sci.* **2014**, *9*, 163–175.
- [91] Bhattarai, S.; Freundlieb, M.; Pippel, J.; Meyer, A.; Abdelrahman, A.; Fiene, A.; Lee, S.-Y.; Zimmermann, H.; Yegutkin, G.; Sträter, N.; El-Tayeb, A.; Müller, C. E. α,β -Methylene-ADP (AOPCP) derivatives and analogues: development of potent and selective ecto-5'-nucleotidase (CD73) inhibitors. *J. Med. Chem.* **2015**, *58*, 6248–6263.
- [92] Bhattarai, S.; Pippel, J.; Meyer, A.; Freundlieb, M.; Schmies, C.; Abdelrahman, A.; Fiene, A.; Lee, S.-Y.; Zimmermann, H.; El-Tayeb, A.; Yegutkin, G.; Sträter, N.; Müller, C. E. X-ray co-crystal structure guides the way to subnanomolar competitive ecto-5'-nucleotidase (CD73) inhibitors. *Adv. Ther.* **2019**, *1900075*, 1–8.
- [93] Debien, L.; Jaen, J. Modulators of ecto-5'-nucleotidase and the use thereof. **2017**, WO2017120508.
- [94] U.S. National Institutes of Health, A study to investigate the safety of AB680 in healthy volunteers. 2019; <https://clinicaltrials.gov/ct2/show/NCT03677973?term=NCT03677973&rank=1>.
- [95] Bowman, C. E.; da Silva, R. G.; Pham, A.; Young, S. W. An Exceptionally Potent Inhibitor of Human CD73. *Biochemistry* **2019**, *XXXX*, XXX–XXX.
- [96] Cacatian, S.; Claremon, D. A.; Jia, L.; Morales-Ramos, A.; Singh, S. B.; Venkatraman, S.; Xu, Z.; Zheng, Y. Purine derivatives as CD73 inhibitors for the treatment of cancer. **2015**, WO 2015/164573.
- [97] Billedeau, R.; Li, J.; Chen, L. Ectonucleotidase inhibitors and methods of use thereof. **2018**, WO 2018/119284 A1.
- [98] Brunschweiger, A. Darstellung und Charakterisierung von Uracil- und Adenin-nucleotidmimetika als selektive Ectonucleotidase-Inhibitoren. Ph.D. thesis, Universität Bonn, 2007.

- [99] Baqi, Y.; Lee, S. Y.; Iqbal, J.; Ripphausen, P.; Lehr, A.; Scheiff, A. B.; Zimmermann, H.; Bajorath, J.; Müller, C. E. Development of potent and selective inhibitors of ecto-5'-nucleotidase based on an anthraquinone scaffold. *J. Med. Chem.* **2010**, *53*, 2076–2086.
- [100] Iqbal, J.; Saeed, A.; Raza, R.; Matin, A.; Hameed, A.; Furtmann, N.; Lecka, J.; Sévigny, J.; Bajorath, J. Identification of sulfonic acids as efficient ecto-5'-nucleotidase inhibitors. *Eur. J. Med. Chem.* **2013**, *70*, 685–691.
- [101] Ripphausen, P.; Freundlieb, M.; Brunschweiger, A.; Zimmermann, H.; Müller, C. E.; Bajorath, J. Virtual screening identifies novel sulfonamide inhibitors of ecto-5'-nucleotidase. *J. Med. Chem.* **2012**, *55*, 6576–6581.
- [102] Baykov, A. A. A Malachite green procedure for orthophosphate determination and its use in alkaline phosphatase-based enzyme immunoassay. *Anal. Biochem.* **1988**, *270*, 266–270.
- [103] Cogan, E. B.; Birrell, G. B.; Griffith, O. H. A robotics-based automated assay for inorganic and organic phosphates. *Anal. Biochem.* **1999**, *271*, 29–35.
- [104] Thermo Fisher Scientific, Malachite green isothiocyanate. <http://www.lifetechnologies.com/order/catalog/product/M689>.
- [105] Renn, C. Unpublished work. **2015**,
- [106] Iqbal, J.; Jirovsky, D.; Lee, S. Y.; Zimmermann, H.; Müller, C. E. Capillary electrophoresis-based nanoscale assays for monitoring ecto-5'-nucleotidase activity and inhibition in preparations of recombinant enzyme and melanoma cell membranes. *Anal. Biochem.* **2008**, *373*, 129–140.
- [107] Qurishi, R. Qualitative und quantitative kapillarelektrophoretische Untersuchungen von Nukleosiden, Nukleotiden und deren Derivaten – Methodentwicklung und Validierung. Ph.D. thesis, University of Bonn, 2002.
- [108] Perrin, M. F. Polarisation de la lumière de fluorescence. Vie moyenne des molécules dans l'état excité. *J. Phys. Radium* **1923**, *1*, 390–401.
- [109] Chen, X.; Levine, L.; Kwok, P. Fluorescence polarization in homogeneous nucleic acid analysis. *Genome Res.* **1999**, *9*, 492–498.
- [110] Owicki, J. C. Fluorescence polarization and anisotropy in high throughput screening: perspectives and primer. *J. Biomol. Screen.* **2000**, *5*, 297–306.

- [111] BellBrook Labs: Transcreener ADP FP assay. *Tech. Man.* **2009**, 1–12.
- [112] BellBrook Labs: Transcreener AMP/GMP FP assay. *Tech. Man.* **2011**, 1–11.
- [113] Fiene, A.; Baqi, Y.; Lecka, J.; Sévigny, J.; Müller, C. E. Fluorescence polarization immunoassays for monitoring nucleoside triphosphate diphosphohydrolase (NTPDase) activity. *Analyst* **2015**, *140*, 140–148.
- [114] Lee, S.-Y. Unpublished work. **2017**,
- [115] Lee, S. Y.; Luo, X.; Namasivayam, V.; Geiss, J.; Mirza, S.; Pelletier, J.; Stephan, H.; Sévigny, J.; Müller, C. E. Development of a selective and highly sensitive fluorescence assay for nucleoside triphosphate diphosphohydrolase1 (NTPDase1, CD39). *Analyst* **2018**, *143*, 5417–5430.
- [116] Renn, C. Assay Development , Identification , Optimization and Pharmacological Characterization of Inhibitors for Ecto-5'-nucleotidase (CD73). Ph.D. thesis, University of Bonn, 2019.
- [117] Yoshikawa, M.; Kato, T.; Takenishi, T. A novel method for phosphorylation of nucleosides to 5'-nucleotides. *Tetrahedron Lett.* **1967**, *50*, 5065–5068.
- [118] Burgess, K.; Cook, D. Syntheses of nucleoside triphosphates. *Chem. Rev.* **2000**, *100*, 2047–2059.
- [119] Cramer, F.; Winter, M. Katalytische Wirkung von Dimethylformamid bei Reaktionen von Phosphorsäureester-chloriden. *Chem. Ber.* **1961**, *94*, 989–996.
- [120] Yoshikawa, M.; Kato, T.; Takenishi, T. Studies of phosphorylation. III. Selective phosphorylation of unprotected nucleosides. *Bull. Chem. Soc. Jpn.* **1969**, *42*, 3505–3508.
- [121] Kovács, T.; Ötvös, L. Simple synthesis of 5-vinyl- and 4-ethynyl-2'-deoxyuridine-5'-triphosphates. *Tetrahedron Lett.* **1988**, *29*, 4525–4528.
- [122] Alder, R.; Bowman, P.; Steele, W.; Winterman, D. The remarkable basicity of 1,8-bis(dimethylamino)naphthalene. *Chem. Commun.* **1968**, *452*, 723–724.
- [123] El-Tayeb, A.; Iqbal, J.; Behrenswerth, A.; Romio, M.; Schneider, M.; Zimmermann, H.; Schrader, J.; Müller, C. E. Nucleoside-5'-monophosphates as prodrugs of adenosine A2A receptor agonists activated by ecto-5'-nucleotidase. *J. Med. Chem.* **2009**, *52*, 7669–7677.
- [124] Imai, K.; Fujii, S.; Takanohashi, K.; Furukawa, Y.; Masuda, T.; Honjo, M. Phos-

- phorylation. IV. Selective phosphorylation of the primary hydroxyl group in nucleosides. *J. Org. Chem.* **1969**, *34*, 1547–1550.
- [125] Kucerová, Z.; Holy, A.; Bald, R. Nucleic acid components and their analogues. CXLVIII. Preparation of some nucleotidic derivatives of orotidine. *Collect. Czech. Chem. Commun.* **1972**, *34*, 1547–1550.
- [126] Ludwig, J. A new route to nucleoside 5'-triphosphates. *Acta Biochim. Biophys.* **1981**, *16*, 131–133.
- [127] El-Tayeb, A.; Qi, A.; Nicholas, R. A. Structural modifications of UMP, UDP, and UTP leading to subtype-selective agonists for P2Y₂, P2Y₄, and P2Y₆ receptors. *J. Med. Chem.* **2011**, *54*, 2878–2890.
- [128] Kalek, M.; Jemielity, J.; Stepinski, J.; Stolarski, R.; Darzynkiewicz, E. A direct method for the synthesis of nucleoside 5'-methylenebis(phosphonate)s from nucleosides. *Tetrahedron Lett.* **2005**, *46*, 2417–2421.
- [129] Junker, A.; Renn, C.; Dobelmann, C.; Namasivayam, V.; Jain, S.; Losenkova, K.; Irjala, H.; Duca, S.; Balasubramanian, R.; Chakraborty, S.; Börgel, F.; Zimmermann, H.; Yegutkin, G. G.; Müller, C. E.; Jacobson, K. A. Structure-activity relationship of purine and pyrimidine nucleotides as ecto-5'-nucleotidase (CD73) inhibitors. *J. Med. Chem.* **2019**, *62*, 3677–3695.
- [130] Kikugawa, K.; Suehiro, H.; Aoki, A. Platelet aggregation inhibitors. X. S-substituted 2-thioadenosine and their derivatives. *Chem. Pharm. Bull. (Tokyo)*. **1977**, *25*, 2624–2637.
- [131] Kikugawa, K.; Suehiro, H.; Ichino, M. Platelet aggregation inhibitors. VI. 2-Thioadenosine derivatives. *J. Med. Chem.* **1973**, *16*, 1381–1388.
- [132] Niiya, K.; Thompson, R. D.; Silvia, S. K.; Olsson, R. A. 2-(N'-Aralkylidenehydrazino) adenosines: Potent and selective coronary vasodilators. *Tetrahedron* **1992**, 4562–4566.
- [133] Ikehara, M.; Uesugi, S. Studies of nucleosides and nucleotides. XXXVIII. Synthesis of 8-bromoadenosine nucleotides. *Chem. Pharm. Bull. (Tokyo)*. **1969**, *17*, 348–354.
- [134] Chattopadhyaya, J. B.; Reese, C. B. Reaction between 8-bromoadenosine and amines. Chemistry of 8-hydrazinoadenosine. *Synthesis* **1977**, *10*, 725–726.
- [135] Long, R. A.; Robins, R. K.; Townsend, L. B. Purine nucleosides. XV. The syn-

- thesis of 8-amino- and 8- substituted aminopurine nucleosides. *J. Org. Chem.* **1967**, *32*, 2751–2756.
- [136] Fox, J. J.; Wempen, I.; Hampton, A.; Doerr, I. L. Thiation of nucleosides. I. Synthesis of 2-amino-6-mercapto-9- β -D-ribofuranosylpurine ("Thioguanosine") and related purine nucleosides. *J. Am. Chem. Soc.* **1958**, *80*, 1669–1675.
- [137] Nadel, Y.; Lecka, J.; Gilad, Y.; Ben-David, G.; Forster, D.; Reiser, G.; Kenigsberg, S.; Camden, J.; Weisman, G. A.; Senderowitz, H.; Sevi-gny, J.; Fischer, B. Highly potent and selective ectonucleotide pyrophosphatase/phosphodiesterase I inhibitors based on an adenosine 5'-(alpha or gamma)-thio-(alpha,beta- or beta,gamma)-methylenetriphosphate scaffold. *J. Med. Chem.* **2014**, *57*, 4677–4691.
- [138] Volpini, R.; Dal Ben, D.; Lambertucci, C.; Marucci, G.; Mishra, R.; Ramadori, A.; Klotz, K.-N.; Trincavelli, M.; Martini, C.; Cristalli, G. Adenosine A2A receptor antagonists: new 8-substituted 9-ethyladenines as tools for in vivo rat models of Parkinson's disease. *Chem Med Chem* **2009**, *4*, 1010–1019.
- [139] Ikehara, M.; Ogiso, Y.; Maruyama, T. Studies on nucleosides and nucleotides. LXXIII. Chlorination of adenosine and its N6-methyl derivatives with t-butyl hypochlorite. *Chem. Pharm. Bull. (Tokyo)*. **1977**, *25*, 575–578.
- [140] Ryu, E. K.; Kim, J. N. The oxidative chlorination of pyrimidine and purine bases, and nucleosides using acyl chloride-dimethyl-formamide- m -chloroperbenzoic acid system. *Nucleosides and Nucleotides* **1989**, *8*, 43–48.
- [141] Horatscheck, A.; Wagner, S.; Ortwein, J.; Kim, B. G.; Lisurek, M.; Belyny, S.; Schütz, A.; Rademann, J. Benzoylphosphonate-based photoactive phosphopeptide mimetics for modulation of protein tyrosine phosphatases and highly specific labeling of SH2 domains. *Angew. Chemie - Int. Ed.* **2012**, *51*, 9441–9447.
- [142] Assimomytis, N.; Sariyannis, Y.; Stavropoulos, G.; Tsoungas, P. G.; Varvounis, G.; Cordopatis, P. Anionic ortho-fries rearrangement, a facile route to arenol-based mannich bases. *Synlett* **2009**, 2777–2782.
- [143] Goodnow, R.; Hamilton, M.; Kowalczyk, A.; Sidduri, A. Preparation of amino acid- and dipeptide-containing integrin antagonist siRNA conjugates for targeted delivery to cells expressing LFA-1. Patent WO 2013110679 A1. 2003.
- [144] Chandran, K.; Nithya, R.; Sankaran, K.; Gopalan, A.; Ganesan, V. Synthesis

- and characterization of sodium alkoxides. *Bull. Mater. Sci.* **2006**, *29*, 173–179.
- [145] Oertell, K.; Chamberlain, B. T.; Wu, Y.; Ferri, E.; Kashemirov, B. A.; Beard, W. A.; Wilson, S. H.; McKenna, C. E.; Goodman, M. F. Transition state in DNA polymerase β Catalysis: Rate-Limiting chemistry altered by base-pair configuration. *Biochemistry* **2014**, *53*, 1842–1848.
- [146] McKenna, C. E.; Khawli, L. A.; Ahmad, W.-Y.; Pham, P.; Bongartz, J.-P. Synthesis of α -halogenated methanediphosphonates. *Phosphorous Sulfur Relat. Elem.* **1988**, *37*, 1–12.
- [147] Mohamady, S.; Jakeman, D. L. An improved method for the synthesis of nucleoside triphosphate analogues. *J. Org. Chem.* **2005**, *70*, 10588–10591.
- [148] McCoy, L. S.; Shin, D.; Tor, Y. Isomorphous emissive GTP surrogate facilitates initiation and elongation of in vitro transcription reactions. *J. Am. Chem. Soc.* **2014**, *136*, 15176–15184.
- [149] Boyle, N. A. Difluoromethylenediphosphonate: A convenient, scalable, and high-yielding synthesis. *Org. Lett.* **2006**, *8*, 187–189.
- [150] Pankiewicz, K. W.; Lesiak, K.; Watanabe, K. A. Efficient synthesis of methylenebis(phosphonate) analogues of P1,P2-disubstituted pyrophosphates of biological interest. A novel plausible mechanism. *J. Am. Chem. Soc.* **1997**, *119*, 3691–3695.
- [151] Chini, E. N.; Chini, C. C.; Espindola Netto, J. M.; de Oliveira, G. C.; van Schooten, W. The Pharmacology of CD38/NADase: An Emerging Target in Cancer and Diseases of Aging. *Trends Pharmacol. Sci.* **2018**, *39*, 424–436.
- [152] Kohyama, N.; Yamamoto, Y. A facile synthesis of AICAR from inosine. *Synthesis* **2003**, *17*, 2639–2642.
- [153] Bressi, J. C.; Choe, J.; HoughHough, M. T.; Buckner, F. S.; Van Voorhis, W. C.; Verlinde, C. L. M. J.; Hol, W. G. J.; Gelb, M. H. Adenosine analogues as inhibitors of *Trypanosoma brucei* phosphoglycerate kinase: Elucidation of a novel binding mode for a 2-amino-N6-substituted adenosine. *J. Med. Chem.* **2000**, *43*, 4135–4150.
- [154] Francom, P.; Robins, M. J. Nucleic acid related compounds. 118. Nonaqueous diazotization of aminopurine derivatives. Convenient access to 6-halo- and 2,6-dihalopurine nucleosides and 2'-deoxynucleosides with acyl or silyl halides. *J.*

- Org. Chem.* **2003**, *68*, 666–669.
- [155] Sandmeyer, T. Ueber die Ersetzung der Amidgruppe durch Chlor in den aromatischen Substanzen. *Berichte der Dtsch. Chem. Gesellschaft* **1884**, *17*, 2650–2653.
- [156] Blackburn, G.; Gait, M.; Loakes, D.; Williams, D. *Nucleic Acids Chem. Biol.*, 3rd ed.; 2015; Chapter 3.
- [157] Gerster, J.F. and Robins, K. Purine nucleosides. XIII. The synthesis of 2-fluoro- and 2-chloroinosine and certain derived purine nucleosides. *J. Org. Chem.* **1965**, *31*, 3258–3262.
- [158] Meier, L.; Monteiro, G.; Baldissera, R.; Mandolesi Sá, M. Simple method for fast deprotection of nucleosides by triethylamine-catalyzed methanolysis of acetates in aqueous medium. *J Braz Chem Soc* **2010**, *21*, 859–866.
- [159] Borrmann, T.; Hinz, S.; Bertarelli, D. C. G.; Li, W.; Florin, N. C.; Scheiff, A. B.; Müller, C. E. 1-Alkyl-8-(piperazine-1-sulfonyl)phenylxanthines: Development and characterization of adenosine A2B receptor antagonists and a new radioligand with subnanomolar affinity and subtype specificity. *J. Med. Chem.* **2009**, *52*, 3994–4006.
- [160] Liu, A. X.; Wang, M.-Y.; Wang, S.-Y.; Wang, Q.; Liu, X.; Wang, M.-y.; Wang, S.-Y.; Wang, Q.; He, L.-N. In situ generated zinc (II) catalyst for incorporation of CO₂ into 2-oxazolidinones with propargylic amines at atmospheric pressure. *ChemSusChem* **2017**, *10*, 1210–1216.
- [161] von Baeyer, A. Ueber ein neue Klasse von Farbstoffen. *Berichte der Dtsch. Chem. Gesellschaft zu Berlin* **1871**, *4*, 555–558.
- [162] Guilbault, G. G. *Pract. Fluoresc.*; Marcel Dekker Inc.: New York, 1990.
- [163] Sjöback, R.; Nygren, J.; Kubista, M. Absorption and fluorescence properties of fluorescein. *Spectrochim. Acta Part A* **1995**, *51*, L7–L21.
- [164] Sun, W.-C.; Gee, K. R.; Klaubert, D. H.; Haugland, R. P. Synthesis of fluorinated fluoresceins. *J. Org. Chem.* **1997**, *62*, 6469–6475.
- [165] Stokes, G. On the change of refrangibility of light. *Philos. Trans. R. Soc. London* **1852**, *142*, 463–562.
- [166] Herzenberg, L.; Parks, D.; Sahaf, B.; Perez, O.; Roederer, M. The history and

- future of the fluorescence activated cell sorter and flow cytometry: a view from Stanford. *Clin Chem* **2002**, *48*, 1819–27.
- [167] Jacobson, O.; Kiesewetter, D. O.; Chen, X. Fluorine-18 radiochemistry, labeling strategies and synthetic routes. *Bioconjug. Chem.* **2015**, *26*, 1–18.
- [168] Huisgen, R. Centenary Lecture - 1,3-Dipolar Cycloadditions. *Proc. Chem. Soc. London* **1961**, 357–396.
- [169] Seela, F.; Xiong, H.; Budow, S. Synthesis and 'double click' density functionalization of 8-aza-7-deazaguanine DNA bearing branched side chains with terminal triple bonds. *Tetrahedron* **2010**, *66*, 3930–3943.
- [170] Chan, T. R.; Hilgraf, R.; Sharpless, K. B.; Fokin, V. V. Polytriazoles as copper(I)-stabilizing ligands in catalysis. *Org. Lett.* **2004**, *6*, 2853–2855.
- [171] Glaser, M.; Erik, A. "Click labeling" with 2-[18F] fluoroethylazide for positron emission tomography. *Bioconjug. Chem.* **2007**, *18*, 989–993.
- [172] Huang, S.; Han, Y.; Chen, M.; Hu, K.; Qi, Y.; Sun, P.; Wang, M.; Wu, H.; Li, G.; Wang, Q.; Du, Z.; Zhang, K.; Zhao, S.; Zheng, X. Radiosynthesis and biological evaluation of 18 F-labeled 4-anilinoquinazoline derivative (18 F-FEA-Erlotinib) as a potential EGFR PET agent. *Bioorganic Med. Chem. Lett.* **2018**, *28*, 1143–1148.
- [173] Seela, F.; Peng, X. 7-Functionalized 7-deazapurine ribonucleosides related to 2-aminoadenosine, guanosine, and xanthosine: Glycosylation of pyrrolo[2,3-d]pyrimidines with 1-O-acetyl-2,3,5-tri-O-benzoyl-D-ribofuranose. *J. Org. Chem.* **2006**, *71*, 81–90.
- [174] Choi, W. B.; Wilson, L. J.; Yeola, S.; Liotta, D. C.; Schinazi, R. F. In situ complexation directs the stereochemistry of N-glycosylation in the synthesis of thialanyl and dioxolanyl nucleoside analogs. *J. Am. Chem. Soc.* **1991**, *113*, 9377–9379.
- [175] Vorbrüggen, H.; Lagoja, I. M.; Herdewijn, P. Synthesis of ribonucleosides by condensation using trimethylsilyl triflate. *Curr. Protoc. Nucleic Acid Chem.* **2007**, *27*, 1.13.1–1.13.16.
- [176] Ingale, S. A.; Leonard, P.; Seela, F. Glycosylation of pyrrolo[2,3-d]pyrimidines with 1-O-acetyl-2,3,5-tri-O-benzoyl- β -d-ribofuranose: substituents and protecting groups effecting the synthesis of 7-deazapurine ribonucleosides. *J. Org.*

- Chem.* **2018**, *83*, 8589–8595.
- [177] Idris, R. Unpublished data. **2019**,
- [178] Idris, R. No Title. Ph.D. thesis, University of Bonn.
- [179] El-Tayeb, A. Synthesis and evaluation of uracil and adenine nucleotide derivatives and analogs as P2Y receptor ligands. Ph.D. thesis, University of Bonn, 2007.
- [180] Chen, L.; Sheppard, T. Synthesis and hybridization properties of RNA containing 8-chloroadenosine. *Nucleosides Nucleotides Nucleic Acids* **2002**, *21*, 599–617.
- [181] Sigma Aldrich, 8-Bromoadenosine (B6272 SIGMA). <http://www.sigmaaldrich.com/catalog/product/sigma/b6272?lang=de®ion=DE>.
- [182] Buenger, G. S.; Nair, V. Dideoxygenated purine nucleosides substituted at the 8-position: chemical synthesis and stability. *Synthesis* **1990**, *10*, 962–966.
- [183] Halbfinger, E. .; Major, D.; Ritzman, M.; Ubl, J.; Reiser, G.; Boyer, J.; Harden, K.; Fischer, B. Molecular recognition of modified adenine nucleotides by the P2Y1-Receptor. 1. A synthetic, biochemical, and NMR approach. *J. Med. Chem.* **1999**, 5325–5337.
- [184] Ikehara, M.; Uno, H. Nucleosides and nucleotides. XXVI. Further studies on the chlorination of inosine derivatives with N,N-dimethylformamide-thionyl chloride complex. *Chem. Pharm. Bull. (Tokyo)*. **1965**, *13*, 221–223.
- [185] Lettre, H.; Ballweg, H. Ribosides of some cytotoxic purine derivatives. *Justus Liebigs Ann. Chem.* **1962**, *656*, 158–162.
- [186] Čechová, L.; Jansa, P.; Šála, M.; Dračínský, M.; Holý, A.; Janeba, Z. The optimized microwave-assisted decomposition of formamides and its synthetic utility in the amination reactions of purines. *Tetrahedron* **2011**, *67*, 866–871.
- [187] Milne, G. W. A. *Drugs: Synonyms & Properties*; Wiley, 2000; p 1280.
- [188] Andrews, K.; Barber, W. The synthesis of 6-dimethylamino-9- β -D-ribofuranosylpurine-5' phosphate. *J. Am. Chem. Soc.* **1958**, 2768–2771.
- [189] Van Tilburg, E. W.; Von Frijtag Drabbe Künzel, J.; De Groote, M.; Volling, R. C.; Lorenzen, A.; IJzerman, A. P. N⁶,5'-disubstituted adenosine derivatives as par-

- tial agonists for the human adenosine A3 receptor. *J. Med. Chem.* **1999**, *42*, 1393–1400.
- [190] Levene, P.; Tipson, R. S. The ring structure of guanosine. *J. Biol. Chem.* **1932**, *97*, 491–495.
- [191] Francom, P.; Janeba, Z.; Shibuya, S.; Robins, M. J. Nucleic acid related compounds. 116. Nonaqueous diazotization of aminopurine nucleosides. Mechanistic considerations and efficient procedures with tert-butyl nitrite or sodium nitrite. *J. Org. Chem.* **2002**, *67*, 6788–6796.
- [192] Fiene, A. Entwicklung und Bewertung verschiedener Methoden zur Aktivitätsbestimmung von Ectonucleotidasen und zur Identifizierung von Inhibitoren. Ph.D. thesis, Bonn University, 2015.
- [193] Lee, S. Y.; Sarkar, S.; Bhattarai, S.; Namasivayam, V.; De Jonghe, S.; Stephan, H.; Herdewijn, P.; El-Tayeb, A.; Müller, C. E. Substrate-dependence of competitive nucleotide pyrophosphatase/phosphodiesterase1 (NPP1) inhibitors. *Front. Pharmacol.* **2017**, *8*, 1–7.
- [194] Blacher, E.; Baruch, B. B.; Levy, A.; Geva, N.; Green, K. D.; Garneau-Tsodikova, S.; Fridman, M.; Stein, R. Inhibition of glioma progression by a newly discovered CD38 inhibitor. *Int. J. Cancer* **2015**, *136*, 1422–1433.
- [195] Lopez, V. Unpublished work. **2019**,
- [196] Servos, J.; Reiländer, H.; Zimmermann, H. Catalytically active soluble ecto-5'-nucleotidase purified after heterologous expression as a tool for drug screening. *Drug Dev. Res.* **1998**, *45*, 269–276.
- [197] Cheng, Y.; Prusoff, W. Relationship between the inhibition constant (K₁) and the concentration of inhibitor which causes 50 per cent inhibition (I₅₀) of an enzymatic reaction. *Biochem. Pharmacol.* **1973**, *22*, 3099–3108.

Danksagung

An dieser Stelle möchte ich meinen besonderen Dank nachstehenden Personen entgegen bringen, ohne deren Mithilfe die Anfertigung dieser Dissertation nicht zustande gekommen wäre.

Zunächst gilt mein besonderer Dank meiner wissenschaftlichen Betreuerin Frau Prof. Dr. Christa Müller, die es mir möglich gemacht hat diese Arbeit in ihrem Arbeitskreis anzufertigen. Liebe Christa, als meine Doktormutter warst du immer offen für Diskussionen und hattest wertvolle Ratschläge parat. Dank dir hatte ich die Möglichkeit viele interessante Erfahrungen zu machen, auch neben der Arbeit im Labor, wie zum Beispiel die Teilnahme an der Organisation der Frontiers Konferenz in Bonn, die Bewerbung für das SFB Projekt, oder auch die Präsentation bei der Exzellenz-Uni Bewerbung. Ich danke dir für dein Vertrauen und den Freiraum, den du mir gegeben hast, wodurch ich eine eigenständige Arbeitsweise erlernen konnte.

Außerdem möchte ich Herrn Prof. Gerd Bendas für die Anfertigung des Zweitgutachtens danken.

Für die Mitwirkung in der Prüfungskommission danke ich Frau PD Dr. Ganna Staal und Herrn Prof. Manthey.

Bei Dr. Ali El-Tayeb möchte ich mich für die Unterstützung und hilfreichen Diskussionen und guten Tipps bedanken, die zum Gelingen der Synthesen beigetragen haben. Dr. Sanjay Bhattarai danke ich für die Einarbeitung in die chemische Phosphorylierung.

Christian dir danke ich ganz herzlich für die pharmakologische Testung meiner Verbindungen an CD73. Unsere Zusammenarbeit lief super. Wir hätten damit schon viel früher anfangen müssen. Du hast nur wenige Monate vor mir angefangen mit deiner Promotion, und zusammen haben wir die Höhen und Tiefen der Promotion erlebt. Durch die gemeinsamen Mittagspausen, unseren Road-Trip nach Ljubljana und andere Erlebnisse bist du zu einem Freund geworden. Ich wünsche dir alles Gute für die Zeit nach der Promotion und hoffe sehr, dass unsere Freundschaft bestehen bleibt.

Ein besonderer Dank geht auch an meinen Nukleotid-Kollegen und Mit-Karnevals-Prinzen Georg I., der einen Teil meiner Projekte übernehmen wird und mit dem ich viele interessante und hilfreiche Diskussionen rund um die Nukleotid-Synthese und die HPLC geführt habe. Vielen Dank auch dafür, dass du dich bereit erklärt hast, diese Arbeit Korrektur zu lesen. In Zukunft wirst du wohl alleine an der HPLC herumschrauben müssen. Ich wünsche dir viel Erfolg bei deiner Promotion und freue mich schon aufs Paper-schreiben mit dir.

Bei Laura bedanke ich mich für die pharmakologische Testung meiner Verbindungen an CD39. Du bist erst seit knapp einem Jahr in unserem Arbeitskreis und ich bin so dankbar, dass wir das SFB Projekt bekommen haben und du auf dieses Thema gesetzt wurdest. Gerade in den letzten Wochen meiner Promotion hast du mich tatkräftig unterstützt, die Selektivitätsstudien voran getrieben, die Daten formatiert und mit mir über die Zukunft des Projekts diskutiert. Auf dich ist immer Verlass!

I also want to thank Sang-Yong, Xihuan, and Riham for the pharmacological evaluation of my compounds at CD39 and CD73, as well as Vittoria and Mirza for the selectivity studies.

Marion, Sabine und Anette danke ich für die Durchführung der LC-MS und NMR-Analytik. Wenn ich Fragen zu meinen Spektren und Chromatogrammen hatte, konnte ich immer zu euch kommen und bei Problemen habt ihr mir stets geholfen diese zu lösen. Vielen Dank dafür!

Des Weiteren möchte ich Thomas und Christoph danken, dass sie mir immer sofort geholfen haben, wenn ich ein mechanisches oder elektronisches Problem hatte. Egal ob es die Pumpe vom Roti war, der Computer vor mir angefangen hat zu qualmen, die Druckerpatrone leer war oder die Sicherung von einem Praktikums-Gerät sich verabschiedet hatte, ihr ward sofort zur Stelle und habt das Problem schnellst möglich gelöst. Danke schön.

Beate bei dir möchte ich mich ganz herzlich bedanken, dass ich mit Fragen immer zu dir kommen konnte, und du dich um alle organisatorischen Dinge gekümmert hast.

Ein besonderer Dank geht an Frau Prof. Eva Tolosa vom UKE Hamburg, die mich eingeladen hat meine Verbindungen in ihrem Labor zu testen. Ich hatte eine wunderbare Zeit in Hamburg und dieser kurze Forschungsaufenthalt war eine klasse Erfahrung. Ganz besonders möchte ich auch Riekje danken für ihre Hilfe und Betreuung während meines Aufenthalts. Bei allen Fragen hast du versucht mir weiter

zu helfen, hast mir geholfen bei der Auswertung und hast sogar nach meiner Abreise noch Experimente für mich durchgeführt. Vielen vielen Dank dafür.

Meinen Forschungsstudenten Renas und Aysegül möchte ich danken für ihre Unterstützung im Labor. I also want to thank Bibby for his help in the lab during the last months. I wish you all the best for your PhD and success with continuing the CD39 project.

Ich möchte dem gesamten Arbeitskreis Müller dafür danken, für die wunderbare Zeit. Im Falle von fachlichen Fragen, gab es immer jemanden, den ich ansprechen konnte. Darüber hinaus haben Erlebnisse wie die jährlichen Weihnachtsfeier, Karneval, Heringessen, Pharmapartys, und unseren Betriebsausflug auf das Weingut dafür gesorgt, dass die 4 Jahre im AK Müller unvergesslich bleiben.

Besonders danken möchte ich vor allem allen aktiven Mitgliedern der "Feierabendbiergruppe" sowie den ehemaligen Doktoranten Clara, Anne, Stephi, und Markus. Unsere Gespräche bei einem kühlen Bierchen glichen manchmal schon fast einer Gruppentherapiesitzung. Und ab und an ist auch die ein oder andere Idee fürs Labor an diesen Abenden entstanden.

Ein herzlicher Dank geht an meine Bürokollegen Vittoria, Ahmed, Aliaa und Christin. Ihr habt immer für eine angenehme Arbeitsatmosphäre gesorgt, in der man sowohl konzentriert arbeiten konnte, als auch gemütlich bei einem Kaffchen quatschen konnte. Christin du hast außerdem immer zuverlässig dafür gesorgt, dass meine Verbindungen fachgerecht registriert wurden. Dear Vittoria, also next to work we had a lot of fun and I will always think of you when I use your "gnocchi-plank". I wish you all the best and success with your thesis.

Danken möchte ich auch meinen Kollegen, mit denen ich gemeinsam das Praktikum des 4. Semesters betreut habe. Insbesondere möchte ich Martin danken für die verlässliche Versorgung mit Kaffee während unseres E-Chemie Blocks.

Ein besonderer Dank gilt am Ende vor allem meiner Familie. Liebe Mama, auch wenn wir nicht viel Zeit miteinander verbringen konnten, hast du mir so viel mitgegeben und ohne dieses Fundament wäre meine schulische und akademische Karriere bestimmt nicht so erfolgreich gewesen. Du wirst immer bei mir sein. Papa und Tina, ihr habt mich immer unterstützt und meine Entscheidungen nie hinterfragt. Zusammen mit meinen Geschwistern Basti, Valeria, und Lea, habt ihr für ein zuhause gesorgt, wo ich immer abschalten konnte. Wenn wir zusammen sind, ist

immer was los und es wird bestimmt nicht langweilig. Ich liebe euch alle. Danke, dass ihr immer für mich da seid.

Zuletzt geht ein großer Dank an meinen Partner Felix. Seit 9 Jahren gehen wir zusammen durchs Leben. Nach 5 Jahre nerviger Fernbeziehung hast du mich auch noch während der Promotion leidlos ertragen. Du hattest immer ein offenes Ohr für mich, wenn es alles schief ging im Labor, und hast dich über jeden meiner Erfolge mit mir gefreut. Jetzt liegt ein neuer Lebensabschnitt vor uns und ich bin übergücklich dich an meiner Seite zu wissen.